DOCTOR OF PHILOSOPHY

Environmental and biological controls of Mg/Ca, Sr/Ca and Mn/Ca ratios in the shells of the bivalves Pinna nobilis, Mytilus edulis and Pecten maximus : implications for palaeo-environmental reconstructions

Freitas, Pedro

Award date:
2007

Awarding institution:
Bangor University

Environmental and Biological Controls of Mg/Ca, Sr/Ca and Mn/Ca Ratios in the Shells of the Bivalves *Pinna nobilis*, *Mytilus edulis* and *Pecten maximus*: Implications for Palaeo-environmental reconstructions

A Thesis submitted to the University of Wales Bangor by

Pedro Seabra Freitas

for the degree of

Philosophiae Doctor

School of Ocean Sciences
University of Wales – Bangor
Porthaethwy (Menai Bridge)
Ynys Môn
LL59 5AB

October 2007

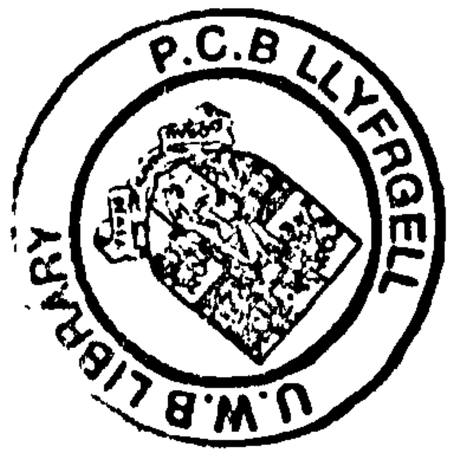

Á Camille e ao Luca.

E ao Duarte, Mark e Martin,
companheiros desta longa viagem…

ACKNOWLEDGEMENTS

This thesis is the result from many collaborations, support and precious helps. I would like to thank all the persons who helped me go through this incredible experience.

First of all, I thank my supervisors at the School of Ocean Sciences, Chris Richardson, Hilary Kennedy and Leon Clarke for their support, enthusiasm, encouragement, expertise and constructive comments that made this journey possible and productive. I would like to thank Fátima Abrantes from my home institution INETI, for all her help, motivation, patience and support throughout the years.

This work could not have happened without the precious help from the technicians at the School of Ocean Sciences, with whom I shared much more than "technical" aspects. It was a pleasure to meet and share all the enthusiasm from these talented and gifted welsh persons: Thanks to Berwyn Roberts, Gwynne P. Jones and Gwynne Hughes for the incredible journey on board of the sampling boats, the care in the tanks, the sharing of seafood, jokes, secrets about collecting and pillaging the welsh seashore, but most of all for the smiles and the warmth in their hearts; thank to Malcolm Budd for the attention and care with the algae culture and being a great landlord. Thanks to Anne Hammerstein for the help during the salinity analysis; Viv Ellis and Ian Pritchard for helping me in the laboratory; thank to Mike Jones, Ian Nicholls and Elwyn Jones for building the cages for the raft and loads of funny jokes; John Rowlands and David Roberts for their help with photography and microscopes.

I would like to thank Paul Kennedy, my guide in the labs, for all his help and technical support in analyses I had to do in the lab, his "good" and "bad" humour, keeping the coffee going and a lot more; and also a big thank you to Stathys Papadimitriou for the nutrient analyses, but mainly for the endless discussions and exchanges, his ever present help and the delicious stuffed peppers.

The technical assistance of Nick Walsh, Sarah James and Jacqui Duffet at the U.K. Natural Environment Research Council ICP-AES Facility at Royal Holloway University of London; of Paul Dennis and Alina Marca at the School of Environmental Sciences, University of East Anglia for seawater oxygen stable-isotope analyses; access to the U.K. Natural Environment Research Council Ion Microprobe Facility at Edinburgh University and the assistance of Richard Hinton and John Craven is acknowledged gratefully. In particular, I thank David Oakes from Ramsay Sound Shellfish Ltd. for kindly supplying the scallop spat. Constructive comments on that substantially improved several chapters were given by Thierry Corrège, Adrian Immenhauser, Andrew Johnson, David Lea, Laura Wasylenki, Vincent Salters, David Thomas, William Andrews and four anonymous reviewers.

The journey through North Wales as been one of discovery. A discovery of cultures, places, activities, but most importantly of people, beautiful people. I thank from my heart the people in Wales and abroad that shared such important time. First the big family of brothers, sisters and cousins: Adriana Candeias and Greg Carson, Duarte Tito, Marta Rufino, Marika Galinidi, Mar Otero, Mark Walton, Martin Skov, and Virginia Salas. Abroad: Mario and Teresa, Judite and Luis, Rita Amado, Francisco Teixeira, Alain Frances and Catarina, Tiago Cunha and Marianne Nuzzo, Rui e Carlos Malato, Luis Rebelo, Silvia and To, Pedro "Cenoura" and Miguel Pato. I thank also those that become good friends during this time and shared so good moments: "Big" Phil Wiles, Richard "Big Nose" Shucksmith, Kate Mcquaid, Sacha Beard, Ana Queiros and João, Raquel, Alexandra Marques, Nigel Hussey, Jan Hiddink, Femke Gent, Hilmar Hinz, Panos Grigoriou, Eva Chatzinikolau, Glória Pereira, Rubina Rodrigues, Maher and Mai-anh Kaladji.

A special thanks to my family, Pai, Mãe, Carlos, Rita, Claudia, Jorge and Gi, for your friendship and your love through some rough times during this PhD. A huge thank you to Domi and Gégé for accepting as friend and as part of their family.

Finally, I would like to thank Camille. For your never ending love and friendship that keeps growing each day. I do not have words strong enough to say the importance you have to me.

The funding during this PhD came from the Fundação para a Ciência e Tecnologia, scholarship Ref: . SFRH/BD/10370/2002. Access to the U.K. Natural Environment Research Council ICP-AES Facility at Royal Holloway University of London, awards No. ICP/196/1201 and OSS/273/1104, as well as to the U.K. Natural Environment Research Council Ion Microprobe Facility at Edinburgh University is acknowledged gratefully.

SUMMARY

Calcium carbonate skeletons produced by organisms such as foraminifera, ostracodes, corals and molluscs have the potential to contain within their isotope and elemental composition signatures (i.e. proxies) that reflect the environment in which the organisms calcified. Bivalves offer the potential for high resolution reconstructions over a wide geographical range and in the fossil record since the Early Ordovician. However, when compared to other biogenic carbonate archives there have been relatively fewer studies that have investigated bivalve mollusc shell geochemistry, especially robust validation studies of likely geochemical proxies. This study contributes to the evaluation and validation of geochemical proxies in bivalves. More specifically, the aim was to investigate and validate the relationships between the elemental composition (Mg/Ca, Sr/Ca and Mn/Ca) of bivalve shell calcite and its primary environmental controlling factors, i.e. seawater temperature, dissolved and particulate Mn concentrations. In addition, the role of secondary control factors (i.e. "vital" effects and small-scale element heterogeneity), as a source of non-environmental variability in bivalve geochemical proxies was also investigated.

Studies on the temperature dependence of Mg/Ca ratios in bivalve calcite shells have produced contradictory results. In the bivalve species studied, *Pinna nobilis* (Chapter 2), *Mytilus edulis* (Chapter 4) and *Pecten maximus* (Chapters 3 and 4), the temperature dependence of shell calcite Mg/Ca ratios was found to be generally weak. The occurrence of a large variability in Mg/Ca ratios at the species, inter- and intra- individual shell levels, as well as through ontogeny, together with a weak temperature control, clearly suggests a strong physiological control of calcite Mg/Ca ratios during shell biomineralization. Bivalve calcite Mg/Ca ratios do not yet appear to be a reliable and precise temperature proxy, at least in the species studied.

In the three bivalve species studied, *Pinna nobilis* (Chapter 2), *Mytilus edulis* (Chapter 5) and *Pecten maximus* (Chapters 3 and 5), shell Sr/Ca ratios were found to be influenced by more than a single physiological control (shell growth rate, metabolic activity and even shell Mg content), which may differ from one species to another, but also vary temporally in a single species. Shell growth rate, assumed to indicate a precipitation rate control, was significantly correlated to shell Sr/Ca ratios in field- and laboratory-grown *P. maximus* and *M. edulis*. The positive relationship observed between absolute respiration rate and Sr/Ca ratios in *M. edulis*, grown both in laboratory and field culturing experiments, provides the first direct evidence of an influence from metabolic activity on bivalve calcite Sr/Ca ratios.

The seasonal variation of Mn/Ca ratios in the shell calcite of field grown *Pecten maximus* specimens followed a similar intra-annual variation to dissolved Mn concentrations described previously (Chapter 5). In *Mytilus edulis*, shell Mn/Ca ratios were found not to be influenced by either dissolved or particulate Mn^{2+} concentrations (Chapter 6). Shell Mn/Ca ratios and shell growth rates showed a remarkably similar seasonal variation. However, such similarity is not indicative of a precipitation rate control since precipitation rate and Mn partition coefficient in synthetic inorganic calcite are inversely related. The influence of shell growth rate on shell Mn/Ca ratios must reflect a physiological control most likely acting at the transport of Mn into the extra-pallial fluid.

Significant small-scale heterogeneity in Mg/Ca, Sr/Ca and Mn/Ca ratios in the shells of *Pecten maximus* and *Mytilus edulis* deposited at a constant temperature was observed (Chapter 7). In particular, elaborate shell features and disturbance growth marks, were associated with significant variations of the elemental content of the shell calcite and may represent an important interference in the use of geochemical proxies in bivalve shell calcite. Importantly, shell Mg/Ca ratios in the inner regions of *P. maximus* shells promise the potential to become a valid palaeotemperature proxy. In both bivalve species studied, elemental/Ca ratios vary significantly in shell deposited from the same extra-pallial fuild and

thus strongly suggests that element incorporation in to the shell carbonate at the crystal-solution interface is a key control step in determining the element composition of shell calcite.

Most of the results in this study contribute to the growing evidence that bivalve calcite element composition is controlled by physiological factors that underlie a tight control of element incorporation during shell biomineralization. Unless the secondary controls (i.e. metabolic and/or kinetic factors) on element incorporation, in particular their influence on the small-scale heterogeneity of shell elemental composition, can be understood in more detail, and subsequently compensated for, the use of the geochemical proxies Mg/Ca, Sr/Ca and Mn/Ca ratios in bivalves for reliable and accurate reconstructions of past or present environmental conditions remains unlikely, at least in the species studied to date.

TABLE OF CONTENTS

LIST OF TABLES

LIST OF FIGURES

Chapter I

General Introduction

Chapter 1

General Introduction

I - General Introduction

1.1 Background

In the past decades there has been a growing interest in understanding and reconstructing past environmental conditions. The knowledge of the causes and controls of Earth's climate are of major importance to the ability to predict and monitor future changes associated with the potential impacts of human activity and disturbance of natural systems. Furthermore, there is a growing need to reconstruct environmental events after they have taken place, assessing the impact of both natural (e.g. storms, productivity, temperature and salinity fluctuations) and anthropogenic (e.g. pollution) occurrences. Instrumental records on the variation of environmental conditions are relatively recent, covering a few centuries at most, rare and spatially limited. To reconstruct past and present environmental conditions prior to the instrumental record or in areas where such records are scarce or absent, the use of natural archives of environmental conditions is necessary and often the only way to retrieve such information. Natural archives, be it in geological (e.g. ice cores, rocks, sediments and speleotherms) or biological structures (e.g. trees, corals, bivalves, etc), record environmental information both as physical and chemical properties.

A proxy is a measurable chemical or physical signal preserved in biological or geological structures that reflect an un-measurable environmental signal. A "proxy"-based approach for the reconstruction of environmental conditions is especially important when and where instrumental records of oceanographic and climatic parameters are absent. An ideal marine geochemical proxy will depend on a single oceanographic parameter, and will enable a perfect reconstruction of the variation of such a parameter in the past. Often, multiple parameters can influence these proxies, thereby confounding their use. It is now clear that the organism metabolic activity significantly interfere with geochemical proxies recorded in the carbonate skeletons

of foraminifera (Spero and Lea, 1993; Spero and Lea, 1996; Lea et al., 1999; Zeebe, 1999b), corals (e.g. McConnaughey, 1989a; McConnaughey, 1989c; e.g. de Villiers et al., 1995; McConnaughey et al., 1997; Adkins et al., 2003; Rollion-Bard et al., 2003), and bivalves (Klein et al., 1996b; Vander Putten et al., 2000; Kennedy et al., 2001; Owen et al., 2002b; Lorrain et al., 2004; Gillikin et al., 2005b; Lorrain et al., 2005; Carré et al., 2006; Gillikin et al., 2006b). Consequently, each new potential proxy needs to be rigorously calibrated and validated and its veracity confirmed (for reviews, see e.g. Wefer et al., 1999; Lea, 2003). To complete such an exercise the role of environmental, and potentially biological, factors in controlling the proxy variation must be understood.

Carbonate minerals are ubiquitous in a wide variety of terrestrial and aquatic environments, constituting a significant component of sediments throughout the world oceans (e.g. Broecker and Peng, 1982). The chemical and isotopic composition of carbonate minerals may reflect the mode and environment of their formation and subsequent alterations, and thus provides a valuable source of information on the Earth's past climates and oceanographic conditions. In particular, successive growth layers of calcium carbonate skeletons (i.e. biogenic accretionary hard parts), or in a stratigraphic sequence of shells, produced by organisms such as foraminifera, ostracodes, corals and bivalves have the potential to contain within their isotope and elemental composition signatures that reflect the environment in which the organisms calcified (e.g. Lea and Boyle, 1989; Lea et al., 1989; Wefer and Berger, 1991; Delaney et al., 1993; Druffel, 1997; Lea et al., 1999; Swart and Grottoli, 2003). Variable growth rates produce distinct growth increments that allow estimating the organism age, attributing a time frame to different portions of the skeleton or assessing the life history of the organism.

The use of elemental/Ca ratios in biogenic carbonates as geochemical proxies has grown rapidly in the last decade, particularly of Mg/Ca and Sr/Ca ratios, and complements the more traditional $\delta^{18}O$ and $\delta^{13}C$ proxies. However, the factors controlling the trace-element composition of biogenic carbonates generally are much less well understood than those governing stable-isotope ratios. The importance of Mg/Ca and Sr/Ca ratio palaeo-thermometry has encouraged active research into the evaluation of biological and environmental (e.g., temperature, salinity and pH)

factors which may influence the incorporation of elements into biogenic carbonates. Compared to other biogenic carbonate archives there have been relatively fewer studies that have investigated bivalve mollusc shell geochemistry, especially robust validation studies of likely geochemical proxies.

1.2 Marine Bivalves

For several decades bivalve shells have been known to provide valid archives of past environmental conditions (e.g. for a review see Richardson, 2001). The potential utility of mollusc shells as palaeoenvironmental archives is due to their incremental deposition, such that they possess in their shell geochemical and physical composition a temporal record reflective of ambient conditions during growth (Jones, 1983; Richardson, 2001). For instance, the initial work carried by Epstein et al. (1951), and later corrected by Epstein et al. (1953), to establish a biogenic carbonate $\delta^{18}O$-water temperature scale was done mainly using gastropods and bivalve molluscs. Marine bivalves also are widely distributed throughout the oceans, from the tropics to the polar regions, whereas many other substrates such as corals are limited in their latitudinal extent, and from coastal estuarine waters to the deep ocean, displaying a range of growth rates and longevity of usually less than 10 years, but in some cases more than 50 years or even more than 300 years for *Artica islandica* (Schöne et al., 2005). Furthermore, bivalve shells are often found in archaeological middens and in fossil records since the Cretaceous. Bivalve shell geochemistry thus provides the potential to reconstruct high temporal resolution records of environmental conditions over a wide range of spatial and also temporal scales, from decades to even centuries if a sclerochronological approach is taken (e.g. Jones, 1983; Weidman et al., 1994).

1.2.1 Morphology

Bivalvia, a class of the phylum Mollusca, are laterally compressed animals possessing 2 valves which enclose the animal tissues (Russell et al., 1996). The shell

consists of two more or less similar valves, which are attached and articulated to one another by the hinge system which includes a ligament, teeth and other specific specializations (Figure 1-1). The umbo is a dorsal protuberance and bears the oldest part of the shell. The valves of the shell are pulled together by one or two adductor muscles, an anterior and a posterior, and in bivalves enclose a well developed mantle (or pallial) cavity, the space between the mantle and the internal organs. The mantle cavity contains essentially seawater, although its composition can be altered during extended closure of the valves. The mantle is a thin organ that lines the inner shell surface, which in bivalves consists of 2 lobes of tissues that completely enclose the animal within the shell. Both the inner surface of the mantle (facing the mantle or pallial cavity) and the outer surface of the mantle (facing the inner shell surface) are covered by a layer of single cell epithelium. The bivalve mantle possesses different tissues: muscle tissue, connective tissue, nerve fibres, haemolymph and may contain most of the gonads. Therefore, the mantle may serve different functions: sensorial, shell formation, reproductive, endocrinal. The mantle margins are organized in 3 folds (Benninger and Le Pennec, 1991; Gosling, 2003): the outer fold, close to the shell edge and responsible for shell formation, which contains the periostracum groove where the periostracum is formed; the middle fold, with a sensory function and the inner fold or vellum, muscular and which controls water flow into the mantle cavity. The mantle is attached to the shell by muscle in the pallial line (not clearly detectable in all species) and runs in a semicircle parallel to the shell edge. A space, the extra-pallial space, contains a fluid named the extra-pallial fluid (EPF), which is enclosed between the mantle and the inner shell surface.

1.2.2 Species Used

Three bivalve species were used in this study: the fan mussel *Pinna nobilis*, the blue mussel *Mytilus edulis* and the scallop *Pecten maximus*. The former species has been shown to calcify under oxygen-isotope equilibrium with surrounding seawater, confirming the potential for high temporal resolution palaeotemperature reconstruction (Kennedy et al., 2001), and together with its large size and fast shell growth rate provides an interesting model to investigate the temperature control of Mg/Ca and Sr/Ca ratios in bivalve calcite. The latter two species, as well as closely related taxa, have been proposed previously as valid archives for palaeoceanographic

studies (e.g. Krantz et al., 1988; Klein et al., 1996a; Hickson et al., 1999; Chauvaud et al., 2005; Gillikin et al., 2006a; Wanamaker et al., 2006) and arguably are two of the most studied bivalve species, thus yielding a valuable wealth of knowledge regarding its ecology and physiology (Brand, 1991; Gosling, 1992).

Figure 1 - 1 – The morphology of the shell of *Mytilus edulis* (from Gosling 2003).

Pinna nobilis (Figure 1-2) is a large (up to 1 m) and long lived bivalve (up to 20 yrs), with relatively fast growth rates (up to 59 cm in 8 yrs) (Richardson et al., 1999). *P. nobilis* is an endemic endangered species of the Mediterranean Sea that occur in sheltered coastal areas in the infralitoral and circalitoral, usually in seagrass meadows between 0.5 and 60 m water depth, with approximately ⅔ of the shell buried in sediments and use byssal threads to attach to sand or gravel bottoms (Moreteau and Vicente, 1982).

Scallops (Figure 1-3), bivalves belonging to the family Pectinidae, are found in all waters of the Northern and Southern Hemispheres. *Pecten maximus* is found in the Northeast Atlantic Ocean from Norway to west Africa, in the western Mediterranean and in the archipelagos of the Açores, Canarias and Madeira (Brand, 1991). *Pecten maximus* is an unattached surface dweller that lives from the low tide mark down to 200 m, but usually at 20-45 m, in clear firm sand and fine or sandy gravel (Brand, 1991). Adults can reach up to 150 mm and bury slightly in the sediment with the flat/left valve upwards. Life span is variable with location, but can reach over 10

years. The valves have two auricules on either side of the umbo and are not symmetric, with the left (upper) valve being flattened and slightly overlapped by the right one, which is convex. The shell of *P. maximus* has several ribs radiating from the umbo (typically 14-15), alternating with grooves. Distinct yearly rings that are deposited during winter are usually easily observed, although they may be absent or easily mistaken by disturbance marks. The shell shows concentric stria all along its length. Scallops have the ability to swim by clapping the valves, usually to avoid predation or for habitat selection.

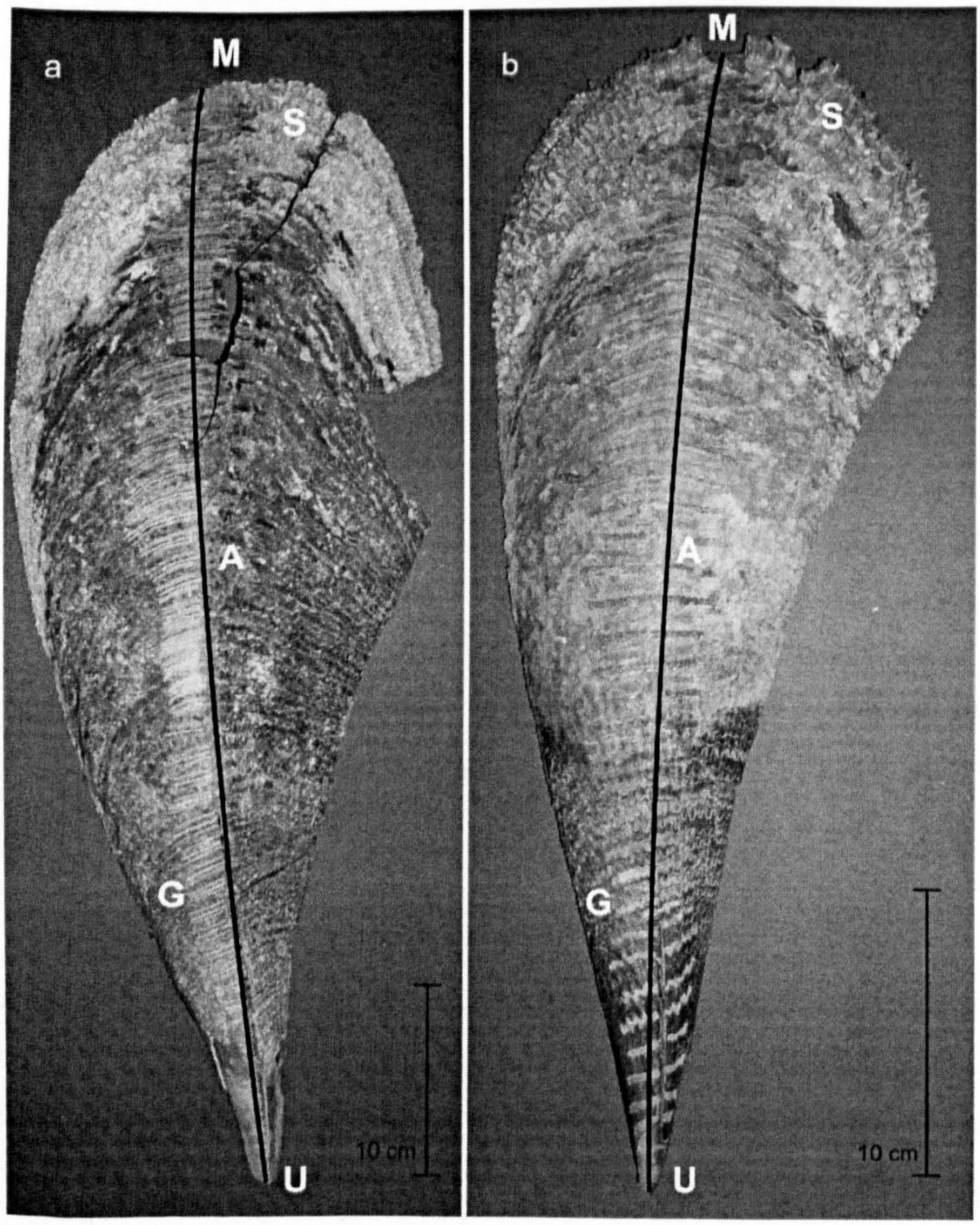

Figure 1 - 2 – The *Pinna nobilis* shells used in this study. Shell features: Shell Margin (M); Spines (S); Shell Main Growth Axis (A); Umbo (U); Sampling Grooves (G).

Figure 1 - 3 – The morphology of the shell of *Pecten maximus* (from Gosling, 2003).

Bivalves from the genus *Mytilus* (Figure 1-1) are attached surface dwellers and have a wide geographical distribution living in temperate water from the Northern and Southern Hemispheres, and occupy a wide range of habitats: from high inter-tidal to sub-tidal, from marine to estuarine waters, from rocky shores to firm sediments (Seed and Suchanek, 1992). Furthermore, *M. edulis* have the capacity to withstand large variations in salinity, temperature, dessication and oxygen content (Seed, 1976). *Mytilus edulis* can reach up to 15 cm, but normally grow to 5-8 cm with a life span of up to 18-24 years. *Mytilus* sp. also are commonly used throughout the world in environmental biomonitoring programs (e.g. for heavy metal pollution).

1.2.3 Growth and Metabolism in Bivalves

Physiological processes are thought to significantly influence the isotopic and element composition of biogenic carbonates (Urey et al., 1951; Lorens and Bender, 1977; McConnaughey, 1989a; Rosenberg and Hughes, 1991; de Villiers et al., 1995; Klein et al., 1996b; Spero and Lea, 1996; McConnaughey et al., 1997; Lea et al., 1999), and thus the growth and metabolic activity of each organism may interfere with the use of geochemical proxies from biogenic carbonates. In bivalves, growth represents the integration of physiological processes of energy acquisition and utilization, and it is dependent on the interaction of endogenous factors, such as size, age, genotype and physiological condition with several environmental factors, mainly food availability and temperature, but also population density, water flow, and pollution (Gosling, 2003). As such, growth rate and reproduction may differ between species, but also vary significantly between populations of the same species, between individuals of the same population, being modulated by seasonal and inter-annual variations of environmental conditions. In bivalves, an ontogenetic change occurs in which the focus of production switches from growth in young and small animals to reproduction in older and larger animals (Gosling, 2003). This change, associated with higher respiratory demands, is probably what causes the observed decrease in growth efficiency and absolute growth with size and age in bivalves.

Shell growth occurs throughout the life of the animal, but a clear ontogenetic decrease in growth rate can be observed in most species. Bivalves may produce growth marks, rings, lines, scales or stria during shell growth, all of which can be used to determine age (Lutz and Rhoads, 1980). The use of growth marks to record age in bivalves is dependent on their periodicity and cause and may not be present or discernable in all species. Annual growth marks are usually associated to seasonal changes in growth rates, but in some cases a spawning mark may also be observed. Marks such as rings or stria may be deposited at a higher periodicity related to tides, daily or lunar spring-neap tidal cycles. Other events such as storms, damage to the shell, handling, parasites and predation may leave their own marks in the shell and be indistinguishable from other growth marks. As can be seen, there is still a large debate concerning the periodicity of deposition of growth increments in different species, which may vary from annual to tidal, and are not present in all species (e.g.

mussels and oysters). Nevertheless, growth marks and growth increments are morphological identities and represent events that can be linked to physiological or environmental factors (Richardson, 2001).

Growth in bivalves is usually measured by changes in soft tissue dry weight or in a shell dimension. Soft tissue weight is seen as the best method as it reflects overall production, on the other hand it needs the sacrifice of the animals and more important it is modulated by seasonal energy storage and reproductive cycles. A shell dimension is usually used and a weight-length regression determined to estimate growth. Shell length, the distance between the anterior and posterior margins, is normally used, although the distance between the dorsal (hinge) and ventral margins, shell height, is also used (Gosling, 2003). The relationship between shell and somatic tissue growth varies in different bivalve species depending on the main energy source for reproduction, i.e. stored energy or external food (Bricelj and Shumway, 1991). In species where gametogenesis mainly depends on energy reserves, shell and somatic tissue growth may not follow the same pattern, with the later being more strongly influenced by the reproductive cycle than in species that meet most of the energy costs of reproduction from external food sources (Bricelj and Shumway, 1991). For instance, in *Mytilus edulis* shell and somatic tissue growth are not necessarily coupled (Hillbish, 1986). In the soft shell clam *Mya arenaria*, shell growth and somatic tissue growth are uncoupled, and the former reflects metabolic activity while the latter reflects the energy budget and storage regulated by reproduction (Lewis and Cerrato, 1997).

The most common method of assessing the energy balance is to determine the components of the following energy budget: $C = P + R + F + U$, where C is the energy input or food consumption and the energy losses includes energy used into shell and somatic tissue production P, respiratory heat loss R, faecal losses F and excretory products U (Bayne and Newell, 1983). Only when the energy balance is positive, i.e. the energy available for production after respiration and excretion have been subtracted from absorption $(C-F)-(R+U) > 0$ (Warren and Davis, 1967), may an animal allocate energy for growth or reproduction, otherwise energy reserves must be used. In mussels, the total metabolic cost of maintenance, including respiration, digestion, absorption, and cost of growth can reach 50% of the total energy intake

(Hawkins and Bayne, 1992). Shell production in *Mytilus* sp. may reach values of 20% of total production (Hawkins and Bayne, 1992). However, there are large uncertainties in estimating the cost of shell formation in bivalves due to methodological difficulties in measuring all the components of the total energy budget. Wilbur and Saleuddin (1983) in their review suggested a value of 1/4 to 1/3 of the total energy budget as the cost of shell growth, which is most likely an underestimation and there are large differences among species with different shell sizes, densities and structures.

Various methods exist to determine metabolic rate (also described as energy demand or turnover rate) in bivalves (De Zwaan and Mathieu, 1992), and in aerobic conditions the rate of oxygen consumption is an indirect measurement of metabolic rate, which can be obtained by converting the rate of oxygen consumption to energy demand (Bayne and Newell, 1983). In anoxic conditions, metabolic rate can be measured by biochemical methods or by direct calorimetry. Metabolic rate is known to be influenced by several variables (e.g. for a review see Bayne and Newell, 1983): temperature, body size, oxygen tension, food concentration, reproductive state, feeding, activity level and physiological condition. Of these, temperature, size and activity level are the most relevant ones (Bayne and Newell, 1983). The rate of metabolism varies with short term temperature variations, with an initial overshoot followed by a period of stabilization after minutes to hours. Many organisms show a longer term adaptation (or acclimation) to changed temperature conditions after days or weeks, adjusting the rate of oxygen consumption to levels similar to the ones that preceded the temperature change (Bayne and Newell, 1983). The scope for activity (the increase in oxygen consumption associated with activity) of *Mytilus edulis* can be 2 to 3 times resting, starved condition, and is mainly associated with feeding activity and indirect costs (posture, mucus productions, ingestion and digestion). In mussels there is evidence that metabolic efficiency decreases with increasing size and age (Gosling, 2003).

1.2.4 Shell Biomineralization

Shell Structure and Morphology

The bivalve shell serves several functions: it acts as a skeleton for muscle attachment, protection from predators, protection from environmental changes and in burrowing species for protection from sediments (Gosling, 2003). The main component of the shell is calcium carbonate ($CaCO_3$) at around 95-99.9 wt% with the remainder being an organic matrix made of macromolecules (Hare, 1963), forming a microlaminate composite of mineral and biopolymers exhibiting exceptional nanoscale regularity, and a strength ~ 3000 times greater than that of the crystals themselves (Currey, 1988).

Most mollusc shells have an outer organic layer, covering the outer surface of the shell, and an inner calcified layer. Bivalve shells possess two distinct crystal polymorphs of $CaCO_3$ with similar crystal structures, calcite and aragonite. Vaterite, a third polymorph, is usually absent (Wilbur and Saleuddin, 1983). Shells from the family Pinnacea and the genus *Pinna* are constituted by a dominant outer prismatic calcite layer with a thin aragonite nacreous inner layer (Watabe, 1988). The general shell structure of *Pecten maximus* consists of both outer and inner irregularly oriented foliated calcite layers (Taylor et al., 1969; Carter, 1990a), with some pectinid species also having a very thin aragonite prismatic pallial myostracum (Taylor et al., 1969). The inner layer of irregularly oriented foliated calcite structure appears to be a secondary feature, deposited late in the life of the animal on the inside of the shell between the umbo and midway along the growth axis. The general structural characteristics of *Mytilus edulis* bivalve shells are reported to be two primary calcium carbonate layers and an outer organic layer, the periostracum, which covers the outer surface of the shell. The outer shell layer is finely prismatic calcite with the inner layer a nacreous aragonite, these being separated by a thin pallial myostracum made up of irregular simple prismatic aragonite (Taylor et al., 1969; Carter, 1990b).

The Extra-Pallial Fluid: The Environment of Shell Deposition

The total shell formation system in molluscs comprises 4 compartments: 1) the external medium, 2) the haemolymph and body tissues, 3) the extra-pallial fluid (EPF) between the mantle and the inner shell surface, 4) the shell (Wilbur and Saleuddin, 1983). Shell formation can be described as two separate parts (Wilbur and

Saleuddin, 1983): 1) EPF formation - active and diffusive processes of intracellular and intercellular ion transport, synthesis and secretion of the EPF organic compounds that will build the organic matrix of the shell and modulate crystallization; 2) Crystallization - a series of physicochemical processes in which crystals of $CaCO_3$ are nucleated, oriented and grow in intimate association with the organic matrix and soluble proteins.

In bivalves, like in other molluscs, shell deposition occurs from the EPF, a liquid present in the space between the mantle epithelium and the calcifying inner shell surface, the extra-pallial space (EPS) (Crenshaw, 1972; Misogianes and Chasteen, 1979; Wilbur and Saleuddin, 1983; Checa, 2000). In bivalves, the muscular attachment of the mantle to the shell along the pallial line, an attachment of the mantle on the inner shell surface, further divides the shell-forming compartment (i.e. EPS) in two distinct zones. The marginal EPS, outside the pallial line, is associated with the highest rate of shell deposition and contributes to increases in the height and length of the shell and is where the outer and mid shell layers are deposited. The central (or inner) EPS, within the pallial line, is associated with both deposition (thickening) and redissolution of shell (Wheeler, 1992; Nair and Robinson, 1998), and is where deposition of the inner shell layer occurs. Usually, the periostracum seals the EPS (the marginal EPS to be precise) isolating it from both , the external (seawater) and internal (haemolymph) environments (Wilbur, 1976; Saleuddin and Petit, 1983; Falini et al., 1996). However, EPS isolation from seawater varies amongst bivalves. In scallops, like in oysters, shell deposition at the shell margin occurs from a periodically exposed EPS, while in *Mytilus edulis* it occurs from a continuously isolated one (Clark II, 1974; Carriker, 1992). In species with periodically exposed EPS, the margins of mantle lobes are frequently withdrawn into the mantle cavity exposing the crystals at the inner shell surface to seawater or mantle cavity fluid (Clark II, 1974; Carriker, 1992).

The element and/or isotopic composition of the EPF may thus differ from both seawater and the haemolymph. For instance, freshwater and marine bivalve have EPFs with different chemical compositions most likely due to a physiological control related to differences in the external medium (Wada and Fujinuki, 1974; Wilbur and Saleuddin, 1983). Bivalves are expected to be able to biochemically regulate the

activity of Ca^{2+} and other ions from the EPF, solution from which mineralization takes place. For instance, the majority of Ca in the EPF is not in free ionic form but bound to organic molecules secreted by the mantle (Crenshaw, 1972; Misogianes and Chasteen, 1979; Nair and Robinson, 1998).

Element Transport to the Extra-Pallial Fluid

In bivalves, any surface of the body, not protected by the shell, may participate in the interaction between the environment and the animal (Simkiss and Mason, 1983; Wilbur and Saleuddin, 1983). The gills, the foot, the mantle and the alimentary tract have all been implicated as sites of metal uptake, with the gills seen as the major uptake site (Simkiss and Mason, 1983; Wilbur and Saleuddin, 1983). Elements in the EPF may be derived from both the external medium and the animal tissues, reaching the EPF after diffusion (i.e. intercellular) or active (i.e. intracellular) transport across the mantle (Crenshaw, 1972; Wilbur and Saleuddin, 1983; Wheeler, 1992). Direct input from the external medium can also occur in the event of rupture of the mantle-shell connection at the shell edge. Furthermore, a mechanism for the transport of ions across the periostracum through the presence of pores was proposed for oysters and most bivalve groups that attach to the substratum (Harper, 1991), and based on the similarity of the periostracum (i.e. its small thickness, <1 μm) extended to the entire pteriomorph group, which includes the three species studied (Hickson et al., 1999). Active transport of ions to the EPF was proposed to be mediated by an enzyme responsible for a Ca^{2+}/H^{+} exchange across the mantle epithelial cells (Wilbur and Saleuddin, 1983). The enzyme Ca^{2+}–ATPase transports Ca^{2+} to the EPF while removing $2H^{+}$ and has been proposed to be involved Ca^{2+} and divalent ion transport across epithelial cells of corals (McConnaughey, 1989c; Cohen and McConnaughey, 2003) and has been also observed in calcifying algae (McConnaughey and Falk, 1996). In bivalves, precipitation of the shell occurs under physiologically controlled concentrations of Ca^{2+} and HCO_3^{-} (Wada and Fujinuki, 1976), and the enzyme carbonic anhydrase, which catalyses the reaction $H_2O + CO_2 \leftrightarrow H_2CO_3 \leftrightarrow H^{+} + HCO_3^{-}$, is involved in the precipitation of $CaCO_3$ (e.g. Crenshaw, 1980).

Recently, Carré et al., (2006) argued that the two proposed pathways for Ca^{2+} transport through the calcifying mantle, a diffusive inter-cellular pathway and an

active intra-cellular pathway based on Ca^{2+} -ATPase, cannot support the Ca^{2+} flux necessary for biomineralization. According to these authors most Ca^{2+} transport must be intra-cellular to avoid ionic deregulation of the internal medium, but Ca^{2+}-ATPase cannot account for the Ca^{2+} flux necessary to sustain mineralization. Carré et al., (2006) thus propose an alternative intra-cellular pathway based on ionic calcium channels, which are widespread in biological tissues, are ion selective and can support very high ionic fluxes. In such a model, calcification rates change the electrochemical potential driving ions through the channel and ultimately the ion selectivity of calcium channels leading to variable transport of divalent ions to the EPF.

Shell Deposition and Growth

The EPF was found to contain a complex mixture of organic compounds, which are involved in the organic matrix-mediated biomineralization of the shell (Crenshaw, 1972; Wada and Fujinuki, 1976; Misogianes and Chasteen, 1979; Wilbur and Saleuddin, 1983; Weiner and Dove, 2003; Addadi et al., 2006). The organic compounds are secreted by the cells of the outer mantle epithelium (Wheeler, 1975; Wilbur and Saleuddin, 1983) and are constituted by similar macromolecules to the materials found in the shell matrix, mainly by proteins, glycoproteins, amino acids and carbohydrates (Misogianes and Chasteen, 1979). As in the plasma, complexation of elements with organic molecules is significant in the EPF and influences the activity of different ions. For instance, of the total Ca in the plasma, the majority (up to 85%) is bound to small chelates, insoluble carbohydrates and soluble macromolecular (Misogianes and Chasteen, 1979; Nair and Robinson, 1998). Bound Ca may serve several functions: represent dissolution of deposited shell, be a preliminary step in shell formation or a reservoir of Ca^{2+} ions for shell formation (Crenshaw, 1972). In *Mytilus edulis*, 56% of the protein content of the EPF was found to be a single histidine rich glycoprotein that bounded Ca^{2+} and was proposed to be a precursor or a building block of the soluble organic matrix of the shell (Hattan et al., 2001).

The compositional and conformational features of the organic matrix are seen as having a significant influence on the structural properties of the shell crystal (Kaplan,

1998). The organic matrix consists of a structural framework of hydrophobic macromolecules that are used to partition the extra-cellular space and provide mechanical support, while acidic macromolecules interact with the ions of the surrounding solution, determine its chemical activity, lower the activation energy for inorganic nucleation, and provide a template structure that direct the resulting mineralization process (for reviews see Weiner and Dove, 2003; Addadi et al., 2006). The composition of the organic component of bivalve shells, varies not only among different taxa (Lowenstam and Weiner, 1989), but also within different shell layers (outer vs inner layers and calcitic vs aragonitic layers) and microstructural layers of the same species (Hare, 1963; Hare and Abelson, 1965; Goodfriend, 1992).

Mount et al., (2004) have recently observed the intra-cellular formation of crystals in the oyster *Crassostrea virginica,* and thus suggested that intra-cellular crystal nucleation may at least complement the organic matrix-mediated biomineralization in bivalves. Furthermore, the transfer of ions and organic molecules by direct contact between the mantle epithelium and the mineralizing matrix has also been suggested, thus reducing the role of the EPF in shell mineralization (Simkiss and Wilbur, 1989; Addadi et al., 2006).

Calcite vs Aragonite

The mineralogy and structure of the shell carbonate is important since calcite and aragonite although crystal polymorphs of calcium carbonate, have different mineral-water fractionation factors (Romanek et al., 1992) and partition coefficients (Morse and Bender, 1990). Calcite (trigonal structure) is thermodynamically more stable than aragonite (orthogonal structure) at ambient temperatures and pressures, and in spite of possessing very similar crystal structures, the major difference between the two polymorphs is in the organization and orientation of the carbonate molecules (Lipmann, 1973).

Control of which of the two $CaCO_3$ polymorphs is formed by marine calcareous organisms has been suggested to depend on environmental factors, such as temperature and salinity (Taylor and Reid, 1990; Cohen and Branch, 1992), but also concentration of ions, mainly Mg^{2+}. The presence of doubly charged ions, especially

Mg^{2+}, in $CaCO_3$ solutions, as well as high temperature, favours the formation of aragonite (Kitano et al., 1976), possibly since the incorporation of Mg in the calcite crystal lattice increases its solubility relative to that of pure calcite (Berner, 1975b). However, several studies have shown that bivalves possess a tight control on which polymorph is deposited. Belcher et al., (1996) observed that soluble proteins determined the carbonate polymorph during crystal growth, and the formation of each of the two crystal polymorphs was accompanied by the synthesis of specific polyanionic proteins. Furthermore, macromolecules from aragonite layers induced *in vitro* formation of aragonite, while macromolecules from calcite layers induced formation of calcite (Falini et al., 1996; Feng et al., 2000). Therefore, differential expression of proteins allows the organism to control and to induce phase changes in the shell crystal (He and Mai, 2001).

Calcite is softer than aragonite, but secretion of calcite by bivalves may present some advantages. In shells where calcite and aragonite coexist there is always a sharp boundary without microstructural intergradation (Taylor et al., 1969; Taylor et al., 1973). Calcite tends to break along well defined cleavage planes and in conjunction with aragonite layers contribute to avoid propagation of fractures along the shell (Carter, 1980). Secretion of calcite may also contribute to minimize shell density. A mixture of $CaCO_3$ polymorphs is usually never found at the same location, but many organisms are capable of precipitating both polymorphs at adjacent locations and some present an ontogenic change in the polymorph used in specific shell structures (He and Mai, 2001). In bivalves, the occurrence of calcite shell layers is rare and occurs only in Pteriomorpha (except Arcoida) and Chamacea of Heterodonta (Kobayashi, 1981). The distribution of calcite in Mytilacea occurs as fibrous prismatic at the outer calcified layer, in Pinnacea it occurs as prismatic at the outer calcified layer and in Pectinacea it occurs as foliated in the inner and outer calcified layers (Kobayashi, 1981).

1.3 Stable Isotope Geochemical Proxies

1.3.1 Isotopes and Isotope Fractionation

Isotopes are atoms of the same element that contain the same number of protons but different number of neutrons. In stable isotopes, i.e. non-radioactive isotopes, there is no decay to produce other isotopes of the same or other element. The basis behind the use of stable isotopes in geochemical studies of Earth systems is the difference in atomic mass between heavier and lighter isotopes (Hoefs, 1997). Such mass difference may cause isotopes to react differently during chemical and physical reactions. Chemically, the isotopes are equivalent and form the same type of chemical bonds, but there are slight physicochemical differences between the isotopes that cause them to have slightly different bond energies. The vibrational frequency of an atom is inversely proportional to the square root of the mass, meaning that the lighter isotopes will have higher vibrational frequencies that the heavier ones (Hoefs, 1997). This causes the chemical bonds formed by lighter isotopes to be weaker that the ones formed by the heavier isotopes, making the lighter isotopes more prone to react than the heavier isotopes.

The isotope species of an element will react at different rates and to different extents, with the light isotope usually reacting faster and to a greater extent. This will cause the reactants and the products of a chemical reaction to have different abundances of the heavy and light isotope. This is termed isotopic fractionation and the degree to which the products of a reaction become enriched or depleted in one of the isotopes can be expressed as a fractionation factor, α, where R is the isotopic ratio of the heavier isotope over the lighter isotope (e.g. Hoefs, 1997):

$$\alpha = R_{products}/R_{reactants} \quad (1)$$

Fractionation factors decrease with increasing reaction temperature and at high enough temperatures α will tend to 1, as the differences due to dissimilar isotopic composition become irrelevant in comparison with the vibrational energy of a given molecule, i.e. the mass differences in the products of a reaction become bigger at lower temperatures and smaller at higher temperatures (Hoefs, 1997). Carbon and oxygen display large chemical fractionations, due to the large relative mass differences between each isotope.

Two types of fractionation occur, thermodynamic (or equilibrium) and kinetic (e.g. Swart, 1983; McConnaughey, 1989a; McConnaughey, 2003). Thermodynamic or equilibrium fractionation occurs, according to a equilibrium constant, in chemical reactions that reach equilibrium, e.g. in materials that are in equilibrium but have different molecular structures or in reactions involving phase changes. Thermodynamic fractionations are temperature and pressure dependent. The isotope species will redistribute themselves within the system to obtain the minimum free energy. For example, in the reaction:

$$H_2{}^{18}O\ (g) + H_2{}^{16}O\ (l) \leftrightarrow H_2{}^{16}O\ (g) + H_2{}^{18}O\ (l) \qquad (2)$$

The products with the lighter isotope require less energy to be maintained in the gas phase and are therefore favoured. The heavier isotope "prefers" the phase with the lowest heat capacity:

Gas	↔	Liquid	↔	Solid
$+^{16}O$	←		→	$+^{18}O$
$+^{12}C$	←		→	$+^{13}C$

Kinetic fractionations occur when the rate of a given physical or chemical processes differs for different isotopes, usually during fast unidirectional reactions such as diffusion or phase changes. For instance, when $CaCO_3$ precipitation is fast enough for HCO_3^- and/or CO_3^{2-} to precipitate before isotopic equilibration with H_2O (McConnaughey, 1989a; McConnaughey, 1989c). Since both C and O are in the same molecule, kinetic effects will influence both elements and cause the carbon and oxygen isotopic composition of $CaCO_3$ to be correlated (e.g. McConnaughey, 1989c; McConnaughey et al., 1997; McConnaughey, 2003). In kinetic fractionations the light element reacts faster than the heavier one, causing the products to be enriched in the former relative to the reactants. Fractionation arises from differences in the rates at which the isotopes pass from the reactants to the products, rates that are usually concentration dependent. Therefore, kinetic fractionations are rate dependent, are usually concentration dependent, depend on the isotopic composition of the reactants and depend on the degree to which the process or reaction has occurred, but are usually temperature independent. Kinetic fractionation may also occur in chemical processes that do not reach equilibrium and it is common in biologically mediated processes, which are often enzyme-catalyzed and occur in a series of step reactions that tend to make them behave as unidirectional (McConnaughey, 2003).

The relative abundance of stable isotopes of an element is usually expressed as a ratio, with the most abundant isotope, usually the lighter, on the denominator. The isotope ratio of a sample is always measured relative to a standard, and the data is expressed in per mil difference to a well defined reference standard, i.e. the Del notation (McKinney et al., 1950).

$$\delta_{sample} = [Ratio_{sample} - Ratio_{standard} / Ratio_{standard}] \times 1000 \text{ (in ‰)} \quad (3)$$

and

$$\alpha = (\delta_{products}+1000)/(\delta_{reactant}+1000) \text{ (in ‰)} \quad (4)$$

The standard for oxygen isotopes in water and most mineral phases is the Vienna Standard Mean Ocean Water (VSMOW), while the standard for carbon isotopes, but also for oxygen isotopes in carbonates, is the Vienna PeeDee Belemnite (VPDB). The conversion between the two standards in water is given by the equation:

$$\delta^{18}O_{VPDB} = \delta^{18}O_{VSMOW} - 0.27‰ \text{ (Hut, 1987)} \quad (5)$$

while for carbonates the conversion is given by the equation:

$$\delta^{18}O_{VPDB} = 1.03091 * \delta^{18}O_{VSMOW} + 30.91 \text{ (Coplen et al., 1983)} \quad (6)$$

Table 1 - 1 – Relative abundance of some stable Isotopes (*Radioactive). From (Gill, 1997).

Atomic Number	Symbol	Analysed as	Mass Number	Abundance	Reference Standard
6	C	CO_2	12	98.888	
			13	1.1112	VPDB
			14^*	10^{-10}	
7	N	N_2	14	99.634	Air
			15	0.366	
8	O	$CO_2(O_2)$	16	99.759	VSMOW
			17	0.037	Or
			18	0.204	VPDB

The analysis of stable oxygen and carbon isotopes have played a major role in palaoceanography since the work of Emiliani (1955), following the previous work of Urey (1947), McCrea (1950) and Epstein et al., (1951; 1953), which interpreted the isotopic record of foraminifera shells from deep-sea cores as climate/temperature cycles. Shackleton and Opdyke (1973) by correlating the oxygen isotope stratigraphy with the magnetic stratigraphy, established the use $\delta^{18}O$ as a dating tool as well as a tool to reconstruct global ice volume (Shackleton, 1967) and temperature fluctuations

(Emiliani, 1955). Furthermore, Shackleton (1977) demonstrated the potential of carbonate $\delta^{13}C$ for studies on water mass movement and palaeoproductivity.

1.3.2 Oxygen Isotopes in Carbonates

The use of oxygen isotope ratios in carbonate material as a temperature indicator is based on the temperature dependent fractionation that occurs during precipitation (Urey, 1947). Urey (1947) suggested that variations in the temperature of seawater would lead to measurable $^{18}O/^{16}O$ ratio of $CaCO_3$ precipitated from that same seawater. McCrea (1950) established a palaeotemperature curve by carrying experiments with inorganically precipitated $CaCO_3$ and showing a clear temperature dependent isotope fractionation of the $^{18}O/^{16}O$ ratio between $CaCO_3$ and water. This is translated in the isotopic exchange reaction:

$$CaC^{16}O^{16}O^{16}O(s) + H_2{}^{18}O(l) \leftrightarrow CaC^{18}O^{16}O^{16}O(s) + H_2{}^{16}O(l) \quad (7)$$

At equilibrium, this isotope exchange reaction causes the carbonates to be significantly enriched in ^{18}O relative to the water, at 25 °C by 28.3‰ (VSMOW). In addition, shell mineralogy is also important for the $\delta^{18}O$ of carbonate material, and calcite is depleted relative to aragonite by about 0.6 to 1.0 ‰ (Tarutani et al., 1969; Grossman and Ku, 1986; Bohm et al., 2000). However, the $\delta^{18}O$ of carbonate material is dependent not only on temperature but also on the $\delta^{18}O$ of the seawater ($\delta^{18}O_{water}$) from which it precipitated (McCrea, 1950; Epstein et al., 1953; Epstein and Mayeda, 1953b; Emiliani, 1955). Roughly, a change of 0.25 ‰ of $\delta^{18}O_{water}$ or 1 in salinity at mid-latitudes corresponds to the equivalent of 1.1°C. The $\delta^{18}O_{water}$ is determined by two major factors (Garlick, 1974; Broecker and Peng, 1982): 1) the mean ocean $\delta^{18}O_{water}$, which in turn depends on the volume of continental ice (^{16}O is preferentially sequestered in ice leaving seawater enriched in ^{18}O) on time scales of 10^4 to 10^5 yrs ($V_{ice}*\delta^{18}O_{ice}+V_{ocean}*\delta^{18}O_{ocean}=V_{total}*\delta^{18}O_{total}$), and on exchange of water between the ocean and the crust on time scales of 10^7 to 10^8 yrs; 2) the local/regional precipitation-evaporation balance (E-P), this is often called the salinity effect since both tend to co-vary with E-P. When evaporation takes place, the ^{16}O will be favoured in the gas phase, causing the liquid phase to be enriched in ^{18}O and the gas phase in ^{16}O, the reverse occurs during precipitation (Dansgaard, 1964). However, the salinity-$\delta^{18}O_{water}$ relationship is variable in the ocean due to variable

$\delta^{18}O$ values of precipitation and river run-off freshwaters (Epstein and Mayeda, 1953b), and due to the Raleigh distillation process is lighter at higher altitudes (Broecker and Peng, 1982; Bigg and Rohling, 2000). The extent to which evaporation and condensation reactions occur will affect the $\delta^{18}O$ of both the reactant and products of such reactions. Such a process, in which the isotopic composition of the product varies with the extent of th reaction, is called a Raleigh distillation. The influence of the different factors that control the variation of the salinity-$\delta^{18}O_{water}$ relationship (i.e. the source of evaporation and distance to that source, precipitation of water with different $\delta^{18}O$) does not allow salinity to be faithfully used as a proxy for $\delta^{18}O_{water}$ and vice versa. However, in certain oceanic areas, especially away from coastal areas and enclosed basins, this relationship is linear indicating a simple dilution effect (e.g. Ingram et al., 1996a; Mueller-Lupp et al., 2003). In coastal and estuarine waters the influence of freshwaters with very different $\delta^{18}O$, as well as environments with high evaporation, may deviate the salinity-$\delta^{18}O_{water}$ relationship. Moreover, it is in coastal and estuarine areas where bivalves are most abundant, but also where the presence of past and present human populations is most strong and where most of the archaeological middens occur.

Palaeotemperature equations

Several studies have developed empirical palaeotemperature equations by determining the $\delta^{18}O$ composition of biogenic carbonates deposited under known temperature and $\delta^{18}Ow$. Epstein et al. (1953) developed an equation for calcitic bivalves, which was later modified by Anderson and Arthur (1983):

$$T\,(°C) = 16 - 4.14*(\delta^{18}O_{calcite} - \delta^{18}O_{water}) + 0.13*(\delta^{18}O_{calcite} - \delta^{18}O_{water})^2 \quad (8)$$

where $\delta^{18}O_{calcite}$is the $\delta^{18}O$ value of CO_2 (VPDB) produced from the reaction of the carbonate with phosphoric acid at 25°C and $\delta^{18}O_{water}$ is the value of (VSMOW) equilibrated with water at 25°C. Grossman and Ku (1986) determined an equation for aragonitic molluscs:

$$T\,(°C) = 19.7 - 4.34 * (\delta^{18}O_{calcite} - \delta^{18}O_{water}) \quad (9)$$

Bivalves precipitate calcite in or near thermodynamic equilibrium (Epstein et al., 1951; Epstein et al., 1953; O'Neil et al., 1969; Wefer and Berger, 1991; Hickson et al., 1999; Chauvaud et al., 2005; Wanamaker et al., 2006). Chauvaud et al., (2005)

and Wannamaker et al., (2006, 2007) have shown *Pecten maximus* and *Mytilus edulis*, respectively, to precipitate calcite close to the isotope equilibrium predicted by the equation obtained for inorganic carbonate by Kim and O'Neil (1997):

$$1000\ln\alpha = 18.03 * 1000/ T(K)-32.42 \quad (10)$$

where α is the fractionation factor and T is in Kelvin. For *P. maximus* (Chauvaud et al., 2005):

$$T\ (°C) = 14.84 - 3.75\ (\delta^{18}O_{calcite} - \delta^{18}O_{water}) \quad (11)$$

while for *M. edulis* (Wanamaker et al., 2007):

$$T\ (°C) = 16.28 - 4.57*(\delta^{18}O_{calcite} - \delta^{18}O_{water}) + 0.06*(\delta^{18}O_{calcite} - \delta^{18}O_{water})^2 \quad (12)$$

There are many palaeotemperature equations in the literature for carbonates produced by different organisms and the choice of equation has varied in different studies (e.g. see Bemis et al., 1998).

1.3.3 Carbon Isotopes

The use of biogenic carbonate stable-carbon isotope composition ($\delta^{13}C_{shell}$) as a proxy for the stable-carbon isotope composition of seawater dissolved inorganic carbon ($\delta^{13}C_{DIC}$) is based on the assumption that in such carbonates, carbon is directly derived from seawater DIC (Mook and Vogel, 1968; Killingley and Berger, 1979; Arthur et al., 1983). The stable carbon isotope composition of biogenic carbonates ($\delta^{13}C_{shell}$) thus has the potential to reflect processes that are related and/or determine seawater $\delta^{13}C_{DIC}$, i.e. salinity, atmospheric CO_2 exchanges, productivity, respiration and consequently nutrient concentration. If one assumes DIC to be mainly composed of HCO_3^-, then to calculate equilibrium values from seawater $\delta^{13}C_{DIC}$, the equilibrium fractionation for experimentally precipitated carbonate relative to HCO_3^-, is simply added to the value of $\delta^{13}C_{DIC}$, i.e. +1.0 ± 0.2 ‰ for calcite and +2.7 ± 0.6 ‰ for aragonite (Romanek et al., 1992).

Grossman (1987) summarised that carbon isotope ratios in almost all biogenic carbonates are to some extent influenced by vital effects, which almost invariably cause depletion relative to equilibrium. There is growing evidence that carbon in marine biogenic carbonates is derived from two sources of carbon, seawater DIC and metabolic DIC that derives from respiratory CO_2 (Keith and Weber, 1965; Weber and Woodhead, 1970; Vinot-Bertouille and Duplessy, 1973; Dillaman and Ford,

1982; Swart, 1983; Tanaka et al., 1986; Spero and Deniro, 1987; McConnaughey et al., 1997; Furla et al., 2000; Kennedy et al., 2001; Owen et al., 2002b; Lorrain et al., 2004; Gillikin et al., 2006b). The magnitude of the vital effect seems to be proportional to the amount of metabolic CO_2 within the organisms internal CO_2 pool (Erez, 1978), which, in turn, should be a function of the organisms ability for gas-exchange with ambient water. Like animal tissues, metabolic CO_2 is highly depleted in ^{13}C, with a $\delta^{13}C$ value from -10 to -25 ‰, relative to seawater DIC that has a $\delta^{13}C$ usually close to 1 ‰ (Craig, 1953; Tanaka et al., 1986; McConnaughey et al., 1997; Lorrain et al., 2002; Lorrain et al., 2004; Gillikin et al., 2006b). Therefore, the larger the proportion of metabolic carbon incorporated in the shell carbonate the lower the shell $\delta^{13}C$ will be, thus masking the seawater $\delta^{13}C_{DIC}$ signal. The proportion of carbon with a metabolic origin in biogenic carbonates is still a subject of some dispute, with suggestions of values as high as 85% (Tanaka et al., 1986), although values of 10 to 20% are now thought to be better estimates (Klein et al., 1996b; McConnaughey et al., 1997; Hickson et al., 1999; Lorrain et al., 2002; Lorrain et al., 2004; Gillikin et al., 2006b; Gillikin et al., 2007). Furthermore, in bivalves, a strong ontogenetic decrease in $\delta^{13}C_{shell}$, and thus an increase in the proportion of metabolic carbon incorporated in the shell carbonate, has been observed by several authors (Krantz et al., 1987; Kennedy et al., 2001; Keller et al., 2002; Elliot et al., 2003; Lorrain et al., 2004), although in some species such decrease of $\delta^{13}C_{shell}$ with age was not observed (Buick and Ivany, 2004; Gillikin et al., 2005c).

The bivalve shell $\delta^{13}C$ signal can thus be seen as a result of the seawater $\delta\ ^{13}C_{DIC}$ signal (varying seasonally and annually), with a variable metabolic signal of up to 2 ‰ (McConnaughey et al., 1997) super-imposed on it. Moreover, the carbon isotope composition of biogenic carbonates has been shown to suffer kinetic, carbonate ion concentration, and metabolic effects. Thus, the use of biogenic carbonate $\delta\ ^{13}C$ as a tracer of palaeo-water $\delta^{13}C_{DIC}$ is far from being straight forward and caution must be employed.

1.3.4 Isotope Vital effects

Biogenic carbonates may deviate from predicted isotope equilibrium and the term "vital effects" has been used to describe the processes responsible for such

disequilibria (Urey et al., 1951): kinetic effects (Swart, 1983; McConnaughey, 1989c; Spero and Lea, 1996; Bijma et al., 1998; Owen et al., 2002a) or carbonate ion effects (Turner, 1982; Romanek et al., 1992; Spero et al., 1997; Zeebe, 1999a; Adkins et al., 2003; McConnaughey, 2003; Rollion-Bard et al., 2003).

Kinetic effects arise from compartmentalization of calcification and from rate dependent reactions such as enzyme catalyzed or diffusion mediated processes, e.g. when CO_2 diffuses across membranes in which molecules bearing the lighter oxygen isotope react preferentially. If the ^{18}O depleted HCO_3^- and/or CO_3^{2-} thus formed, precipitate to form shell $CaCO_3$ before equilibration with H_2O, such isotopic disequilibrium will be expressed in the shell carbonate. Kinetic effects originate from slower hydration and hydroxylation of CO_2 of any origin, not necessarily respired, by molecules bearing the heavier isotopes ^{18}O and ^{13}C (McConnaughey, 1989b). Kinetic effects will act on both O and C isotopes as both are on the same molecule, lowering the predicted $\delta^{18}O$ and $\delta^{13}C$ of carbonates, and thus cause a correlation between the two (e.g. McConnaughey, 1989c; McConnaughey et al., 1997; McConnaughey, 2003).

McCrea (1950) observed that the $\delta^{18}O$ of inorganically precipitated carbonates varied with pH, which was later suggested to result from equilibration with the different carbonate species, each one with their own fractionation factor with water (Usdowski et al., 1991; Usdowski and Hoefs, 1993). The $\delta^{18}O_{VSMOW}$ of the carbonate species at equilibrium with H_2O of 0 ‰ at 19°C (and 25°C for CO_2, see Rollion-Bard et al., 2003) is: 41.2 ‰ for CO_2 (Kim and O'Neil, 1997), 34.3 ‰ for HCO_3^- (Zeebe and Wolf-Gladrow, 2001), 18.4 ‰ for CO_3^{2-} (Usdowski et al., 1991) and -41.1 ‰ for OH^- (McCrea, 1950). Since the concentration of HCO_3^- and CO_3^{2-} will change with increasing pH, the former decreasing and latter increasing, and in addition HCO_3^- is enriched in ^{18}O relative to CO_3^{2-}, the $\delta^{18}O$ of DIC decreases with increasing pH. If shell $CaCO_3$ is formed from a mixture of carbonate species in proportion to their relative contribution to DIC, then the $\delta^{18}O$ of $CaCO_3$ (and $\delta^{13}C$) will also decrease with increasing pH (Spero et al., 1997; Zeebe, 1999b; Adkins et al., 2003). As no kinetic effects are involved in such reactions, these are equilibrium reactions. However, Rollion-Bard et al., (2003) observed in deep-sea corals a large deviation of

$\delta^{18}O$ from equilibrium hydroxylation that could not be attributed only to the carbonate ion effect. These authors suggested that pH will change the proportion of HCO_3^- derived from hydration and hydroxylation. Since hydroxylation takes considerably more time to reach equilibrium than hydration (Johnson, 1982), at higher pH carbonate $\delta^{18}O$ would be expected to be lower as more HCO_3^- is derived from hydroxylation. Nevertheless, such a model is controversial and some authors suggest that the effects observed by Rollion-Bard et al., (2003) can be explained by kinetic effects alone (Cohen and McConnaughey, 2003; McConnaughey, 2003).

Furthermore, neither the kinetic or carbonate ion effects, as understood in foraminifera and corals, appear to be applicable to bivalve $\delta^{18}O_{calcite}$. Bivalves precipitate their calcite in or close to oxygen isotopic equilibrium (Wefer and Berger, 1991; Chauvaud et al., 2005; Wanamaker et al., 2006; Wanamaker et al., 2007), shell $\delta^{18}O_{calcite}$ and $\delta^{13}C_{calcite}$ are usually not significantly correlated (Owen et al., 2002b; Elliot et al., 2003), and the EPF pH is known to vary significantly (Wada and Fujinuki, 1976; Crenshaw, 1980). In addition, the presence of carbonic anhydrase in the shell matrix (Miyamoto et al., 1996) or of "carbonic anhydrase" compounds in the organic matrix (e.g. see Mann, 2001), will reduce the occurrence of kinetic effects by catalyzing the hydration of CO_2 (Weiner and Dove, 2003). Moreover, if a significant amount of the carbonate species in the EPF are derived directly from seawater and are equilibrated with it.

1.4 Elemental Geochemical Proxies of Carbonates

1.4.1 Principles of Elemental Substitution in Calcium Carbonates

Natural carbonates contain a variety of co-precipitated ions other that Ca^{2+}, which reflect their mode and environment of formation. The incorporation of trace elements into carbonates has been the subject of research in a wide variety of disciplines and the knowledge of the environmental factors that control carbonate elemental composition is extremely useful in performing reconstructions of

palaeoenvironments and in monitoring present ones, be it temperature, salinity, nutrient concentration, productivity, pH, pCO_2, metal concentrations, etc.

The use of elemental/Ca ratios as indicators of environmental conditions at the time of carbonate precipitation arises from the fact that divalent cations, which have an ionic radius similar to Ca^{2+} (i.e. Mg^{2+}, Sr^{2+}, Ba^{2+} and to a lesser extent Cu^{2+}, Mn^{2+} and Pb^{2+}), are able to substitute for Ca^{2+} ions in the carbonate lattice (Speer, 1983). A solid solution can occur when ions of one element substitute for ions of another element in a lattice, forming a single crystalline phase. Such substitution is strongly influenced by the fact that the different elements, which substitute for Ca^{2+} in the $CaCO_3$ crystal lattices (e.g. Mg^{2+}, Sr^{2+}, Mn^{2+}, Ba^{2+} and Pb^{2+}), are chemically different from Ca^{2+} (e.g. ionic radius, mass, etc). Therefore, the incorporation of divalent cations into $CaCO_3$ crystal lattices may depend on several factors, apart from thermodynamic or kinetic considerations. The more similar the substituting ion is to Ca^{2+} the closer to ideal mixing solid solution the resulting crystal will be (Morse and Bender, 1990). Ions that have ionic radii larger than Ca^{2+} (e.g. Sr^{2+}, Pb^{2+} and Ba^{2+}) generally substitute for Ca^{2+} in the orthorhombic aragonite lattice, rather than in the rhombohedral structure of calcite, while the calcite lattice can accommodate more easily divalent metal ions that have smaller ionic radii than Ca^{2+} (e.g. Mg^{2+}, Cu^{2+}, Mn^{2+} and Zn^{2+}) (Tesoriero and Pankow, 1996). Low partition coefficients (see below) may reflect the incapacity of the calcite lattice to accommodate large divalent ions, such as Ba^{2+} ($r = 1.49$ Å) and Sr^{2+} ($r = 1.32$ Å) in Ca^{2+} ($r = 1.14$ Å) sites without significant structural deformation (Onuma et al., 1979), and non-lattice substitution may become the preferred substitution mechanism (Pingitore, 1986).

The perception that the elemental composition of biogenic carbonates, i.e. Mg and Sr, was temperature dependent occurred simultaneously and in parallel to the use of stable isotopes in geosciences (Chave, 1954). Mg and Sr form the most important solid solutions in the $CaCO_3$ series, Mg with calcite while the larger ionic radius of Sr^{2+} leads it to form a solid solution with aragonite (Speer, 1983). The main interest in the use of elemental composition of biogenic carbonates as proxies of palaeotemperature lies in the independence from salinity, since the ratios of some elements (i.e. Mg/Ca and Sr/Ca) are not expected to vary with salinity (Broecker and Peng, 1982; Dodd and Crisp, 1982). The combination of elemental and isotope

proxies provides the ability to simultaneously estimate both temperature and $\delta^{18}O_{water}$, i.e. of factors related to it such as ice volume and salinity. The use of Mg/Ca and Sr/Ca ratios in biogenic carbonates, especially in foraminifera and corals, have gone through major advances in the last 10 to 15 years and thus appear to be the so long-sought source of oxygen isotope and salinity independent temperature information (Weber, 1973; Rosenberg, 1980; Beck et al., 1992; Nurnberg et al., 1996a; Lea et al., 1999; Elderfield and Ganssen, 2000; Lea et al., 2000; Rosenheim et al., 2004).

Partition coefficients

Studies on inorganic carbonates have focused on the measurement of partition coefficients that relate the composition of the carbonate to the solution from which it precipitates, as well as on the factors that influence elemental partition coefficients, such as temperature, crystal and solution composition, precipitation rate, mineralogy, and surface processes (e.g. sector zoning). Morse and Bender (1990) and Rimstidt et al., (1998) provide good reviews on the experimental determination of partition coefficients at or near room temperature. Studies on biogenic carbonates have taken a more empirical and practical approach focusing on the relationships between elemental carbonate content and environmental variable(s) that determine it or are in some way related to it. Partitions coefficients are a way of describing the partition of an element between a solution and a solid, where D_E is the partition coefficient of the element E:

$$D_E = (E/Ca)_{solid} / (E/Ca)_{solution} \quad (13)$$

It must be noted that partition coefficients are not equivalent to stoichiometric constants and can only be related to thermodynamic equilibrium constant by solid (f_i) and liquid (γ_i) activity coefficients if true equilibrium is attained (e.g. Morse and Bender, 1990). If the molar ratios of E and Ca in the solid phase and in the ECO_3 mineral to calcite are the same, D is related to K as:

$$D = K [(\gamma_{E2+} / \gamma_{Ca2+}) / (f_{ECO3} / f_{CaCO3})] \quad (14)$$

Partition coefficients reflect phenomenological measurements of concentrations in the respective phases under a given set of conditions, and several factors (e.g. reaction rate), apart from the obviously relevant thermodynamically variables

(pressure, temperature and composition) may exert significant influence on *D* (Morse and Bender, 1990). Furthermore, *D* is dependent on solution phase activity coefficients and in order to apply them to another solution there is the need to correct for changes in such coefficients. In bivalves, the shell is precipitated from the EPF rather than directly from seawater, which may have a different chemical composition relative to seawater (Crenshaw, 1972; Wada and Fujinuki, 1976; Misogianes and Chasteen, 1979).

Incorporation processes

The incorporation of ions from solution in to carbonate crystals may occur from surface-solution ion exchange, i.e. sorption. Ions can be sorbed (i.e. taken out of solution and attached to a foreign surface) by true adsorption, by absorption or diffusion into the solid, by surface precipitation (to form a single, distinct adherent phase) or by co-precipitation (to form an adherent precipitate which might be a solid-solution incorporating a second sorbate or even a mixture of precipitates) (Stipp et al., 1992). It is important to distinguish between processes that originate a uniformly distribution in the carbonate crystal such as co-precipitation, and the ones which cause a heterogeneous distribution on the surface of carbonate minerals, e.g. adsorption. Sorption on the surface of calcite was shown to be strong for Cd^{2+}, Zn^{2+}, Mn^{2+}, Co^{2+}, Ni^{2+} (in decreasing order of selectivity), while Ba^{2+} and Sr^{2+} are weakly sorbed, e.g. (Lorens, 1981b; Davis et al., 1987; Zachara et al., 1988; Zachara et al., 1991; Reeder, 1996; Tesoriero and Pankow, 1996), with the adsorption constants for each element following the sequence expected from their ionic radii, according to the degree to which their radii match the ionic radius of Ca^{2+} (Comans and Middelburg, 1987). Strongly sorbed cations have solid-liquid partition coefficients greater than unity, ionic radii less than or close to that of Ca^{2+}, are miscible in calcite and form anhydrous carbonates having the calcite structure, the weakly sorbed cations have solid-liquid partition coefficients less than unity, ionic radii larger than Ca^{2+}, are immiscible in calcite, and form anhydrous carbonates with the aragonite structure (Zachara et al., 1991). In addition, crystal-fluid interface processes have been shown to influence the composition of synthetic calcite, such as diffusive transport conditions to the mineral surface (Wasylenki et al., 2005a) and sector zoning where

elemental composition vary significantly in different non equivalent vicinal crystal faces (e.g. Reeder and Paquette, 1989; Paquette and Reeder, 1995). Watson (1996; 2004) proposed a surface enrichment model in which the composition of the crystal reflects equilibrium element concentrations in the near-surface region of the crystal

1.4.2 Mg/Ca Ratios

The underlying basis for Mg palaeothermometry is that Mg forms a solid solution with calcite (Speer, 1983), and the substitution of Ca^{2+} by Mg^{2+} in calcite is endothermic and therefore is favoured at higher temperatures. Temperature appears to be a dominant factor in the incorporation of Mg^{2+} in inorganic carbonates (Chave, 1954; Katz, 1973b; Burton and Walter, 1987; Mucci, 1987a; Oomori et al., 1987; Morse and Bender, 1990), but also in biogenic ones (Klein et al., 1996a; Nurnberg et al., 1996a; Lea et al., 1999; Elderfield and Ganssen, 2000; Lear et al., 2002).

Any reaction for which there is change in enthalpy or heat of reaction (ΔH) will be exponentially dependent on temperature, as shown in van't Hoff equation:

$$d\ln K / d(1/T) = - \Delta H / R \qquad (15)$$

Where T is the temperature in degrees Kelvin, R is the gas constant and K the equilibrium constant for the reaction. The greater absolute ΔH, the greater temperature dependence the reaction will have. A recent estimate of ΔH for Mg substitution in calcite is 21 kJ/mol, suggesting that the Mg/Ca content of a thermodynamically ideal calcite will increase exponentially by ~3% per degree between 0° and 30°C (Koziol and Newton, 1995).

Biogenic calcites have been found to have lower Mg content and a temperature dependence of Mg substitution higher than the one observed in calcite from inorganic precipitation experiments, and thus suggest a clear vital effect on biogenic calcite Mg/Ca ratios (Nurnberg et al., 1996a; Rosenthal et al., 1997; Lea et al., 1999). Furthermore, the clear species-specific temperature dependence of Mg/Ca ratios that has been observed in foraminifera calcite (Rosenthal et al., 1997; Lea et al., 1999; Elderfield and Ganssen, 2000; Lear et al., 2002) suggests that parameters other than temperature also can influence the Mg/Ca ratios of biogenic calcites and calibrations

have to be performed for each species (Nurnberg et al., 1996a; Lea et al., 1999; Elderfield and Ganssen, 2000; Lear et al., 2002; Skinner and Elderfield, 2005). For example, biological parameters such as gametogenesis, ontogeny, growth rate and size, as well as environmental and physical parameters such as salinity, pH and post-depositional dissolution, have all been proposed to significantly influence foraminiferal Mg/Ca ratios (Delaney et al., 1985; Lea et al., 1999; Elderfield et al., 2001; Bentov and Erez, 2005). Furthermore, observations of significant small-scale intra-shell heterogeneity in Mg contents indicates a strong biological control on the Mg/Ca ratio of biogenic calcites, such as observed in foraminifera (Rio et al., 1997; Hathorne et al., 2003; Eggins et al., 2004; Bentov and Erez, 2005; Sadekov et al., 2005), ostracodes (Rio et al., 1997) and bivalves (Lorens and Bender, 1977; Lorens and Bender, 1980; Rosenberg and Hughes, 1991; Vander Putten et al., 2000; Rosenberg et al., 2001). Nevertheless, the large exponential response of biogenic calcite Mg/Ca to temperature, combined with the fact that shell Mg/Ca can be precisely measured, makes this a promising and powerful tool for palaeotemperature reconstructions.

In calcitic bivalve molluscs the occurrence of a temperature control on shell Mg/Ca ratios has been the subject of several studies that have returned contrasting results, but nevertheless shell Mg/Ca ratios have been used to reconstruct palaeotemperatures from fossil bivalves (e.g. Klein et al., 1997; Immenhauser et al., 2005). In an early study, a weak positive correlation between shell calcite Mg concentration with temperature was reported for three species from the genus *Mytilus* (Dodd, 1965). More recently, Klein et al. (1996a) described a clear temperature dependence of Mg/Ca ratios for the mussel *Mytilus trossulus*, as did Vander Putten et al., (2000) for *Mytilus edulis* (blue mussel), but in the latter case an apparently seasonal breakdown in the relationship between Mg/Ca and temperature also was reported. For other bivalve species, such as *Pecten maximus* (king scallop), Lorrain et al., (2005) reported an absence of a significant correlation between Mg/Ca ratios and temperature for this species. Furthermore, several studies report, or suggest, the occurrence of significant non-thermodynamic controls on the Mg content of bivalve mollusc calcite, such as salinity (Dodd, 1965), solution Mg/Ca ratios (Lorens and Bender, 1980), the animal's metabolism (Lorens and Bender, 1977; Lorens and Bender, 1980; Vander Putten et al., 2000) or even variations in the activity of fructose diphosphase, a Mg-dependent enzyme involved in gluconeogenesis

(Vasil'ev, 2005). Moreover, significant small-scale heterogeneity in Mg content also has been described for bivalve shell calcite. Such variability has been associated with stress (Lorens and Bender, 1980), metabolic activity (Rosenberg and Hughes, 1991) and control of shell crystal elongation (Rosenberg et al., 2001). In conclusion, constrained calibration and validation studies need to be completed for Mg/Ca ratios in the calcite of marine bivalves to fulfil its potential as a palaeotemperature proxy.

1.4.3 Sr/Ca Ratios

$SrCO_3$ does not form a solid solution in calcite but it does with aragonite due to the large ionic radius of Sr^{2+} (Speer, 1983). Although, Sr^{2+} also substitutes for Ca^{2+} in the calcite crystal lattice (Pingitore et al., 1992) it is not possible to use thermodynamic parameters to predict or describe the temperature dependence of such substitution.

Inorganic precipitation experiments have shown Sr incorporation in aragonite to be inversely related to temperature (Kinsman and Holland, 1969a; Dietzel et al., 2004) but independent on precipitation rate (Zhong and Mucci, 1989). However, in experimentally precipitated inorganic calcite, Sr/Ca ratios are strongly dependent on precipitation rate, increasing with increasing precipitation rate (Lorens, 1981a; Morse and Bender, 1990; Tesoriero and Pankow, 1996), and also are influenced by the Sr/Ca ratio of the solution from which precipitation occurred (Mucci and Morse, 1983; Pingitore and Eastman, 1986), and the Mg content of the solution and solid mineral which favours the incorporation of other elements by distorting the mineral lattice (Mucci and Morse, 1983; Ohde and Kitano, 1984; Morse and Bender, 1990).

Sr/Ca ratios from biogenic carbonates have been proposed or used to obtain information on past seawater temperatures (Weber, 1973; Beck et al., 1992; Guilderson et al., 1994; Hughen et al., 1999; McCulloch et al., 1999; Rosenheim et al., 2004), but also on past ocean Sr/Ca ratios (Martin et al., 1999; Stoll et al., 1999). In biogenic carbonates, kinetic effects are thought to strongly influence Sr incorporation in biogenic aragonite, where control by precipitation rate is not expected, such as in corals (de Villiers et al., 1995; Cohen et al., 2001) and bivalves

(Gillikin et al., 2005a; Gillikin et al., 2005b; Carré et al., 2006), but also in biogenic calcite such as foraminifera (Lea et al., 1999), coccoliths (Stoll and Schrag, 2000; Rickaby et al., 2002; Stoll et al., 2002a; Stoll et al., 2002b) and bivalves (Lorrain et al., 2005). A positive temperature influence on Sr/Ca ratios has also been observed in foraminifera (Lea et al., 1999), coccolithophores (Stoll et al., 2002a, b) and bivalves (Dodd, 1965; Lorrain et al., 2005) but can be attributed to a kinetic influence and a co-variation between temperature and growth rates.

In bivalve calcite, the mechanisms controlling Sr incorporation continue to be investigated and the matter of some debate, and physiological controls (Klein et al., 1996b; Lorrain et al., 2005), are thought to influence Sr/Ca ratios, and a secondary influence of salinity also has been suggested (Klein et al., 1996b). However, while kinetic effects have been observed in the dependence of Sr/Ca ratios on shell growth rates (Lorrain et al., 2005), the suggestion of a metabolic control of Sr/Ca ratios in bivalves has been derived from indirect evidence, rather than direct observation, gathered from the relationship of Sr/Ca ratios with $\delta^{13}C$, as well as the intra-individual variability (fast growing sections relative to slow growing sections) of Sr/Ca ratios (Klein et al., 1996b).

1.4.4 Mn/Ca Ratios

If a consistent relationship can be established between the Mn content of biogenic carbonates and the dissolved and/or particulate Mn concentrations of seawater, Mn/Ca ratios of marine calcifying organisms potentially could provide a useful proxy for dissolved and particulate Mn concentrations and thus for those redox processes that can determine the concentration of this element in seawater. Because of the association of numerous elements (such as carbon, sulphur, phosphorus and several trace elements), organic matter and redox conditions with the redox cycle of Mn, the latter may play an important role in tracing the biogeochemical cycles of many elements, as well as the response of coastal systems to seasonal and long term eutrophication (e.g. Murray, 1975; Turekian, 1977; Balistrieri and Murray, 1986; Hunt and Kelly, 1988; Burdige, 1993).

In inorganic calcite manganese has been shown to substitute for calcium in the crystal lattice, and to be incorporated into the calcite mineral by the formation of a dilute solid solution of $MnCO_3$ in $CaCO_3$ (Pedersen and Price, 1982; Pingitore et al., 1988). In inorganic calcite, precipitation rate also has been shown to influence the incorporation of Mn^{2+}, and the partition coefficient for Mn was found to be inversely correlated to the rate of precipitation (Mucci, 1987b; Mucci, 1988; Pingitore et al., 1988; Dromgoole and Walter, 1990). In addition, small changes D_{Mn} have been observed with solid or solution composition for calcites precipitated from artificial seawater, probably due to the effect of Mg^{2+} present in seawater (Franklin and Morse, 1983; Mucci, 1988). The effect of temperature on D_{Mn} is still controversial with studies reporting both positive and inverse relationships, although in calcite deposited from synthetic solutions under controlled precipitation rates, the increase in D_{Mn} with increasing temperature was of similar magnitude to the effect of precipitation rate (Dromgoole and Walter, 1990). Also, sector zoning of Mn in calcite, where elemental composition vary significantly in different non equivalent vicinal crystal faces, has been observed in natural calcite cements and induced in synthetic calcite crystals (e.g. Reeder and Grams, 1987; e.g. Reeder and Paquette, 1989; Paquette and Reeder, 1995).

The manganese content of bivalve shells is seen as a potential record of ambient Mn concentrations. However, it is unclear if the Mn content of aragonite or calcite bivalve shells reflect the dissolved or particulate Mn concentrations. In particular, the aragonitic shells of freshwater unionoid bivalves have been shown to be valid archives of dissolved Mn levels associated with riverine anthropogenic inputs (Lindh et al., 1988; Jeffree et al., 1995; Markich et al., 2002), but also of both dissolved and biogenic particulate Mn concentrations associated with lacustrine upwelling and related changes in productivity (Langlet et al., 2007). In the calcite of marine bivalves, investigations relating shell Mn/Ca ratios to environmental variables have led to the suggestion of a possible control of shell Mn/Ca ratios by both particulate and/or dissolved Mn concentrations (Arthur et al., 1985; Vander Putten et al., 2000; Langlet et al., 2006). Elevated shell Mn/Ca ratios have been suggested to be related to spring bloom-induced increases in particulate and/or dissolved Mn in the bivalve *Mytilus edulis* (Vander Putten et al., 2000), or to increased riverine discharge events and associated increases in particulate and/or dissolved Mn in the tropical mangrove

bivalve *Isognomon ephippium* (Lazareth et al., 2003). Gillikin (2005), however, suggested that food is not an important source of Mn to the calcite of *M. edulis* from an experimental study on the elemental composition of the haemolymph, tissue, shell and seawater. Langlet et al., (2006), by repeatedly marking animals in seawater with artificially elevated dissolved Mn concentrations, produced the first direct evidence for the rapid uptake of dissolved Mn^{2+} into the shell calcite of the oyster *Cassostrea gigas*.

Further calibration work is required to validate robustly bivalve shell Mn/Ca ratios as a potential proxy for seawater dissolved manganese concentrations, as well as to determine the extent of any physiological controls on shell Mn/Ca ratios.

1.5 Limitations of Biogenic Carbonate Archives

1.5.1 Growth Rates and Sampling Techniques: Influence on Time Averaging and Resolution

In biogenic carbonate archives, skeletal growth produces distinct growth increments and thus can significantly influence the preservation of environmental signals within skeletal structures. Variable growth rates influence the amount of time during which a portion of skeletal structures were deposited, i.e. the time window that each sample represents. Other factors affecting the retrieval of proxy data from biogenic hard parts are the size of the growth structures from which information is to be extracted and the minimum size the sampling technique can produce.

Shell growth in bivalves is incremental with shell being extended by adding discrete increments from the extra-pallial fluid (EPF) at the shell margin (Lutz and Rhoads, 1980). This results in a pattern of older shell towards the umbo and younger shell towards the shell margin, but also results in a change in age across the shell, i.e. from the older outer shell surface to the younger inner shell surface. Therefore, variations in sample size, depth of sampling and sampling interval will influence the time

represented by any given shell sample. Furthermore, variations in shell growth rate also influence the time-averaging of any given sample, i.e. for shell samples collected with the same size, interval and up to the same depth, the higher the growth rate the shorter the time represented by a sample (Wilkinson and Ivany, 2002; Goodwin et al., 2003; Ivany et al., 2003; Goodwin et al., 2004). Time-averaging thus results in sub-sampling of the full amplitude of the seasonal cycle of any given parameter. Furthermore, growth cessations occur in bivalves when temperatures exceed the thermal tolerances of the organisms (Jones and Quitmyer, 1996), or growth rates are reduced even when temperature approach but do not exceed the thermal tolerances (Goodwin et al., 2001) or thresholds of other parameters that control growth, e.g. salinity, food, reproductive cycle. Shell growth reduction or cessation results in a temporally distorted or discontinuous sampling, which becomes biased towards the seasons of maximum growth through sub-sampling of one period of the seasonal cycle relative to another or even missing one or both extremes of the seasonal cycle of the relevant environmental parameter (e.g. temperature). Nevertheless, relevant information on environmental conditions during growth can still be retrieved from bivalve shells if enough is known about the ecology, growth and ontogeny of any given species (Jones, 1983; Wefer and Berger, 1991; Richardson, 2001).

1.6 Rationale and aims of this study

This dissertation contributes to the use of bivalves as a palaeo-tool for the reconstruction of past environmental conditions. Its aim is to investigate and validate the relationships between the elemental composition (Mg/Ca, Sr/Ca and Mn/Ca) of bivalve shell calcite and its primary environmental controlling factors, mainly seawater temperature, dissolved and particulate element concentration. A special focus will be placed on the role of secondary controlling factors, i.e. vital effects such as kinetic effects, shell growth rate and metabolic activity. In addition, the small-scale element composition heterogeneity in bivalve shells is investigated as a potential variability source of bivalve calcite elemental/calcium ratios.

In this dissertation, a combined field and laboratory culture approach was taken whereby the stable O and C isotope and elemental composition of shell carbonate for a defined interval of growth was compared to a contemporaneous data set of environmental and biological parameters. Specifically, no laboratory calibration of the Mg/Ca ratio–temperature relationship in bivalve calcite, or of the influence of metabolic and kinetic controls on Sr/Ca ratios in bivalve calcite, has been performed under constrained and constant seawater temperatures. The constrained chronology of new shell growth obtained for both field and laboratory experimentally grown animals has allowed completion of a reliable comparison of shell elemental/Ca ratios to measurements of contemporaneous seawater temperature, salinity and other relevant environmental variables, as well as to biological variables such as shell growth rate, size and metabolic activity. A laboratory culturing approach enables manipulation of specimens, control of additional environmental factors, and measurement of other parameters, such as size and growth rate. It must be acknowledged, however, that laboratory aquaria are not a true representation of the animal's natural habitat. Nevertheless, a laboratory culturing approach is the only means whereby complex environmental variables can be constrained and only one variable, i.e. seawater temperature in this study, varied. However, the outcomes of laboratory culturing studies are only of value when validated by field-based studies, albeit with the latter suffering from a lesser degree of constraint of environmental variables.

The temperature dependence of Mg/Ca ratios in bivalve calcite was investigated in field-grown specimens of *Pinna nobilis* (chapter 2), *Pecten maximus* (chapter 3) and *Mytilus edulis* (chapter 4) and laboratory-grown specimens of *P. maximus* (chapter 4) and *M. edulis* (chapter 4). More specifically, the aim was to derive empirical Mg/Ca ratio to temperature calibrations to enable paleotemperature reconstructions, and to investigate the non-temperature variability and its possible physiological sources (ontogeny, metabolic activity and shell growth rate) that may render invalid the establishment of such calibrations.

The physiological sources (ontogeny, metabolic activity and shell growth rate), as well as the influence of environmental parameters such as temperature and salinity, on Sr/Ca ratios of bivalve calcite also was investigated in field-grown specimens of

Pinna nobilis (chapter 2), *Pecten maximus* (chapter 3) and *Mytilus edulis* (chapter 5) and laboratory-grown specimens of *P. maximus* and *M. edulis* (chapter 5).

An assessment of the association between the variation of shell Mn/Ca ratios and the seasonal changes of seawater dissolved Mn^{2+} concentrations also has been made for field-grown specimens of *Pecten maximus* (chapter 3). In addition, the relationship between dissolved and particulate Mn^{2+} concentrations and shell Mn/Ca ratios was assessed in field-grown specimens of *Mytilus edulis* (chapter 6). This dataset also has enabled the additional consideration of the significance of shell growth rate effects on shell Mn/Ca ratios.

Finally, an initial assessment of the extent of any small-scale heterogeneity in Mg/Ca, Sr/Ca and Mn/Ca ratios in bivalve shell calcite laboratory-grown specimens of *Pecten maximus* and *Mytilus edulis* (chapter 7) has been analysed using SIMS. Small-scale heterogeneity may provide further insights into explaining the sources and processes of elemental/Ca ratios variability observed in bivalve calcite.

Chapter 1

General Introduction

Chapter II

Mg/Ca, Sr/Ca and stable-isotope ($\delta^{18}O$ and $\delta^{13}C$) ratio profiles from the fan mussel *Pinna nobilis*: Seasonal records and temperature relationships

Publications related to this chapter:

Freitas P., Clarke L. J., Kennedy H., Richardson C. and Abrantes F., 2005. Mg/Ca, Sr/Ca and stable-isotope ($\delta^{18}O$ and $\delta^{13}C$) ratio profiles from the fan mussel *Pinna nobilis*: Seasonal records and temperature relationships. *Geochemistry Geophysics Geosystems*, 6, Q04D14, doi:10.1029/2004GC000872.

Third Party material excluded from digitised copy.
Please refer to original text to see this material.

Chapter III

Environmental and biological controls on elemental (Mg/Ca, Sr/Ca and Mn/Ca) ratios in shells of the king scallop *Pecten maximus*

Publications related to this chapter:

Freitas P., Clarke L. J., Kennedy H., Richardson C. and Abrantes F., 2006. Elemental (Mg/Ca, Sr/Ca and Mn/Ca) and stable-isotope ($\delta^{18}O$ and $\delta^{13}C$) records from shells of the scallop *Pecten maximus* (Bivalvia): Preliminary results from field deployments. *Geochimica et Cosmochimica Acta*, 70, 5119-5133.

Third Party material excluded from digitised copy.
Please refer to original text to see this material.

Chapter IV

Inter- and intra-specimen variability masks reliable temperature control on shell Mg/Ca ratios in laboratory and field cultured *Mytilus edulis* and *Pecten maximus* (bivalvia)

IV - Inter- and intra-specimen variability masks reliable temperature control on shell Mg/Ca ratios in laboratory and field cultured *Mytilus edulis* and *Pecten maximus* (bivalvia)

4.1 Abstract

The Mg/Ca ratios of biogenic calcites are commonly seen as a valuable palaeo-proxy for reconstructing past ocean temperatures. The temperature dependence of Mg/Ca ratios in bivalve calcite has, however, been the subject of contradictory observations. The palaeoceanographic use of a geochemical proxy, like Mg/Ca ratios, is dependent on initial, rigorous calibration and validation of relationships between the proxy and the ambient environmental variable to be reconstructed. In this study, Mg/Ca ratio data are reported for the shell calcite of two bivalve species, *Mytilus edulis* (common mussel) and *Pecten maximus* (king scallop), for the first time grown in laboratory culturing experiments at controlled and constant aquarium seawater temperatures over a range from ~10 to ~20°C. Furthermore, Mg/Ca ratio data of laboratory-grown *M. edulis* specimens were compared with data from specimens of this same species grown in a field-culturing experiment. Only a weak, albeit significant, shell Mg/Ca ratio–temperature relationship was observed in the two bivalve species: *M. edulis* (r^2 = 0.37, $p<0.001$ laboratory cultured specimens and r^2 = 0.50, $p<0.001$ for field cultured specimens) and *P. maximus* (r^2 = 0.21, $p<0.001$, laboratory cultured specimens only). In the two species, shell Mg/Ca ratios also were not found to be controlled by shell growth rate and salinity. Furthermore, measurement of Mg/Ca

ratios in the shells of multiple specimens illustrated that a large degree of variability in the measured shell Mg/Ca ratios was significant at the species, inter- and intra-individual shell levels. The study data suggest that the use of bivalve calcite Mg/Ca ratios as a reliable, precise and accurate temperature proxy still remains limited, at least in the species studied to date. Such limitations are most likely due to the presence of significant physiological effects on Mg incorporation in bivalve calcite, with such variability differing both within single shells and between shells of the same species that were precipitated under the same ambient conditions.

4.2 Introduction

Carbonate skeletal remains, i.e. foraminifera, corals, ostracodes and bivalves, are valuable archives of information for palaeo-reconstruction of changes in physical and chemical oceanographic conditions. The incremental growth of biogenic carbonates, such as the shells of marine bivalve molluscs or the coral skeleton, has the potential to record high-resolution time-series of those environmental conditions in which the organism grew. Furthermore, marine bivalves occupy widely distributed habitats in the modern-day oceans, as well as being relatively common throughout the fossil record since the Cretaceous. Information on past environmental conditions that are preserved in carbonates can be obtained through the use of proxies, i.e. physical and chemical signals that provide information on sought after variables that cannot be measured directly, such as seawater temperature or salinity. However, a proxy is rarely dependent on a single variable, and the influence of other secondary independent variables complicates, to a lesser or larger extent, proxy use in palaeo-studies; such factors must be assessed rigorously via calibration and validation studies prior to successful application (for reviews, see e.g. Wefer et al., 1999; Lea, 2003).

The use of the oxygen-isotope composition ($^{18}O/^{16}O$ ratios expressed as $\delta^{18}O$ values) of biogenic carbonate archives as a proxy for seawater temperature (for reviews, see e.g. Emiliani, 1966; Wefer and Berger, 1991) is one of the most powerful tools in palaeoceanographic studies (e.g. Shackleton, 1967; Shackleton and Opdyke, 1973;

Gagan et al., 2000), but its use is complicated by factors other than temperature, namely variation in the oxygen-isotope composition of seawater, pH and kinetic effects (e.g. McConnaughey, 1989a; Spero et al., 1997). By comparison, the predicted thermodynamic control of Ca^{2+} substitution by Mg^{2+} in inorganically precipitated calcite (Chilingar, 1962; Katz, 1973a; Mucci, 1987b; Oomori et al., 1987) and the observed temperature dependence of Mg/Ca ratios in some biogenic calcites (Chave, 1954; Dwyer et al., 1995; Klein et al., 1996a; Nurnberg et al., 1996a; Rosenthal et al., 1997; Lea et al., 1999; Dwyer et al., 2000; Elderfield and Ganssen, 2000; Lear et al., 2002) have resulted in Mg/Ca ratios being seen as a salinity-independent temperature proxy that makes an ideal companion to the $\delta^{18}O$–temperature proxy. However, the clear species-specific temperature dependence of Mg/Ca ratios that has been observed in foraminiferal calcite (Rosenthal et al., 1997; Lea et al., 1999; Elderfield and Ganssen, 2000; Lear et al., 2002) suggests that parameters other than temperature also can influence the Mg/Ca ratios of biogenic calcites. For example, biological parameters such as gametogenesis, ontogeny, growth rate and size, as well as environmental and physical parameters such as salinity, pH and post-depositional dissolution, have all been proposed to significantly influence foraminiferal Mg/Ca ratios (Delaney et al., 1985; Lea et al., 1999; Elderfield et al., 2001; Bentov and Erez, 2005). Furthermore, observations of significant small-scale intra-shell heterogeneity in Mg contents indicates a strong biological and/or kinetic control on the Mg/Ca ratio of biogenic calcites, such as observed in foraminifera (Rio et al., 1997; Hathorne et al., 2003; Eggins et al., 2004; Bentov and Erez, 2005; Sadekov et al., 2005), ostracodes (Rio et al., 1997) and bivalves (Lorens and Bender, 1980; Rosenberg et al., 2001).

In calcitic bivalve molluscs the occurrence of a temperature control on shell Mg/Ca ratios has been the subject of several studies that have returned contrasting results, but nevertheless shell Mg/Ca ratios have been used to reconstruct palaeotemperatures from fossil bivalves (Klein et al., 1997; e.g. Immenhauser et al., 2005). In an early study, a weak positive correlation between shell calcite Mg concentration with temperature was reported for three species from the genus *Mytilus* (Dodd, 1965). More recently, Klein et al., (1996a) described a clear temperature dependence of Mg/Ca ratios for the mussel *Mytilus trossulus*, as did Vander Putten et al., (2000) for *Mytilus edulis* (blue mussel), but in the latter case an apparently seasonal breakdown

in the relationship between Mg/Ca and temperature also was reported. A clear seasonal relationship between shell Mg/Ca ratios and calcification temperature for the large fan mussel *Pinna nobilis* has also been reported (Chapter 2), albeit with an additional ontogenetic influence.For other bivalve species, such as *Pecten maximus* (king scallop), there also exists no clear temperature relationship; Lorrain et al., (2005) reported an absence of a significant correlation between Mg/Ca ratios and temperature for this species while a weak, albeit significant, Mg/Ca ratio to temperature relationship was also observed (Chapter 3), with the relationship breaking down during winter months. Furthermore, several studies report, or suggest, the occurrence of significant non-thermodynamic controls on the Mg content of bivalve mollusc calcite, such as salinity (Dodd, 1965), solution Mg/Ca ratios (Lorens and Bender, 1980) or the animal's metabolism (Lorens and Bender, 1977; Lorens and Bender, 1980; Vander Putten et al., 2000). Significant small-scale heterogeneity in Mg content has also been described for bivalve shell calcite. Such variability has been associated with stress (Lorens and Bender, 1980), metabolic activity (Rosenberg and Hughes, 1991) and control of shell crystal elongation (Rosenberg et al., 2001).

The purpose of this study was to advance an understanding of the degree of variability of Mg/Ca ratios in calcite bivalve shells using a controlled laboratory aquarium culturing approach. Specifically, no laboratory calibration of the Mg/Ca ratio–temperature relationship in bivalve calcite has previously been performed under constrained and constant seawater temperatures. This approach is a significant advancement on previous studies, since it enables manipulation of specimens, control of environmental variables, and measurement of other parameters, such as size and growth rate. It must be acknowledged, however, that laboratory aquaria are not a true representation of the animal's natural habitat. However, the outcomes of laboratory culturing studies are only of value when validated by field-based studies, albeit with the latter suffering from a lesser degree of constraint of environmental variables. In summary, the ultimate goal of this investigation was to determine whether a reliable calibration of the Mg/Ca ratio–temperature relationship could be obtained for the shell calcite from two bivalve species, *Mytilus edulis* (blue mussel) and *Pecten maximus* (king scallop), grown under constrained and constant temperature

laboratory aquaria conditions. Finally, the *M. edulis* laboratory culturing data have been compared with data from field-grown specimens of this same species.

4.3 Material and Methods

4.3.1 Laboratory Culture Experiment

Two species of marine bivalve mollusc were cultured in constant-temperature aquaria in the School of Ocean Sciences, University of Wales Bangor, U.K. *Mytilus edulis* specimens were collected in December 2003, from naturally settled spat (1 cm < size < 2 cm; age < one year) in Cable Bay, a site on the coast of Anglesey, northwest Wales, while *Pecten maximus* specimens (1 cm < size < 2 cm; age < one year) were collected from a commercial fishery, Ramsay Sound Shellfish, Isle of Skye, Scotland, in November, 2003. Once moved into the laboratory environment, all animals were acclimated at a temperature of ~13°C for more than two months. Subsequently, animals of similar size were moved into separate aquaria each under different but constant temperatures and controlled food and light conditions; the aquaria were routinely cleaned of all detritus. For the duration of the experiments, animals were kept in individual plastic mesh cages within each aquarium. Acclimation to the different temperatures in each aquarium was achieved by increasing/decreasing water temperature by 1°C every 2 days before commencement of the experimental periods. A mixed algae solution of *Pavlova lutheri*, *Rhinomonas reticulata* and *Tetraselmis chui* was collected every morning from stock cultures, split into equal volumes of eight litres and then supplied to the aquaria, from containers with a drip-tap, throughout that day at rates of ~5.5 ml/min. Because of the limited number of aquaria available, two separate temperature-controlled experiments were completed with three aquaria used in each.

The two separate culturing experiments were performed to evaluate the influence of temperature on shell Mg/Ca ratios of *Mytilus edulis* and *Pecten maximus* in the laboratory environment. During experiment one, from 23rd February to 7th April, 2004, nominal seawater temperatures in the three available aquaria were maintained

at 12, 15 and 18°C, and only *M. edulis* was cultured. In experiment two, from 6th May to 18th June 2004, nominal seawater temperatures were maintained at 10, 15 and 20°C and both *M. edulis* and *P. maximus* were cultured. In each aquarium, with individual thermostat temperature control via a heating/glycol cooling system, the nominal seawater temperatures were controlled by setting upper and lower temperature thresholds on the individual control systems, with a maximum resolution achievable by these controllers of 1°C. For improved constraint, seawater temperature was also monitored in each aquarium every 15 minutes using submerged temperature loggers (Gemini Data Loggers TinyTag - TGI 3080; accuracy of ± 0.2°C and resolution <0.05°C; Figure 4-1). The intermittent lack of temperature control in some aquaria is a limitation of the aquarium system used and most manifest at the lowest nominal temperature of 10°C, when the cooling system sometimes struggled to compensate for fluctuations in the temperature of the external seawater supply. Natural seawater is pumped from the proximal Menai Strait into settling tanks before being introduced as a common supply into the laboratory aquaria.

Once the animals had acclimatised, individual specimens were removed at weekly intervals (with the exception of the last growth interval in experiment two, which was longer than a week for both the 15°C and 20°C aquaria) to be processed. Each time the *Mytilus edulis* specimens were removed from the aquaria they were exposed to the air for 5 to 6 hours, while *Pecten maximus* specimens were kept in small holding tanks for periods of 30 to 45 minutes. Both methods resulted in emplacement of a disturbance mark on the surface of the shells. The shells then were photographed and digitally imaged using the AnalySIS software package. The combination of disturbance marks and photographs was used to identify and measure all shell growth between emersions and provided a time control of the new shell growth laid down throughout the experiments. Subsequently the term "growth interval" has been used to describe the time intervals between emersions of animals (Table 4-1). The duration of the experiments, and hence the number of growth intervals, varied with species and aquarium temperature (Table 4-1).

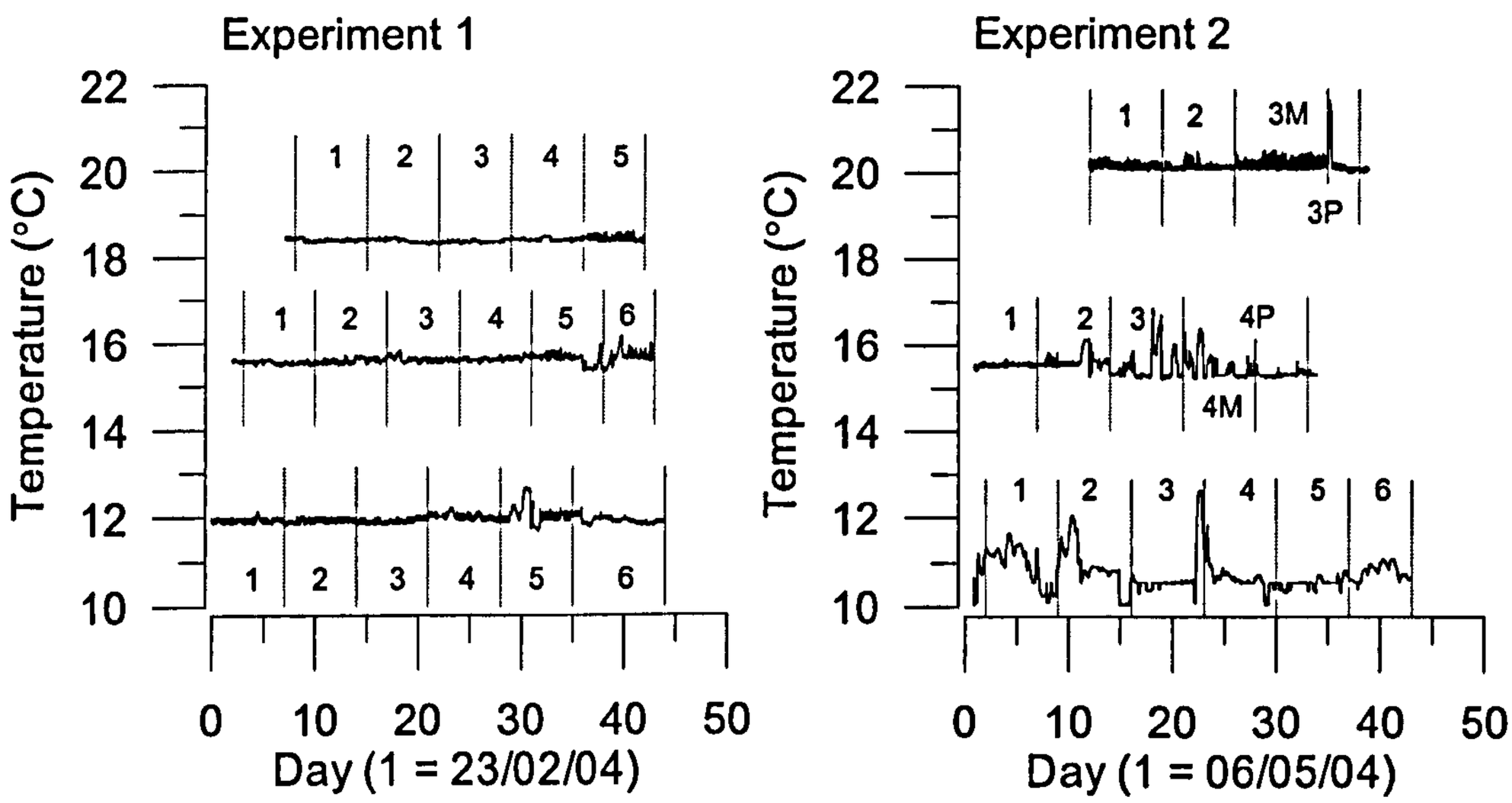

Figure 4 - 1 – Variation of seawater temperature measured every 15 minutes in all the aquaria during experiments one and two. Vertical lines define limits of growth intervals in each tank. In experiment two, the last growth interval was of different duration for the two species, and the suffixes M and P indicate the last growth interval for *Mytilus edulis* and *Pecten maximus*, respectively.

Table 4 - 1 – Start dates of the two culturing experiments and duration of growth intervals (days) in each aquarium for which new shell growth was evident.

Experiment 1

Species	Aquarium Interval		12°C						15°C						18°C				
			1	2	3	4	5	6	1	2	3	4	5	6	1	2	3	4	5
Mytilus edulis	Start Date	2004	23/02						25/02						01/03				
	Duration	Days	7	7	7	7	7	9	7	7	7	7	7	6	7	7	7	7	7

Experiment 2

Species	Aquarium Interval		10°C						15°C					20°C			
			1	2	3	4	5	6	1	2	3	4M	4P	1	2	3M	3P
Mytilus edulis *Pecten maximus*	Start Date	2004	07/05						06/05					17/05			
	Duration	Days	7	7	7	7	7	7	7	7	7	7	12	7	7	10	13

In experiment two the last growth interval was of different duration for the two species grown at 15 and 20°C and the suffixes M and P indicate the last growth interval for *Mytilus edulis* and *Pecten maximus*, respectively.

Seawater samples for measurement of salinity and $\delta^{18}O_{seawater}$ were collected using sealed salinity bottles every other day from the 15°C aquarium in both experiments. Samples were collected from one aquarium only, since the seawater supply was common in all aquaria and water turnover time was short (~7–8 hours for a volume of ~650 litres). Samples were analysed for $\delta^{18}O_{seawater}$ at the School of Environmental Sciences, University of East Anglia, by off-line equilibration with CO_2 and subsequent measurement of isotope ratios using a Europa-PDZ Geo 20/20 isotope-ratio mass spectrometer, with normalisation relative to a laboratory standard, North Sea Water (accepted value of -0.14 ‰ VPDB). The precision of replicate $\delta^{18}O_{seawater}$

analyses is 0.05 ‰ (1 σ; N = 30) and all data are reported in per mil (‰) deviations relative to the to the VPDB scale (Hut, 1987), where $\delta^{18}O_{seawater}$ (VPDB) = $\delta^{18}O_{seawater}$ (VSMOW) – 0.27 ‰. Salinity was determined using an AutoSal 8400 Autosalinometer calibrated with International Association for Physical Sciences of the Ocean (I.A.P.S.O.) standard seawater (analytical accuracy and resolution of ± 0.003 equivalent PSU) for a subset of samples that covered the entire range of the $\delta^{18}O_{seawater}$ variation. The temperature and $\delta^{18}O_{seawater}$ data were collected at a higher than weekly frequency, hence average values were calculated for each growth interval (Appendix 3).

4.3.2 Field Culturing Experiment

Specimens of the bivalve *Mytilus edulis* were suspended 1 metre below a moored raft in the Menai Strait (north Wales, U.K.; Figure 3-1, pp 71) from the 8th December 2004 to the 12th December 2005. The animals were all less than 1 year old when deployed, obtained from one spat cohort and initially ranged from 2.0 to 2.7 cm in shell length. This raft is moored in the close vicinity (ca. 500 m) of the School of Ocean Sciences, University of Wales Bangor in a section of the Menai Strait where the water column is completely mixed, due to strong turbulent tidal mixing (Harvey, 1968). Animals were deployed in mesh cages and each shell was identified by a mark hand drilled on its surface. Two different, but parallel, experimental approaches were taken: 1) "short" deployment specimens were placed into cages for 16 short, well-defined and consecutive growth intervals that together covered the duration of the entire field experiment. The duration of each growth interval varied during the experiment according to expected seasonal changes in shell growth rate; 2) In contrast to the short-deployment specimens, "annual" deployment specimens were placed in the field for the entire duration of the experiment. To ensure that short-deployment specimens were in the same physiological condition as their annual-deployment counterparts, and to avoid the inevitable period of acclimation if animals were deployed directly from laboratory conditions, the former were taken at the start of each growth interval from a stock of animals deployed in the beginning of the experiment and kept in a separate cage.

At the end of each growth interval (which also was the beginning of the next growth interval) all short specimens from the preceding deployment and all annual-deployment specimens were removed from the raft, together with a new set of short-deployment specimens taken from the stock that were to be used during the next growth interval deployment. All of these shells then were photographed and digitally imaged using the AnalySIS software package. Between each deployment growth interval both short- and annual- deployment *Mytilus edulis* specimens were exposed to the air for 5 to 6 hours resulting in emplacement of a disturbance mark on the surface of the shells. The combination of disturbance marks and photographs was used to identify and measure all shell growth for each growth interval, as well as shell height (i.e. the distance from the umbo to the shell margin along the main axis of growth), and thus provide a time control of the new shell growth laid down throughout the field experiment by assuming shell growth rate to be constant during each growth interval.

Seawater temperature was monitored every two hours throughout the experimental deployment period using submerged temperature loggers placed in the mesh cages containing the animals (Gemini Data Loggers TinyTag - TGI 3080; accuracy of ± 0.2°C). Surface seawater samples for measurement of $\delta^{18}O_{seawater}$ were collected every two to five weeks, in the vicinity of the moored raft, using sealed salinity Winchester glass bottles. Samples were analysed for $\delta^{18}O_{seawater}$ as described in section.

4.3.3 Shell Preparation and Surface Milling

Laboratory Culture Experiment

The surfaces of the left hand valve of *Pecten maximus* shells were cleaned with a brush and any encrusting material removed using a 0.4 mm wide steel carbide burr (Minerva Dental Ltd) attached to a hand-held dental drill. The left hand valve of *Mytilus edulis* shells were cleaned in a similar manner to the *Pecten maximus* shells but, in addition, the outer organic periostracum was milled away with the drill until periostracum-free shell was visible in the entire sampling area. Shell powder samples subsequently were taken from the new shell growth by milling to a depth of ca. 200

μm. Accurate milling was completed under a binocular microscope fitted with an eyepiece graticule, and depth and width of milling were controlled carefully. Each milled powder sample was taken from the main axis of shell growth: in *P. maximus* from the mid 2–3 axial ridges (ribs), and in *M. edulis* from the middle section, to avoid the increase in shell curvature that occurs away from the main growth axis (Figure 4-2). Only one powder sample was milled from each individual growth interval and, particularly at the lower temperatures, the milled powder from one or more growth intervals had to be combined to provide enough shell material for analysis. Whenever the amount of sample permitted, single milled powder samples were split into separate aliquots for Mg/Ca and stable-isotope ratio determinations, otherwise only Mg/Ca ratios were measured (Appendix 3).

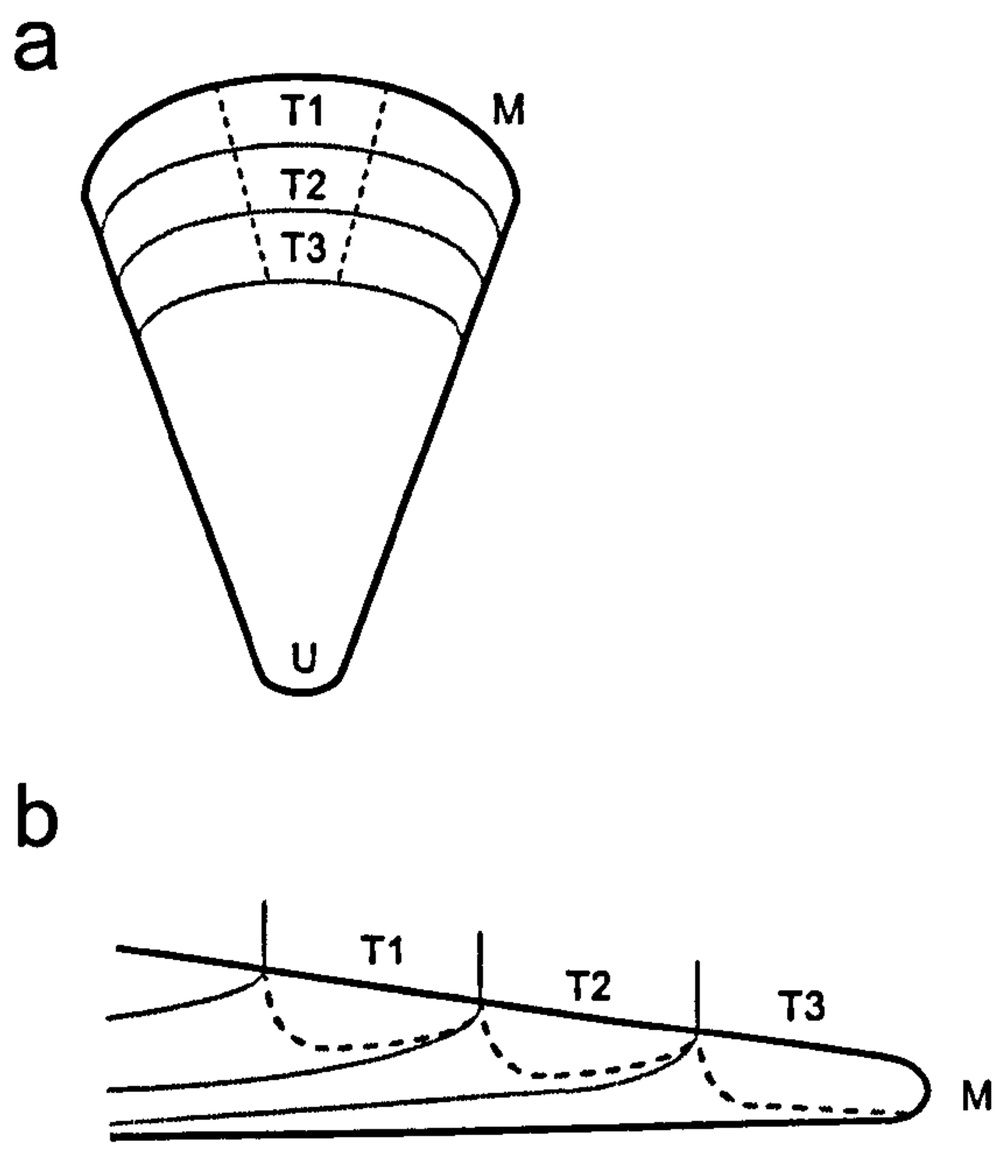

Figure 4 - 2 – Schematic representation of a shell representing the sampling approach for *Mytilus edulis* and *Pecten maximus* shells. a) View of the outer shell surface from above and b) Longitudinal section of the shell. M is the shell margin; U is the shell umbo; grey lines define the boundaries between growth intervals identified by T1, T2 and T3. Samples of shell calcite were collected for each growth interval along the main axis of growth, avoiding areas of excessive shell curvature, and up to a depth of ca. 200 μm in the areas delimited by the dotted lines in a) and b).

Lorens and Bender (1980) have described that the stress of capture and adaptation to a new laboratory environment induced the deposition of a region of shell (termed "transition zone calcite" by those authors) with higher Mg/Ca ratios. Therefore, it is possible that the regular handling disturbance (for measurement purposes) imposed on the animals of both species during the present study may explain some of the

variability of shell calcite Mg/Ca ratios that have been observed. However, Lorens and Bender (1980) only inferred the "transition zone" between new and old calcite using spot chemical compositions measured by electron microprobe, and their transition zone that exhibited higher Mg/Ca ratios occurs perpendicular to the shell surface. Also, no scale was reported in the Lorens and Bender (1980) study making it difficult to determine the size of the region of "transition zone calcite". Therefore, in the current study the sampling of individual growth intervals by hand-milling of powder samples between the disturbance marks on the surface of the shell, that represent the times of immersion during the experimental period, has minimized the influence of handling disturbances on measured Mg/Ca ratios.

Field Culture Experiment

The left hand valve of two short-deployment *Mytilus edulis* specimens were sampled for each growth interval, while three annual-deployment *M. edulis* specimens (A2, A6, A20) were sequentially sampled for all growth intervals as described for the laboratory culture experiment. Whenever the amount of shell growth permitted more than one sample was collected from a single growth interval. On such occasions the new shell growth was equally divided between the number of samples collected ($2 \leq N \leq 4$).

4.3.4 Shell Stable-Isotope and Elemental Ratio Analyses

The shell milled powder sample preparation and analytical methodologies used in this study are as described in detail in chapters 2 and 3. Shell and water oxygen stable-isotope data are reported in per mil (‰) deviations relative to VPDB and VSMOW, respectively. The overall analytical precision for shell $\delta^{18}O$ measurements based on analyses of an internal laboratory standard run concurrently with all *Mytilus edulis* and *Pecten maximus* samples analysed in this study is 0.08 ‰ (1 σ; N = 32). Sufficient material was not available from any one growth interval to enable replicate isotope analyses for an assessment of true sample precision; however, Freitas et al. (2006) used the same method as reported here and obtained a $\delta^{18}O$ precision of 0.06 ‰ for five replicate measurements of the same milled powder sample obtained from one *P. maximus* specimen.

Calibration for Mg/Ca ratio determinations was performed via an established ICP-AES intensity-ratio method (de Villiers et al., 2002), using synthetic standard solutions in the range 0–25 mmol/mol for Mg/Ca, and most at Ca concentrations of 50 (N = 304) and 60 μg/ml (N = 161). The smallest milled powder samples were analysed at 30 μg/ml (N = 102). Measurements were made using the Perkin Elmer Optima 3300RL ICP-AES instrument housed at the NERC ICP Facility, Royal Holloway University of London. Instrumental drift was monitored by running an intermediate (16 mmol/mol) calibration standard every 5 to 10 samples and data then were corrected accordingly. Analytical precision (expressed as relative standard deviation or RSD) was 0.5 % for the laboratory experiments (N = 86) and 1.3 % for the field experiment (N = 29). In the laboratory experiments, sufficient material was not available from any one growth interval to enable replicate analyses for an assessment of true sample precision; in the field experiment, however, sample precision was 6.2 % RSD for replicate measurements (N = 3) of the same milled powder samples obtained from five *Mytilus edulis* specimens. Furthermore, the same method as reported here was used in chapter 3 and obtained a Mg/Ca ratio precision of 3.5 % RSD for five replicate measurements of the same milled powder sample obtained from one *Pecten maximus* specimen. For comparison with past and future datasets, Mg/Ca ratio measurements also are reported for a set of solutions prepared by the Elderfield group at the University of Cambridge, U.K. (Greaves, pers. comm., 2003; cf. de Villiers et al., 2002), as well as for three solutions (BAM-RS3, ECRM-752 and CMSI-1767) that have been proposed as certified reference materials (CRMs) for Mg/Ca ratio measurements in carbonates (Greaves et al., 2005) and that are subject to an ongoing international inter-laboratory calibration study (Table 4-2). For each CRM, approximately 50 mg of powder was dissolved in 50 g of 0.075M HNO_3 (Merck Ultrapur), resulting in Ca concentrations in solution of ca. 400 µg/ml. Subsequently, 1.5 ml of each solution was centrifuged for 10 minutes and an aliquot then was pipetted into clean 12 ml centrifuge tubes and diluted to 10 ml to give final Ca concentrations of 50 and 30 µg/ml in order to match the sample and standard solutions. The linearity of the intensity-ratio calibration lines, combined with the independent assessment of the accuracy of the analytical procedure (Chapter 2 and

3), confirms the veracity of the *Mytilus edulis* and *Pecten maximus* Mg/Ca ratios obtained in this study.

Table 4 - 2 – Comparison of expected (Greaves et al., 2005) with measured Mg/Ca ratios for three certified reference material (CRMs) solutions.

CRM solution	Expected	Inter-laboratory	This study	% Difference
BAM-RS3	0.80	0.80 ± 0.01 (N = 6)	0.78 ± 0.12 (N = 9)	-3.0
ECRM-752	3.90	3.50 ± 0.04 (N = 6)	3.82 ± 0.07 (N = 13)	-2.1
CMSI-1767	6.10	5.58 ± 0.09 (N = 6)	5.76 ± 0.07 (N = 11)	-5.7

The values in the third column are those returned from the University of Wales Bangor as part of an ongoing international inter-laboratory comparison exercise, with the replicates representing six separate dissolutions of each CRM (1 ml of each solution was centrifuged for 10 minutes at ~6000 rpm and ca. 0.75 ml from each solution then diluted to final solution Ca concentrations of 60 μg/ml). By comparison, the replicates reported for this study in the fourth column are repeated measurements of a single dissolution completed for each CRM and diluted to Ca concentrations of 50 or 30 μg/ml. All measurements were made on the same Perkin Elmer Optima 3300RL ICP-AES instrument.

4.3.5 Statistical Analyses

Two-sample *t*-tests were used to determine statistically whether significant differences existed between measured shell Mg/Ca ratios precipitated at different seawater temperatures in pairs of constant-temperature aquaria. Herein, probability levels less than 5% ($p<0.05$) are considered significantly different. Linear regressions and ANOVA analyses of shell Mg/Ca ratios and seawater temperature were performed using the software package MINITAB. Regressions were compared by testing the equality of variance in the regression residuals, since unequal variance in the regression residuals (*F*-test, $p<0.05$) indicates significantly different regressions. GLM ANOVA has been used to test for differences in the slope and intercepts of the regressions. The variability in shell Mg/Ca ratios attributable to different factors was determined using fully nested ANOVA.

4.4 Results

4.4.1 Culture Conditions and Confirmation of Shell Precipitation in Thermodynamic Equilibrium

Seawater temperature was stable during experiment one, but more variable during experiment two, especially in the lower (10°C) and mid (15°C) temperature aquaria

(Figure 3). Nevertheless, clear temperature differences were maintained in the three different aquaria in each of the experiments (Figure 3). Aquaria mean seawater temperatures were 11.96±0.12°C, 15.61±0.12°C and 18.39±0.05°C during experiment one, and 10.76±0.41°C, 15.54±0.25°C and 20.23±0.22 °C during experiment two. Variation of $\delta^{18}O_{seawater}$ was different in the two experiments, with variable but increasing values from -0.10 to 0.10 ‰ during experiment one. In experiment two $\delta^{18}O_{seawater}$ decreased from initially high values (~0.08 ‰) to the lowest values observed (-0.33 ‰) in the middle of the experiment and then increased to 0.00 ‰.

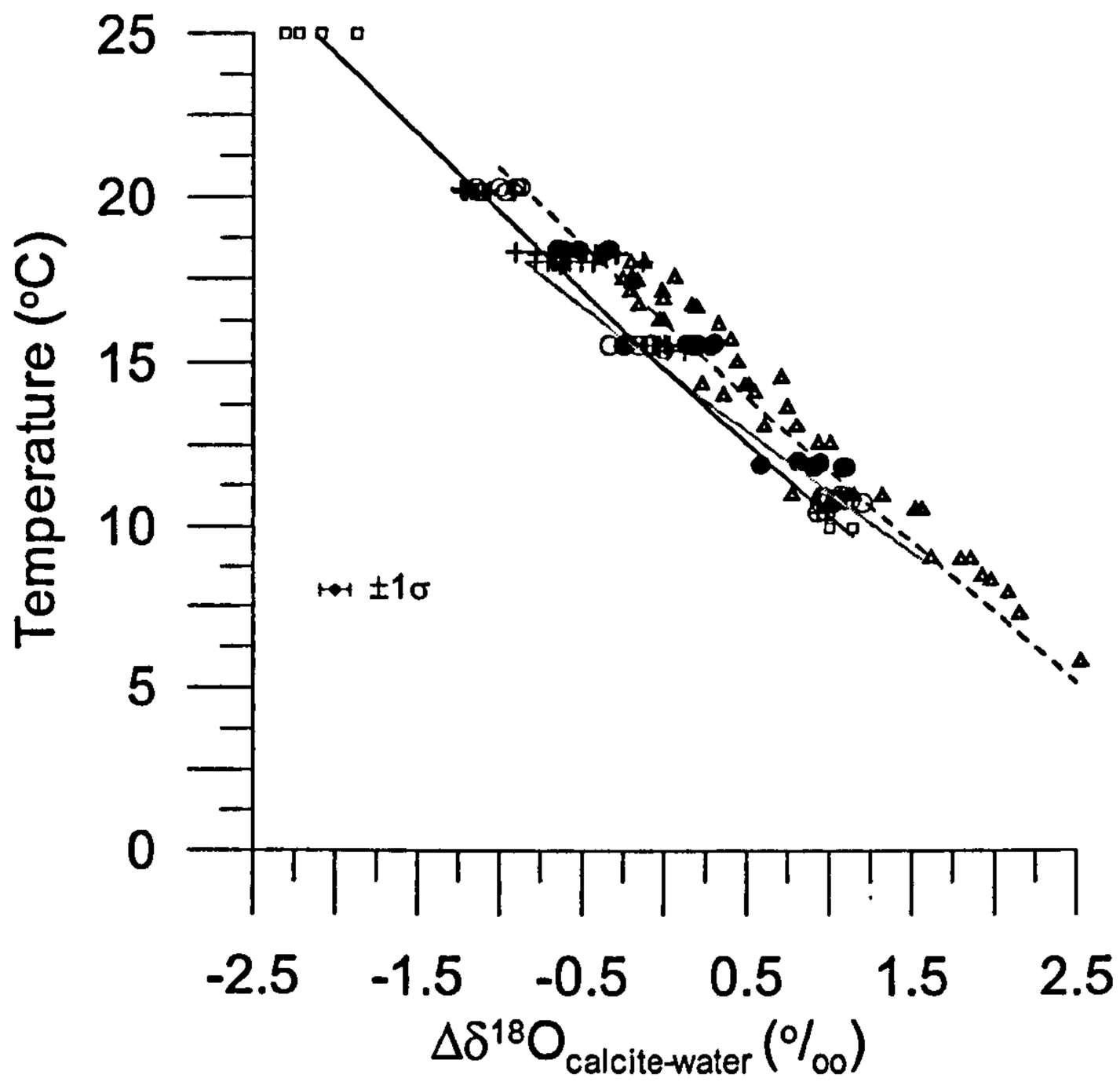

Figure 4 - 3 – Seawater temperatures plotted against mean $\Delta\delta^{18}O$ values ($\delta^{18}O_{carbonate}$ - $\delta^{18}O_{seawater}$, on the VPDB and VSMOW scale, respectively) for laboratory cultured *Mytilus edulis* (● - experiment one and ○ - experiment two) and *Pecten maximus* (+ - experiment two only), and field cultured *M. edulis* (Δ). Plotted also are the data (□ – solid black line) for inorganic calcite deposited from seawater in oxygen-isotope thermodynamic equilibrium from Kim and O'Neil (1997), but also species-specific palaeotemperature equations obtained for *P. maximus* (solid grey line) by Chauvaud et al., (2005) and *M. edulis* (dashed black line) by Wannamaker et al., (2007). Due to the use of different acid fractionation factors between the present study and Kim and O'Neil (1997), 0.25‰ was substracted from their original $\delta^{18}O_{carbonate}$ values. For comparison, twice the analytical error for $\delta^{18}O_{carbonate}$ - $\delta^{18}O_{seawater}$ (±0.09 ‰) also is shown

During the field culturing experiment, seawater temperature exhibited a clear seasonal pattern, and $\delta^{18}O_{seawater}$ was less seasonally variable (Figure 4a). Seawater temperature decreased from ca. 10.0°C in December 2004 to a minimum temperature

of ca. 5.0°C in the end of February, followed by a rise to ca. 9.5°C during mid March–late April (from day 105 to 140) and then a further rise up to a maximum temperature of ca. 19.0°C in early–mid July (ca. day 225). From that time to early September (ca. day 280) seawater temperature remained high at ca. 18.0°C, before it decreased to ca. 9.0°C in December 2005. During the field culturing experiment, $\delta^{18}O_{seawater}$ varied from -0.48 to 0.03 ‰, with a mean value of -0.20 (±0.13) ‰, with lower values usually occurring during winter and higher values during spring and summer (Figure 4a).

The variation of oxygen-isotope data ($\Delta\delta^{18}O_{carbonate\text{-}seawater}$ = shell $\delta^{18}O$ values minus seawater $\delta^{18}O$ values) of *M. edulis* and *P. maximus* with temperature (Figure 5) was compared to previously derived data for the precipitation of inorganic calcite from seawater in oxygen-isotope thermodynamic equilibrium (Kim and O'Neil, 1997), but also to species-specific palaeotemperature equations obtained for *P. maximus* (Chauvaud et al., 2005) and *M. edulis* (Wanamaker et al., 2006; Wanamaker et al., 2007). *P. maximus* and *M. edulis* $\Delta\delta^{18}O_{carbonate\text{-}seawater}$ values at each temperature are similar for both species, similar for laboratory- and field-grown *M. edulis* specimens and similar to oxygen-isotope equilibrium values (Figure 5). Thus, during both the laboratory and field culturing experiments deposition of new shell material occurred in or close to oxygen-isotope equilibrium.

4.4.2 Shell Mg/Ca Records and Variability of Shell Calcite Mg/Ca Ratios from Laboratory Cultured Mytilus edulis and Pecten maximus

Measured shell Mg/Ca ratios range from 2.84 to 9.50 mmol/mol in *Mytilus edulis* (experiments one and two) and from 8.08 to 29.92 mmol/mol in *Pecten maximus* (experiment two) over the experimental temperature range (Figure 4-4). Four main features are clear from the shell Mg/Ca ratio data: 1) Variability of shell Mg/Ca ratios at each temperature is very large for both species (Figures 4-4 and 4-5). 2) Despite the high degree of variability, a significant ($p<0.001$ for both species), albeit weak, correlation exists between seawater temperature and shell Mg/Ca ratios in both species (r^2 = 0.38 and 0.57 for *Mytilus edulis* in experiment one and two, respectively; r^2 = 0.21 for *P. maximus* in experiment two). 3) In experiment two, during which both species were grown at the same temperatures and in the same

aquaria, shell Mg/Ca ratios are approximately three times higher in *P. maximus* than in *M. edulis* (*t*-test, $p<0.001$, degrees of freedom ≥ 41 for all temperatures). 4) For *M. edulis* that was cultured in both experiment one and two there is a significant difference in the Mg/Ca ratio to temperature relationship between experiments and shell Mg/Ca ratios were higher in experiment two than in experiment one (Figure 4-4).

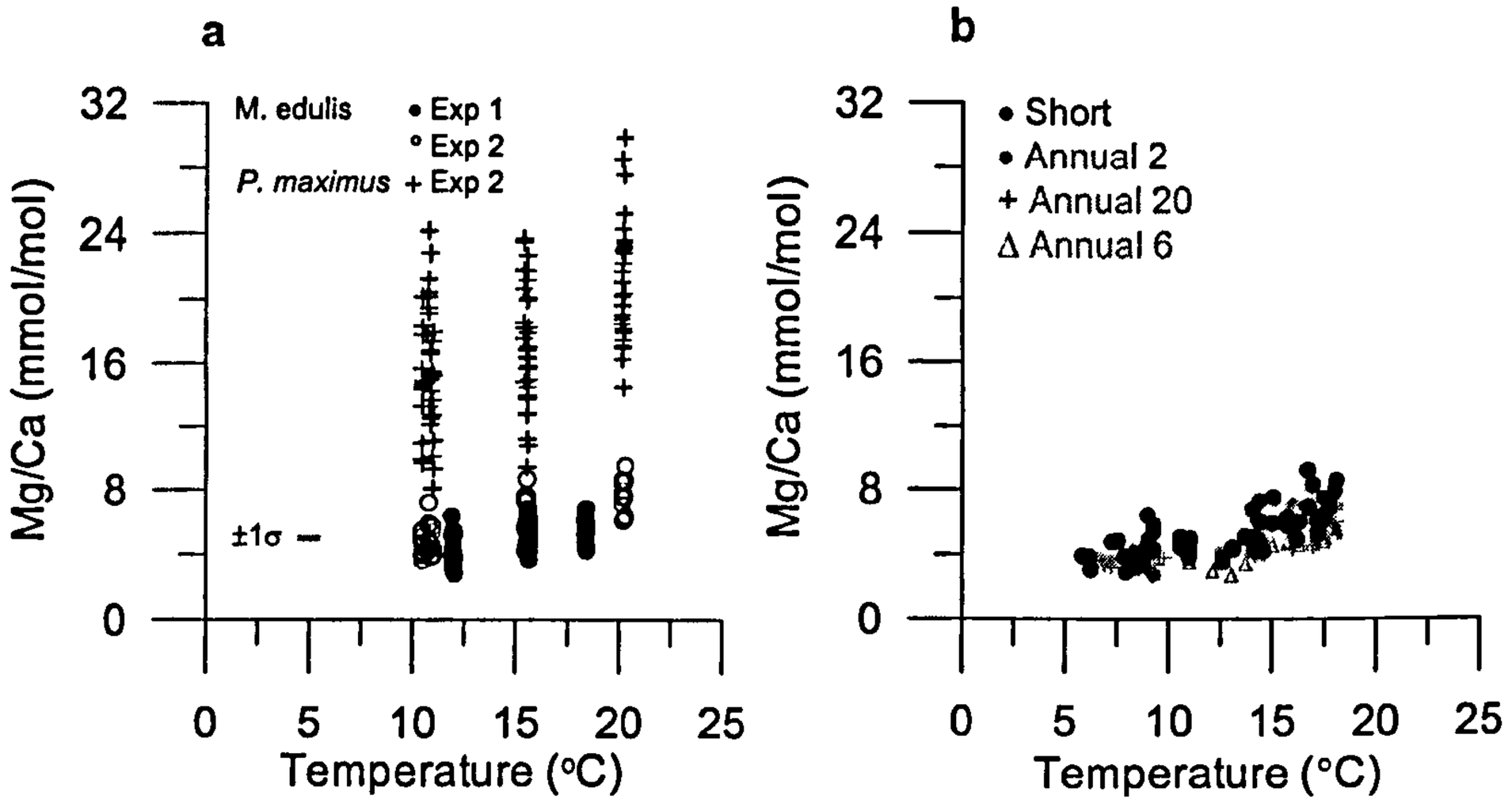

Figure 4 - 4 – Shell Mg/Ca ratios against seawater temperature from: a) laboratory cultured *Mytilus edulis* (● - experiment one and ○ - experiment two) and *Pecten maximus* (+ - experiment two only); b) field cultured *M. edulis* (● – short-deployment specimens; annual-deployment specimens, see Chapter 6 for a detailed description of field experiment design: ● - A2, Δ - A6 and + - A20). Each point represents a paired seawater temperature value and Mg/Ca ratio obtained for individual growth intervals. For comparison, twice the analytical error (±0.10 mmol/mol) also is shown.

Irrespective of the observation that shell Mg/Ca ratios are significantly, albeit weakly, correlated with temperature in both bivalve species, the significant differences evident in the absolute shell Mg/Ca ratios of the two species indicate a clear species-specific Mg/Ca ratio–temperature relationship for the two bivalve species investigated in this study. Furthermore, the degree of variability of shell Mg/Ca ratios at each temperature also is higher in *Pecten maximus* than in *Mytilus edulis*. Unequal variance in the residuals indicates significantly different regressions of Mg/Ca ratios with temperature between *M. edulis* and *P. maximus* from experiment two (*F*-test, $p < 0.05$). The linear fit of Mg/Ca ratios (mmol/mol) to seawater temperature (°C), with 95% confidence intervals, is for *M. edulis* Mg/Ca = 1.286 (± 0.84,) + 0.320 (± 0.072) * T (N = 59) while for *P. maximus* is Mg/Ca = 9.886 ± 2.96 + 0.520 ± 0.19 * T (N = 111). ANOVA analysis of the regressions of

Mg/Ca with temperature shows that the slope of the linear regressions does not differ significantly ($F = 2.13$, $p = 0.146$), but that the intercept does ($F = 37.67$, $p<0.001$).

Mytilus edulis shell Mg/Ca ratios also are statistically different between the two experiments, with higher values during experiment two (Figure 4-4). The correlation between *M. edulis* shell Mg/Ca ratios and temperature also is stronger in experiment two than in experiment one ($r^2 = 0.38$ and 0.57 in experiment one and two, respectively, $p<0.001$ in both experiments), although this may be due solely to the smaller number of individuals analysed in experiment two compared to experiment one, i.e. the capture of a smaller degree of Mg/Ca ratio variability, as well the greater temperature range for the experiment two regression. Unequal variance in the residuals confirms significantly different regressions of Mg/Ca ratios with temperature in *M. edulis* between experiments one and two (F-test, $p<0.05$). Further analysis of variance of the regressions of *M. edulis* Mg/Ca ratios and temperature shows that the slope of the regressions is not significantly different ($F = 2.50$, $p = 0.116$), but that the intercept ($F = 127.92$, $p<0.001$) is different in the two experiments.

Evidence exists for statistically significant (t-test, $p<0.05$) inter-individual shell variability of shell Mg/Ca ratios between individuals cultured within any one aquarium (Figure 4-5). Maximum differences between mean shell Mg/Ca ratios from different *Mytilus edulis* individuals cultured in the same aquarium were: 1.3 mmol/mol at 12°C (N = 7), 1.9 mmol/mol at 15°C (N = 6) and 2.1 mmol/mol at 18°C (N = 6) in experiment one and 1.2 mmol/mol at 10°C (N = 6), 3.3 mmol/mol at 15°C (N = 6) and 3.0 mmol/mol at 20°C (N = 6) in experiment two. For *Pecten maximus* maximum differences between mean Mg/Ca ratios from different individuals cultured in experiment two were: 8.9 mmol/mol at 10°C (N = 8), 9.2 mmol/mol at 15°C (N = 10) and 9.0 mmol/mol at 20°C (N = 10).

In addition to inter-individual shell variability, there is also a degree of intra-individual shell variability in Mg/Ca ratios within the dataset, i.e. between milled samples taken from different growth intervals (Figure 4-5). For either species, the proportion of individual shells that produced Mg/Ca ratios significantly different among samples milled from the same specimen (i.e. the difference between any two

Mg/Ca measurements was larger than twice the analytical error) was similar at each temperature. However, *P. maximus* showed a higher frequency of milled samples with different Mg/Ca ratios within an individual shell (> 97% in all aquaria) than did *M. edulis*, (68% < experiment one < 73%, and 72% < experiment two < 83%).

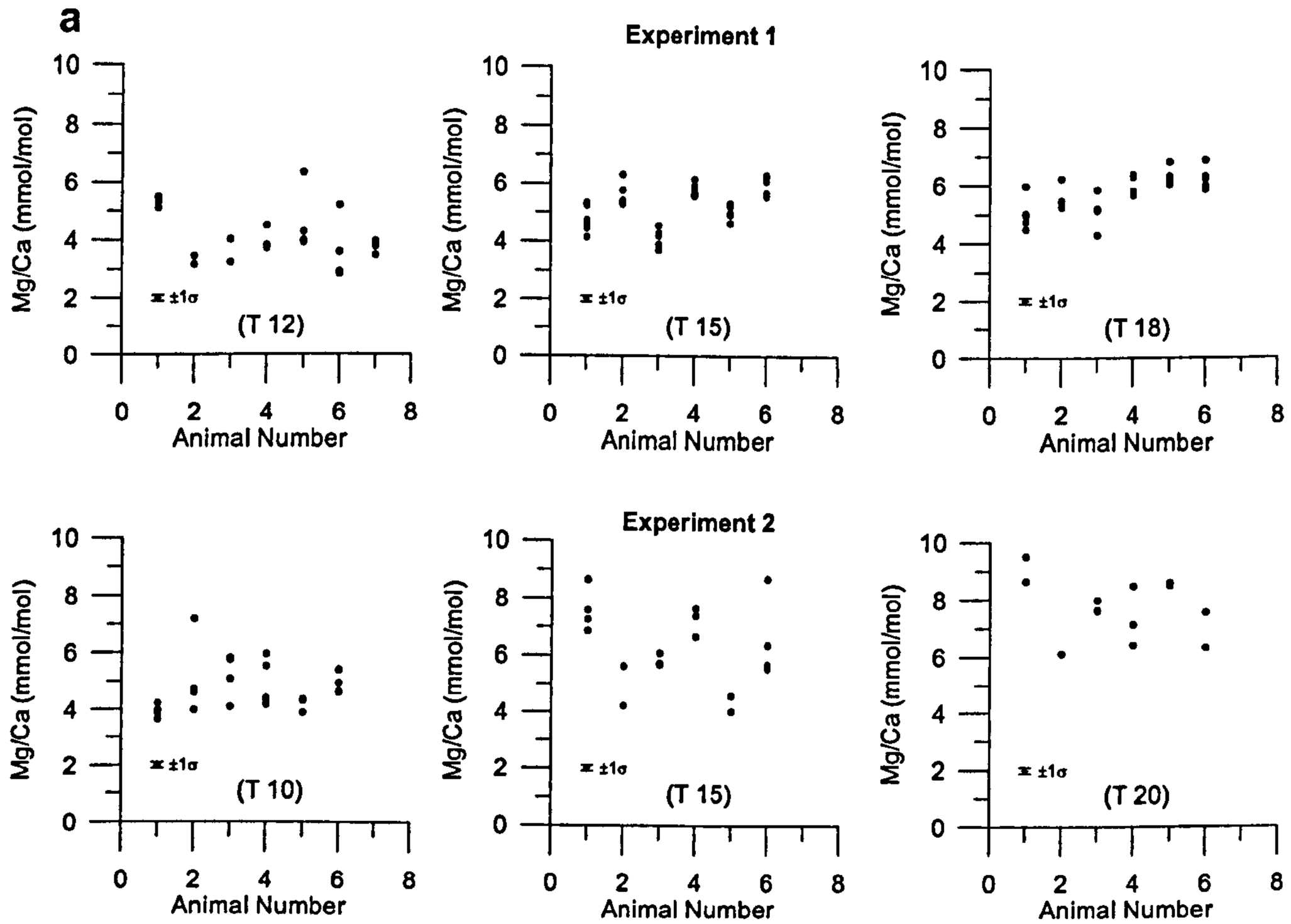

Figure 4 - 5 – Shell Mg/Ca samples plotted against animal number for each aquarium (temperature in brackets) in order to illustrate inter- and intra-individual shell variability of Mg/Ca ratios in a) *Mytilus edulis* and b) *Pecten maximus*. For each animal, individual data points correspond to Mg/Ca ratios of new shell growth deposited in the experiment during different growth intervals. For comparison, twice the analytical error (±0.10 mmol/mol) also is shown.

4.4.3 Shell Mg/Ca Records and Variability of Shell Calcite Mg/Ca Ratios from Field Cultured Mytilus edulis

In field cultured *Mytilus edulis*, measured shell Mg/Ca ratios range from 2.96 to 9.16 mmol/mol in the short specimens; from 2.86 to 8.34 mmol/mol in the A2 specimen; from 2.78 to 5.97 mmol/mol in the A6 specimen and from 2.75 to 6.11 mmol/mol in the A20 specimen (Figure 4-4).

In field cultured *Mytilus edulis*, a significant ($p<0.001$ for all specimens), albeit not strong, correlation exists between seawater temperature and shell Mg/Ca ratios (Figure 4-4): $r^2 = 0.54$ for the short specimens ($N = 62$); $r^2 = 0.77$ for the A2 specimen ($N = 28$); $r^2 = 0.72$ for the A6 specimen ($N = 34$) and $r^2 = 0.81$ for the A20 specimen ($N = 30$). However, the correlation between shell Mg/Ca ratios and temperature is weaker ($r^2 = 0.50$, $p < 0.001$) when all data from all specimens is pooled together. Furthermore, variance of the residuals was only equal for the regressions of Mg/Ca ratios with temperature between *M. edulis* specimens between short and A2 specimens and between A6 and A20 (F-test, $p > 0.05$). In all other specimens, unequal variance of residuals indicates significantly different regressions of Mg/Ca ratios with temperature (F-test, $p < 0.05$). ANOVA analysis of the regressions of Mg/Ca with temperature between short and A2 specimens, and between A20 and A6 specimens, shows that the slope of the linear regressions does not differ significantly ($F = 2.70$, $p = 0.104$ and $F = 1.40$, $p = 0.242$, respectively), but that the intercept does ($F = 126.11$, $p<0.001$ and $F = 196.31$, $p<0.001$, respectively). Evidence thus exists for significant inter-individual variability of shell Mg/Ca ratios and its relationship with temperature from *M. edulis* specimens grown in the same field culture conditions. Maximum shell Mg/Ca ratios, in particular, are markedly different between individual specimens and range from 5.97 to 9.16 mmol/mol.

For the same range of temperature, shell Mg/Ca ratios of *M. edulis* grown in the laboratory- and field-culturing experiments showed a similar range (Figure 6). However, the correlation between Mg/Ca ratios and temperature was stronger in field cultured ($0.54 < r^2 < 0.81$) than in laboratory cultured *M. edulis* specimens ($0.38 < r^2 < 0.57$). Furthermore, ANOVA analysis of the regressions of Mg/Ca with

temperature between laboratory cultured and field cultured *M.edulis* specimens shows that the slope of the linear regressions does not differ significantly ($F = 0.70$, $p = 0.799$), but that the intercept does ($F = 224.68$, $p<0.001$).

4.5 Discussion

4.5.1 Inter-Species, Inter-Individual and Intra-Individual Variability in Shell Mg/Ca Ratios

In addition to the weak, but significant, relationships with seawater temperature, the shell Mg/Ca ratio data obtained in this study also clearly show a large degree of variability in absolute shell Mg/Ca ratios in both *Mytilus edulis* and *Pecten maximus* species. As in other bivalve geochemical and physical proxies (for review, see e.g. Richardson, 2001), variability of shell Mg/Ca ratios occurs at different levels, requiring consideration of differences between the two bivalve species cultured (inter-species level), between shells of different individuals grown simultaneously in the same aquarium and under the same culture conditions (inter-individual shell level) and within individual shells, i.e. between milled samples taken from one individual shell that correspond to different growth intervals during the experimental period (intra-individual shell level).

Differences in shell Mg/Ca ratios of the same species have been observed in previous field-based studies at levels of both inter- and intra-individual shell variability (Rosenberg and Hughes, 1991; Klein et al., 1996a; Vander Putten et al., 2000; Freitas et al., 2005; Lorrain et al., 2005; Freitas et al., 2006). For example, Klein et al. (1996) presented data from two field-collected shells (British Columbia, Canada) of the mussel *Mytilus trossulus* which clearly show large Mg/Ca ratio differences at inter- (up to 2.5 mmol/mol) and intra- (up to 1.5 mmol/mol) individual shell levels, in addition to a temperature relationship ($r^2 = 0.74$, $p<0.001$) over a range from 5.5 to 22.7°C. By comparison, Vander Putten et al. (2000) reported inter-individual differences in Mg/Ca ratios between four *Mytilus edulis* field-grown shells (Schelde Estuary, Netherlands) as high as ~7 mmol/mol. Similarly, Lorrain et al. (2005)

presented data from four *Pecten maximus* specimens collected from the Bay of Brest, France, where differences of up to 6 mmol/mol in Mg/Ca ratios were observed between individual specimens for shell samples that corresponded to the same time of calcification. Most recently, in three *P. maximus* specimens grown in a field-based experiment, and for a similar temperature range to that used in the present laboratory culturing study (10 to 20°C), differences were observed in Mg/Ca ratios of up to 7.5 mmol/mol between shells (Chapter 3). Specifically, for $\delta^{18}O$-derived calcification temperatures of 10 ± 0.5°C (N = 8) and 15 ± 0.5°C (N = 6), Mg/Ca ratios varied by up to 4.06 and 5.61 mmol/mol, respectively (Chapter 3). The inter- and intra-individual variability of Mg/Ca ratios in shell calcite of *M. edulis* and *P. maximus* grown in field-based and laboratory culturing studies thus are of similar magnitude.

Significant differences in absolute shell Mg/Ca ratios can be observed between the two cultured bivalve species (Figure 4-4); *P. maximus* shell Mg/Ca ratios being approximately three times higher than those in *M. edulis*. Large variations in the Mg content of biogenic calcite from different species has been observed previously in bivalves (Lorens and Bender, 1980; Klein et al., 1996a; Vander Putten et al., 2000; Lorrain et al., 2005). The Mg/Ca ratio data obtained in this study for laboratory cultured *M. edulis* and *P. maximus* have been compared to previously published data for other marine bivalve species investigated in field-based studies (Figure 4-6). On the whole, a large degree of overlap can be observed between the Mg/Ca ratio data derived from the laboratory and field cultured *M. edulis* and *P. maximus* specimens. Nevertheless, laboratory and field cultured *M. edulis* show lower shell Mg/Ca ratios than data reported from field experiments for *M. edulis* (Vander Putten et al., 2000), although the latter data were obtained by laser ablation ICP-MS and there is the potential for calibration issues between datasets. The Mg/Ca ratios for *M. edulis* cultured in this study are, however, similar to Mg/Ca ratios reported for *M. trossulus* (Klein et al., 1996a), a close relative of *M. edulis*. Shell Mg/Ca ratios in the *P. maximus* animals cultured in this study are similar to Mg/Ca ratios reported for specimens of the same species grown or collected in field studies (Lorrain et al., 2005; Chapter 3), but extend to higher values and also show a larger variability than in specimens grown at a field location adjacent to the present aquarium based study (Chapter 3). This latter observation suggests that the influence of any non-temperature control (i.e. physiological factors) on *P. maximus* shell Mg/Ca ratios

may well be stronger under laboratory culture conditions than in field-based situations that more closely mimic the conditions best suited for optimal growth of natural populations.

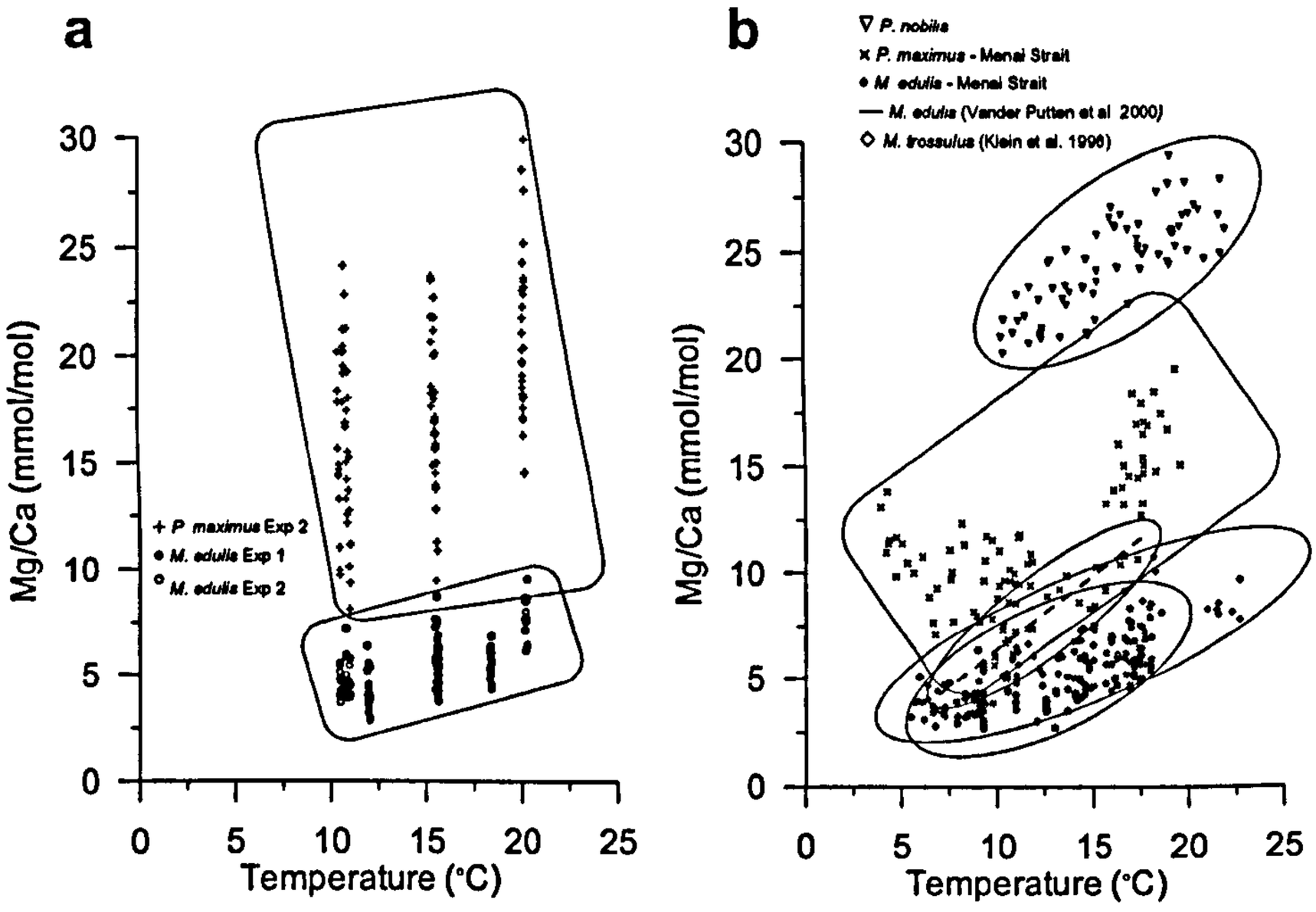

Figure 4 – 6 – Comparison of bivalve calcite shell Mg/Ca ratios, plotted against temperature, from: a) laboratory culturing completed in this study for *Pecten maximus*[1] and *Mytilus edulis*[1]; and b) field culturing completed in this study for *Mytilus edulis*[1] and other field-based studies, for the species: *Mytilus edulis* (Vander Putten et al., 2000)[1], *Pecten maximus* (Chapter 3)[2], *Mytilus trossulus* (Klein et al., 1996a)[1] and *Pinna nobilis* (Chapter 2)[2]. [1 denotes temperature is measured seawater temperature; 2 denotes temperature is $\delta^{18}O_{calcite}$-derived calcification temperature].

4.5.2 Imprecise Temperature Control on Shell Mg/Ca Ratios

Despite the observation that the shell and seawater oxygen-isotope composition relationship was significantly correlated to seawater temperature, indicating shell deposition in or near to oxygen-isotope thermodynamic equilibrium (Figure 4-3), one obvious feature of the measured shell Mg/Ca ratios obtained from specimens of *Mytilus edulis* and *Pecten maximus* cultured in the constant-temperature aquaria in this study is that there is only a weak dependence on temperature (Figure 4-4 and Table 4-3). Nevertheless, in *M. edulis* specimens cultured in the field, shell Mg/Ca ratios were significantly correlated with temperature ($0.54 < r^2 < 0.81$). However, the inter-individual variability of Mg/Ca ratios is large (Figure 4-4) and results in a weaker correlation ($r^2 = 0.50$, $p < 0.001$) when data from all specimens is pooled together. Furthermore, linear regressions of Mg/Ca ratios with temperature are

different between individual specimens and thus do not support the use of a single valid regression for all specimens. Such an observation contrasts markedly with the well-documented temperature dependent incorporation of Mg into inorganic calcite experimentally precipitated from seawater (Chilingar, 1962; Katz, 1973a; Burton and Walter, 1987; Mucci, 1987b; Oomori et al., 1987) and in other biogenic calcites (e.g. Dwyer et al., 1995; Nurnberg et al., 1996a; Stoll et al., 2001). Clearly, as has been observed previously in some field studies, the weak temperature dependence of shell Mg/Ca ratios in the two marine bivalve species that were cultured is a feature specific to the incorporation of Mg into the calcite shells of these organisms and must therefore relate to their specific biomineralization processes, including any secondary physiological influences.

The suggestion of additional, physiological controls on Mg/Ca ratios in bivalve calcite (i.e. metabolic or kinetic controls) is supported further by the significant difference in the absolute shell Mg/Ca ratios in *Mytilus edulis* grown at 15°C in two aquaria in experiments one and two of ~1.1 mmol/mol (*t*-test, $p = 0.004$, $DF = 24$), but also by the large inter- and intra-individual variability of Mg/Ca ratios observed in both the laboratory and field cultured bivalves (Figure 4-4). These observations clearly indicate that specimens from the same species cultured at different times at the same seawater temperature can have different shell Mg/Ca ratios. It is therefore important to recognise that other non-thermodynamic factors in the two experiments must also have influenced shell Mg/Ca ratios. Furthermore, it is not possible to discount the possibility that the *M. edulis* animals cultured in experiment two were better conditioned for the laboratory environment than those in experiment one, due to their longer acclimation in the experimental aquaria prior to commencement of the experimental period.

Given the experimental design in this study, only factors that were entirely independent of seawater temperature can be discussed as additional potential controls on shell Mg/Ca ratios. This consideration thus prohibits a detailed discussion of the influence of shell growth rate on shell Mg/Ca ratios, since growth rates co-vary significantly with temperature in both the laboratory (for *Pecten maximus*, $r^2 = 0.62$, $p < 0.001$; for *Mytilus edulis*, $r^2 = 0.23$, $p = 0.001$ and $r^2 = 0.15$, $p = 0.032$ in experiment one and two, respectively) and field culture experiments (for *M. edulis*,

$0.26 < r^2 < 0.43$, $p < 0.002$). Nevertheless, as reported by Lorens and Bender (1980) for cultured *M. edulis* specimens, shell Mg/Ca ratios also were only weakly correlated to shell growth rates in both the laboratory and field culture experiments (Table 4-3).

Table 4 - 3 – Summary of correlations between Mg/Ca and temperature, shell growth rate (SGR – μm/day) and salinity for all laboratory (temperature = experiment one and two) and field culture experiments.

Experiment		Temperature r^2	Temperature p	SGR r^2	SGR p	Salinity r^2	Salinity p
Temperature							
M. edulis	Exp 1	0.38	< 0.001	0.19	0.006	-	> 0.05
	Exp 2	0.57	< 0.001	0.33	< 0.001	-	> 0.05
	Exp 1+2	0.37	< 0.001	0.23	< 0.001	-	> 0.05
P. maximus	Exp 2	0.21	< 0.001	0.09	0.002	0.21	< 0.001
Field							
M. edulis		0.50	<0.001	0.22 to 0.41	< 0.004	-	-

A metabolic control, i.e. the physiological exclusion of Mg from its shell-forming fluid (the extra-pallial fluid or EPF), on calcite Mg content has been proposed previously for *Mytilus edulis* (Lorens and Bender, 1977; Lorens and Bender, 1980). Metabolic control also was suggested as a possible way of explaining an observed seasonal breakdown in the relationship between Mg/Ca and temperature reported for *M. edulis* (Vander Putten et al., 2000). An apparent ontogenetic control of Mg/Ca ratios has been described in the fan mussel *Pinna nobilis*, although a temperature control on shell Mg/Ca ratios also was present in this species (Chapter 2). For *Pecten maximus*, recent field-based studies have shown the absence of a significant correlation between shell Mg/Ca ratios and seawater temperature (Lorrain et al., 2005) or a strong seasonal variation in the strength of the correlation between shell Mg/Ca ratios and seawater temperatures, again suggesting that other factors must influence Mg/Ca ratios in *P. maximus* shell calcite (Chapter 3).

Seawater salinity is a truly independent variable in the laboratory culture experiment, but not in the field culture experiment where it co-varies with seawater temperature ($r^2 = 0.50$, $p<0.001$). Any differences in seawater salinity between the laboratory experiments thus could influence the amount of magnesium available for

incorporation, assuming that shell Mg/Ca ratios are not solely related to seawater Mg/Ca ratios. Indeed, Lorens and Bender (1980) have shown that shell Mg/Ca ratios increase with increasing solution Mg concentrations, albeit at much higher concentrations than would be expected from natural changes in seawater salinity. Although, an earlier study by Dodd (1965) observed the opposite trend of increasing Mg concentrations in *Mytilus edulis* shell calcite with decreasing salinity. In addition, salinity has been reported to significantly influence the Mg/Ca ratios of foraminifera calcite (Lea et al., 1999). In *M. edulis*, salinity was not significantly correlated with shell Mg/Ca ratios in the two laboratory experiments in this study ($p>0.05$), and only weakly, in *Pecten maximus* ($r^2 = 0.21$, $p<0.001$). The strength of this correlation between shell Mg/Ca ratios and salinity is of comparable magnitude to that between temperature and shell Mg/Ca ratios ($r^2 = 0.21$, $p<0.001$). Nevertheless, temperature and salinity together ($r^2 = 0.37$, $p<0.001$) still do not explain much more of the observed shell Mg/Ca variability in *P. maximus* than just temperature alone.

4.5.3 Are Mg/Ca Ratios in Bivalve Calcite an Unreliable Palaeotemperature Proxy?

Bivalve molluscs, like other calcifying organisms, are capable of regulating or at least influencing to variable extents, the Mg content of their calcium carbonate skeletons (Dodd, 1965; Lorens and Bender, 1977; Neri et al., 1979; Onuma et al., 1979; Lorens and Bender, 1980; Rosenberg and Hughes, 1991; Rosenberg et al., 2001). This phenomenon can be expressed by temperature-dependent partition coefficients (D_{Mg}) between the solid mineral phases and ambient seawater medium ($D_{Mg} = Mg/Ca_{calcite} / Mg/Ca_{seawater}$). In other words, the differences in the Mg content of calcite secreted by different taxa, as well as differences in Mg/Ca ratios between and within individuals of a single species, suggest a strong physiological control of the incorporation of Mg into biogenic calcites. Examples of such physiological effects that may influence, either directly or indirectly, the Mg content of bivalve shell calcite are: variable chemical composition of the precipitating fluid, i.e. the EPF, resulting from biological control on differential transport of ions into and out of the EPF; variable calcification rates; and differences in crystal growth orientation and morphology (Mucci and Morse, 1983; Reeder and Grams, 1987; Debeney et al., 2000; Erez, 2003; Wasylenki et al., 2005a).

Small-scale heterogeneous distribution of Mg may represent a particularly relevant source of error in the use of bivalve calcite Mg/Ca ratios as a palaeotemperature proxy. Lorens and Bender (1980) have described significant small-scale variability of Mg/Ca ratios, from <5 to 40 mmol/mol over scales of 100's μm, in the very first new shell growth from *Mytilus edulis* cultured in natural seawater under controlled conditions at temperatures between 22 and 24°C. Significant small-scale variability of Mg/Ca ratios has also been observed in *M. edulis* and *Pecten maximus* shells grown in the same experiment as the present study (Chapter 6). Small scale variations in Mg concentrations in *M. edulis* calcite have been shown to derive from Mg being concentrated along the margins of calcite prisms, especially along the terminations of the crystals, with the alignment of adjacent crystals then producing compositional growth bands within the shell (Rosenberg et al., 2001). The latter observation lead to the suggestion that in *M. edulis* Mg and also sulphur in the shell could control rates of shell crystal elongation, shell curvature along different axes and ultimately the Mg distribution throughout the shell (Rosenberg et al., 2001).

The use of Mg/Ca ratios from bivalve calcite shells as a reliable and accurate temperature proxy thus remains unlikely at present, at least in the species studied to date. The now well-documented variation of Mg/Ca ratios in bivalve calcite at species-specific, inter- and intra-individual shell levels prevents the establishment of valid Mg/Ca ratio–temperature relationships, even for individual species. Furthermore, there exists support for a strong physiological control of Mg/Ca ratios in bivalve shells (Lorens and Bender, 1977; Lorens and Bender, 1980; Rosenberg and Hughes, 1991; Vander Putten et al., 2000; Rosenberg et al., 2001) present study, although the mechanisms by which such control acts are still not fully clear, as well as for extensive small-scale heterogeneity in shell Mg contents (Lorens and Bender, 1980; Rosenberg et al., 2001; Chapter 6). Future research should address these issues in greater detail, if ever this geochemical proxy is to be used as a reliable and accurate temperature proxy in bivalve calcite.

4.6 Conclusions

In a laboratory and field culturing experiments only a weak dependence on temperature, as well as a large degree of variability, has been observed for shell Mg/Ca ratios in calcite sampled from two marine bivalve species, *Mytilus edulis* and *Pecten maximus*. Such variability is significant at the species, inter- and intra-individual shell levels, and most likely reflects the influence of additional secondary physiological factors influencing shell biomineralisation and Mg content. Shell Mg/Ca ratios were different between *M. edulis* and *P. maximus*, being three to five times greater in the latter species. The variability of shell Mg/Ca ratios for laboratory cultured *M. edulis* in the present study was similar to the variability observed in previous field-grown specimens. Laboratory cultured *P. maximus* specimens, however, showed approximately twice the variability of shell Mg/Ca ratios than has been reported previously for field-grown specimens. In the two species, shell Mg/Ca ratios were not found to be controlled by shell growth rate and salinity. The Mg/Ca ratio data obtained in the present laboratory and field culturing of *M. edulis* and *P. maximus*, together with supporting evidence from previous field studies, clearly suggests that bivalve Mg/Ca ratios do not yet appear to be a reliable and precise temperature proxy. Strong metabolic controls and extensive small-scale heterogeneity in shell Mg content may even prevent unique Mg/Ca ratio to temperature relationships for individual species to be defined. Unless the secondary controls (i.e. metabolic and/or kinetic factors) on Mg incorporation, and their influence on the small-scale heterogeneity of shell Mg content, can be understood in more detail, and subsequently compensated for, the use of this geochemical proxy as a reliable and accurate temperature proxy remains unlikely, at least in the species studied to date.

Chapter V

Sr/Ca ratios in the calcite shells of the marine bivalves *Mytilus edulis* and *Pecten maximus*: Evidence of physiological controls from laboratory and field culturing experiments.

V - Sr/Ca ratios in the calcite shells of the marine bivalves *Mytilus edulis* and *Pecten maximus*: Evidence of physiological controls from laboratory and field culturing experiments

5.1 Abstract

The minor and trace element composition of natural carbonates has been widely used in paleoclimatic studies. The Sr/Ca ratios preserved in the skeletons of corals and sclerosponges have been successfully used as temperature proxies. In abiogenic calcite, Sr/Ca ratios are strongly controlled by precipitation rate and previous work on aragonitic and calcitic bivalve shells suggests a major control of Sr/Ca ratios by growth rate, but the role of metabolic activity on shell Sr/Ca ratios remains inconclusive. The influence of physiological (shell growth rate and metabolic activity) controls on the Sr/Ca ratios of shell calcite was investigated in two marine bivalve species, *Mytilus edulis* (blue mussel) and *Pecten maximus* (king scallop), grown in laboratory and field (*M. edulis* only) culturing experiments. Seawater temperature was clearly not a significant control of bivalve calcite Sr/Ca ratios, while shell growth rate was found to exert a significant influence on shell Sr/Ca ratios of *M. edulis*, but only a weak influence on shell Sr/Ca ratios of *P. maximus*. The positive relationship observed between absolute respiration rate, a measure of metabolic activity, and Sr/Ca ratios in *M. edulis* grown in the laboratory and field culturing experiments provides the first direct evidence of a metabolic activity control in bivalve calcite Sr/Ca ratios. In addition, a significant inverse relationship between Sr/Ca and shell $\delta^{13}C$ ratios was observed in *M. edulis, P. maximus* and *Pinna nobilis*, and thus further supports a control of shell Sr/Ca ratios by metabolic

activity. High metabolic activity is thus suggested to increase both the transport of Sr^{2+} and low $\delta^{13}C$ metabolic carbon into the EPF, ultimately resulting in higher shell Sr/Ca ratios as well as lower shell $\delta^{13}C$ ratios.

5.2 Introduction

Natural carbonates contain a variety of co-precipitated ions other than Ca, which reflect their mode and environment of formation. However, element incorporation in biogenic carbonates is only partially dependent on environmental factors and physiological effects (often called vital effects), both kinetic and metabolic, may also significantly influence the incorporation of elements such as Mg and Sr in biogenic carbonates (e.g. Lorens and Bender, 1980; Delaney et al., 1985; Rosenberg and Hughes, 1991; de Villiers et al., 1995; this study; Klein et al., 1996b; Lea et al., 1999; Elderfield et al., 2001; Bentov and Erez, 2005). Such biological effects, and the mechanisms through which they act, thus must be thoroughly assessed to validate the potential use of these geochemical proxies from biogenic carbonate archives.

Strontium is the second most abundant cationic impurity in carbonates after Mg, and its incorporation is significantly influenced by mineralogy, forming a solid solution with aragonite due to its large ionic radius (Speer, 1983), but also substitutes for Ca in the calcite crystal lattice (Pingitore et al., 1992). Inorganic precipitation experiments have shown Sr incorporation in aragonite to be inversely related to temperature (Kinsman and Holland, 1969b; Dietzel et al., 2004) but independent on precipitation rate (Zhong and Mucci, 1989). In experimentally precipitated inorganic calcite, Sr/Ca ratios are strongly dependent on precipitation rate (Lorens, 1981a; Morse and Bender, 1990; Tesoriero and Pankow, 1996), and also are influenced by the Sr/Ca ratio of the solution from which precipitation occurred (Mucci and Morse, 1983; Pingitore and Eastman, 1986), and the Mg content of the solution and solid mineral which favours the incorporation of other elements by distorting the mineral lattice (Mucci and Morse, 1983; Ohde and Kitano, 1984; Morse and Bender, 1990).

Sr/Ca ratios from biogenic carbonates have been proposed or used to obtain information on past seawater temperatures (Weber, 1973; Beck et al., 1992; Guilderson et al., 1994; Hughen et al., 1999; McCulloch et al., 1999; Rosenheim et al., 2004), but also on past ocean Sr/Ca ratios (Martin et al., 1999; Stoll et al., 1999). Nevertheless, in biogenic carbonates, kinetic effects are thought to strongly influence Sr incorporation in biogenic aragonite, where control by precipitation rate is not expected, such as in corals (e.g. de Villiers et al., 1995; Cohen et al., 2001) and bivalves (Takesue and van Geen, 2004; Gillikin et al., 2005b; Carré et al., 2006), but also in biogenic calcite such as foraminifera (Lea et al., 1999), coccoliths (Stoll and Schrag, 2000; Rickaby et al., 2002; Stoll et al., 2002a; Stoll et al., 2002b) and bivalves (Lorrain et al., 2005; Chapter 3). A positive temperature influence on Sr/Ca ratios of biogenic calcite also has been observed in foraminifera (Lea et al., 1999), coccoliths (Stoll et al., 2002a; Stoll et al., 2002b) and bivalves (Dodd, 1965; Lorrain et al., 2005; Chapter 3) but can be attributed to a kinetic influence and a co-variation between temperature and growth rates.

In bivalve calcite, the mechanisms controlling Sr incorporation continue to be investigated and the matter of some debate, and both kinetic (Lorrain et al., 2005; Chapter 3) and metabolic (Klein et al., 1996b) effects have been proposed to influence Sr/Ca ratios, and a secondary influence of salinity also has been suggested (Klein et al., 1996b). However, while kinetic effects have been observed in the dependence of Sr/Ca ratios on shell growth rates (Lorrain et al., 2005; Chapter 3), the suggestion of a metabolic control of Sr/Ca ratios in bivalves has been derived from indirect evidence, rather than direct observation, gathered from the relationship of Sr/Ca ratios with $\delta^{13}C$, as well as the intra- individual variability (fast growing sections relative to slow growing sections) of Sr/Ca ratios (Klein et al., 1996b). Furthermore, kinetic and metabolic effects on the elemental composition of biogenic carbonates are interlinked and are difficult, if not impossible to distinguish (e.g. de Villiers et al., 1995; Nurnberg et al., 1996a; Lea et al., 1999; Lea, 2003; Gillikin et al., 2005b; Carré et al., 2006).

To determine the influence of physiological controls on Sr/Ca ratios of bivalve calcite, two marine bivalve species, *Mytilus edulis* (blue mussel) and *Pecten maximus* (king scallop), were grown in a controlled laboratory aquarium culturing approach.

Animals were grown at five different, but constant, seawater temperatures over the range from 10 to 20 °C and under the same food regime. In addition, respiration and shell growth rates were decoupled from seawater temperature in an experiment with food regimes, but constant temperature. Furthermore, *M. edulis* specimens were grown in the field during one year to validate the results obtained from the laboratory culturing approach. Specifically, the aim was to investigate the role of temperature, shell growth rate, shell Mg content and metabolic activity in controlling shell Sr/Ca ratios of bivalve calcite. The purpose of this study was to advance the understanding of the physiological controls of Sr/Ca ratios in the calcite shells of the two bivalve species which have been proposed previously, as well as closely related taxa, as archives for palaeoceanographic studies (e.g. Krantz et al., 1988; Klein et al., 1996a; Hickson et al., 1999; Chauvaud et al., 2005; Gillikin et al., 2006a; Wanamaker et al., 2007).

5.3 Material and Methods

5.3.1 Laboratory Culture Experiment

Two species of marine bivalve mollusc were cultured in aquaria in the School of Ocean Sciences, University of Wales Bangor, U.K. *Mytilus edulis* specimens were collected in December 2003, from naturally settled spat (10 mm < size < 20 mm; age < one year) in Cable Bay, a site on the coast of Anglesey, northwest Wales, while *Pecten maximus* specimens (10 mm < size < 20 mm; age < one year) were collected from a commercial fishery, Ramsay Sound Shellfish, Isle of Skye, Scotland, in November, 2003. Once moved into the laboratory environment, all animals were acclimated at a temperature of ~13°C for more than two months. Both water temperature and food availability were used to further investigate the control of growth rate on Sr/Ca ratios in these bivalves. Animals of similar size were moved into separate aquaria each under different but constant temperatures and controlled food and light conditions; the aquaria were routinely cleaned of all detritus. A mixed algae solution of *Pavlova lutheri*, *Rhinomonas reticulata* and *Tetraselmis chui* was collected every morning from stock cultures, split into equal volumes of eight litres

and then supplied to the aquaria, from containers with a drip-tap, throughout that day at rates of ~5.5 ml/min. Because of the limited number of aquaria available, two separate temperature-controlled experiments were completed with three aquaria used in each. Clear temperature differences were maintained in the three different aquaria in each of the experiments. Aquaria mean seawater temperatures were 11.96 ±0.12°C, 15.61 ±0.12°C and 18.39 ±0.05°C during experiment one, and 10.76 ±0.41°C, 15.54 ±0.25°C and 20.23 ±0.22°C in 20°C aquarium during experiment two. The objective of the third experiment was to decouple respiration rate and shell growth rate from seawater temperature. In this experiment, temperature was similar in two aquaria (18.28°C ±0.10 in the low food aquarium and 18.01°C ±0.13 in the high food aquarium), but the amount of food was four times higher in one aquarium than in the other.

Once the animals had acclimatised, individual specimens were temporarily removed from each aquarium at weekly intervals (with the exception of the last growth interval in experiment two, which was longer than a week for both the 15°C and 20°C aquaria). During emersion *Mytilus edulis* specimens were exposed to the air for 5 to 6 hours, while *Pecten maximus* specimens were kept in small holding tanks for periods of 30 to 45 minutes. Both methods resulted in emplacement of a disturbance mark on the surface of the shells. The shells then were photographed and digitally imaged using the AnalySIS software package. Subsequently, the term "growth interval" has been used to describe the time intervals between emersions of animals. The duration of the experiments, and hence the number of growth intervals, varied with species and aquarium temperature (for a detailed description, see Chapter 4). At the end of each experiment, the tissue was removed from the each shell, dried to constant weight and tissue dry weight measured.

5.3.2 Field Culture Experiment

Specimens of the bivalve *Mytilus edulis* were suspended 1 m below a moored raft in the Menai Strait (north Wales, U.K.) from the 8th December 2004 to the 12th December 2005 (Figure 3-1, pp 71). The animals were all less than 1 year old when deployed, obtained from one spat cohort and initially ranged from 20 to 27 mm in shell length. The raft is moored in the close vicinity (ca. 500m) of the School of

Ocean Sciences, University of Wales Bangor in a section of the Menai Strait where the water column is homogenous with depth, due to strong turbulent tidal mixing (Harvey, 1968). Animals were followed for short, defined and consecutive growth intervals (N = 16) that together cover the duration of the entire field experiment. To ensure that specimens were adapted to field conditions in the beginning of each growth interval, animals were taken at the start of each growth interval from a stock of animals deployed in the beginning of the field experiment and kept in a separate cage.

The duration of each growth interval varied during the experiment according to expected seasonal changes in shell growth rate and in seawater parameters. At the end of each growth interval, which also is the beginning of the next interval, specimens were removed from the raft together with a new set of stock specimens to be used during the next growth interval. Each time the *Mytilus edulis* specimens were exposed to the air for 5 to 6 hours resulting in emplacement of a disturbance mark on the surface of the shells. The shells then were photographed and digitally imaged using the AnalySIS software package. The animal tissue was removed from the shell, dried to constant weight and tissue dry weight determined.

5.3.3 Shell Growth Rate Measurements

The combination of disturbance marks and photographs was used to identify and measure all shell growth for each growth interval, as well as shell height (i.e. the distance from the umbo to the shell margin along the main axis of growth), and thus provide a time control of the new shell growth laid down throughout the laboratory and field experiments. Shell growth rates were calculated assuming shell growth rate (SGR, $\mu m\ day^{-1}$) to be constant during each growth interval. Both in the laboratory and field experiments SGR was determined for all specimens, albeit in the former only for a sub-set of the growth intervals (Appendix 4).

Shell growth rates (SGR), i.e. the daily linear increase in shell height, have been commonly used in bivalves as indicative of precipitation rate (Klein et al., 1996b; Purton et al., 1999; Gillikin et al., 2005b; Carré et al., 2006), which is known to strongly control the incorporation of Sr in synthetic calcite (Lorens, 1981a; Pingitore,

1986; Morse and Bender, 1990; Tesoriero and Pankow, 1996; Gabitov and Watson, 2006). Lorrain et al., (2005), however, found in *Pecten maximus* that the daily increase in shell surface area (DSAI) or shell weight (DSWI), estimated from strong morphometric relationships with shell height, represent best the amount of $CaCO_3$ precipitated in the shell and both their relationships with Sr/Ca ratios were stronger than SGR. Subsequently, a stronger relationship between Sr/Ca and DSAI has been also observed (Chapter 3), than with SGR in *P. maximus*. In the present study, DSAI was measured at each growth interval using the AnalySIS software package and DSWI was estimated using the same approach as Lorrain et al., (2005). However, no differences were found in the strength of the relationships between Sr/Ca and SGR, DSAI and DSWI in *Mytilus edulis* and *P. maximus* (Table 5-1) and thus only SGR has been used as indicative of shell precipitation rate.

Table 5 - 1 – Summary of correlations between Sr/Ca and shell growth rate (SGR – μm/day), daily shell area increment (DSAI – mm^2/day) and daily shell weight increment (DSWI – μg/day) for all the experiments.

Experiment	SGR		DSAI		DSWI	
	r^2	p	r^2	p	r^2	p
Temperature						
M. edulis	0.17	<0.001	-	>0.05	0.21	<0.001
P. maximus	0.24	<0.001	0.19	<0.001	0.30	<0.001
Food						
M. edulis	0.57	<0.001	0.66	<0.001	0.40	<0.001
P. maximus	0.10	0.012	0.14	0.006	-	>0.05
Field						
M. edulis	0.40	<0.001	0.38	<0.001	0.20	<0.001

5.3.4 Respiration Rate Measurements

The resting absolute respiration rate (ARR, mmolO_2/h) of *Mytilus edulis* and *Pecten maximus* animals was measured in all specimens at the end of each experiment, and for field cultured *M. edulis* in all short-deployment specimens at the end of each growth interval. Various methods exist to determine metabolic rate (also described as energy demand or turnover rate) in bivalves (De Zwaan and Mathieu, 1992), and in aerobic conditions the rate of oxygen consumption is an indirect measurement of metabolic rate, which can be obtained by converting the rate of oxygen consumption

to energy demand (Bayne and Newell, 1983). Individual animals were removed from the experiment aquaria and placed in a respirometry chamber with a volume of 100 ml. The respirometry chamber consisted of a cylindrical transparent perspex apparatus of 10.5 cm diameter and 4.5 cm height, with a volume of 100 ml. Temperature in the respirometry chamber was kept at ±0.5°C from the individual experimental aquaria by a surrounding water jacket attached to a recirculating water bath. A groove at the base of the respirometry chamber accommodated a polythene-covered magnetic spin bar with a plastic mesh separating the groove from the remainder of the chamber and providing support for the animals. The respirometry chamber was placed on a magnetic stirrer set at the maximum speed that would minimise the diffusion boundary layer and guarantee a homogenous distribution of dissolved oxygen in the chamber without disturbing the animal. A complete seal in all apertures, including the lid, was ensured by rubber o-rings and all air bubbles were removed from the chamber using a third aperture that was subsequently closed with a plastic screw. A polarographic dissolved oxygen probe with automatic temperature compensation and a HiTemp temperature sensor probe (both DCP Microelements) were inserted through apertures in the lid of the chamber. The oxygen electrode contained an electrolyte solution (Strathkelvin Instruments) which was checked and changed before each batch of measurements. The oxygen and temperature probes were attached to a LogIT DataMeter 1000 (DCP Microelements) and logged in a computer using the DataLogging Insight software package.

Calibration to 0 and 100% oxygen saturation was performed using 0.2 μm filtered and U.V. irradiated seawater (FSW) containing dissolved sodium dithionite for 0% saturation and air saturated FSW kept at measurement temperature in the water bath for 100% saturation. A control run was performed before each set of measurements to determine blank ARR and to ensure the respirometry chamber was free from significant bacterial contamination. Animals were placed in the chamber, the lid closed and the sensor probes inserted. Any air bubbles were removed and the animals allowed to settle in FSW close to oxygen saturation. After a period of stabilization, the decrease in oxygen saturation was measured for a period of 15 to 30 minutes depending on animal size and seawater temperature. The rate of decrease in oxygen saturation then was converted to the rate of oxygen consumption ($mmolO_2/h$) by calculating the amount of oxygen in the chamber. The precision of replicate

measurements of ARR (N = 3) in *Mytilus edulis* specimens (N = 8), expressed as relative standard deviation or RSD, was better than 7%. However, the bivalve *Pecten maximus* is known to be an active swimmer, through clapping of the valves, usually to avoid predation and for habitat selection. The high activity levels of *Pecten maximus* animals in the respiration chamber prevented the accurate measurement of resting absolute respiration rate in this species. Replicate measurements of individual animals showed RSD higher than 50%. It was impossible, therefore, to measure accurately resting ARR in *P. maximus*.

5.3.5 Shell Preparation and Milling

Shell powder samples were taken from the new shell growth by milling to a depth of ca. 200 μm. Accurate milling was completed under a binocular microscope fitted with an eyepiece graticule, and depth and width of milling were controlled carefully. Each milled powder sample was taken from the main axis of shell growth: in *Pecten maximus* from the mid 2–3 axial ridges (ribs), and in *Mytilus edulis* from the middle section, to avoid the increase in shell curvature that occurs away from the main growth axis. In the laboratory experiment, only one powder sample was milled from each individual growth interval and, particularly at the lower temperatures, the milled powder from one or more growth intervals had to be combined to provide enough shell material for analysis. Whenever the amount of sample permitted, single milled powder samples were split into separate aliquots for elemental and stable-isotope ratio determinations ($\delta^{18}O$ values reported in chapter 4), otherwise only element/Ca ratios were measured. In the field experiment, shell powder samples were collected from two specimens for each growth interval. Whenever the amount of shell growth permitted more than one sample was collected from a single growth interval. In such occasions, the new shell growth was equally divided between the numbers of samples collected ($2 \leq N \leq 4$). Both for the laboratory and field experiment, shell preparation and sampling is described in more detail elsewhere (Chapters 4 and 6).

5.3.6 Shell Stable-Isotope and Elemental Ratio Analyses

The shell milled powder sample preparation and analytical methodologies used in this study are as described in detail in Chapter 2 and 3. Stable-isotope data are

reported in per mil (‰) deviations relative to VPDB and the overall analytical precision for shell $\delta^{13}C$ measurements based on analyses of an internal laboratory standard run concurrently with all *Mytilus edulis* and *Pecten maximus* samples analysed in this study is 0.08 ‰ (1 σ; N = 32).

Table 5 - 2 – Comparison of expected (Greaves et al., 2005) with measured Sr/Ca ratios for three certified reference material (CRMs) solutions.

CRM solution	Expected	This study
BAM-RS3	0.19	0.20 ± 0.02 (N = 9)
ECRM-752	0.20	0.19 ± 0.01 (N = 13)
CMSI-1767	-	1.54 ± 0.01 (N = 11)

The values in the third column are those returned from the University of Wales Bangor as part of an ongoing international inter-laboratory comparison exercise, with the replicates representing six separate dissolutions of each CRM (1 ml of each solution was centrifuged for 10 minutes at ~6000 rpm and ca. 0.75 ml from each solution then diluted to final solution Ca concentrations of 60 µg/ml). By comparison, the replicates reported for this study in the fourth column are repeated measurements of a single dissolution completed for each CRM and diluted to Ca concentrations of 60 µg/ml. All measurements were made on the same Perkin Elmer Optima 3300RL ICP-AES instrument.

Calibration for Sr/Ca ratio determinations was performed via an established ICP-AES intensity-ratio method (de Villiers et al., 2002), using synthetic standard solutions in the range 1.0-1.8 mmol/mol for Sr/Ca, and most at Ca concentrations of 50 and 60 µg/ml. The smallest milled powder samples were analysed at 30 µg/ml. Measurements were made using the Perkin Elmer Optima 3300RL ICP-AES instrument housed at the NERC ICP Facility, Royal Holloway University of London. Instrumental drift was monitored by running an intermediate (1.5 mmol/mol) calibration standard every 5 to 10 samples and data then were corrected accordingly. Analytical precision (expressed as relative standard deviation or RSD) was 0.8 % for the laboratory experiments (N = 11) and 0.3 % for the field experiment (N = 29). In the laboratory experiments, sufficient material was not available from any one growth interval to enable replicate analyses for an assessment of true sample precision; in the field experiment, however, sample precision was 1.3 % RSD for replicate measurements (N = 3) of the same milled powder samples obtained from five *Mytilus edulis* specimens. For comparison with past and future datasets, Sr/Ca ratio measurements also are reported for three solutions (BAM-RS3, ECRM-752 and CMSI-1767) that have been proposed as certified reference materials (CRMs) for Sr/Ca ratio measurements in carbonates (Greaves et al., 2005) and that are subject to an ongoing international inter-laboratory calibration study (Table 5-2). The linearity of the intensity-ratio calibration lines, combined with the independent assessment of

the accuracy of the analytical procedure (see also chapters 2 and 3), confirms the veracity of the *M. edulis* and *Pecten maximus* Sr/Ca ratios obtained in this study.

5.4 Results

5.4.1 Shell Sr/Ca Records

In the laboratory temperature experiments, measured shell Sr/Ca ratios range from 1.18 to 1.76 mmol/mol in *Mytilus edulis*, and for *Pecten maximus* shell Sr/Ca ratios range from 1.38 to 1.76 mmol/mol during experiment two only (Figure 5-1). In the laboratory food regime experiment, *M. edulis* shell Sr/Ca ratios range from 1.01 to 1.29 mmol/mol in the low food aquarium and from 1.36 to 1.87 mmol/mol in the high food aquarium (Figure 5-1a). In *P. maximus* shell Sr/Ca ratios range from 1.42 to 1.73 mmol/mol in the low food aquarium and from 1.46 to 1.78 mmol/mol in the high food aquarium (Figure 5-1b). In the field experiment, *M. edulis* shell Sr/Ca ratios range from 0.82 to 1.23 mmol/mol.

No single parameter controlled shell Sr/Ca ratios in both species. In the laboratory temperature and field experiments, shell Sr/Ca ratios in both species were significantly correlated to Mg/Ca, salinity, shell growth rate, $\delta^{13}C$ ratios and to ARR in *Mytilus edulis* only (Tables 5-1 and 5-3).

Table 5 - 3 – Summary of correlations between Sr/Ca and other parameters for all the experiments.

Experiment	Mg/Ca		Temperature		Salinity		$\delta^{13}C$		ARR	
	r^2	p	r^2	p	r^2	p	r^2	p	r^2	p
Temperature										
M. edulis	0.10	<0.001	-	>0.05	0.16	<0.001	0.34	<0.001	0.59	<0.001
P. maximus	0.45	<0.001	0.18	<0.001	0.29	<0.001	0.53	<0.001	-	-
Food										
M. edulis	0.32	<0.001	-	-	-	>0.05	0.84	<0.001	0.36	<0.001
P. maximus	0.15	0.002	-	-	-	>0.05	0.55	0.006	-	-
Field										
M. edulis	0.28	<0.001	0.52	<0.001	0.28	<0.001	0.50	<0.001	0.58	<0.001

a Mytilus

Experiment 1

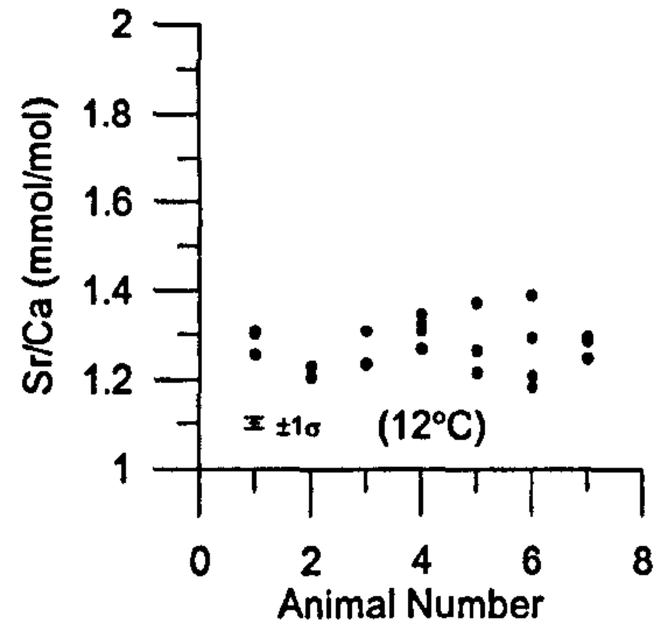

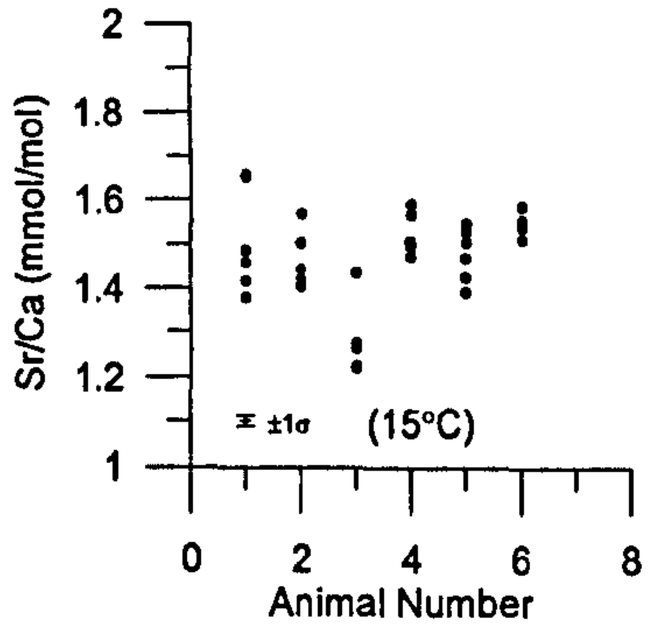

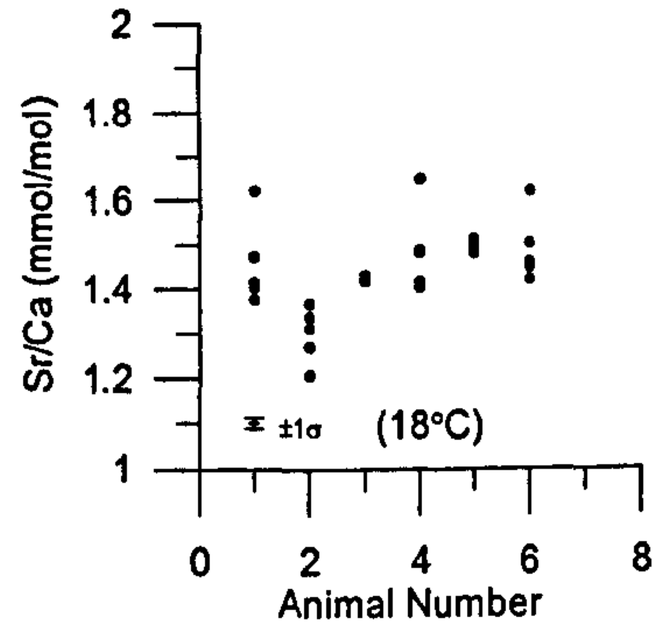

Experiment 2

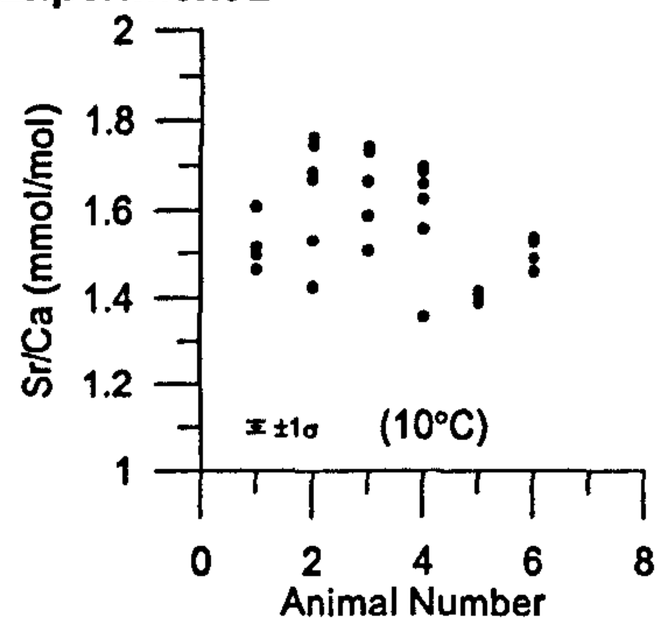

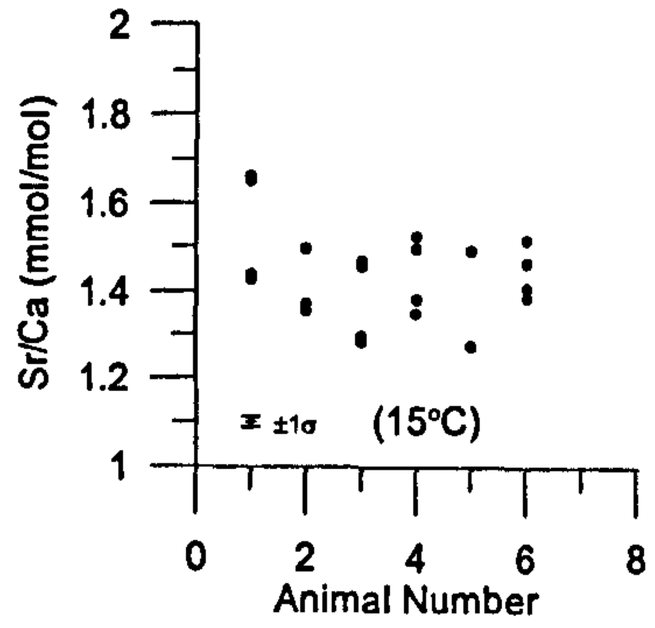

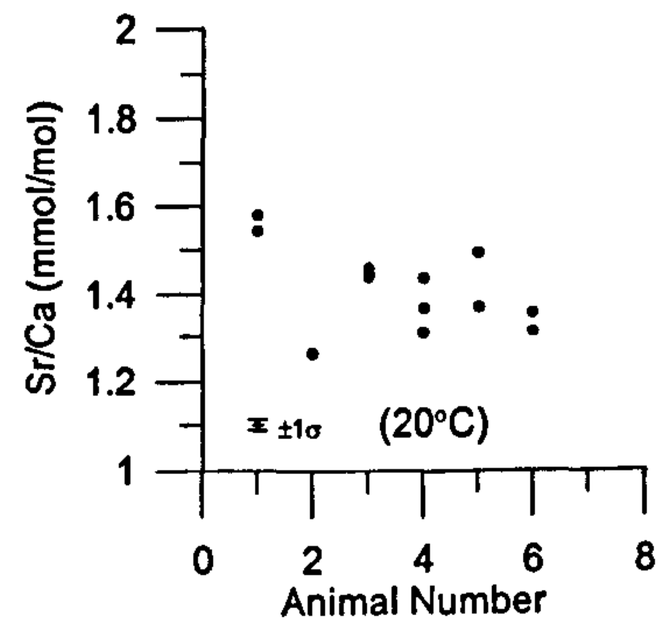

Experiment 3

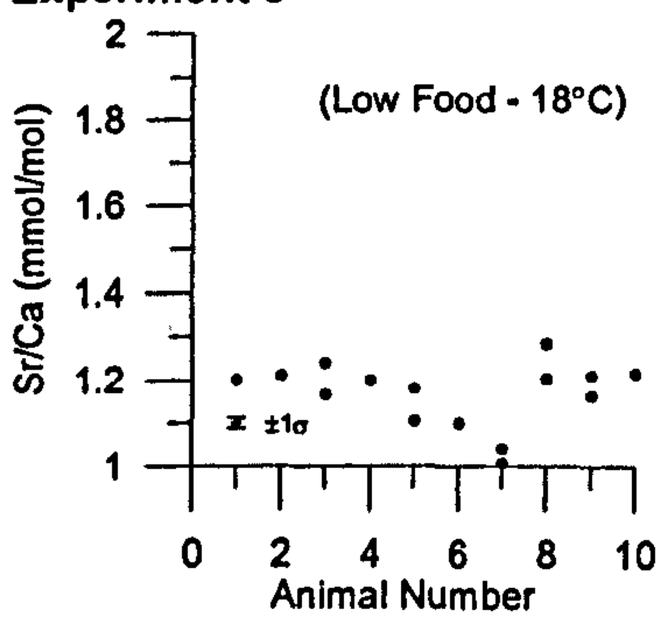

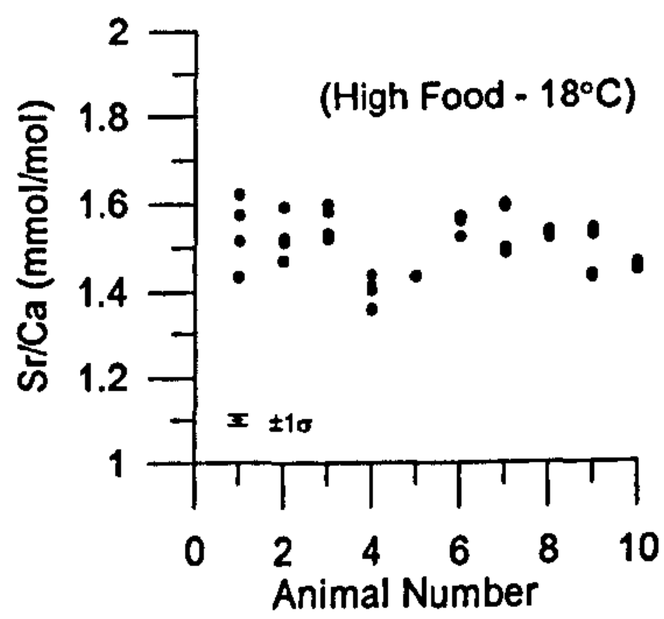

b Pecten

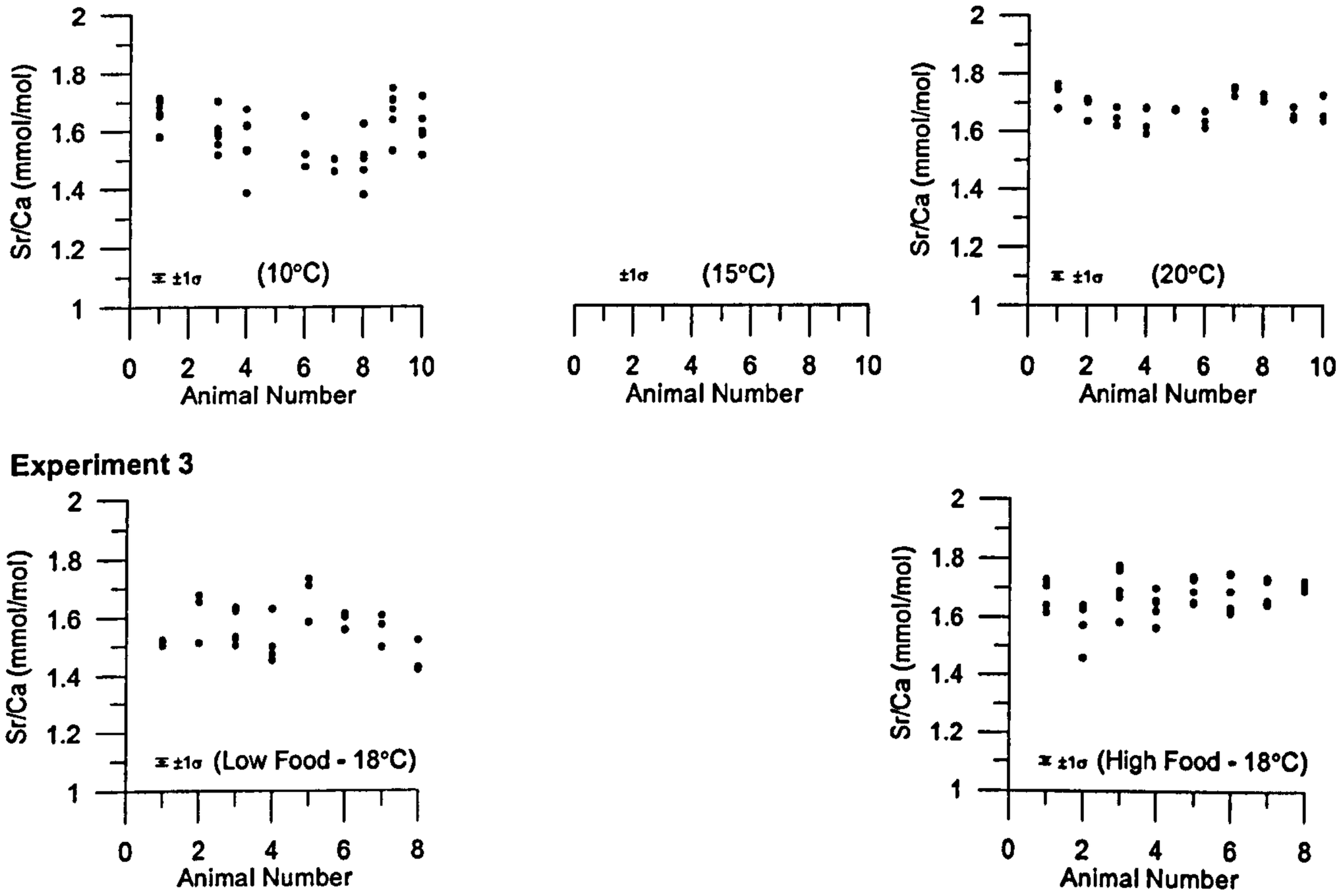

Figure 5 - 1 – Shell Sr/Ca samples plotted against animal number for each aquarium (temperature in brackets) in order to illustrate inter- and intra-individual shell variability of Sr/Ca ratios in a) *Mytilus edulis* and b) *Pecten maximus*. For each animal, individual data points correspond to Sr/Ca ratios of new shell growth deposited in the experiment during different growth intervals. For comparison, twice the analytical error (± 0.01 mmol/mol) also is shown.

5.4.2 Shell Growth Rate Records

In the laboratory temperature experiments *Mytilus edulis* shell growth rates (SGR) vary from 29 to 284 µm/day in *M. edulis* during experiments one and two, while for *Pecten maximus* SGR range from 33 to 394 µm/day during experiment two (Figure 5-2). In the laboratory food regime experiment, *M. edulis* SGR range from 21 to 48 µm/day in the low food aquarium and from 27 to 225 µm/day in the high food aquarium (Figure 5-2). In *P. maximus* SGR ranges from 32 to 138 µm/day in the low food aquarium and from 41 to 180 µm/day in the high food aquarium (Figure 5-2). In *M. edulis* and *P. maximus*, SGR was significantly lower in the low food aquarium relative to the high food aquarium (t-test, $p < 0.001$ and $p = 0.004$, respectively). In the field experiment, *M. edulis* specimens SGR range from 19 to 347 µm/day (Figure 5-2).

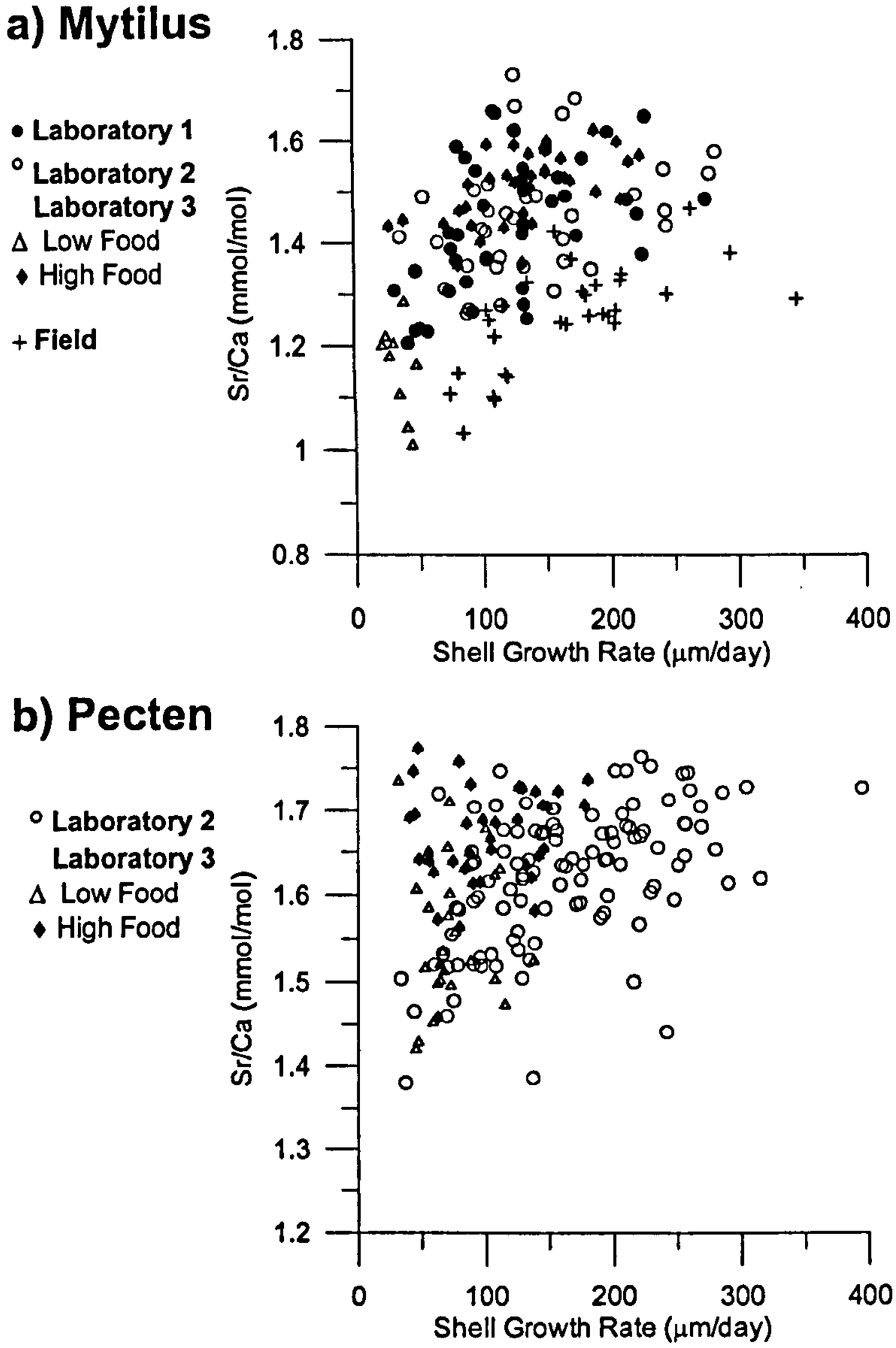

Figure 5 - 2 – Shell Sr/Ca ratios plotted against shell growth rates from a) *Mytilus edulis* (Laboratory and Field experiments) and b) *Pecten maximus* (Laboratory experiments, only).

Shell growth rate values observed both in the laboratory and field experiments are within the range of shell growth rates (0 to 350–400 µm/day) reported for *Mytilus edulis* (Bayne and Worral, 1980; Hillbish, 1986) and *Pecten maximus* of similar age from non-manipulated populations (Chauvaud et al., 1998a; Lorrain et al., 2000; Chauvaud et al., 2005; Lorrain et al., 2005)

No single parameter showed a dominant control of SGR of both species. Seawater temperature was found to be significantly correlated to *Mytilus edulis* and *Pecten maximus* SGR, albeit weakly in the former, in the laboratory temperature experiments ($r^2 = 0.15$, $p < 0.001$ and $r^2 = 0.62$, $p < 0.001$, respectively), as well as in

the field experiment in *M. edulis* ($r^2 = 0.43$, $p < 0.001$). In addition, in *M. edulis* only, SGR was significantly correlated with ARR, albeit weakly in the laboratory temperature and food experiments ($r^2 = 0.32$, $p = 0.001$ and $r^2 = 0.14$, $p = 0.004$, respectively), but stronger in the field experiment ($r^2 = 0.58$, $p = 0.001$).

5.4.3 Shell $\delta^{13}C$ Records

In the laboratory temperature experiments, *Mytilus edulis* shell $\delta^{13}C$ ratios range from -1.9 to -0.6 ‰ during experiments one and two, while for *P. maximus* shell $\delta^{13}C$ ratios range from 0.0 to 1.2 ‰ during experiment two (Figure 5-3). During experiment two, when the two species were grown together in the same aquaria, shell mean $\delta^{13}C$ ratios were significantly lower (t-test, $p < 0.001$) in *M. edulis* than in *P. maximus* (Figure 5-3). In the laboratory food regime experiment, *M. edulis* shell $\delta^{13}C$ ratios range from -0.7 to -0.1 ‰ in the low food aquarium and from -1.8 to -0.8 ‰ in the high food aquarium; whereas in *P. maximus* shell $\delta^{13}C$ ratios range from -0.2 to 0.3 ‰ in the low food aquarium and from -0.3 to 0.1 ‰ in the high food aquarium (Figure 5-3). In the field experiment, *M. edulis* shell $\delta^{13}C$ ratios range from -2.5 to -0.2 ‰ (Figure 5-3).

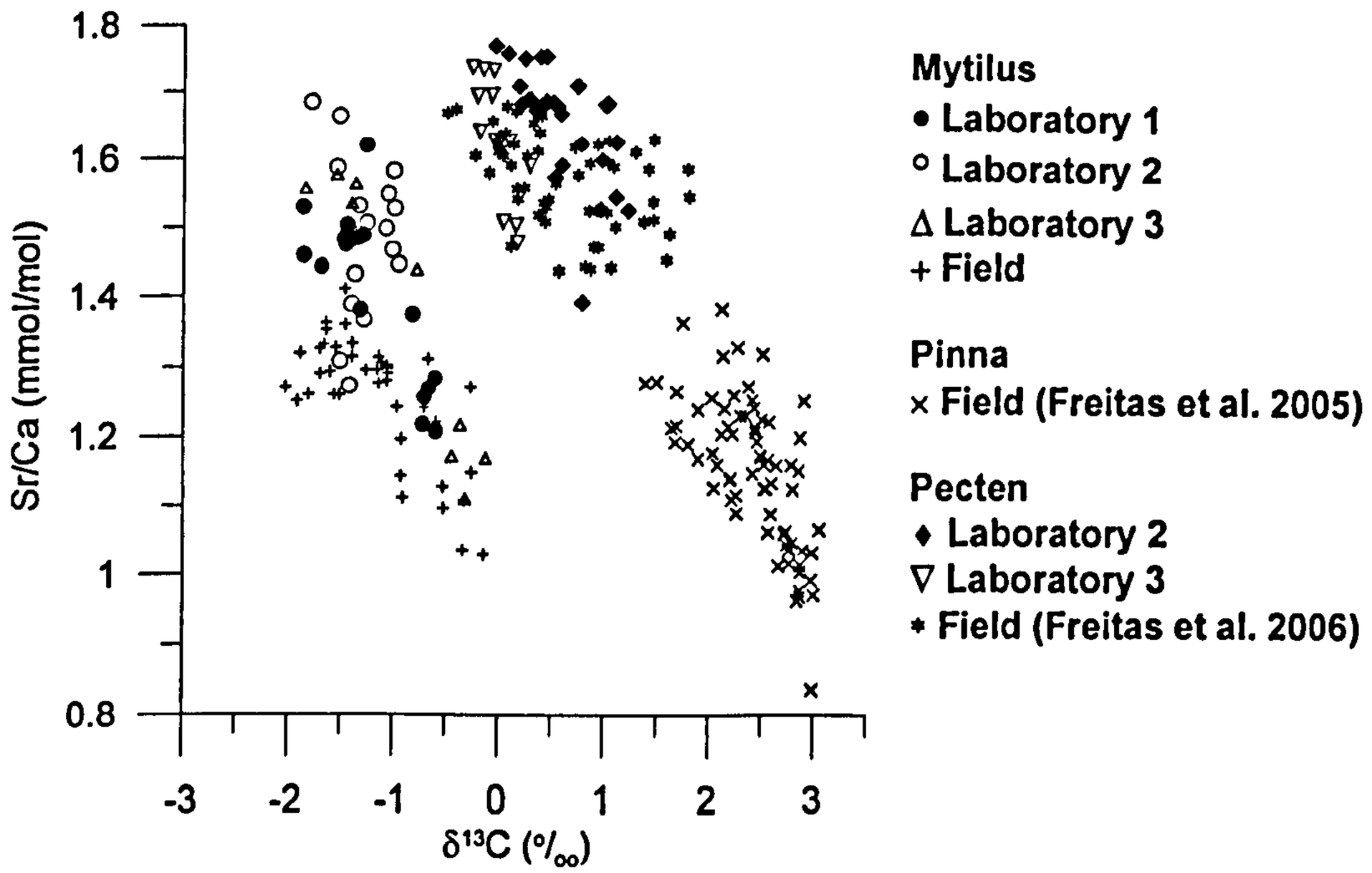

Figure 5 - 3 – Shell Sr/Ca ratios from *Mytilus edulis* (Laboratory and Field experiments) and *Pecten maximus* (Laboratory experiments, only) plotted against shell $\delta^{13}C$ ratios. Shown is also data from field grown *P. maximus* (Chapter 3) and *Pinna nobilis* (Chapter 2).

In *Mytilus edulis* and *Pecten maximus*, shell mean $\delta^{13}C$ were higher (t-test, $p < 0.001$ and $p = 0.032$, respectively) in the low food aquarium relative to the high food aquarium, i.e. strong metabolic influence in the high food aquarium in both species. Nevertheless, in the present study the metabolic control of $\delta^{13}C$ ratios was species specific, and the incorporation of carbon with a metabolic origin was larger in *M. edulis* than in *P. maximus*, i.e. when both species where grown side-by-side in the same aquaria and under the same food regime during experiments two and three, shell $\delta^{13}C$ ratios were significantly lower in the former than in the latter species (t-test, $p < 0.001$).

5.4.4 Respiration Rate Records

In the laboratory temperature experiments, *Mytilus edulis* ARR range from 0.006 to 0.023 $mmolO_2\ h^{-1}$ in experiments one and two (Figure 5-4). In the laboratory food regime experiment, *M. edulis* ARR ranges from 0.004 to 0.010 $mmolO_2\ h^{-1}$ in the low food aquarium and from 0.005 to 0.024 $mmolO_2\ h^{-1}$ in the high food aquarium (Figure 5-4). In the field experiment, *M. edulis* ARR range from 0.033 to 0.442 $mmolO_2\ h^{-1}$ (Figure 5-4).

Mytilus edulis resting respiration rate is known to depend on temperature and animal size (e.g. Bayne and Newell, 1983). In the laboratory temperature, however, ARR was not significantly correlated to seawater temperature ($p > 0.05$), but in the field experiment, ARR was significantly correlated to seawater temperature ($r^2 = 0.67$, $p < 0.001$). Animal size strongly influenced ARR in all experiments, as indicated by the significant positive correlations between ARR and shell height and tissue dry weight observed in the laboratory temperature ($r^2 = 0.71$, $p < 0.001$ and $r^2 = 0.71$, $p < 0.001$, respectively), in the food regime experiment ($r^2 = 0.74$, $p < 0.001$ and $r^2 = 0.88$, $p < 0.001$, respectively) and in the field experiment ($r^2 = 0.36$, $p < 0.001$ and $r^2 = 0.46$, $p < 0.001$, respectively).

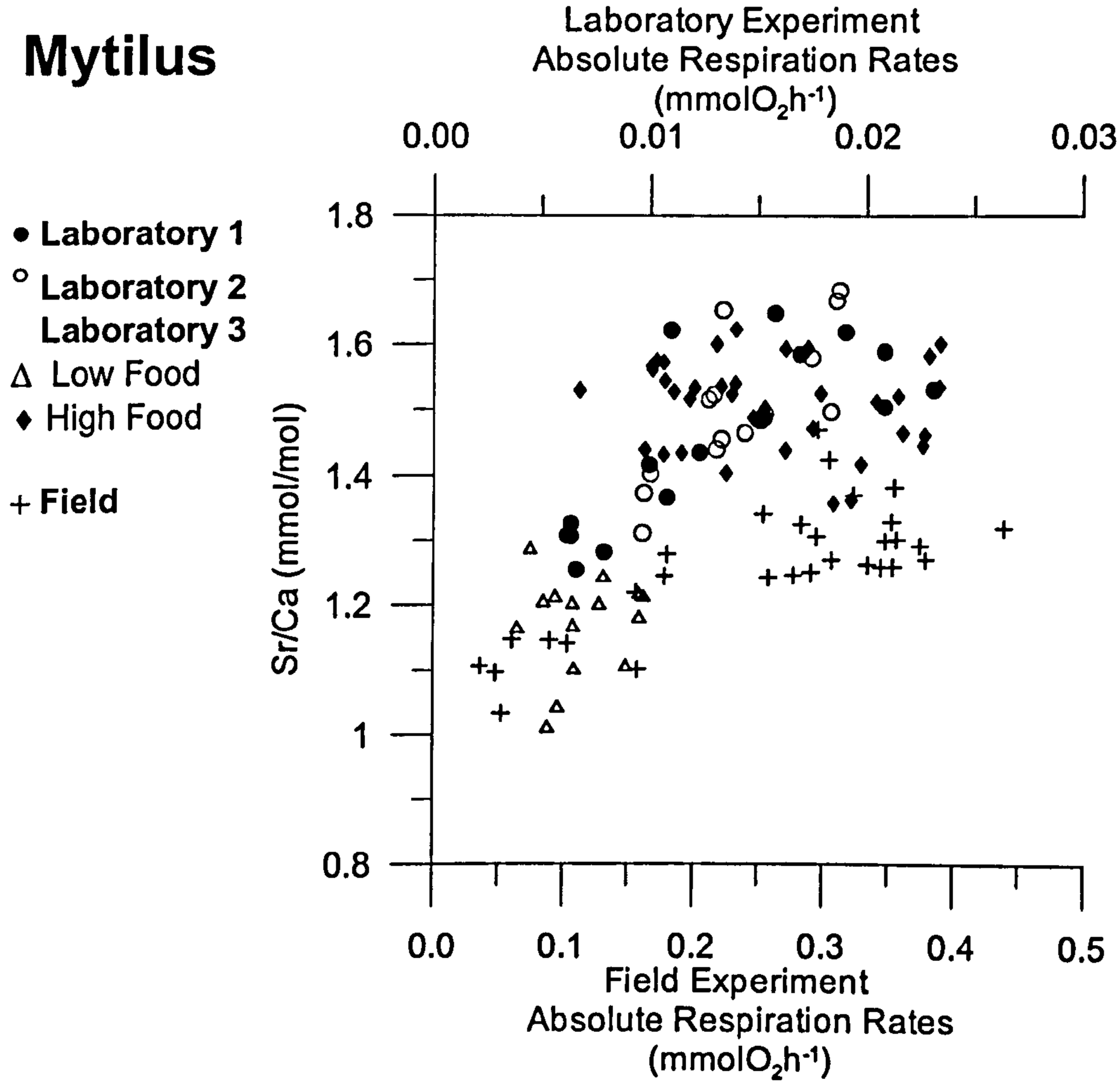

Figure 5 - 4 – Shell Sr/Ca ratios from *Mytilus edulis* (Laboratory and Field experiments) and *Pecten maximus* (Laboratory experiments, only) plotted against absolute respiration rate (ARR, $mmolO_2/h$). Note that ARR from laboratory and field grown *M. edulis* are plotted in different axis.

5.4.5 Relationships of Shell Sr/Ca Ratios with Metabolic Activity Related Parameters: Absolute Respiration Rates and Shell $\delta^{13}C$ Ratios

In *Mytilus edulis*, shell Sr/Ca ratios were significantly correlated to ARR in all experiments, while in both species shell Sr/Ca ratios were significantly correlated to shell $\delta^{13}C$ ratios (Table 5-3). In addition, in the laboratory food regime experiment, shell mean Sr/Ca ratios of both species were also significantly lower in (t-test, $p < 0.001$) in the low food and low metabolic activity aquarium compared to the high food and high metabolic activity aquarium. In both species, therefore, shell Sr/Ca ratios were influenced by metabolic activity. In the laboratory food regime experiment, SGR and metabolic activity (measured by ARR) were dissociated from its temperature dependence. Indeed, *Mytilus edulis* mean SGR and ARR were lower

(t-test, $p < 0.001$) in the low food aquarium relative to the high food aquarium. Metabolic activity of *M. edulis* animals was thus significantly higher in the high food aquarium than in the lower food aquarium.

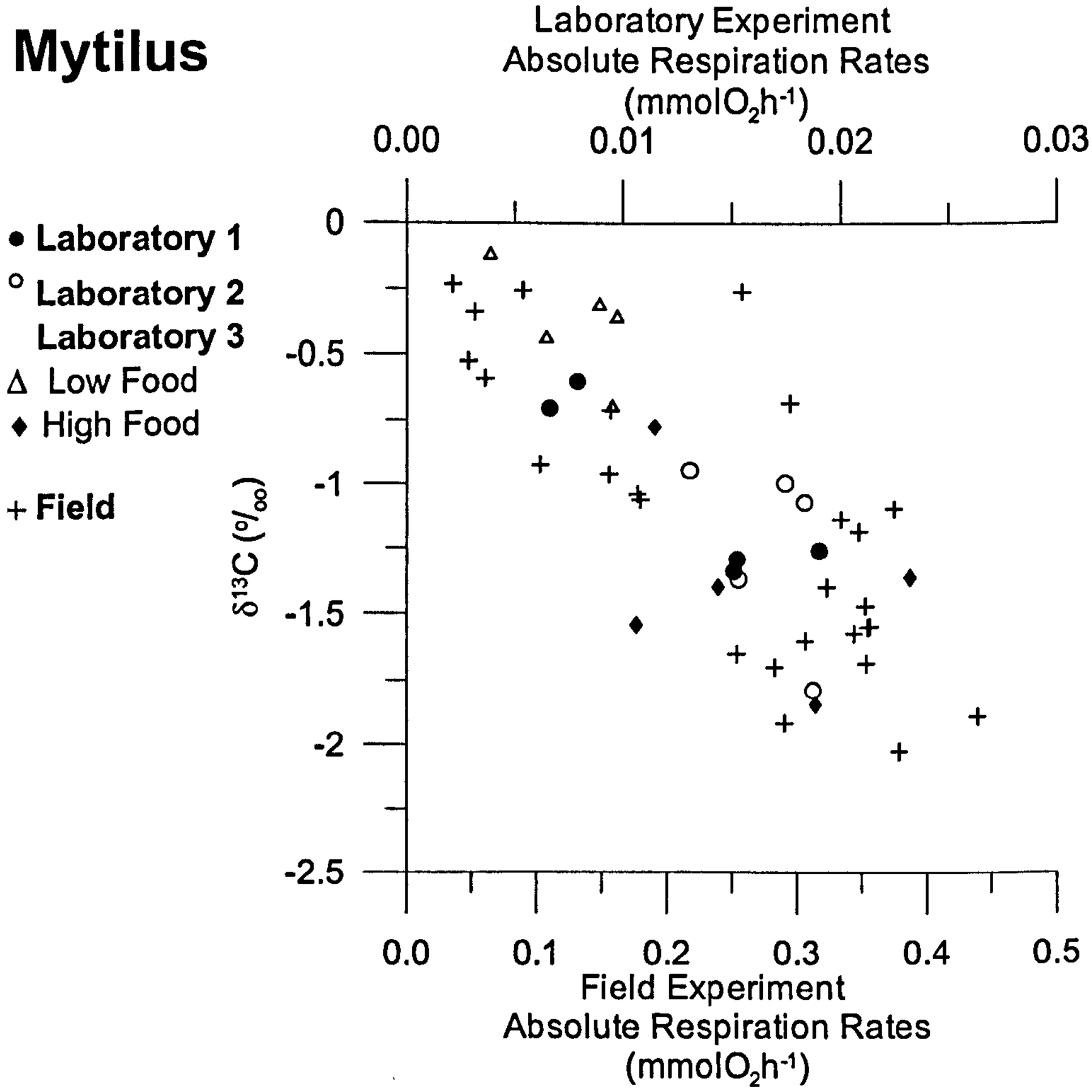

Figure 5 - 5 – Absolute respiration rate (ARR, $mmolO_2/h$) of *Mytilus edulis* from both laboratory and field experiments plotted against shell $\delta^{13}C$ (‰) ratios. Note that ARR from laboratory and field grown *M. edulis* are plotted in different axis.

In *Mytilus edulis*, SGR also explains a significant proportion of the variability of Sr/Ca ratios in the laboratory food and field experiments (Table 5-1). In contrast to previous observations in bivalves (Lewis and Cerrato, 1997), SGR and ARR were only weakly correlated or only strongly correlated in the field experiment ($r^2 = 0.58$, $p = 0.001$). However, such correlations can be attributed to co-variation of both SGR and ARR with seawater temperature ($r^2 = 0.43$, $p < 0.001$ and $r^2 = 0.67$, $p < 0.001$, respectively).

In *Mytilus edulis*, ARR and shell $\delta^{13}C$ ratios were significantly inversely correlated in all experiments (Figure 5-5), supporting the use of shell $\delta^{13}C$ ratios as reflecting metabolic activity: in the laboratory temperature experiment ($r^2 = 0.57$, $p = 0.012$), in the laboratory food regime experiment ($r^2 = 0.57$, $p = 0.001$) and in the field experiment ($r^2 = 0.58$, $p < 0.001$).

5.5 Discussion

In bivalve calcite, the mechanisms controlling trace element incorporation continue to be investigated and the matter of some debate, with both kinetic (Vander Putten et al., 2000; Lorrain et al., 2005; Chapter 3) and metabolic (Klein et al., 1996b) controls thought to influence bivalve calcite Sr/Ca ratios. Shell Mg content has been also observed to influence shell Sr/Ca ratios in *Pecten maximus* (Chapter 3). However, shell Mg content was not a major control of shell Sr/Ca ratios in the present study (Table 5-3).

5.5.1 Physiological Controls of Shell Sr/Ca Ratios

Kinetic controls of Sr incorporation in bivalve calcite have been hypothesized to control shell Sr/Ca ratios of *Mytilus edulis* (Vander Putten et al., 2000), but a strong dependence of bivalve calcite Sr/Ca ratios on SGR, indicating the presence of a strong kinetic control, has only been observed recently in *Pecten maximus* (Lorrain et al., 2005). In addition, SGR has been observed to exert a strong control on the shell Sr/Ca ratios of the aragonitic bivalves *Saxidomus giganteus* (Gillikin et al., 2005b) and *Mesodesma donacium* and *Chione subrugosa* (Carré et al., 2006).

In *Pecten maximus*, shell Sr/Ca ratios have been found to be strongly correlated with the daily increment in shell area (DSAI) and shell weight (DSWI), thought to represent better the increase in shell $CaCO_3$ deposited than SGR (Lorrain et al., 2005). However, no differences were found in the strength of the relationships between Sr/Ca and SGR, DSAI and DSWI in *Mytilus edulis* and *P. maximus* (Table 5-1) and thus only SGR has been used as indicative of shell precipitation rate and the

presence of kinetic effects. In this study, shell Sr/Ca ratios of *P. maximus* were significantly, albeit weakly correlated with SGR, which therefore can only explain a small proportion of the observed variability in shell Sr/Ca ratios (Figure 5-2 and Table 5-1), and such kinetic influence is weaker than previously reported (Lorrain et al., 2005; Chapter 3). Nevertheless, in *M. edulis* SGR still explains a significant proportion of the variability of Sr/Ca ratios from animals grown in the laboratory food experiment and field experiment (Table 5-1). However, it is unclear if the kinetic control of Sr incorporation in shell calcite occurs at the crystal-solution interface or during transport of Sr from the surrounding medium to the extra-pallial space as proposed by Carré et al., (2006).

In bivalve calcite, metabolic effects have been suggested to strongly control shell Sr/Ca ratios (Klein et al., 1996b). However, contrary to Mg (Rosenberg and Hughes, 1991), the suggestion of a metabolic control of Sr/Ca ratios in bivalve calcite has been derived from indirect evidence, rather than direct observation. Regarding Sr, the relationship of Sr/Ca ratios with $\delta^{13}C$, as well as the intra- individual variability (fast growing sections relative to slow growing sections) of Sr/Ca ratios have supported the suggestion of a strong metabolic control of shell Sr/Ca ratios in the calcite of *Mytilus trossulus* (Klein et al., 1996b).

Direct evidence for the influence of metabolic activity on bivalve shell Sr/Ca ratios was observed for the first time in *Mytilus edulis* grown both in the laboratory and field experiments. Shell Sr/Ca ratios were significantly positive correlated with absolute resting respiration rate (ARR) (Figure 5-4 and Table 5-3), a measure of metabolic rate (Bayne and Newell, 1983). Furthermore, in *M. edulis* grown at the same temperature, shell Sr/Ca ratios were significantly higher in specimens kept at a higher metabolic activity (i.e. higher ARR) than in those kept at a lower metabolic activity (Figure 5-4). In *M. edulis*, Rosenberg and Hughes (1991) observed that intra-shell variations of Mg content along the shell edge are linked to local variations in the metabolic activity of the adjacent mantle, and higher Mg content was associated with higher mantle metabolic activity. The metabolic control of shell Sr/Ca ratios reported here for *M. edulis*, however, reflects the influence of the animal's total metabolic activity on the Sr content of a defined shell region along the main axis of shell growth, the area of the shell with the least curvature.

In addition, the significant relationship between Sr/Ca and $\delta^{13}C$ ratios, which reflect metabolic activity due to the incorporation of respired carbon in the shell carbonate (Tanaka et al., 1986; Klein et al., 1996b; Kennedy et al., 2001; Owen et al., 2002b; Lorrain et al., 2004; Gillikin et al., 2006b; Gillikin et al., 2007) and were significantly correlated with ARR (Figure 5-5), further supports a metabolic control of shell Sr/Ca in *Mytilus edulis* animals grown in both the laboratory and the field conditions, but also in *P. maximus* animals grown in the laboratory only (Figure 5-3 and Table 5-3).

In *Mytilus edulis*, however, the influence of metabolic activity on shell Sr/Ca ratios differed between laboratory and field grown *M. edulis* (Figure 5-4), i.e. the slopes from the linear regressions of ARR and Sr/Ca are significantly different (ANOVA, $F = 52.6$, $p < 0.001$). Respiration rate of *M. edulis* is strongly dependent on animal size (Bayne and Newell, 1983), particularly in the laboratory experiment (section 5.3.4), and thus differences in the size attained may explain the observed differences in the range of ARR values between laboratory and field grown animals (Figure 5-6). However, a general difference in the metabolic activity between *M. edulis* animals grown in the laboratory and field conditions is further supported by a difference in the relationship between shell height and ARR, i.e. for the same shell height ARR were lower in laboratory relative to field grown animals (Figure 5-6). Differences in food supply, as well as in water flow, most likely cause animals grown in the laboratory or in the field to be in a different physiological condition (Bayne and Worral, 1980) and may explain the observed differences in metabolic activity between the laboratory and field experiments.

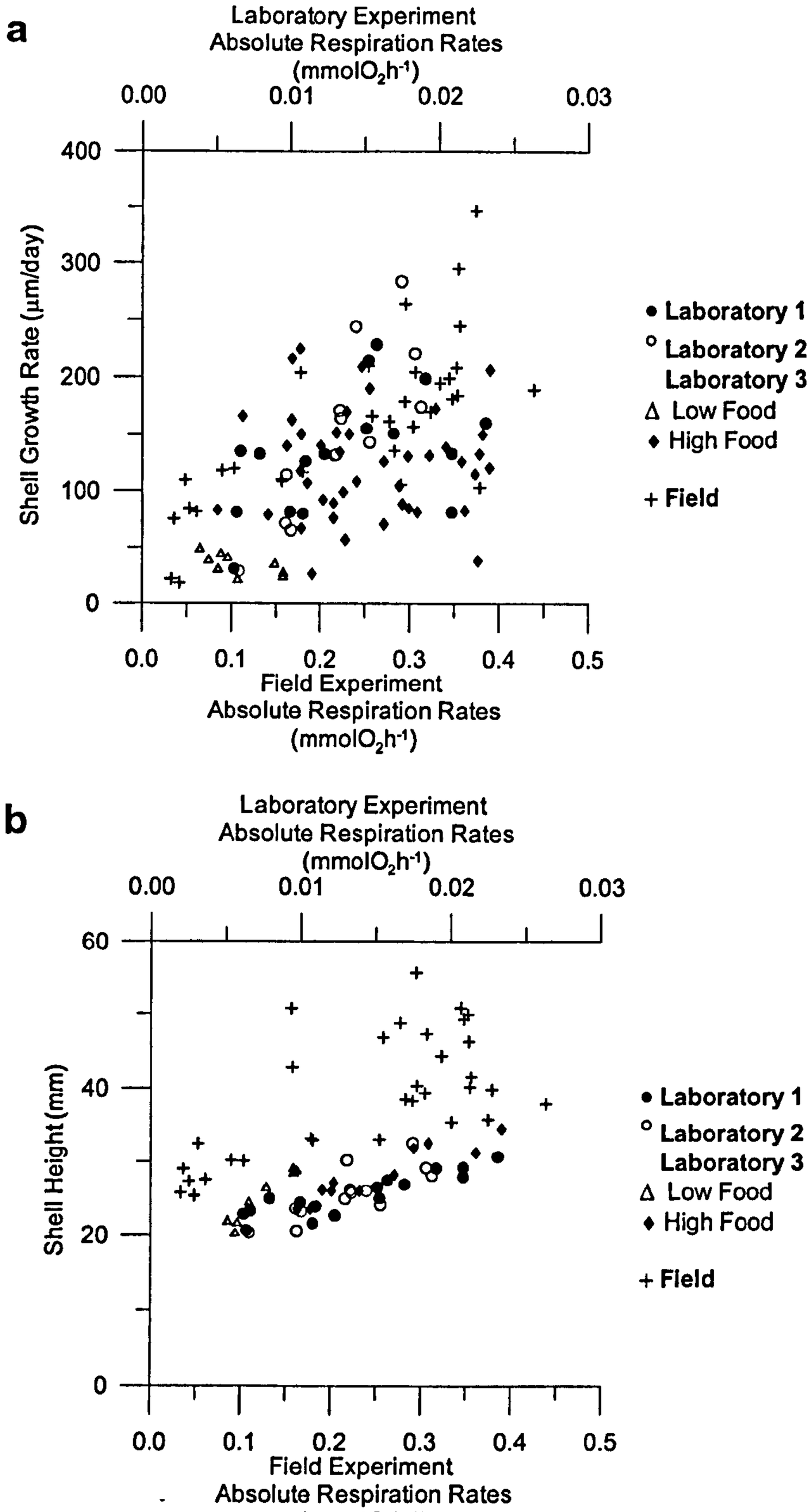

Figure 5 - 6 – Absolute respiration rate (ARR, $mmolO_2/h$) of *Mytilus edulis* from both laboratory and field experiments plotted against: a) shell growth rate (SGR, μm/day) and b) shell height (mm). Note that ARR from laboratory and field grown *M. edulis* are plotted in different axis.

However, a model of a general metabolic control of shell Sr/Ca ratios in bivalve calcite or aragonite cannot be established at present. Indeed, while in *Mytilus edulis*

shell Sr/Ca ratios are clearly associated with metabolic activity (i.e. ARR and $\delta^{13}C$), previously published calcite Sr/Ca and $\delta^{13}C$ ratios data of *Pecten maximus* (Chapter 3), M*ytilus trossulus* (Klein et al., 1996b) and *Pinna nobilis* (Chapter 2), as well as of the aragonitic bivalves *Mercenaria mercenaria* and *Saxidomus giganteus* (Gillikin et al., 2005b) show contrasting results (Figure 5-3). In the aragonitic bivalves *Mercenaria mercenaria* and *Saxidomus giganteus*, shell Sr/Ca and $\delta^{13}C$ ratios were uncorrelated (Gillikin et al., 2005b). In *Mytilus trossulus*, a close relative of *M. edulis*, shell Sr/Ca ratios of two specimens were found to be either positive correlated, albeit weakly ($r^2 = 032$, $p = 0.003$), or uncorrelated with shell $\delta^{13}C$ ratios (Klein et al., 1996b). However, both shell Sr/Ca and $\delta^{13}C$ ratios were significantly correlated with salinity (Klein et al., 1996b), particularly shell $\delta^{13}C$ ratios ($r^2 = 0.85$, $p < 0.001$), suggesting shell $\delta^{13}C$ ratios may reflect changes in seawater $\delta^{13}C$ of dissolved inorganic carbon rather than an influence of metabolic activity. In field grown *P. maximus* specimens (Chapter 3) and in field collected specimens of *Pinna nobilis* (Chapter 2), however, significant relationships ($r^2 = 0.29$ $p < 0.001$ and $r^2 = 0.44$, $p < 0.001$, respectively) were observed between Sr/Ca ratios and $\delta^{13}C$ ratios (Figure 5-3), suggesting a possible metabolic control of Sr/Ca ratios in these two bivalve species.

5.5.2 What Controls Shell Sr/Ca ratios in Mytilus edulis and Pecten maximus?

At present, three different models have been proposed to describe kinetic (Gillikin et al., 2005b; Carré et al., 2006) and metabolic controls of bivalve shell Sr/Ca ratios (Klein et al., 1996b).

In *Mytilus trossulus*, Sr^{2+} incorporation in shell calcite was proposed to be modulated by metabolic efficiency in the mantle epithelium, where increased metabolic pumping of Ca^{2+} relative to Sr^{2+} would cause lower Sr/Ca ratios and lower $\delta^{13}C$ (Klein et al., 1996b). Gillikin et al., (2005b), however, has shown the metabolic pumping model of Klein et al. (1996) to be flawed in assuming a positive relationship between Sr/Ca ratios and $\delta^{13}C$ in bivalves, which is the opposite of what was observed in the present study and other studies (Gillikin et al., 2005b; Chapter 2), and on the basis of current knowledge of calcification, particularly on the

incapacity of Ca^{2+}-ATPase to sustain a high enough transport of Ca^{2+} to the site of calcification at high precipitation rates (Cohen and McConnaughey, 2003).

Gillikin et al. (2005) suggested that increased activity of Ca^{2+}-ATPase, an enzyme involved in the transport of Ca^{2+} to the site of calcification (Cohen and McConnaughey, 2003), at higher metabolic activity increases calcification rate and should decrease Sr/Ca ratios by increasing Ca^{2+} pumping disproportional to Sr^{2+}, due to the higher affinity of Ca^{2+} -ATPase for Ca^{2+}. However, this implies that Sr/Ca ratios and shell growth rates should be inversely correlated, which is the opposite of what is observed in bivalves (Klein et al., 1996b; Gillikin et al., 2005b; Lorrain et al., 2005; Carré et al., 2006). Gillikin et al., (2005b), suggested that increased Sr/Ca ratios in the central extra-pallial fluid (EPF) during periods of rapid shell growth (Wada and Fujinuki, 1976), if valid for the marginal EPF, could explain the relationship between shell Sr/Ca ratios and calcification rate.

Recently, Carré et al., (2006) proposed a new model for control of Sr/Ca ratios that explains the unexpected (Zhong and Mucci, 1989) positive relationship between Sr/Ca and SGR observed in aragonite bivalves (Stecher et al., 1996; Takesue and van Geen, 2004; Gillikin et al., 2005b), as well as in the calcite from *Mytilus trossulus* (Klein et al., 1996b) and *Pecten maximus* (Lorrain et al., 2005; Chapter 3). Carré et al., (2006) argue that the two proposed pathways for Ca^{2+} transport through the calcifying mantle (Wheeler, 1992; Klein et al., 1996b), a diffusive inter-cellular pathway and an active intra-cellular pathway based on Ca^{2+} -ATPase (Cohen and McConnaughey, 2003; Gillikin et al., 2005b), cannot support the Ca^{2+} flux necessary for biomineralization. According to these authors most Ca^{2+} transport must be intra-cellular to avoid ionic deregulation of the internal medium, but Ca^{2+} -ATPase cannot account for the Ca^{2+} flux necessary to sustain mineralization. Carré et al., (2006) thus propose an alternative intra-cellular pathway based on ionic calcium channels, which are widespread in biological tissues, are ion selective and can support very high ionic fluxes. In such a model, high calcification rates change the electrochemical potential driving ions through the channel and decrease the ion selectivity of calcium channels leading to an increase in the transport of Sr to the EPF, and ultimately to higher shell Sr/Ca ratios.

Gillikin et al., (2005b) and Carré et al., (2006) models thus are based on kinetic effects due to transport across biological membranes that are driven by shell growth rate. However, such growth rate based models cannot explain Sr/Ca variations in shells with stable growth rate or in very slow growing species that may not involve Ca^{2+}-channels in ionic transport (Carré et al., 2006). Furthermore, Gillikin et al., (2005b) and Carré et al., (2006) models are not necessary to explain the observed dependence of shell Sr/Ca ratios on SGR in calcite, which are known from experimentally precipitated inorganic calcite to be precipitation rate dependent (Lorens, 1981a; Morse and Bender, 1990; Tesoriero and Pankow, 1996), a dependence that can occur at the crystal-solution interface (Reeder and Paquette, 1989; Paquette and Reeder, 1995; Wasylenki et al., 2005b).

The present study supports Gillikin et al., (2005b) view on the Klein et al., (1996b) model, by showing an inverse relationship between shell Sr/Ca and $\delta^{13}C$ ratios in *Mytilus edulis* and *Pecten maximus*, but it does not support, however, the view that shell Sr/Ca ratios are controlled by the activity of Ca^{2+}-ATPase since this would cause an inverse relationship between Sr/Ca ratios and SGR, which is the opposite of what was observed. Furthermore, it is clear that no generalization can be made regarding the relationship between shell Sr/Ca and $\delta^{13}C$ ratios in bivalves, which can be absent (Gillikin et al., 2005b; this study), inverse (Chapter 2 and 3, this study) or even positive (Klein et al., 1996b). The observation that SGR and ARR are unrelated in *M. edulis*, suggests that the model of Carré et al., (2006) is not valid for this species, i.e. that high metabolic activity would drive calcification rate and thus lower the ion selectivity of the proposed Ca channel transport pathway and favour Sr^{2+} transport over Ca^{2+} to the EPF. In *Mytilus edulis*, therefore, shell Sr/Ca ratios were found to be under a joint, but distinct, control by SGR and ARR. Such observation suggests that the influence SGR and ARR on shell Sr/Ca ratios acts through different mechanisms, the former most likely at the crystal-solution interface and the latter through Sr^{2+} transport to the EPF.

5.6 Summary

To determine the physiological controls on Sr/Ca ratios in bivalve calcite, *Mytilus edulis* and *Pecten maximus* specimens were grown in laboratory and field (*M. edulis* only) culturing experiments. The well-defined chronology of newly deposited shell growth allowed to accurately determine the influence of seawater temperature, shell Mg content, shell growth rates and metabolic activity on the shell Sr/Ca ratios. Seawater temperature was clearly not a significant control of bivalve calcite Sr/Ca ratios, while shell growth rate was found to exert a significant influence on shell Sr/Ca ratios of *M. edulis*, but only a weak influence on shell Sr/Ca ratios of *P. maximus*. The positive relationship observed between absolute respiration rate and Sr/Ca in *M. edulis* grown in the laboratory and field culturing experiments provides the first direct evidence of the influence of metabolic activity on bivalve calcite Sr/Ca ratios. Further support for a metabolic control of shell Sr/Ca ratios also comes from the significant inverse relationship between shell Sr/Ca and $\delta^{13}C$ ratios in *M. edulis*, *P. maximus* and *Pinna nobilis*. However, such metabolic control of Sr/Ca ratios cannot be applied to bivalves in general.

In *Mytilus edulis*, shell Sr/Ca ratios were found to be under a joint control, albeit unrelated, by precipitation rate (i.e. SGR) and metabolic activity (i.e. ARR) that most likely acts through different mechanisms, the former at the crystal-solution interface and the latter through Sr^{2+} transport to the EPF. In addition, high metabolic activity is suggested to increase both the transport of Sr^{2+} and low $\delta^{13}C$ metabolic carbon into the EPF, ultimately resulting in higher shell Sr/Ca ratios as well as lower shell $\delta^{13}C$ ratios. Further research into the relationship between metabolic activity and shell Sr/Ca ratios is needed to fully understand the mechanisms of metabolic control of Sr incorporation in bivalve shells.

Chapter VI

An examination of potential controls on shell Mn/Ca ratios in the calcite of the bivalve *Mytilus edulis*

VI - An examination of potential controls on shell Mn/Ca ratios in the calcite of the bivalve *Mytilus edulis*

6.1 Abstract

The Mn/Ca ratios in the calcite of marine bivalves have been suggested to reflect both the dissolved and/or particulate Mn concentrations of seawater. However, a clear understanding of what controls shell Mn/Ca ratios is still lacking and a clear quantitative relationship between dissolved and/or particulate Mn and shell Mn/Ca ratios in either calcitic or aragonitic molluscs must be established and validated before any application of a bivalve Mn/Ca palaeoproxy. To study the influence of seawater dissolved and particulate Mn concentrations on bivalve shell calcite Mn/Ca ratios, *Mytilus edulis* specimens were grown in a field experiment in the Menai Strait, U.K., for a one-year period. A single maximum (0.54 μmol/l) during spring dominated the annual variation of seawater dissolved Mn concentrations, while seawater particulate Mn concentration was highest (up to 0.18 μmol/l) during autumn and winter, although smaller increases in particulate Mn during the phytoplankton spring bloom were also observed. In *M. edulis*, shell Mn/Ca ratios of newly precipitated calcite showed a double-peak annual variation with maximum values (up to 0.19 mmol/mol) during early spring and early summer. None of the two maximum of shell Mn/Ca ratios can be explained by an increase in either seawater dissolved or particulate Mn concentrations. Shell Mn/Ca ratios thus were not controlled by dissolved or particulate Mn concentrations. In *M. edulis*, the double-peak seasonal variation of shell Mn/Ca ratios was remarkably similar to the seasonal variation of shell growth rates. The influence of shell growth rate on shell Mn/Ca ratios is the opposite of the inverse relationship observed unequivocally between precipitation rate and Mn partition coefficient in synthetic inorganic calcite, and thus must reflect a physiological influence on shell Mn content. It is suggested the latter most likely acts through an increase in the transport of Mn into the extra-pallial fluid, raising its Mn content, and ultimately causing higher shell Mn/Ca ratios. The use of Mn content

from marine bivalve shell calcite as a proxy for the dissolved and/or particulate Mn concentrations, and thus the biogeochemical processes that control them, is unlikely until such physiological controls are better understood and eventually compensated for.

6.2 Introduction

Marine bivalves are widely distributed throughout the oceans, from the tropics to the polar regions and from coastal estuarine waters to the deep ocean, displaying a range of growth rates and longevity. The shells of marine bivalves are deposited incrementally and the elemental and isotopic composition of their shell changes in response to variations in the environment in which they live. Hence marine bivalve shells have the potential to record high-resolution time-series of the environmental conditions in which the organism grew, such as temperature (e.g., Williams et al., 1982; Klein et al., 1996a; e.g., Kennedy et al., 2001; Elliot et al., 2003; Schoene et al., 2003; Schoene et al., 2004; Chauvaud et al., 2005), salinity (Ingram et al., 1996b; Klein et al., 1996b) and trace-element concentration (Fuge et al., 1993; Raith et al., 1996; Stecher et al., 1996; Price and Pearce, 1997; Vander Putten et al., 2000; Richardson, 2001; Gillikin et al., 2005a; Gillikin et al., 2006a; Pearce and Mann, 2006). The incorporation of manganese in riverine and marine calcitic and aragonitic bivalve shells has been suggested as a possible proxy for either dissolved or particulate manganese (Lindh et al., 1988; Jeffree et al., 1995; Vander Putten et al., 2000; Markich et al., 2002; Lazareth et al., 2003; Freitas et al., 2006; Langlet et al., 2006; Langlet et al., 2007).

The dominant factor that affects the aquatic geochemistry of Mn is the change in oxidation state between two oxidation states, the soluble Mn^{2+} ion and the insoluble Mn^{4+} ion (e.g. Burton and Statham, 1988), which undergo transformations between the dissolved and particulate phases mainly in response to changes in pH and redox conditions (e.g. Glasby and Schulz, 1999 and references therein). The rate of dissolved Mn oxidation is slow and so it may persist for some time in the water column (Wilson, 1980). Dissolved Mn^{2+} can be removed from solution by oxidation

to Mn^{4+} in insoluble manganese oxides through abiogenic oxidation (e.g. Bruland, 1983), photo-oxidation (Nico et al., 2002), as well as by uptake into, or oxide precipitation onto surfaces of bacteria (Emerson et al., 1982; Sunda and Huntsman, 1985; Sunda and Huntsman, 1987) and phytoplankton (Richardson et al., 1988; Lubbers et al., 1990; Richardson and Stolzenbach, 1995; Schoemann et al., 1998; Roitz et al., 2002). Dissolved Mn sources include release via bacterial reduction of Mn-oxides (Klinkhammer and McManus, 2001) and photo-reduction of Mn-oxides, but mainly from freshwater inputs and benthic fluxes when bacterial remineralisation of organic matter exhausts dissolved oxygen in the sediment pore waters and alternative oxidants such as Mn oxides are used (Burton and Statham, 1988; Burdige, 1993; Laslett, 1995; Tappin et al., 1995; Millward et al., 1998; Burnett et al., 2003). Benthic fluxes of Mn^{2+} to the water column are enhanced in the warmer summer months, when biological activity is increased and oxygen concentrations are generally lower (Hunt, 1983; Sundby et al., 1986; Dehairs et al., 1989; Berelson et al., 2003). Particularly, the seasonal inputs of organic material (e.g. phytoplankton-derived) in coastal areas have been shown to be associated with the release of Mn^{2+} from surface sediments to the water column (Sundby et al., 1981; Hunt, 1983; Sundby et al., 1986; Dehairs et al., 1989; Thamdrup et al., 1994; Slomp et al., 1997; Millward et al., 1998; Hall et al., 1999).

The biogeochemical cycle of Mn in marine and estuarine waters is associated with numerous elements (such as carbon, sulphur, phosphorus and several trace elements), organic matter and redox conditions, and thus Mn may play an important role in tracing the biogeochemical cycles of many elements, as well as the response of coastal systems to seasonal and long term eutrophication (e.g. Murray, 1975; Turekian, 1977; Balistrieri and Murray, 1986; Hunt and Kelly, 1988; Burdige, 1993). For instance, the hydroxides of Mn act as efficient scavengers of other metals (e.g. Glasby, 1984) and when Mn remobilisation occurs in sub-oxic sediments, metals associated with the Mn-oxyhydroxide coatings may also be released (e.g. Duinker et al., 1982). If a consistent relationship can be established between the Mn content of biogenic calcites and the dissolved and/or particulate Mn concentrations of seawater, the Mn/Ca ratios of marine calcifying organisms potentially can provide a proxy for dissolved and particulate Mn concentrations and thus for those redox processes that can control the concentration of this element in seawater.

In inorganic calcite, manganese has been shown to substitute for calcium in the crystal lattice, and to be incorporated into the calcite mineral by the formation of a dilute solid solution of $MnCO_3$ in $CaCO_3$ (Pedersen and Price, 1982; Pingitore et al., 1988). In inorganic calcite, precipitation rate also has been shown to influence the incorporation of Mn^{2+}, and Mn concentration in calcite was found to be to be inversely correlated to the rate of precipitation (Lorens, 1981a; Mucci, 1988; Pingitore et al., 1988; Dromgoole and Walter, 1990). In addition, the composition of the precipitation solution has been found to influence the partition of Mn in calcites precipitated from artificial seawater, probably due to the effect of Mg^{2+} ion present in seawater (Franklin and Morse, 1983; Mucci, 1988). The effect of temperature on the incorporation of Mn in synthethic calcites is still controversial with studies reporting both positive and inverse relationships, although in calcite deposited from synthetic solutions under controlled precipitation rates, the positive temperature effect was of similar magnitude to the effect of precipitation rate (Dromgoole and Walter, 1990).

The manganese content of bivalve shells is seen as a potential record of ambient Mn concentrations. In particular, the aragonitic shells of freshwater unionoid bivalves have been shown to be valid archives of dissolved Mn levels associated with riverine anthropogenic inputs (Lindh et al., 1988; Jeffree et al., 1995; Markich et al., 2002), but also of both dissolved and biogenic particulate Mn concentrations associated with lacustrine upwelling and related changes in productivity (Langlet et al., 2007). In the calcite of marine bivalves, investigations relating shell Mn/Ca ratios to environmental variables have led to the suggestion of a possible control of shell Mn/Ca ratios by particulate and/or dissolved Mn (Vander Putten et al., 2000; Lazareth et al., 2003; Freitas et al., 2006; Langlet et al., 2006) concentrations. Elevated shell Mn/Ca ratios have been suggested to be related to spring bloom-induced increases in particulate and/or dissolved Mn in the bivalve *Mytilus edulis* (Vander Putten et al., 2000), or to increased riverine discharge events and associated increases in particulate and/or dissolved Mn in the tropical mangrove bivalve *Isognomon ephippium* (Lazareth et al., 2003). The seasonal variation of Mn/Ca ratios in the calcitic *Pecten maximus* in the Menai Strait, U.K. (chapter 3), has been shown to follow a similar trend to dissolved Mn described previously at the same location (Morris, 1974). The source of the seasonal signal in the water and hence the record in the shell was suggested to be due to benthic recycling. Langlet et al. (2006), by

repeatedly marking animals of the oyster *Cassostrea gigas* in seawater with artificially elevated dissolved Mn concentrations, produced the first direct evidence for the rapid uptake of dissolved Mn^{2+} into the calcite of bivalve shells. These studies demonstrate the potential of Mn/Ca ratios archived in bivalve shells as a bio-monitor for anthropogenic inputs and as record of dissolved and/or particulate Mn concentrations from both freshwater and marine environments. But despite these encouraging results a clear understanding of what controls shell Mn/Ca ratios, i.e. dissolved and/or particulate Mn concentrations, is still lacking. In addition, a clear quantitative relationship between dissolved and/or particulate Mn and shell Mn/Ca ratio in either calcitic or aragonitic molluscs must be established and validated before any application of a bivalve Mn/Ca palaeoproxy.

It is apparent, despite a wide range of studies, that little or no clear understanding of the effects and interplay that environmental conditions and physiological processes have on the incorporation of Mn in bivalve shells has been obtained. In this study, the relationship between dissolved and particulate Mn^{2+} concentrations and shell Mn/Ca ratios in bivalve calcite has been assessed. Specimens of the blue mussel, *Mytilus edulis*, were grown in a field experiment for a one-year period. The constrained chronology of new shell growth obtained has allowed completion of a reliable comparison between shell Mn/Ca ratios and measurements of contemporaneous seawater dissolved and particulate Mn concentrations, shell growth rate and other relevant environmental variables. This dataset also has enabled the additional consideration of the significance of shell growth rate effects on shell Mn/Ca ratios. Such an approach develops further a reliable evaluation of the use Mn content from marine bivalve shells as a proxy for dissolved or particulate Mn concentrations.

6.3 Material and Methods

6.3.1 Field Culturing Experiment

Specimens of the bivalve *Mytilus edulis* were suspended 1 metre below a moored raft in the Menai Strait (Figure 3-1, pp 71) from the 8th December 2004 to the 12th December 2005. The animals were all less than 1 year old when deployed, obtained from one spat cohort and initially ranged from 20 to 27 mm in shell length. This raft is moored in the close vicinity (ca. 500 m) of the School of Ocean Sciences, University of Wales Bangor in a section of the Menai Strait where the water column is completely mixed, due to strong turbulent tidal mixing (Harvey, 1968). Animals were deployed in mesh cages and each shell was identified by a mark hand drilled on its surface. Two different, but parallel, experimental approaches were taken: 1) Short-deployment specimens were placed into cages for 16 short, well-defined and consecutive growth intervals that together covered the duration of the entire field experiment. The duration of each growth interval varied during the experiment according to expected seasonal changes in shell growth rate and in seawater parameters, particularly in dissolved Mn^{2+} concentration; 2) In contrast to the short-deployment specimens, annual-deployment specimens were placed in the field for the entire duration of the experiment. To ensure that short-deployment specimens were in the same physiological condition as their annual-deployment counterparts, and to avoid the inevitable period of acclimation if animals were deployed directly from laboratory conditions, short-deployment specimens were taken at the start of each growth interval from a stock of animals maintained in the Menai Strait from the beginning of the experiment and kept under the same conditions, but located in a separate cage.

At the end of each growth interval, all short-deployment specimens and all annual-deployment specimens, were removed from the raft, together with a new set of short-deployment specimens taken from the stock that were to be used during the next growth interval deployment. All of these shells then were photographed and digitally imaged using the AnalySIS software package. During this manipulation, *Mytilus edulis* specimens were exposed to the air for 5 to 6 hours resulting in emplacement of a disturbance mark on the surface of the shells. The combination of disturbance marks and photographs was used to identify and measure all shell growth for each growth interval, as well as shell height (i.e. the distance from the umbo to the shell margin along the main axis of growth). The data provide a time control of the new shell growth laid down throughout the field experiment by assuming shell growth

rate to be constant during each growth intervals. Furthermore, the known deployment and retrieval times of the *M. edulis* specimens thus have allowed for direct comparison of shell Mn/Ca ratios with contemporaneous measurements of seawater parameters. At the end of each growth interval, the tissue was removed from each shorth-deployment specimen, dried to constant weight at 60°C and tissue dry weight measured.

6.3.2 Seawater Temperature, Salinity, Chlorophyll-a and Nutrient Concentrations, Particulate and Dissolved Mn^{2+} Measurements

For the duration of the field experiment the following key seawater parameters were measured every two to five weeks (Figures 6-2 and 6-3; Appendix 5): seawater temperature, salinity, nutrient concentration (nitrate and nitrite, phosphate and silicate), chlorophyll-*a* and total particulate and dissolved Mn^{2+} concentration. Seawater temperature was monitored every two hours throughout the experimental deployment period using submerged temperature loggers placed in the mesh cages containing the animals (Gemini Data Loggers TinyTag - TGI 3080; accuracy of ± 0.2°C). Surface seawater samples for measurement of salinity were collected, in the vicinity of the moored raft, using sealed salinity Winchester glass bottles. Salinity was determined using an AutoSal 8400 Autosalinometer calibrated with International Association for Physical Sciences of the Ocean (I.A.P.S.O.) standard seawater (analytical accuracy and resolution of ± 0.003 equivalent PSU). For chlorophyll-*a*, a separate surface seawater sample and back at the laboratory agitated to ensure homogeneity and then filtered (500–1000 ml) through Whatman GF/C filters of 47 mm diameter (nominal pore size 1.2 μm and frozen for storage. Subsequently, samples were defrosted and chlorophyll-*a* extracted for 18 hours at 4°C with 90% acetone and measured using a Turner Design 10-AU fluorometer calibrated against a chlorophyll-*a* standard (method adapted from (Parsons et al., 1984). The filtrate from the chlorophyll-*a* samples was collected in 30 ml clean polythene bottles and kept frozen until subsequent determination of the major dissolved inorganic nutrients. Nitrate plus nitrite (hereafter, nitrate), dissolved inorganic phosphorus (DIP) and silicic acid, were determined using standard colourimetric methodology (Grasshof et al., 1983), as adapted for flow injection analysis (FIA), on a LACHAT Instruments Quick-Chem 8000 autoanalyzer (Hales et al., 2004).

Particulate Mn was determined following a method adapted from Millward et al., (1998). Samples were collected from the same container used for chlorophyll-a sampling and then filtered (120–650 ml) through 0.4 μm polycarbonate filters of 47 mm diameter, which were mounted in clean glass filter holders, washed with milli-Q water and frozen for storage in clean individual petri dishes. After thawing, the filter and the particulate matter were digested in clean centrifuge tubes for 10 hours at room temperature using 1.5 ml of 1M HCl (Aristar). This fraction of the particulate Mn represents easily reducible Mn oxides and does not include the Mn in detrital mineral grains. Following digestion, the sample was centrifuged for one hour to settle the undissolved material and 1 ml of the supernatant diluted between 50 to 400 times depending on Mn concentration. The Mn concentration in the digest solutions was analysed using a Varian Instruments 220Z Zeeman graphite furnace atomic absorption spectrometer with Zeeman background correction calibrated with synthetic solutions made up in 1M HCL (Mn concentration range 0–15 μg l^{-1}). Procedure blanks were prepared likewise by leaching blank filters. Replicate measurements of a particulate Mn sample run concurrently with the samples (2.62 ± 0.10 μg l^{-1}; N = 16) returned an analytical precision of 3.8 % (RSD), while measurements of replicate particulate Mn samples (2.47 ± 0.09 μg l^{-1}; N = 6) showed a best sample precision of 3.5 % (RSD).

Samples of surface seawater also were collected for the determination of dissolved Mn^{2+} using 100 ml *polythene* syringes. These samples were filtered *in-situ* through an in-line syringe and 0.4 μm polycarbonate filters. The filtrate was collected into a 30-mL *HDPE* bottle, after discarding the first 10 ml aliquot, and then frozen on return to the laboratory until analysis. Samples were analysed for dissolved Mn concentration using a Varian Instruments 220Z Zeeman graphite furnace atomic absorption spectrometer with Zeeman background correction using a method adapted from Su and Huang (1998). A chemical modifier, $Pd(NO_3)_2$, was added to the samples and standards at a concentration of 2000 μg/ml to overcome matrix interferences. Calibration was achieved by standard additions (total Mn concentration range 0.9–30.9 μg l^{-1}) using 0.2 μm filtered and ultraviolet irradiated Menai Strait seawater. Certified reference seawater (CASS-4, National Research Council, Canada) was analysed with each batch of samples to validate the accuracy

of the dissolved Mn measurements. Replicate measurements of CASS-4 (2.91 ± 0.11 μg l^{-1}; N = 24) returned a recovery of 104.5 % relative to the certified Mn concentration value (2.78 ± 0.19 μg l^{-1}) and an analytical precision of 4.6 % (RSD), while replicate measurements (N = 3) of two seawater samples showed a best sample precision of 8.8 % (RSD).

6.3.3 Shell Preparation and Milling

The left hand valve of *Mytilus edulis* shells from the short and annual deployments were cleaned with a brush and the outer organic periostracum was milled away with the drill until periostracum-free shell was visible in the entire sampling area. Two short specimens were sampled for each growth interval, while three annual specimens were sequentially sampled for all growth intervals. Shell powder samples were taken from the new shell growth by milling to a depth of ca. 200 μm using a 0.4 mm wide steel carbide burr (Minerva Dental Ltd) attached to a hand-held dental drill. Accurate milling was completed under a binocular microscope fitted with an eyepiece graticule, and depth and width of milling were controlled carefully. Each milled powder sample was taken from the main axis of shell growth to avoid the increase in shell curvature that occurs away from the main growth axis. Whenever the amount of shell growth permitted more than one sample was collected from a single growth interval. On such occasions the new shell growth was equally divided between the number of samples collected ($2 \leq N \leq 4$).

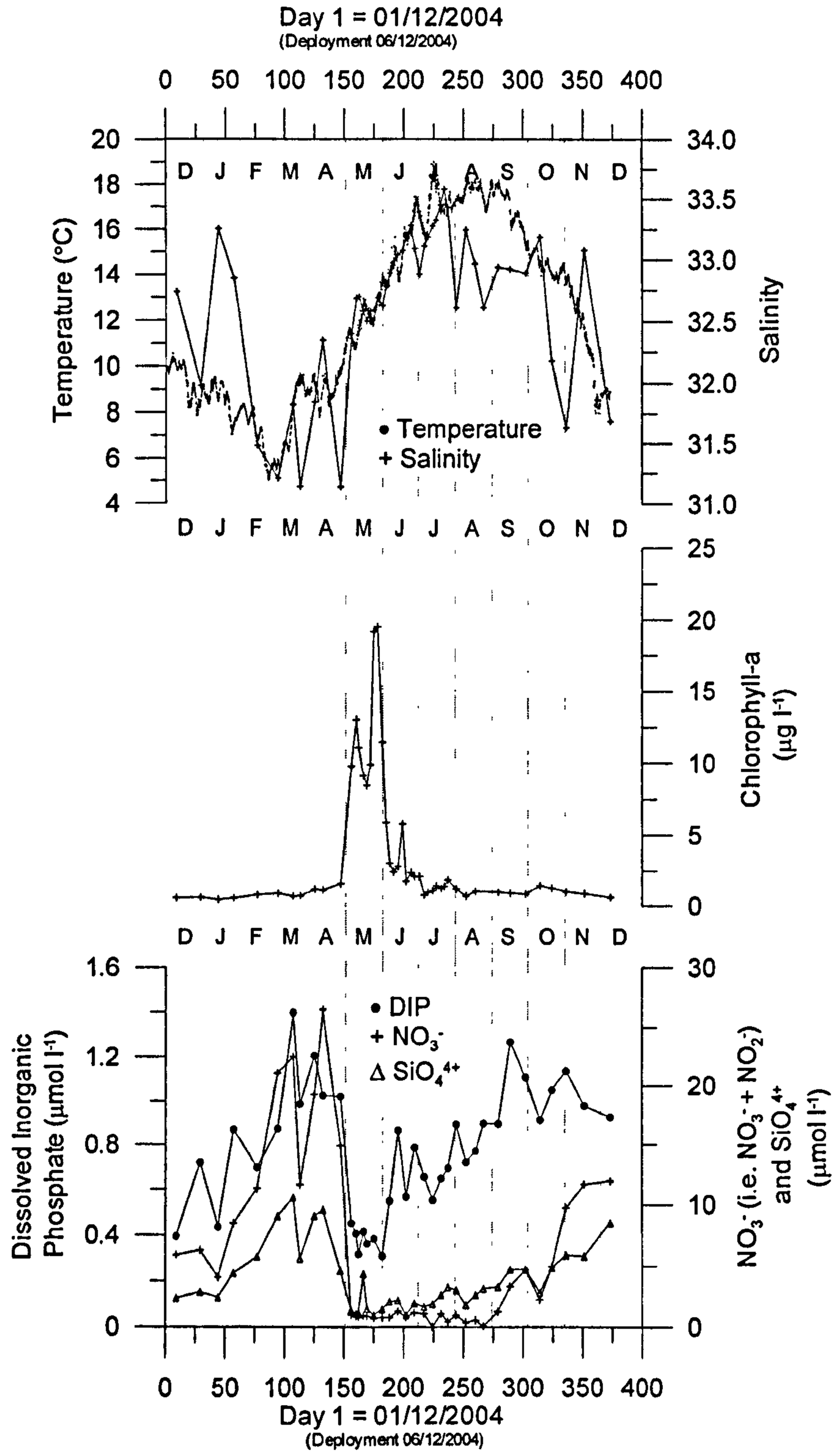

Figure 6 - 1 – Variation of seawater temperature, salinity, chlorophyll-*a* concentration, and nutrient concentrations (dissolved inorganic phosphate, nitrate + nitrite and silicic acid) measured in surface waters of the Menai Strait from December 2004 to December 2005.

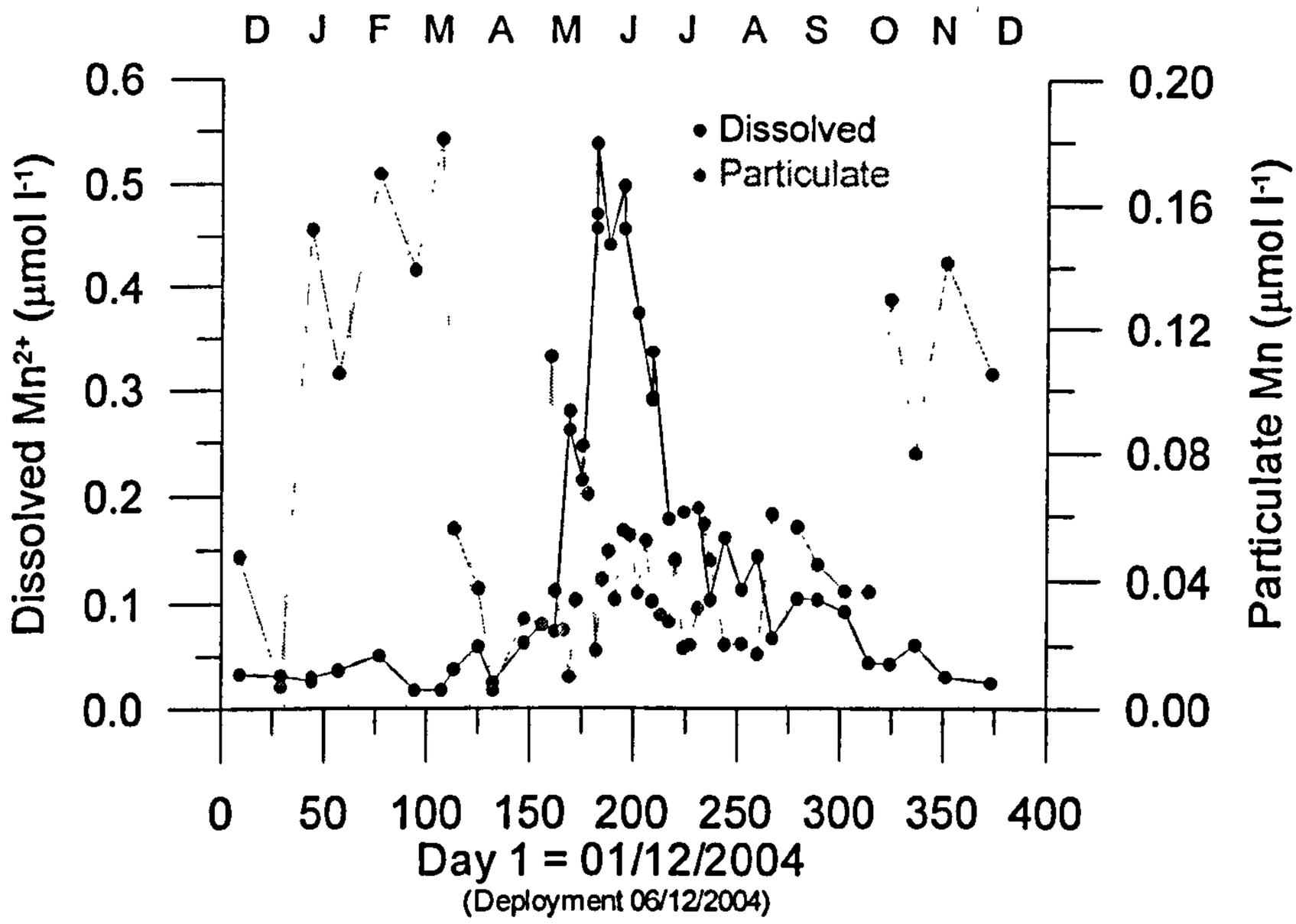

Figure 6 - 2 – Variation of dissolved and particulate Mn concentrations measured in surface waters of the Menai Strait from December 2004 to December 2005.

6.3.4 Shell Mn/Ca Ratio Analyses

Calibration for Mn/Ca ratio determinations was performed via an established ICP-AES intensity-ratio method (de Villiers et al., 2002), using synthetic standard solutions in the range 0.03–0.30 mmol/mol for Mn/Ca ratios at Ca concentrations of 60 µg/ml. Sample preparation is described in detail elsewhere (Chapters 2 and 3) Measurements were made using the Perkin Elmer Optima 3300RL ICP-AES instrument housed at the NERC ICP Facility, Royal Holloway University of London. Instrumental drift was monitored by running an intermediate (0.1 mmol/mol) calibration standard every 10 samples and data then were corrected accordingly. Analytical precision (expressed as relative standard deviation or RSD; N = 33) was 4.0 % for Mn/Ca ratios, while replicate measurements of the same milled powder samples obtained from four *Mytilus edulis* specimens showed a precision better than 7.5 % RSD. For comparison with future datasets, Mn/Ca ratio measurements are reported (Table 6-1)for three solutions (BAM-RS3, ECRM-752 and CMSI-1767) that have been proposed as certified reference materials (CRMs) for measurement of element/Ca ratios in carbonates (Greaves et al., 2005).

Table 6 - 1 – Measured Mn/Ca ratios for three certified reference material (CRMs) solutions (Greaves et al., 2005).

CRM solution	This study
BAM-RS3	0.011 ± 0.003 (N = 8)
ECRM-752	0.141 ± 0.003 (N = 8)
CMSI-1767	0.075 ± 0.002 (N = 8)

The replicates reported for this study are repeated measurements of a single dissolution completed for each CRM and diluted to Ca concentrations of 60 µg/ml. All measurements were made on the same Perkin Elmer Optima 3300RL ICP-AES instrument.

6.4 Results

6.4.1 Seawater Temperature, Salinity, Nutrient and Chlorophyll-a Concentrations in the Menai Strait

Seawater temperature exhibited a clear seasonal pattern (Figure 6-1). Seawater temperature decreased from ca. 10.0°C in December 2004 to a minimum temperature of ca. 5.0°C in the end of February, followed by a rise to ca. 9.5°C during mid March–late April (from day 105 to 140) and then a further rise up to a maximum temperature of ca. 19.0°C in early–mid July (ca. day 225). From that time to early September (ca. day 280) seawater temperature remained high at ca. 18.0°C, before it decreased to ca. 9.0°C in December 2005. Salinity in the Menai Strait also exhibited variation throughout the experimental period (Figure 6-1), with maxima of 33.3 and 33.6 in January and July, respectively, while salinity minima of 31.1 and 31.6 occurred in March–April and November–December, respectively.

During the experimental period, chlorophyll-*a* increased from pre-spring bloom values of ca. 1.2 µg l^{-1}, after the end of April 2005 (ca. day 150), and reached a maximum of 19.5 µg l^{-1} in May 2005 (day 178) (Figure 6-1). There was a rapid decrease in nutrient concentrations in early April, while no increase in chlorophyll-a concentrations were observed until late April. The broad maxima in chlorophyll (with a double maximum on days 160 and 178) existed for over a 4 week period from the end of April (day 150) through the beginning of June (day 185 (Figure 6-1), which itself, was concurrent with the minima in nitrate, silicate and phosphate (Figure 6-1). Chlorophyll-*a* concentration then returned to pre-bloom values in July (Figure 6-1).

6.4.2 Dissolved and Particulate Mn^{2+} concentrations in the Menai Strait

Dissolved Mn^{2+} concentrations were <0.06 µmol l^{-1} from December 2004 until the beginning of May 2005 (day 155), when values increased rapidly to a maximum of up to 0.54 µmol l^{-1}, during the period between the end of May (day 160) and mid June (day 200). Dissolved Mn^{2+} concentrations then decreased to values of ca. 0.18 µmol l^{-1} by early July (day 213) and at a slower rate of decrease to values of ca. 0.09 µmol l^{-1} by early October (day 315). From October to December 2005 dissolved Mn^{2+} concentrations remained low and similar to values measured in the last months of 2004 and first months of 2005. The marked annual variation in dissolved Mn was somewhat similar to chlorophyll-*a* concentrations in terms of the occurrence of a broad double maxima concentrations (Figures 6-2 and 6-3), albeit with the maximum concentrations being observed later than the maximum in chlorophyll-*a*.

Particulate Mn concentrations showed a marked annual variation with two distinct broad maxima from 0.18 to 0.14 µmol l^{-1} during January-March and October–November 2005, respectively. Two smaller, but still distinct particulate Mn maxima (0.11 µmol l^{-1} on day 160 and 0.08 µmol l^{-1} on day 175) occurred in May 2005 concurrent with the spring bloom double maximum in chlorophyll-a concentrations (Figures 6-2 and 6-3). Lower particulate Mn concentrations of 0.01 to 0.11 µmol l^{-1} occurred from April to September 2005 (Figure 6-2).

6.4.3 Shell Growth Rates and Tissue Dry Weights

Shell growth rates (SGR) exhibited two distinctive growth maxima in late April (ca. day 140) and mid–late June (ca. day 200) (Figure 6-3). Growth rates increased from the lowest values of ca. 20 µm/day in December 2004 to the early maxima of up to 204 µm/day in April 2005 (ca. day 140). Shell growth rates then decreased to a minima of 50–100 µm/day in mid May (ca. day 160), before a sharp increase to maximum values of up to 381µm/day by mid June (ca. day 200). Shell growth rates then decreased to 44–109 µm/day in December 2005. The annual variation of SGR

of different animals, and also of short- and annual- deployment specimens, is similar during the experiment (Figure 6-3), and mean annual SGR were not significantly different (t-test, $p > 0.05$) between individuals. Nevertheless, at any given time differences in SGR occur between individual individuals. For instance, from August onwards SGR were higher in the short-deployment than in the annual-deployment specimens, while in the two SGR maxima, SGR of individual animals range from 137 to 204 μm/day in the April maximum and from 250 to 381 μm/day in the June maximum (Figure 6-3).

Tissue dry weight of short-deployment specimens only, increased steadily in early April 2005 (ca. day 125) from the lowest values of < 0.1 g in the winter months from December 2004 to March 2005 towards maximum values from late July to October 2005, after which tissue dry weight values were highly variable (Figure 6-3).

6.4.4 Shell Mn/Ca Records

In both short- and annual-deployment specimens, shell Mn/Ca ratios showed a double-peak variation that was similar in timing to the maxima in SGR (Figure 6-2). Shell Mn/Ca ratios increased from low values of 0.02–0.06 mmol/mol during winter (December 2004–March 2005) to first maxima of 0.09–0.17 in late April (ca. day 140), before decreasing to minima of 0.03 to 0.04 mmol/mol in the end of May (ca. day 175). Second maxima in Mn/Ca ratios, of up to 0.19 mmol/mol, occurred during June (ca. day 190). After June, shell Mn/Ca ratios decreased to values below ca. 0.04 until December 2005. Mean annual shell Mn/Ca ratios were significantly different between short- and annual- deployment specimens (t-test, $p = 0.008$), but there were no significant differences between the three annual specimens (t-test, $p > 0.05$). Shell Mn/Ca ratios were significantly correlated, albeit weakly, to SGR in both short- ($r^2 = 0.34$, $p < 0.001$) and annual-deplyment specimens ($r^2 = 0.13$, $p < 0.001$), as well as to dissolved Mn^{2+} concentration in both short- ($r^2 = 0.34$, $p < 0.001$) and annual-deployment specimens ($r^2 = 0.38$, $p < 0.001$).

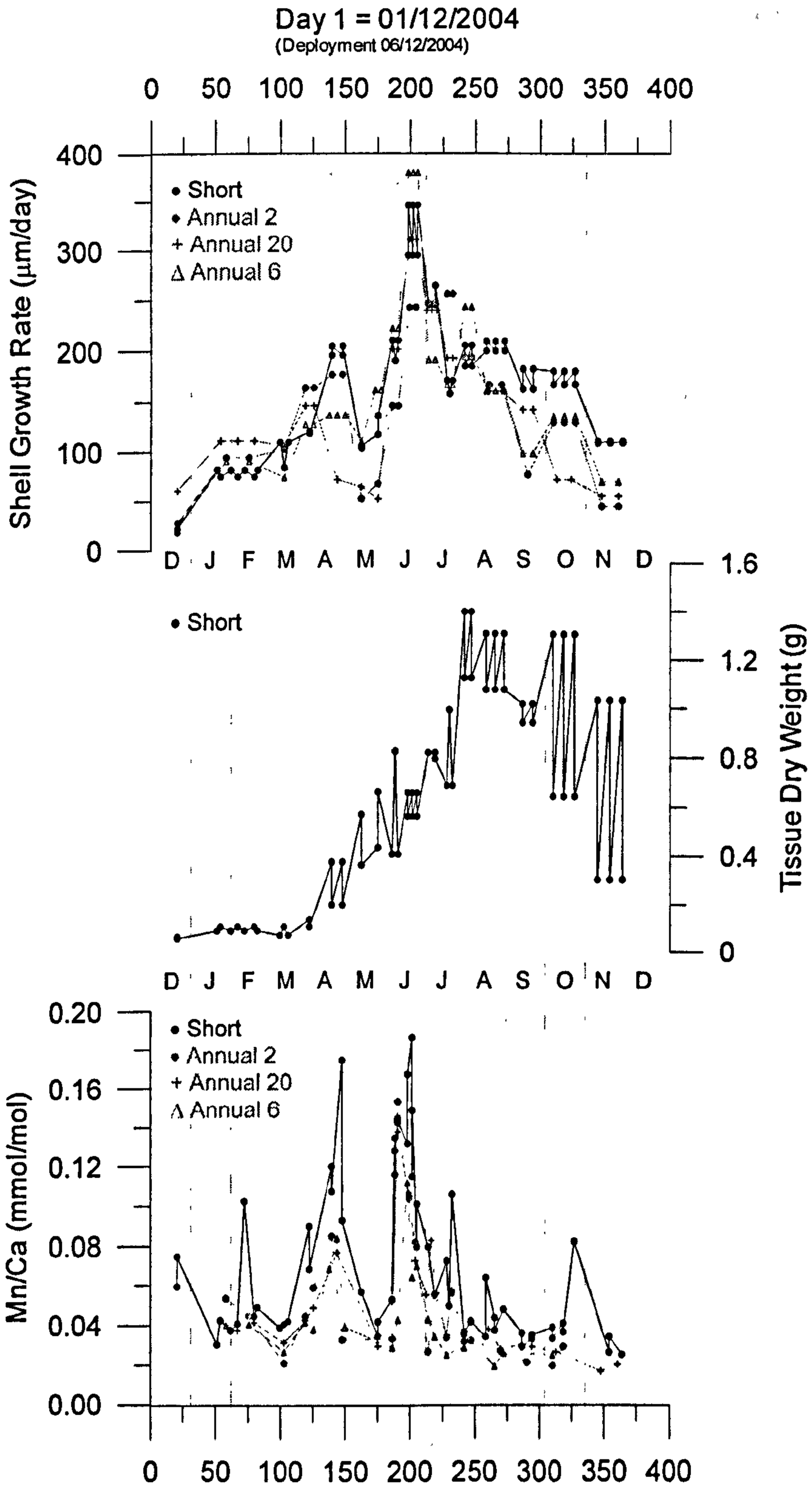

Figure 6 - 3 – Variation of shell growth rates, tissue dry weight (short-deployment specimens only) and shell Mn/Ca ratios of *Mytilus edulis* specimens grown in the Menai Strait from December 2004 to December 2005.

6.5 Discussion

6.5.1 Variation of Dissolved and Particulate Mn Concentrations in the Menai Strait: The influence of Biogeochemical Processes

In the Menai Strait (Morris, 1971), as in other coastal locations (Morris, 1971; Davidson and Marchant, 1987; Richardson et al., 1988; Lubbers et al., 1990; Richardson and Stolzenbach, 1995; Schoemann et al., 1998; Roitz et al., 2002), dissolved and particulate Mn concentrations during spring are closely associated with phytoplankton blooms. Increased particulate Mn concentrations have been observed at or after the peak of the phytoplankton bloom (Morris, 1971; Schoemann et al., 1998). Two clear particulate Mn maxima (0.11 μmol l^{-1} on day 160 and 0.08 μmol l^{-1} on day 175) were observed concurrently with the spring bloom double maximum in chlorophyll-*a* concentrations, but preceding maximum dissolved Mn concentrations (Figures 6-2 and 6-3). A similar sequence of concurrent maxima in particulate Mn and chlorophyll-a, which coincide with a minimum in dissolved Mn that then increases, also was observed on day 234 (Figures 6-2 and 6-3). Increased dissolved Mn concentrations are often observed to occur after the peak of primary production, when chlorophyll-*a* concentration is decreasing and heterotrophic activity is high (Schoemann et al., 1998), Maximum dissolved Mn concentrations followed the onset of the spring bloom, as defined by an increase in chlorophyll-*a* and occurred approximately at the time of the expected increase in heterotrophic activity in the Menai Strait (Figures 6-2 and 6-3), which lags by one to two weeks the *Phaeocystis* and chlorophyll-*a* bundance maxima (Blight et al., 1995). In the Menai Strait and in the coastal waters of the North Sea (Morris, 1971; Lubbers et al., 1990; Schoemann et al., 1998), Mn surface adsorption to *Phaeocystis* bladder colonies and diatoms is thought to be an important mechanism by which particulate Mn levels may increase during bloom conditions, while sedimentation and degradation of decaying colonies causes the slow decrease in particulate Mn levels (Morris, 1971) that followed each of the two particulate Mn maxima (Figure 6-2, days 160 and 175).

Release of dissolved Mn will occur during decomposition of phytoplankton derived organic material in the sediment (Morris, 1971; Sundby et al., 1981; Hunt, 1983; Sundby et al., 1986; Dehairs et al., 1989; Thamdrup et al., 1994; Slomp et al., 1997; Schoemann et al., 1998), in sub-oxic micro-environments within suspended aggregates (Klinkhammer and McManus, 2001) and associated to high heterotrophic acitivity (Schoemann et al., 1998), Some of the dissolved Mn will then adsorb or precipitate to suspended particulate material, while the remainder will stay in solution in the water column (Schoemann et al., 1998). The latter will contribute to the observed post-bloom increase in dissolved Mn concentrations (Figures 6-2 and 6-3). The balance between the sedimentary/reductive sinks and the phytoplankton uptake/adsorption sources, most likely will control the variation in particulate Mn concentrations during the summer (Figure 6-2). The decrease in heterotrophic activity over the summer, associated with the exhaustion of the phytoplankton bloom derived organic matter, would result in the observed decrease in dissolved Mn concentrations during the summer, while particulate Mn concentrations subsequently increased to a autumn and winter maxima (Figure 6-2). In the coastal waters of the North Sea German Bight, a winter maximum in particulate Mn concentration has been shown to be associated with Mn poor particles but a high suspended particulate matter (SPM) load (Dellwig et al., 2007). In addition, in the Humber and the Thames estuaries higher particulate Mn concentration during winter have been attributed to minimal biogenic production and higher sediment resuspension by seasonally-elevated wind speeds and larger swell (Turner and Millward, 2000). In the Menai Strait, suspended particulate matter is dominated by inorganic terrigenous particles (Kratzer et al., 2000), varies seasonally with lower values in the summer and higher values in winter, and has been suggested to respond to long-term variations in wind-forcing (Kratzer et al., 2003), In addition, the number of days with gales and the monthly mean wind speed from the Valley weather station, within ca. 25 km from the Menai Straits, show a marked seasonal variation with higher values in winter and lower values in summer (www.metoffice.gov.uk/climate/uk/location/wales.winds /html and www.llansadwrn-wx.co.uk/w_graphs05.html), Consequently, the autumn and winter maxima of particulate Mn in the Menai Strait during 2005 most likely result from higher SPM concentrations relative to the spring and summer.

Nevertheless, the influence of freshwater inputs of dissolved Mn, which can be significant in the coastal waters of the Irish Sea (Laslett, 1995) and North Sea (e.g. Dellwig et al., 2007), cannot be discarded. Furthermore, the marked seasonal variation of dissolved Mn in the Menai Strait during 1969 and 1970 was suggested not to be related with the spring bloom or particulate Mn concentration maxima (Morris, 1974), both of which it preceded, but to an increase during spring in the release of Mn from the sediments of the Menai Strait (Morris, 1974).

6.5.2 Shell Mn/Ca ratios in Mytilus edulis Controlled by Dissolved or Particulate Mn?

There is no clear consensus from the literature of whether dissolved or particulate Mn controls the Mn/Ca ratio in bivalve carbonate (Lindh et al., 1988; Jeffree et al., 1995; Vander Putten et al., 2000; Markich et al., 2002; Lazareth et al., 2003; Langlet et al., 2006; Langlet et al., 2007), and the relative importance of dissolved and particulate seawater Mn as sources of Mn to the shells of marine bivalves remains largely unknown. A significant correlation ($0.58 < r^2 < 0.72$, $p < 0.001$) between seawater temperature and shell Mn content has been was observed by Langlet et al., (2006), in agreement with the observations for synthetic inorganic calcite (Dromgoole and Walter, 1990). However, in this study the *Mytilus edulis* shell Mn/Ca ratios were not significantly correlated to temperature ($p > 0.05$).

For the *Mytilus edulis* shells investigated in this study, a simple relationship between shell Mn/Ca ratios and dissolved and/or particulate Mn concentrations has not been observed. In multiple specimens of *M. edulis*, Mn/Ca ratios above 0.04 mmol/mol occurred as two clear peaks, the first between day 100 and 175 and the second between day 175 and 225 (Figure 6-3). By comparison, in the water column, the highest particulate Mn concentrations were observed over the winter periods between days 25 to 125 and day 315 to 365 (Figure 6-2), while the peak in dissolved Mn occurred between day 160 and 270 (Figure 6-2). Thus there is no overlap between timing of the particulate Mn and Mn/Ca maxima, but there was an overlap between the dissolved Mn and the second of the Mn/Ca maxima.

Notwithstanding this overlap, the documented maximum in dissolved Mn preceded, by ca. two weeks, the second of the two peaks in *Mytilus edulis* shell Mn/Ca ratios (Figures 6-3 and 6-4). A lag of a few days has been observed between the response of shell calcite Mn contents to an experimentally induced increase in ambient Mn concentrations in the freshwater bivalve *Hyridella depressa* (Jeffree et al., 1995), but a lag of less than 24h has been observed in the marine bivalve *Cassostrea edulis* (Langlet et al., 2006), Therefore, it would be reasonable to expect the occurrence of a similar duration lag in the field experiment. Thus neither maximum in shell Mn/Ca ratios can be explained by an increase in dissolved Mn. For the first Mn/Ca peak there was no preceding or concurrent increase in dissolved Mn and for the 2nd Mn/Ca maxima the increase in shell Mn concentrations occurred too long after the observed peak in dissolved Mn concentrations.

Outside the period of the autumn and winter particulate Mn maxima, there are smaller increases in particulate Mn during the phytoplankton spring bloom chlorophyll-*a* maximum on day 160 and day 175. In this study a lag of ca. 30 days occurred between the last of the two spring-bloom particulate Mn maxima, at the end of May, and the second peak in shell Mn/Ca in the middle of June. A longer lag period for the incorporation of particulate Mn than dissolved Mn may be appropriate as particles have to be ingested and then transported through the animals' body prior to incorporation into the shell. As for dissolved Mn, there was no preceding or concurrent increase in particulate Mn that could account for the first Mn/Ca peak. Thus, in *Mytilus edulis* shell Mn/Ca ratios do not appear to be under the sole influence of either dissolved and/or particulate Mn concentrations.

6.5.3 Shell Growth Rates and Mn/Ca ratios in Mytilus edulis: A Physiological Control?

In this study, there is evidence for a physiological influence on shell Mn/Ca ratios due to the significant relationship with shell growth rates (SGR; $r^2 = 0.34$ in short-deployment specimens and $r^2 = 0.13$ in annual-deployment specimens; $p < 0.001$ for all). Such a relationship is weak and thus can only explain a small proportion of the total variability in shell Mn/Ca ratios. However, the support for a physiological

influence on *Mytilus edulis* shell Mn content comes from the remarkable similarity in the seasonal variation of shell Mn/Ca ratios and SGR (Figure 6-3).

The two distinct SGR peaks most likely were driven by different processes: 1) the early peak fuelled by an increase in seawater temperature and probably fuelled by energy reserves, since no relevant changes in phytoplankton biomass (from chlorophyll-*a* measurements) were observed at that time (Figure 6-1); 2) The second peak in SGR was most likely fuelled by an increased food supply following the spring bloom. The reduction in SGR during May, i.e. between the two reduction in SGR is not accompanied by a decrease in tissue dry weight, which increased steadily from March until September–October (Figure 6-2), suggesting that during that time energy use was focused on tissue growth, most likely gametogenesis and spawning (Seed and Suchanek, 1992), and thus diverted away from shell growth. Nevertheless, whatever the reasons for the observed seasonal changes in SGR in this study, shell Mn/Ca ratios and SGR varied synchronously, with two marked peaks evident in both records during early spring (March–early May) and early summer (late May–June).

If it is assumed that a positive relationship between shell Mn/Ca ratios and SGR relates to mineral precipitation rate during shell calcification, then the above described relationship is the opposite of the inverse relationship observed unequivocally between precipitation rate and Mn partition coefficient in synthetic inorganic calcite (Lorens, 1981a; Mucci, 1988; Pingitore et al., 1988; Dromgoole and Walter, 1990). Therefore, the significant positive relationship observed between SGR and shell Mn/Ca ratios in *Mytilus edulis*, cannot be indicative of a precipitation rate control but must reflect one or more physiological processes.

Wada and Fujinaki, (1976) found that Mn/Ca ratios in the shell-forming fluid (the extra-pallial fluid or EPF) of the central extra-pallial space (the space between the mantle and the inner shell surface or EPS) of four marine bivalve species was higher during periods of increased growth than in periods of reduced growth. Further evidence for a physiological control on the Mn content in the EPF of bivalves, albeit in freshwater species (Pietrzak et al., 1976), are the observations that the Mn concentrations in the EPF of unionid bivalves are maintained within a narrow range (from 0.05 to 0.09 μmol l^{-1}) independently of the external Mn concentration (from ca.

0 to 0.85 μmol l^{-1}). If such observations are applicable to the marginal EPF, where shell deposition in the shell margin occurs and which is separated from the central EPF by the attachment of the mantle to the inner shell surface along the pallial line, one logical hypothesis to explain the data obtained in this study is that SGR influences the concentration of Mn in the EPF, i.e. high rates of shell deposition would cause an increase in the transport of Mn into the EPF, raising its Mn content, and ultimately causing higher shell Mn/Ca ratios. Furthermore, only a small fraction of the Mn in the EPF of *Mytilus edulis* is present as free ionic Mn, with the remainder bound with organic molecules (Misogianes and Chasteen, 1979), which most likely repsesents a physiological control on the activity of Mn in the EPF.

In *Mytilus edulis*, Mn/Ca ratios of shell calcite were not controlled by either dissolved or particulate seawater Mn concentrations, but were under the control of one or more physiological processes that most likely act through an increase in the transport of Mn into the extra-pallial fluid. The use of Mn content from marine bivalve shell calcite as a proxy for the dissolved and/or particulate Mn concentrations, and thus the biogeochemical processes that control them, is thus unlikely until such physiological controls are better understood and eventually compensated for.

6.6 Summary

In *Mytilus edulis*, grown in a field culturing experiment in the Menai Strait for one year, shell Mn/Ca ratios were found not to be influenced by dissolved or particulate Mn concentrations. Shell Mn/Ca ratios of *M. edulis* specimens showed a double-peak variation with maximum values during early spring and early summer, while only a single maximum dominated the annual variation of dissolved Mn. Particulate Mn was highest throughout autumn and winter and was at minima at the time of the two spring shell Mn/Ca maxima. Support for a physiological influence on *M. edulis* shell Mn content comes from the remarkable similarity in the double-peak seasonal variation of both shell Mn/Ca ratios and shell growth rates. However, such an observation is the opposite of the inverse relationship observed unequivocally

between precipitation rate and Mn partition coefficient in synthetic inorganic calcite. It ia suggested that the influence of shell growth rate on shell Mn/Ca ratios must reflect a physiological influence most likely acting through an increase in the transport of Mn into the extra-pallial fluid, raising its Mn content, and ultimately causing higher shell Mn/Ca ratios.

Chapter VII

Ion microprobe assessment of the heterogeneity of Mg/Ca, Sr/Ca and Mn/Ca ratios in *Pecten maximus* and *Mytilus edulis* (bivalvia) shell calcite precipitated at constant temperature

VII - Ion microprobe assessment of the heterogeneity of Mg/Ca, Sr/Ca and Mn/Ca ratios in *Pecten maximus* and *Mytilus edulis* (bivalvia) shell calcite precipitated at constant temperature

7.1 Abstract

Small-scale heterogeneity of biogenic carbonate elemental composition can be a significant source of error in the precise and accurate use of elemental/Ca ratios as geochemical palaeoenvironmental proxies. In this study, ion microprobe (secondary ionisation mass spectrometry; SIMS) has been used to obtain high-spatial resolution Mg/Ca, Sr/Ca and Mn/Ca ratio profiles through new shell calcite, from single structural layers, of the marine bivalves *Pecten maximus* (king scallop) and *Mytilus edulis* (blue mussel). For both mollusc species the new shell calcite was precipitated at a constant temperature of ca. 20°C in a laboratory aquaria culturing experiment. In the *P. maximus* shell Mg/Ca, Sr/Ca and Mn/Ca ratios varied consistently between SIMS profiles, from the outer to the inner shell surfaces, with: an outermost shell of highest and most variable element/Ca ratios and a mid region to innermost shell with lower and rather invariant Mg/Ca ratios, whereas Sr/Ca and Mn/Ca ratios were lowest in the mid region but higher closer to the innermost shell. In the *M. edulis* shell, Mg/Ca, Sr/Ca and Mn/Ca ratios also were more spatially variable than in *P. maximus*, but varied over a smaller range of values. The *M. edulis* new shell growth also exhibited different Mg/Ca and Sr/Ca ratios within individual growth increments deposited contemporaneously but at different locations within the shell. In addition, elevated Mg/Ca, Sr/Ca and Mn/Ca ratios are associated with the deposition of elaborate shell features, i.e. a shell surface stria in *P. maximus*; surface shell

disturbance marks in both species also perturb shell Mg/Ca and Sr/Ca ratios compared to the rest of the shell. Since the latter shell features are a common occurrence in all marine bivalve shells they will thus influence strongly the outermost shell Mg/Ca ratios and hence compromise application of any Mg/Ca–temperature relationship based on conventional milling techniques. In contrast, invariant Mg/Ca ratios observed in the mid region and inner part of the *P. maximus* shell suggests potential application of Mg/Ca ratios from such material as a palaeotemperature proxy in this particular species. Small-scale element distribution in the shells of *P. maximus* and *M. edulis* is suggested to derive from the combined influence of the organic matrix and mantle metabolic activity in element incorporation during shell biomineralization. Furthermore, in both *P. maximus* and *M. edulis*, a large variation in elemental/Ca ratios in shell deposited from the same EPF was observed and thus suggests that element incorporation at the shell crystal-solution interface, and not transport to the EPF, most likely is the key control step of shell element composition.

7.2 Introduction

The elemental composition of marine biogenic carbonates has been thought to provide a powerful tool to obtain information on Earth's present and past climates and oceanographic conditions. The basis of this approach is the observed dependence of the elemental compositions of marine biogenic calcite and aragonite minerals on several ambient environmental parameters, such as temperature, salinity, nutrient levels, carbonate ion concentration and seawater chemistry. Application of this kind of palaeoceanographic proxy-based approach is dependent, however, on rigorous testing of the veracity of relationships between the geochemical proxies and controlling environmental parameters, and must be documented and tested by both laboratory and field-based calibration and validation studies. High degrees of variability recorded in these proxy–parameter relationships will reduce the precision with which past environmental conditions can be reconstructed, and the potential source(s) of such variability need(s) to be recorded and understood.

Several factors are known to complicate any simple dependence of element/Ca ratios in biogenic and synthetic calcites on the associated environmental variables of interest. For instance, growth rates, salinity, pH, and biological kinetic and/or metabolic factors have all been proposed to influence the Mg and Sr composition of biogenic calcites (Lorens and Bender, 1977; Lorens and Bender, 1980; Elderfield et al., 1996; Klein et al., 1996a; Klein et al., 1996b; Lea et al., 1999; Rickaby et al., 2002; Freitas et al., 2006) while precipitation rate, solution composition and near-surface kinetics have been shown to influence elemental incorporation into synthetic calcite precipitated from controlled solutions (e.g. Lorens, 1981a; Mucci and Morse, 1983; Pingitore and Eastman, 1986; Dromgoole and Walter, 1990; Morse and Bender, 1990; Paquette and Reeder, 1995). The reliable and accurate use of elemental/Ca ratios in marine biogenic calcites as geochemical proxies, thus is dependent on understanding in more detail, and subsequently compensate for, the role of secondary controls (i.e. metabolic and/or kinetic factors) on element incorporation into biogenic and inorganic calcites.

The factor or factors that determine the small-scale (<100 μm) element composition will most likely control to a large extent the observed non-environmental variation (i.e. not associated with changes in environmental parameters) of elemental/Ca ratios in bivalve calcite at a larger scale. Conventional 'bulk' sampling techniques, i.e. that mill to depths of up to a few hundred microns in order to obtain powders for solution elemental analyses, could integrate any compositional heterogeneity to variable extents in different samples, thereby reducing spatially resolved records and introducing a significant unknown error. Such compositional heterogeneity has been reported previously for Mg/Ca ratios in *Mytilus edulis* (Lorens and Bender, 1980; Rosenberg and Hughes, 1991; Rosenberg et al., 2001). Thus, application of analytical techniques that allow elemental determinations at a spatial resolution commensurate with the natural incremental growth pattern in bivalve mollusc shells is necessary in order to gain a greater knowledge of the extent and causes of any small-scale heterogeneity of elemental ratios within bivalve shell calcite. For instance, such knowledge allows a greater appreciation of the implications that this compositional heterogeneity may have on the limited temperature control and large variability of Mg/Ca ratios reported for some bivalves, i.e. *M. edulis* (Dodd, 1965; Klein et al., 1996a; Vander Putten et al., 2000) and *Pecten maximus* (Lorrain et al.,

2005; Chapter 3), as well as for the potential use of the Mg/Ca ratio–temperature proxy, or Sr/Ca and Mn/Ca ratios, in bivalve calcite for palaeoceanographic reconstructions.

For archives that retain a potential palaeotemperature proxy, such as Mg/Ca, it is as critical to test the veracity of the proxy under a single constant temperature as it is under a range of temperatures. In contrast to other biominerals produced by marine organisms, the high spatial resolution distribution of elements within molluscan shell calcite deposited at a constant temperature has not been studied in any detail. The majority of mloluscan studies to date have focussed on small scale temporal variability in shell chemistry, rather than testing small scale variability under more stable and controlled conditions. Ion microprobe, or secondary ionisation mass spectrometry (SIMS), has proven extremely useful for assessing small-scale heterogeneity (~10 μm) in the distribution of thermodynamically-controlled elements (i.e. Mg and Sr) within the shells of planktonic (Bice et al., 2005) and benthonic foraminifera (Allison and Austin, 2003), as well as corals (Allison, 1996; Cohen et al., 2001; Meibom et al., 2004). In molluscs, however, the SIMS technique has only been used previously to investigate high spatial resolution time-series variability of pollutant-type elements in bivalve shells (Jeffree et al., 1995; Siegele et al., 2001; Markich et al., 2002). Electron microprobe (Lorens and Bender, 1980; Lutz, 1981; Rosenberg and Hughes, 1991; Rosenberg et al., 2001; Dauphin et al., 2003; Dauphin et al., 2005), particle-induced X-ray emission (PIXE) (Swann et al., 1991; Siegele et al., 2001), cathodoluminescence emission (Langlet et al., 2006), proton microprobe (Coote and Trompetter, 1995), synchrotron radiation-based X-ray fluorescence (Thorn et al., 1995; Kurunczi et al., 2001) and laser ablation ICP-MS (e.g. Raith et al., 1996; Price and Pearce, 1997; Leng and Pearce, 1999; Toland et al., 2000; Vander Putten et al., 2000; Lazareth et al., 2003; Langlet et al., 2007) also have been used to determine spatial variability in the elemental composition of molluscan shells, albeit again related to high resolution reconstructions in animals experiencing time varying environmental conditions.

Only a few studies have focused on the small-scale variability (~10 μm) of element composition within bivalve shells when environmental conditions would predict invariant element composition and the majority of these studies have focussed on

Mg/Ca ratios because of its potential application as a palaeotemperature proxy (Lorens and Bender, 1980; Rosenberg and Hughes, 1991; Rosenberg et al., 2001; Dauphin et al., 2003; Langlet et al., 2006). At the spatial scale of individual crystals, precipitated over very short time scales it would have been expected that element/Ca ratios would be invariant but Dauphin et al., (2003) observed variation in the Mg and S content of the organic rich inter- and intra prismatic structures of the shell prismatic calcite in *Pinna nobilis* and *Pinctada margartifera*. Therefore, changes in the amount of the shell organic matrix, but also in the size of the shell calcite crystals, could have a significant impact on the shell Mg content. Langlet et al. 2006 observed Mn incorporation in the shell calcite of the oyster *Cassostrea gigas* to be related to the dissolved Mn concentration, as well as to seawater temperature, and to vary within the shell over tens of microns up to several millimetres at daily, tidal and seasonal scales. Significant small-scale variability of Mg/Ca and Sr/Ca ratios (from <5 to 40 mmol/mol and 0.6 to 1.6 mmol/mol, respectively) over scales of 100's μm, has been observed in new shell growth from *Mytilus edulis* cultured in natural seawater under controlled conditions at temperatures between 22 and 24°C, but also in semi-artificial 'seawater' solutions with varying Mg/Ca and Sr/Ca ratios (Lorens and Bender, 1980). In that study, the stress of capture and adaptation to a new laboratory environment induced the deposition of a shell region (termed "transition zone calcite" by those authors) with Mg/Ca and Sr/Ca ratios up to five and two times higher, respectively, than surrounding shell material. Furthermore, Rosenberg et al., (2001) demonstrated, using digital electron probe microscopy, that small scale variations in Mg concentrations in *M. edulis* calcite were due to Mg being concentrated along the margins of calcite prisms, especially along the terminations of the crystals, with the alignment of adjacent crystals then producing compositional growth bands within the shell. In *M. edulis*, the Mg content of the outer calcite shell layer also was shown to be higher in regions with slow-growth, high shell curvature and with high mantle (the organ that controls calcification) activity, than in shell areas with fast shell growth, low shell curvature and low mantle activity (Rosenberg and Hughes, 1991). It also has been suggested that *M. edulis* uses Mg (and sulphur) to control shell crystal elongation and hence shell form along different axes (Rosenberg et al., 2001). Despite the relatively intensive studies on Mg/Ca ratios there has been little or no examination of spatial variability in Sr/Ca and/or Mn/Ca despite their potential utility as palaeoproxies.

In an initial preliminary assessment of the extent of any small-scale heterogeneity in Mg/Ca, Sr/Ca and Mn/Ca ratios in bivalve shell calcite, new shell material precipitated by *Pecten maximus* (king scallop) and *Mytilus edulis* (blue mussel) in a constant-temperature laboratory culturing experiment has been analysed using the ion microprobe or SIMS technique. These two bivalve species, as well as closely related taxa, have been proposed previously as archives for palaeoceanographic studies (e.g. Krantz et al., 1988; Klein et al., 1996a; Hickson et al., 1999; Chauvaud et al., 2005; Gillikin et al., 2006a; Wanamaker et al., 2006; Wanamaker et al., 2007) and hence are suitable materials for such an investigation of the extent of spatial variability in bivalve shell elemental concentrations. Since culturing took place under constant temperature conditions, any observed variation of element/Ca ratios will be independent of temperature, thus allowing consideration of other potential controlling factors. This methodological approach is especially valid for Mg/Ca ratios in bivalve calcite, which should be invariant within the new shell growth if a simple thermodynamic influence is the predominant control on this geochemical proxy, and also may provide further insights into explaining the reported weak or no temperature control and large variability of bivalve calcite Mg/Ca ratios (Dodd, 1965; Taylor et al., 1969; Carter, 1990a; Klein et al., 1996a; Vander Putten et al., 2000; Lorrain et al., 2005; Freitas et al., 2006).

7.3 Material and Methods

Single specimens of *Pecten maximus* (shell height - 34.5 mm) and *Mytilus edulis* (shell height - 29.3 mm) were selected from a group of individuals that had been cultured for 27 and 24 days, respectively, in laboratory constant-temperature aquaria. Seawater temperature in the aquarium was measured by *in-situ* logger (Gemini Data Loggers TinyTag - TGI 3080) as 20.33±0.13°C (N = 2952) and 20.21±0.13°C (N = 2304) for the duration of the two culturing periods. A full and detailed description of the culturing experiment set-up can be found elsewhere (Chapter 4). For both species studied, approximately 5–6 mm of new shell was precipitated during the total

experimental period; emergence (*M. edulis*) or handling (*P. maximus*) of each animal occurred at the beginning of the culturing period and twice more during the experiment and resulted in three "growth intervals" (denoted as T1, T2 and T3 on Figures 7-1 and 7-2), separated from one another by disturbance marks on the surface of the shell (denoted by the black vertical lines on Figures 7-1 and 7-2), with each "growth interval" representing ca. one weeks shell growth.

One shell of each species was mounted in blocks using *Robnor resins* epoxy resin (direct equivalent of araldite CY1301 and MY778) and Aradur hardener (HY951) and subsequently sectioned parallel to the main growth axis. Polished sections were digitally photographed under a light microscope and then sputter-coated with gold to inhibit build up of charge on the sample during SIMS analysis. Following SIMS analysis, the resin blocks were re-polished, etched in 0.5% acetic acid with 12.5% gluteraldehide, sputter-coated with gold and imaged under a Cambridge-S120 scanning electron microscope.

The general shell structure of *Pecten maximus* consists of both outer and inner irregularly oriented foliated calcite layers (Taylor et al., 1969), with some pectinid species also having a very thin aragonite prismatic pallial myostracum (Taylor et al., 1969; Carter, 1990b). Neither the inner layer, nor the myostracum, was observed in the new growth region of the *P. maximus* specimen subject to SIMS analyses. The general structural characteristics of *Mytilus edulis* bivalve shells are reported to be two primary calcium carbonate layers and an outer organic layer, the periostracum, which covers the outer surface of the shell. The outer shell layer is finely prismatic calcite with the inner layer a nacreous aragonite, these being separated by a thin pallial myostracum made up of irregular simple prismatic aragonite (Hinton, 1995). Only the outer prismatic calcite layer was observed in the new growth region of the *M. edulis* specimen subject to SIMS analyses. Therefore, for both species the SIMS profiles only spanned a single, outer, structural layer of both bivalve mollusc species.

a)

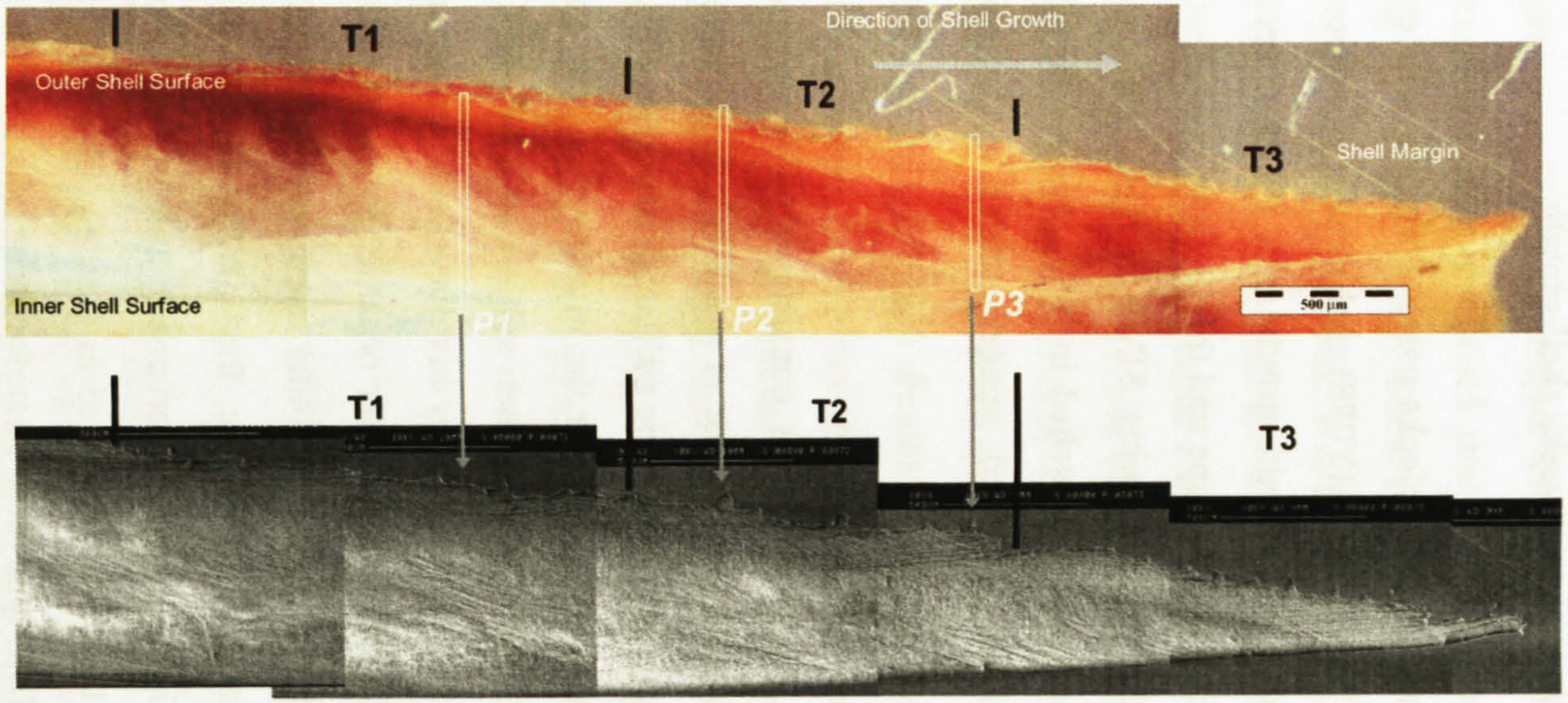
T1
T2
T3
Direction of Shell Growth
Outer Shell Surface
Inner Shell Surface
Shell Margin
500 µm
P1
P2
P3

b)

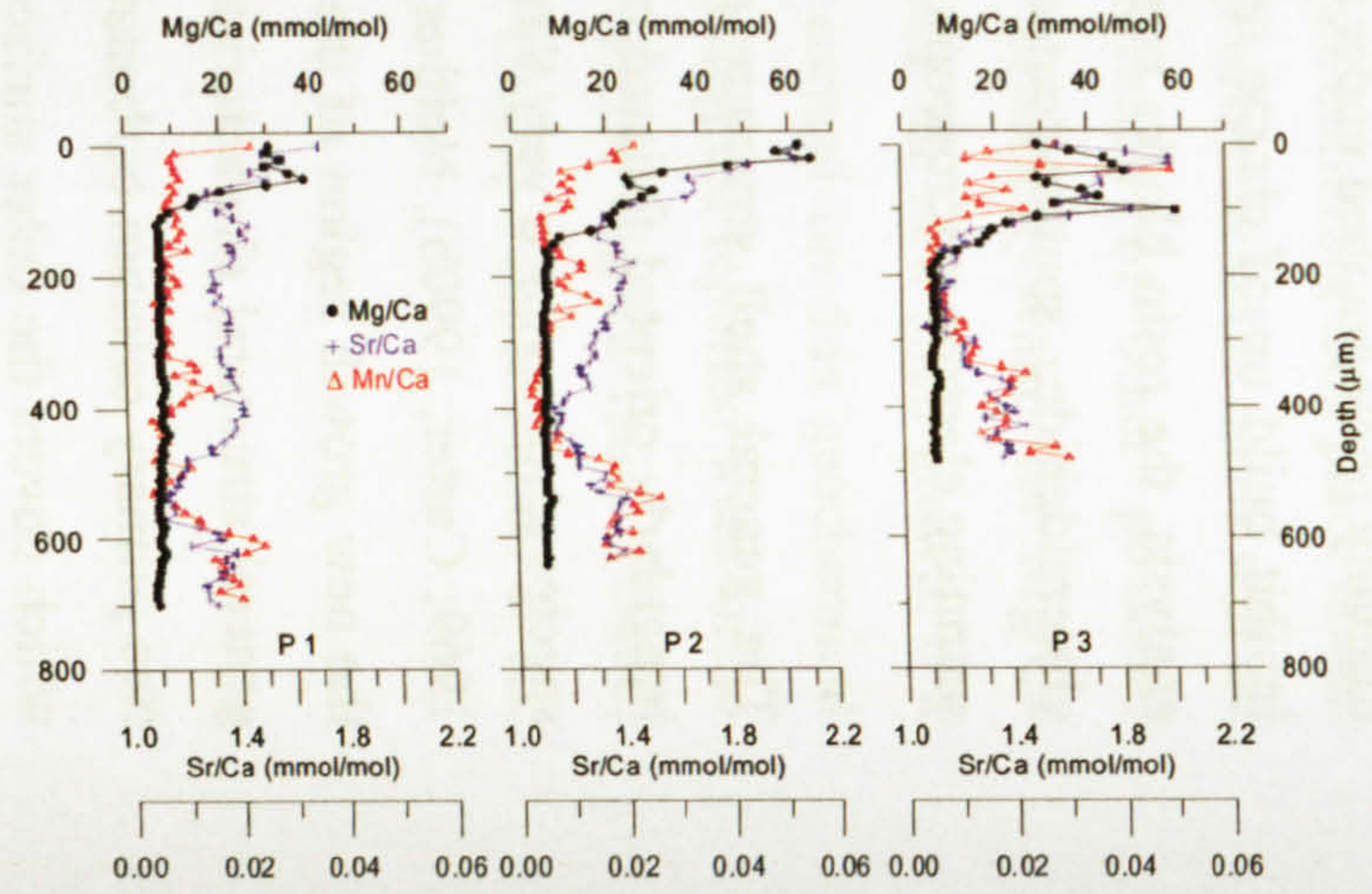
Mg/Ca (mmol/mol)
0 20 40 60
0 200 400 600 800
Depth (µm)
• Mg/Ca
+ Sr/Ca
Δ Mn/Ca
P 1
P 2
P 3
1.0 1.4 1.8 2.2
Sr/Ca (mmol/mol)
0.00 0.02 0.04 0.06

Figure 7 - 1 – a) Light microscope photograph and SEM image of *Pecten maximus* with location of SIMS profiles marked. Two profiles sampled particular features of the *P. maximus* shell, i.e. a shell stria (P2) and the region of a shell surface disturbance mark (P3). The black vertical lines mark the boundaries between three different "growth intervals", T1, T2 and T3, and these disturbance marks correspond to times when the *P. maximus* specimen was handled and photographed in a small holding tank. b) SIMS Mg/Ca (black line), Sr/Ca (blue line) and Mn/Ca (red line) ratio profiles for the *P. maximus* specimen, with depth measured from the outer shell surface towards the inner shell surface. The shell umbo is located towards the left of the figure and the shell growing margin towards the right of the figure. Direction of shell growth is from left to right in the image.

a)

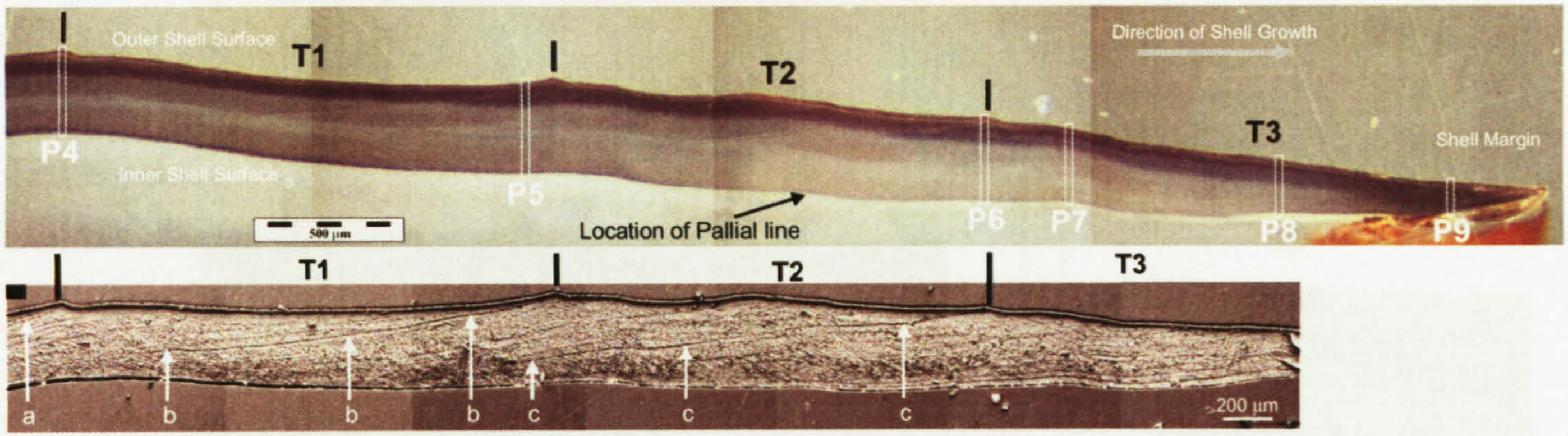
Outer Shell Surface
Inner Shell Surface
T1
T2
T3
P4
P5
P6
P7
P8
P9
Direction of Shell Growth
Shell Margin
500 µm
Location of Pallial line
a
b
b
b
c
c
c
200 µm

b)

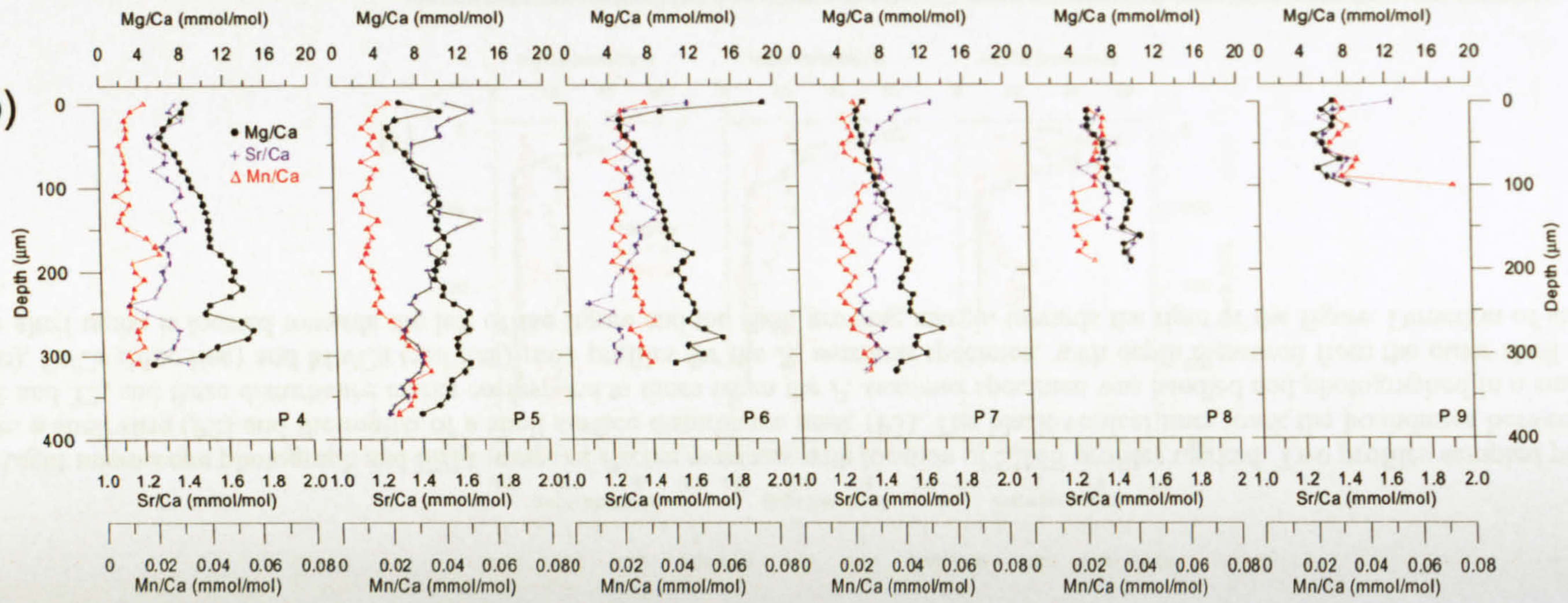
Mg/Ca (mmol/mol)
Sr/Ca (mmol/mol)
Mn/Ca (mmol/mol)
Depth (µm)
Mg/Ca
Sr/Ca
Mn/Ca
P 4
P 5
P 6
P 7
P 8
P 9

Figure 7 - 2 – a) Light microscope photograph and SEM image of *Mytilus edulis* with location of SIMS profiles marked. Letters a, b and c identify internal disturbance lines that are associated with the shell surface disturbance marks formed during emersion of the specimen at the beginning of the three growth intervals, T1, T2 and T3, denoted by the black vertical lines (see text and Figure 7-4 for fuller discussion). In the light microscope photograph, the periostracum, which covers the outer shell surface and extends to the shell margin, is followed by a blue coloured region of ca. 100 μm thickness and then by a grey-blue coloured region down to the inner shell surface. The pallial line, a mark on the inner shell surface due to attachment of the mantle, marks the appearance of a thin blue band on the inner shell surface and also of darker shading of the inner grey-blue shell region towards the umbo side of the pallial line, i.e. to the left in the photograph. Differences in the shell colour observed in the light microscope photograph are not associated with differences in crystal arrangement observed in SEM images, which is similar throughout the shell. b) SIMS Mg/Ca (black line), Sr/Ca (blue line) and Mn/Ca (red line) ratio profiles for the *M. edulis* specimen, with depth measured from the outer shell surface towards the inner shell surface. The shell umbo is located towards the left of the figure and the shell growing margin towards the right of the figure. Direction of shell growth is from left to right in the image.

Ion microprobe analyses were completed at the NERC Ion Microprobe Facility, Edinburgh University, U.K., using a Cameca ims-4f ion microprobe instrument. The optimisation of this instrument and application of the SIMS technique (Allison, 1996) for the determination of element/Ca ratios in biogenic carbonates is described in more detail elsewhere (c.f. Allison and Austin, 2003). The samples were analysed using an 8–10 nA $^{16}O^-$ primary ion beam, accelerated at -10.7 keV. The sample was held at +4.5 keV resulting in total impact energy of ~15 keV. The image setting was for 25 μm and a field aperture (number 2) was inserted to restrict the analysed area on the sample to 8–10 μm in diameter. The depth of these SIMS analyses is probably about 0.1–0.2 microns (Hinton, *pers. comm.* 2007). Line profiles from the outer to inner surfaces of the two shells were undertaken in the new shell growth only using a step-size of 10 μm resolution (Appendix 6). Three profiles were completed on the *Pecten maximus* shell (profiles P1 to P3 in Figure 7-1) and six profiles on the *Mytilus edulis* shell (profiles P4 to P9 in Figure 7-2); for both shells individual profiles traversed the full shell thickness, but in some cases also included other shell features, i.e. shell surface disturbance marks in both species (Figures 7-1 and 7-2) and a shell surface stria (growth ridge present in the surface of the left valve) in *P. maximus* (Figure 7-1). An energy offset of -75 eV was applied to the sample and data collected with a ±20 eV energy window in order to minimise measurement of interferences caused by molecular ions. The ims-4f was operated in low mass resolution ($M/\Delta M$ = 400–500) and secondary positive ions were counted by an electron multiplier at the following masses, for counting times appropriate to the expected relative elemental concentrations: mass 22.5 (average background counts of <1/second; 10 seconds); ^{26}Mg (5s); ^{30}Si (2s); ^{44}Ca (2s); ^{55}Mn (5s); ^{88}Sr (2s); ^{138}Ba (10s). Prior to data collection, initial pre-spluttering was completed for 20 seconds. Data were collected for 10 consecutive cycles of the sequential switching of the magnetic field. The ^{88}Sr signal was corrected for interference from the Ca^{2+} dimer (principally $^{44}Ca^{44}Ca^+$) using a constant Sr/Ca ratio of 0.0001, and the ^{44}Ca signal was used to identify where the individual line profiles crossed from the resin to the shell and vice versa. Silicon and barium were not above detection limits throughout the two samples. A single-point calibration was completed using the OKA carbonatite standard (Lutz and Rhoads, 1980), with nine repeat analyses of this material used to determine a sample

precision of 2.19 %RSD (relative standard deviation) for the determination of Mg/Ca ratios.

7.4 Intra-shell Spatial Heterogeneity of Elemental/Ca Ratios

In *Pecten maximus*, the minimum and maximum Mg/Ca ratios measured within the shell were 5.24 and 64.89 mmol/mol, respectively (Table 7-1). By comparison, *Mytilus edulis* showed lower Mg/Ca ratios than *P. maximus* overall, with minimum and maximum ratios of 4.96 and 19.06 mmol/mol, respectively (Table 7-1). In *P. maximus*, the minimum and maximum Sr/Ca ratios measured within the shell were 1.09 and 2.07 mmol/mol, respectively, while in *M. edulis* the minimum and maximum Sr/Ca ratios measured within the shell were 1.10 and 1.70 mmol/mol, respectively (Table 7-1). The minimum and maximum Mn/Ca ratios measured within the *P. maximus* shell were 0.004 and 0.051 mmol/mol, respectively; in *M. edulis* minimum and maximum shell Mn/Ca ratios were 0.006 and 0.073 mmol/mol, respectively (Table 7-1).

7.4.1 Pecten maximus

In *Pecten maximus* (Figure 7-1) two main features characterise the Mg/Ca ratio profiles: 1) In all profiles, Mg/Ca ratios decrease from maxima in the outermost shell to a minimum value at depths of ca. 110–170 μm. The greatest maxima were observed in regions of modified shell structures, i.e. the shell stria (profile P2) and disturbance growth mark (profile P3); 2) Below the sub-surface minima, Mg/Ca ratios in the inner shell were relatively invariant, both within (P1: depths of 110–700 μm, 7.02±0.67 mmol/mol, N = 60; P2: depths of 160–640 μm, 7.12±0.41 mmol/mol, N = 49; and P3: depths of 170–480 μm, 7.17±0.44 mmol/mol, N = 32) and between each of the three profiles, which show no significant difference in mean Mg/Ca ratios between each profile (*t*-test, $p>0.05$ for all comparisons).

Table 7 - 1 – Summary Mg/Ca, Sr/Ca and Mn/Ca ratio data (mmol/mol) for the nine ion microprobe profiles (P1 to P9). 1σ is the mean standard deviation. RSD is the relative standard deviation, i.e. 1σ/mean*100.

Mg/Ca	Min	Max	Range	Mean	N	1 σ	RSD (%)
P. maximus							
P1	5.24	38.38	33.14	9.97	71	7.9	79
P2	6.27	64.89	58.62	13.03	65	13.41	103
P3	6.59	58.90	52.31	16.02	49	14.26	89
M. edulis							
P4	4.96	14.56	9.60	9.99	32	2.52	25
P5	5.14	12.75	7.61	9.70	38	2.10	22
P6	5.10	19.06	13.96	10.11	32	2.87	28
P7	5.65	13.92	8.27	9.07	33	2.15	24
P8	5.54	10.53	4.99	8.01	19	1.54	19
P9	5.21	8.43	3.22	6.56	11	0.95	15

Sr/Ca	Min	Max	Range	Mean	N	1 σ	RSD (%)
P. maximus							
P1	1.13	1.72	0.59	1.35	71	0.10	7
P2	1.15	2.07	0.92	1.39	65	0.21	15
P3	1.09	1.98	0.89	1.38	49	0.24	17
M. edulis							
P4	1.14	1.42	0.28	1.33	32	0.06	5
P5	1.24	1.70	0.46	1.44	38	0.10	7
P6	1.10	1.59	0.49	1.29	32	0.09	7
P7	1.29	1.65	0.36	1.38	33	0.07	5
P8	1.24	1.51	0.27	1.37	19	0.08	6
P9	1.28	1.63	0.35	1.39	11	0.11	8

Mn/Ca	Min	Max	Range	Mean	N	1 σ	RSD (%)
P. maximus							
P1	0.005	0.049	0.044	0.011	71	0.007	60
P2	0.004	0.051	0.047	0.012	65	0.008	65
P3	0.005	0.049	0.044	0.015	49	0.008	56
M. edulis							
P4	0.006	0.023	0.017	0.013	32	0.004	31
P5	0.009	0.036	0.027	0.019	38	0.007	39
P6	0.015	0.033	0.018	0.024	32	0.005	20
P7	0.015	0.032	0.017	0.022	33	0.004	20
P8	0.017	0.029	0.012	0.023	19	0.004	19
P9	0.026	0.073	0.047	0.035	11	0.013	37

Three main features characterize the *Pecten maximus* Sr/Ca ratio profiles (Figure 7-1): 1) Shell Sr/Ca ratios were highest in the upper 100–120 µm of the profiles (1.6 to 2.1 mmol/mol), especially in the shell structures sampled in profiles P2 and P3, i.e. the stria (up to 2.1 mmol/mol) and disturbance growth mark (up to 2.0 mmol/mol); 2)

Deep sub-surface minima in shell Sr/Ca ratios (1.1 to 1.2 mmol/mol) were apparent 200–300 μm above the inner shell surface; 3) Shell Sr/Ca ratios then increase from the minima to higher values towards the inner shell surface.

Taking the whole of each profile, the Sr/Ca and Mg/Ca ratios were significantly correlated (Table 7-2; all $p<0.001$) in profiles P1, P2 and P3. The greatest degree of correlation was found in the 110–180 μm closest to the outer shell surface where both Sr/Ca and Mg/Ca reach maxima (Table 7-2, all $p<0.001$). From this outermost section (deeper than 110–180 μm) to the inner shell surface no significant relationship was observed between Sr/Ca and Mg/Ca in any of the profiles.

Table 7 - 2 – Summary of correlations between Mg/Ca, Sr/Ca and Mn/Ca ratios for the three ion microprobe profiles (P1 to P3) in the *Pecten maximus* shell. 'Outermost' defines a shell region between the upper shell surface and 110 μm, 150 μm and 200 μm depth for profiles P1, P2 and P3, respectively. 'Innermost' defines a shell region lower than 490 μm, 390 μm and 170 μm depth in the profiles P1, P2 and P3, respectively. 'All' represents the entire profiles.

P. maximus	Mg vs Sr r^2	Mg vs Mn r^2	Mn vs Sr r^2
Outermost			
P1	0.48	0.06	0.48
P2	0.87	0.88	0.81
P3	0.77	0.49	0.45
Innermost			
P1	-	-	0.55
P2	-	-	0.82
P3	-	-	0.63
All			
P1	0.35	-	-
P2	0.83	-	0.08
P3	0.78	0.12	0.29

The *Pecten maximus* Mn/Ca ratio profiles (Figure 7-1) were characterised by three main features : 1) Shell Mn/Ca ratios were highest in the ca. 100 μm proximal to the outer shell surface, particularly in the shell features sampled in profile P2 and P3, the stria (up to 0.023 mmol/mol) and disturbance growth mark (up to 0.050 mmol/mol), respectively; 2) Shell Mn/Ca ratios were lowest at the mid-depths within the profiles (0.004 to 0.016 mmol/mol); 3) Shell Mn/Ca ratios increase to higher values towards the inner shell surface (0.030 to 0.051 mmol/mol). Taking the whole of each profile, the Mn/Ca and Mg/Ca ratios were not significantly correlated (Table 7-2). In the 110–200 m closest to the outer shell surface of *P. maximus*, Mn/Ca ratios were significantly correlated to Sr/Ca in P1, P2 and P3 (Table 2; all $p < 0.001$), and also

were significantly correlated to Mg/Ca ratios in the shell features sampled in profile P2 and P3, the stria and disturbance growth mark (Table 7-2; both $p < 0.001$). In addition, shell Mn/Ca ratios also were significantly correlated to Sr/Ca ratios in the 170–490 μm closest to the inner shell surface (Table 7-2; $r^2 = 0.55$, $r^2 = 0.82$ and $r^2 = 0.63$, for profiles P1, P2 and P3 respectively; all $p < 0.001$).

7.4.5 Mytilus edulis

Spatial variability of Mg/Ca, Sr/Ca and Mn/Ca ratios in the *Mytilus edulis* shell (Figure 7-1) was less systematic than in *Pecten maximus* (Figure 7-2). Three main features characterise the *M. edulis* shell Mg/Ca ratios in profiles P4, P5, P6, P7 and P8: 1) Mg/Ca ratios generally decrease from the outer surface of the shell to minimum values at ca. 20–40 μm depth below the shell surface; 2) Below the sub-surface minimum there was a general increase in Mg/Ca ratios from the minimum value to maximum values at depths of ca. 240–270 μm below the shell surface; 3) Mg/Ca ratios then usually decrease to a lower (but not always the lowest in that profile) values at the inner shell surface. The remaining profile P9 shows no particular trend with profile depth depth. *M. edulis* shell Sr/Ca ratios were highest in the upper 50–100 μm of four of the profiles (P5, P6, P7 and P9) and range from 1.6 to 1.7 mmol/mol (Figure 7-2)., Shell Mn/Ca ratios showed no clear pattern with profile depth, but mean Mn/Ca ratios decreased from profile P9 towards profile P4, i.e. mean profile Mn/Ca ratios decreased along the main growth axis from the shell margin towards the umbo region (Figure 7-2). Shell Mg/Ca, Sr/Ca and Mn/Ca ratios were not significantly correlated in any of the *M. edulis* profiles ($p > 0.05$).

7.5 Relationships Between Element/Ca Ratios and Shell Features and Structure

7.5.1 Pecten maximus

Mg/Ca, Sr/Ca and Mn/Ca ratios are particularly high and variable in the stria (P2) and disturbance mark (P3), respectively. SEM images (Figure 7-3a and b and insets) illustrate that the three *Pecten maximus* ion microprobe profiles, situated in the new growth region of the shell, traversed only one layer of irregularly oriented foliated calcite. Nevertheless, highly variable Mg/Ca, Sr/Ca and Mn/Ca ratios are associated with some differences in the crystal arrangement and size particularly within the stria (profile P2) and to a lesser extent within the region of the surface disturbance mark (profile P3), which are comprised of a relatively unorganized arrangement of the calcite crystals. Mg/Ca ratios are of lower magnitude and relatively invariant in the mid region to innermost shell, whereas Sr/Ca and Mn/Ca ratios vary significantly in this region of the shell and must be controlled by some other factor other than crystal arrangement. Clearly, shell features, such as the stria and disturbance growth marks, and associated variations in crystal arrangement and size have an influence in Mg/Ca ratios in *P. maximus* beyond a simple thermodynamic control..

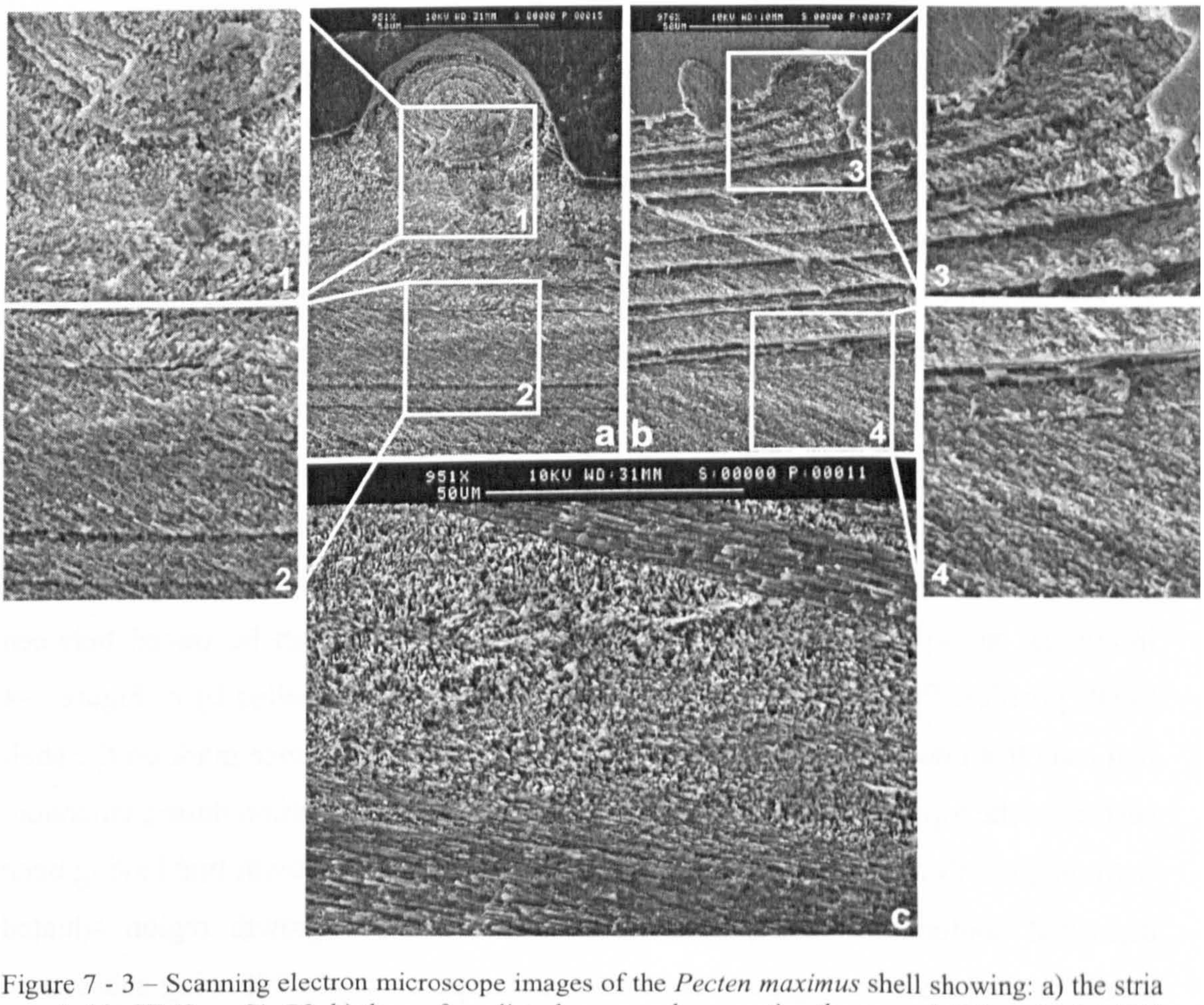

Figure 7 - 3 – Scanning electron microscope images of the *Pecten maximus* shell showing: a) the stria sampled in SIMS profile P2; b) the surface disturbance mark separating the second (T2) and third (T3) growth intervals sampled in SIMS profile P3; c) an example of the crystal arrangement within the mid region to lowermost parts of the shell as sampled by all three SIMS profiles. Insets 1, 2, 3 and 4 are

more detailed images of the contrasting crystal orientation in the shell surface stria (a) and disturbance mark (b). Scale bar in images a, b and c is 50 μm; images 1, 2, 3 and 4 have dimensions of 50 x 50 μm.

7.5.2 Mytilus edulis

All of the *Mytilus edulis* SIMS analyses only sampled the outer prismatic calcite layer (Figures 7-2 and 7-4), even profiles P4 and P5 that were located between the shell margin and the pallial line, the latter being a mark observed on the inner shell surface that is caused by attachment of the animals' body, i.e. by the mantle (Figure 7-2a). Internal disturbance/growth lines are easily identifiable in the SEM images of the *M. edulis* shell (Figures 7-2a and 7-4) and these run oblique to the outer and inner shell surfaces. The disturbance marks on the surface of the shell ('hump-like' features where profiles P4, P5 and P6 are directly or proximally situated; Figures 7-2a and 7-4) and their associated internal disturbance lines (the most prominent lines labelled a, b and c on Figures 7-2a and 7-4) were formed during emersion of the animals between growth intervals, whereas the other internal growth lines formed while the animal remained immersed. Because of the nature of the incremental growth pattern in bivalve mollusc shells (Lorens, 1981a; Morse and Bender, 1990; Tesoriero and Pankow, 1996) internal growth lines can be used to identify shell deposited contemporaneously at different locations within the shell. This incremental growth pattern of bivalve shells is such that within individual profiles, the uppermost data points are representative of shell material deposited at the shell margin at one point in time, with data points lower in the profile being representative of shell material precipitated subsequently, away from the shell margin at other point in time, thus contributing to the increase in shell thickness. Therefore, the age of the new shell material sampled decreases down each SIMS profile. In addition, each individual growth line, representing a common time line, can be traced between SIMS profiles. For example, the internal disturbance line (labelled b) in Figure 7-4 that runs from near the base of SIMS profile P4 to the disturbance mark on the shell surface at the top of profile P5 delineates a break in shell deposition during emersion, with the growth region immediately above and adjacent the growth line having been deposited contemporaneously prior to emersion and the growth region situated immediately below having been deposited contemporaneously following subsequent immersion. A similar structural relationship and internal disturbance line (labelled c)

can be seen running from near the base of profile P5 and the disturbance mark on the shell surface at the top of profile P6 (Figures 7-2 and 7-4). Throughout the shell the individual internal growth bands, defined by two growth lines, also thicken towards the margin of the shell (Figure 7-4).

It could be expected, therefore, that shell deposited between the same two growth lines (i.e. within a growth band) would have a constant Mg/Ca ratio due to contemporaneous precipitation at a constant seawater temperature, independent of location of new crystallisation within the shell. Calcite Sr/Ca and Mn/Ca ratios, on the other hand, are influenced by mineral precipitation rate, the former is positively correlated to precipitation rate (Lorens, 1981a; Mucci, 1988; Pingitore et al., 1988; Dromgoole and Walter, 1990) and the latter inversely correlated to precipitation rate (Clark II, 1974; Carriker, 1992). Shell growth rate varies with location of shell deposition along the inner shell surface: higher towards the shell margin and lower away from it (i.e. the thickness of an individual growth band decreases away from the margin of the shell; Figure 7-4). Sr/Ca and Mn/Ca ratios, thus, are not expected to be constant throughout an individual internal band.

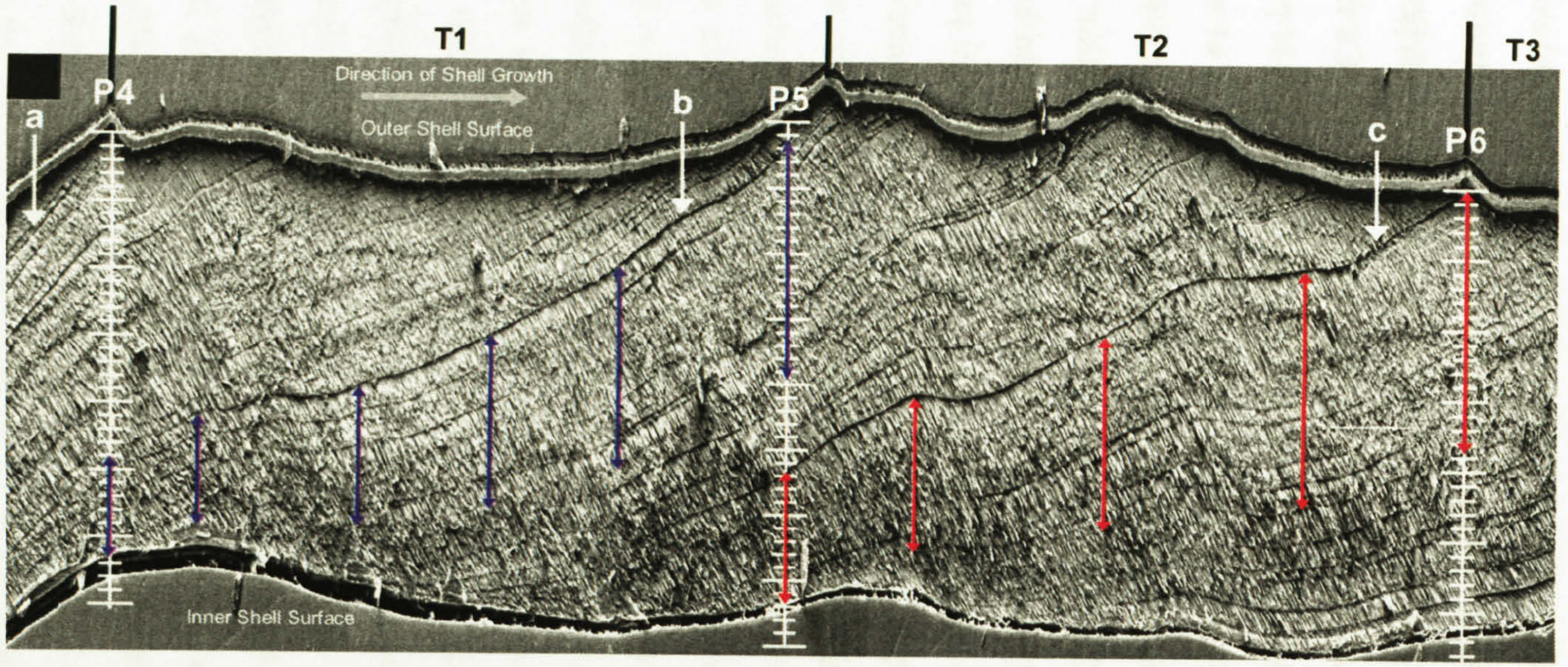
T1
T2
T3
Direction of Shell Growth
Outer Shell Surface
Inner Shell Surface
P4
P5
P6
a
b
c

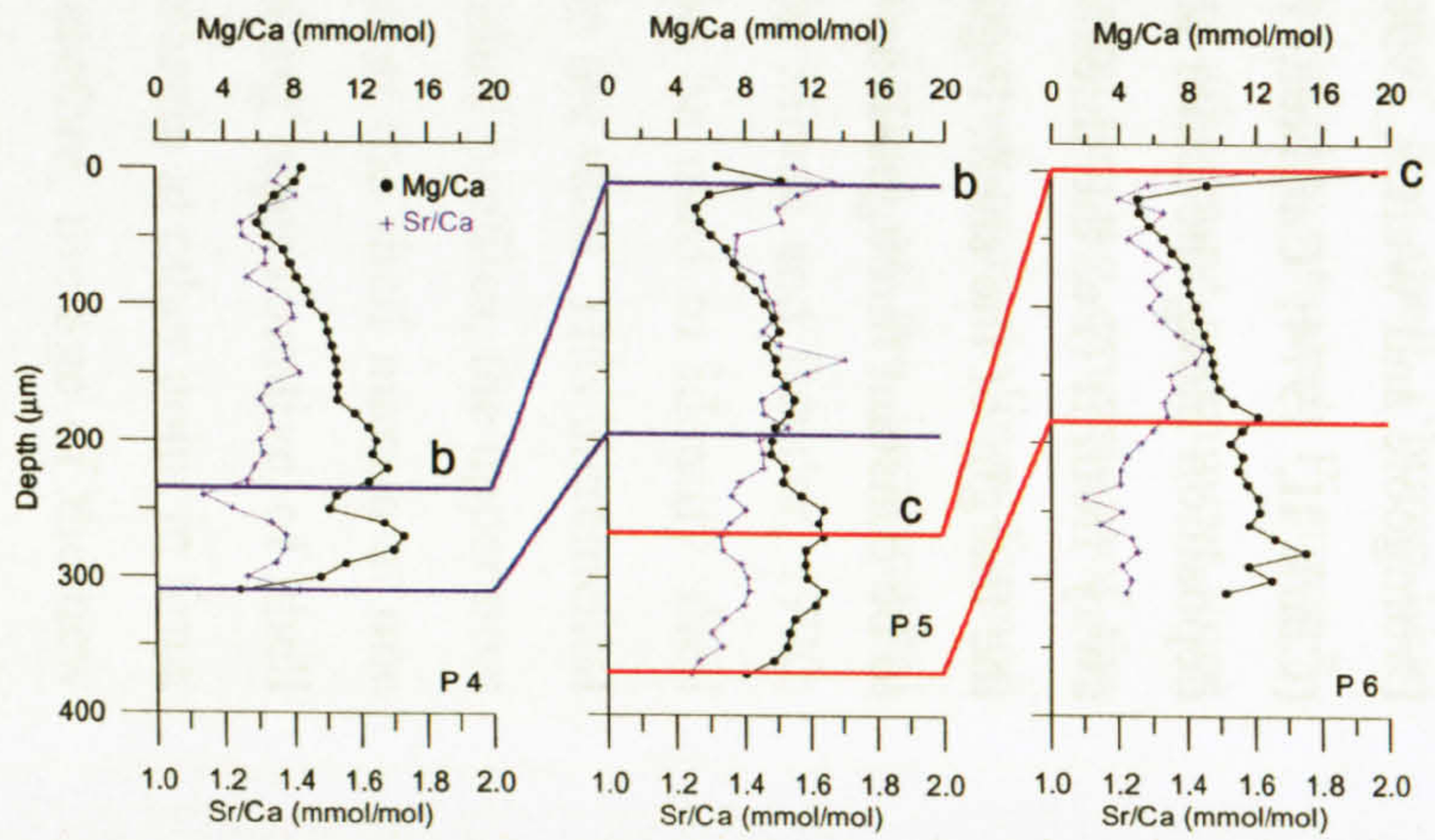
Mg/Ca (mmol/mol)
0 4 8 12 16 20
Mg/Ca
+ Sr/Ca
Depth (µm)
0
100
200
300
400
b
c
P 4
P 5
P 6
1.0 1.2 1.4 1.6 1.8 2.0
Sr/Ca (mmol/mol)

Figure 7 - 4 – Scanning electron microscope images of the *Mytilus edulis* shell with associated SIMS Mg/Ca and Sr/Ca ratio profiles, with the location of each SIMS profile and individual spots indicated by the vertical line and tick marks, respectively. The "hump-like" features on the shell surface are disturbance marks deposited when the shell was emersed at the beginning of each of the three growth intervals (T1, T2 and T3), two of which were sampled directly by SIMS profiles P4, and P6. Three internal disturbance lines (labelled a, b and c) are associated with surface disturbance marks (see also Figure 7-2) and delimit the start of new shell deposited during growth intervals T1, T2 and T3, respectively. The blue and red arrows define two separate growth increments within the shell (see text for discussion), with the appropriate parts of the three SIMS profiles that correspond to these parts of the shell coloured accordingly. The shell umbo is located towards the left of the figure and the shell growing margin towards the right of the figure. Direction of shell growth is from left to right in the image. (*Note*: for presentation purposes the image has been stretched vertically by a factor of 4). The shell umbo is located towards the left of the figure and the shell margin towards the right of the figure. Direction of shell growth is to the right.

Interestingly, Mg/Ca and Sr/Ca ratios differ within two individual growth bands that were not affected by experimental emersion disturbance (Figure 7-4; regions delimited by internal disturbance lines b and c and the inner shell surface, and by the blue and red lines) even though they relate to contemporaneous periods of shell deposition. For example, during the period of shell deposition covered by the growth increment T2, sampled by SIMS profiles P4 and P5 and delimited by the blue lines in Figure 7-4, the shell precipitated at the shell margin (at the top of profile P5) exhibits a general increase in Mg/Ca ratios with profile depth (mean of 8.5 mmol/mol, 1 σ = 1.9, N = 18); a similar pattern is evident for Sr/Ca ratios (mean of 1.49 mmol/mol, 1 σ = 0.08, N = 18), which albeit more variable, also follow the Mg/Ca variation. In contrast, the new shell material deposited contemporaneously in the innermost shell away from the shell margin (near the base of SIMS profile P4) has much more variable Mg/Ca ratios (mean of 11.0 mmol/mol, 1 σ = 3.1, N = 8) and Sr/Ca ratios (mean of 1.31 mmol/mol, 1 σ = 0.09, N = 8). A very similar pattern can be observed for new shell precipitated contemporaneously at the start of growth interval T3, following emplacement of internal growth disturbance line c and delimited by the red coloured lines between profiles P5 and P6. The new shell precipitated at the shell margin (at the top of profile P6) exhibits a rapid decrease and then general increase in Mg/Ca (mean of 8.90 mmol/mol, 1 σ = 3.1, N = 19) and Sr/Ca ratios (mean of 1.33 mmol/mol, 1 σ = 0.08, N = 19), whereas the new shell material deposited contemporaneously on the inner shell surface (near the base of SIMS profile P5) exhibits a general trend of decreasing Mg/Ca (mean of 11.14 mmol/mol, 1 σ = 1.4, N = 11) and Sr/Ca ratios (mean of 1.34 mmol/mol, 1 σ = 0.06, N = 11) with profile depth.

Lorens and Bender (1980) have described previously a similar influence of disturbance on *Mytilus edulis* shell Mg/Ca and Sr/Ca ratios, whereby the stress of capture and adaptation to a new laboratory environment induced the deposition of a shell region (termed "transition zone calcite" by those authors) with high organic matrix content, high Mg/Ca (> 40 mmol/mol) and Sr/Ca (> 1.4 mmol/mol) ratios. Subsequent shell growth then exhibited decreasing Mg/Ca (to < 10 mmol/mol) and Sr/Ca (to < 0.6 mmol/mol) ratios as the animals adapted to their new environment. However, Lorens and Bender (1980) only inferred the "transition zone" between new

and old calcite using spot chemical compositions measured by electron microprobe, and their transition zone that exhibited higher Mg/Ca and Sr/Ca ratios occurs perpendicular to the shell surface, an observation that is inconsistent with the incremental growth pattern of *M. edulis*, i.e. growth lines actually run oblique to the shell surface. By comparison, in this study ion microprobe determined Mg/Ca and Sr/Ca ratios have been compared directly to SEM images of shell growth banding and indicate a more complex relationship between elemental composition and shell structure.

7.6 Potential Causes of the Observed Small Scale Element/Ca Ratio Heterogeneity within *Pecten maximus* and *Mytilus edulis* Shell Calcite

Of all the elements investigated in this study, Mg in the outermost sections of *Pecten maximus* shell provides the clearest indication for the likely presence of control(s), other than temperature, on the elemental composition of bivalve calcite formed during shell biomineralization. By comparison, the low and stable interior *P. maximus* shell Mg/Ca ratios are consistent with temperature being the main control on Mg incorporation. This hypothesis is strengthened by the evidence that the Mg/Ca ratios were relatively invariant both within and between each of the three profiles in the mid region and lowermost shell sampled, even though deposition occurred at different times and locations along the inner shell surface.

The extent of the small-scale heterogeneity of element/Ca ratios differs significantly between *Pecten maximus* and *Mytilus edulis*, suggesting that the processes controlling elemental incorporation into shell calcite also differ between these two marine bivalve species. *Pecten maximus* produces elaborate shell features during biomineralization, such as surface striae, while *M. edulis* has a more smooth shell surface that is also covered by an organic periostracum, a shell component which is absent in the former species. Furthermore, shell deposition at the shell margin occurs differently in the two species. In scallops, like in oysters, shell deposition at the shell

margin occurs from an extra-pallial space (EPS) that is periodically exposed to the ambient seawater medium, while in *M. edulis* biomineralization occurs from a continuously isolated EPS (Clark II, 1974; Carriker, 1992). In bivalve species with periodically exposed EPS the margins of the mantle (the soft-tissue organ that controls calcification) are frequently withdrawn into the mantle cavity, exposing the crystals along the inner shell surface to seawater or mantle cavity fluid from the shell margin to the attachment of the mantle on the inner shell surface at the pallial line (Mucci and Morse, 1983; Ohde and Kitano, 1984; Morse and Bender, 1990).

It is probable that different species-specific shell biomineralization processes contribute to the variable small-scale heterogeneity of elemental composition observed in *Pecten maximus* and *Mytilus edulis*. Several inorganic and biological processes can be considered as potential explanations for the differential incorporation of elements into bivalve shells and may explain the significant small-scale heterogeneity of Mg, Sr and Mn content in *P. maximus* and *M. edulis* shell calcite that has been observed in the present study.

7.6.1 Elemental composition of shell calcite

The Mg content of calcite is known to influence the incorporation of other elements during calcite precipitation, whereby substitution of Ca^{2+} by Mg^{2+} distorts the crystal lattice and favours the incorporation of other elements, namely ones with large ionic radii, such as Sr^{2+} and Mn^{2+} (Mann, 2001; Weiner and Dove, 2003; Addadi et al., 2006). In *Pecten maximus*, significant positive correlations were observed between Mg/Ca and Sr/Ca and Mn/Ca ratios in the outermost 100–200 μm of the shell, particularly in the shell stria and disturbance mark. Therefore, shell Mg may influence Sr and to a lesser extent Mn incorporation in the outermost part of the shell, where Mg/Ca ratios are highest (Figure 7-1). However, such control is absent in the mid region and innermost part of the shell, which has low and stable Mg/Ca ratios (Figure 7-1). In that part of the shell, Sr and Mn are significantly correlated to each other (Table 7-2), suggesting that a common process, or processes, other than Mg content controls both Sr and Mn incorporation.

7.6.2 Composition and the amount of the shell organic matrix

Biogenic minerals are composed of both an inorganic and organic fractions in which the latter controls crystal nucleation and growth (e.g. (Dalbeck et al., 2006) and may influence element incorporation into the mineral. In *Mytilus edulis*, an increase of Mg concentration from the outer shell surface towards the inner shell surface, similar to the one observed in the present study, has been previously reported and suggested to be associated with differences in crystal size and in the organic matrix component (Berner, 1975a). In addition, Lorens and Bender (1980) suggested that in the shell calcite of *M. edulis*, sulphur reflects the amount of the organic matrix. These authors suggested that the *M. edulis* compensates for increased Mg levels in the EPF, which inhibits calcite nucleation and crystal growth (Lorens and Bender, 1980), by secreting additional S-bearing organic matrix. Therefore, the high S/Ca and Mg/Ca ratios observed in shell regions deposited under stress conditions reflect increased organic matrix content, although Mg is not thought to be bound to S-organic matrix (Rosenberg and Hughes, 1991; Rosenberg et al., 2001). For instance, Dauphin et al. (2003) observed in the shell prismatic calcite of *Pinna nobilis* and *Pinctada margartifera* that Mg content was lower in the organic prismatic walls relative to the inorganic calcite mineral. Nevertheless, Mg and S co-vary in the shell calcite of *M. edulis* (2007) and it has been suggested that *M. edulis* uses Mg and S (as a component of the matrix) to control shell crystal elongation and hence shell form along different axes (Rosenberg et al. 2001). Furthermore, England et al., (2007) used electron microprobe analyses to investigate elemental distribution within the shells of two extant species of brachiopod that had been sampled from the same environment. One species, *Novocrania anomala*, exhibited no significant difference in Mg concentrations between shell layers. However, in *Terebratulina retusa* Mg concentrations did differ between shell layers. More significantly, England et al., (2001) also demonstrated that the distribution of Mg within *Terebratulina retusa* correlated with sulphur and they proposed that sulphur could be used as a measure of the sulphated organic matrix of the shell and that a proportion of the measured Mg content of the shell of this species is associated with the sulphated fraction of the shell organic matrix and not just the inorganic calcite mineral. Therefore, it is plausible that the elevated Mg/Ca ratios in the outermost shell of *Pecten maximus* but also in some regions of the *M. edulis* shell, are associated with a greater proportion of

sulphated organic matrix in that part of the shell, compared to the mid region and innermost parts of the shell.

In addition, Rosenberg et al., (Lorens and Bender, 1980) observed in *M. edulis* that Mg is concentrated along the margins of calcite prisms, especially along the terminations of the crystals, with the alignment of adjacent crystals then producing compositional growth bands within the shell. In *Pecten maximus* and *M. edulis*, disturbance growth marks correspond to the extremities of calcite crystals (Figures 7-3 and 7-4). Since shell disturbance growth marks are associated with increased organic matrix (Wasylenki et al., 2005a), variations in both the amount of the organic matrix and the abundance (and size) of the calcite crystals associated with disturbance growth marks may explain the variable Mg/Ca ratios associated with such marks observed in *P. maximus* and *M. edulis* (Figures 7-1 and 7-4).

7.6.3 Crystal-fluid interface processes

Crystal-fluid interface processes have been shown to influence the composition of synthetic calcite. Diffusive transport conditions to the mineral surface (e.g. Reeder and Paquette, 1989; Paquette and Reeder, 1995) and sector zoning, where elemental composition varies significantly in different non-equivalent vicinal crystal faces (Taylor et al., 1969; Carter, 1990a) have all been observed to influence the elemental composition of calcite crystals. It is plausible that such processes occur during shell biomineralization and influence its element composition. However, it is unclear how these processes could be responsible for the larger scale variation of Mg/Ca, Sr/Ca and Mn/Ca observed in *Pecten maximus* and *Mytilus edulis* shells. For instance, the structure of *P. maximus* shell consists of both an outer and inner irregularly oriented foliated calcite layers (e.g. Morse and Bender, 1990), thus the SIMS profiles sample multiple crystals and a variety of crystal faces, however, Mg/Ca ratios are stable throughout the mid and innermost shell region (Figure 7-1).

7.6.4 Mineral precipitation rate

In calcite, Mg incorporation is not thought to be influenced by mineral precipitation rate, both in synthetic (Lorens and Bender, 1980) and in bivalve calcite (Lorens,

1981a; Pingitore et al., 1988; Dromgoole and Walter, 1990; Morse and Bender, 1990). Increasing precipitation rate has been shown to cause an increase in Sr/Ca ratios, but a reduction in Mn/Ca ratios in calcite (Lorrain et al., 2005; Chapters 2 and 5). In addition, in *Pecten maximus* and *Mytilus edulis*, a strong kinetic control of Sr/Ca ratios has been reported previously (Klein et al., 1996b; Gillikin et al., 2005a; Carré et al., 2006; Chapter 6). However, in *P. maximus* Sr and Mn positively co-vary in the innermost shell regions (Figure 7-1 and Table 7-2) and thus a simple influence of precipitation rate in Sr and Mn incorporation in *P. maximus* calcite is not clear.

7.6.5 Metabolic effects

Physiological metabolic effects, related to element transport processes from seawater and the mantle to the EPF, have been proposed to influence the Mg, Sr and Mn incorporation in bivalve shells (Rosenberg and Hughes, 1991). For instance, in *Mytilus edulis*, shell portions with high organic matrix, Mg, S and minor element content are energetically more costly to produce than Ca rich shell areas (Gillikin et al., 2005a; Carré et al., 2006; Chapters 5 and 6). In addition, in bivalves, shell Sr/Ca and Mn/Ca ratios have been found to be positively correlated to metabolic activity (Mucci and Morse, 1983; Pingitore and Eastman, 1986; Dromgoole and Walter, 1990). Therefore, elevated Mg/Ca, Sr/Ca and Mn/Ca ratios in the outermost shell of *Pecten maximus*, but also in some regions of the *M. edulis* shell, could be associated with higher mantle metabolism during shell biomineralization, relative to regions of the shell with lower Mg/Ca, Sr/Ca and Mn/Ca ratios, i.e. the mid region and lowermost shell, which would be associated with lower mantle metabolism during shell biomineralization.

7.6.6 Composition of the extra-pallial fluid (EPF), the precipitating solution in bivalves

The elemental composition of the solution from which calcification occurs is known to have a strong influence on the incorporation of Mg, Sr and Mn in calcite (e.g. Morse and Bender, 1990). Apart from element concentration, the activity coefficients (i.e. the fraction of ions available for chemical interactions) of elements are known to strongly influence elemental incorporation into synthetic calcite (Crenshaw, 1972;

Misogianes and Chasteen, 1979; Nair and Robinson, 1998). Bivalves are known to be able to biochemically regulate the activity of Ca^{2+} and other ions from the EPF solution from which calcfification takes place. For instance, the majority of Ca in the EPF is not in free ionic form but bound to organic molecules secreted by the mantle (Hattan et al., 2001), some of which have been suggested to be a precursor or a building block of the soluble organic matrix of the shell (Woodward and Davidson, 1968; Crenshaw, 1975). The organic matrix has also been suggested to sequester Ca and then release Ca to seed calcite crystal growth (Simkiss and Wilbur, 1989; Checa, 2000; Addadi et al., 2006).

In both *Pecten maximus* and *Mytilus edulis*, a large variation in elemental/Ca ratios in shell deposited from the same marginal EPF was observed and thus suggests that element incorporation at the shell crystal-solution interface, and not transport to the EPF, most likely is the key control step of shell element composition. The close association between the mantle epithelium and the shell surface, which are separated by a small distance and may be in contact with each other, allows the transfer of ions and organic molecules to occur virtually by direct contact (Richardson, 2001), and thus could provide the potential for small-scale variations in the chemical and physical conditions at different precipitation sites.

Whatever processes influence elemental incorporation into the calcite shells of *Pecten maximus* and *Mytilus edulis*, clearly these processes must vary with time and location of shell deposition in order to produce the small-scale heterogeneity of element composition observed.

7.7 Small-Scale Element Heterogeneity and Implications for the Use of Geochemical Proxies in Bivalves

It is clear from the ion microprobe elemental data collected in this study that for both bivalve species investigated highly variable Mg/Ca, Sr/Ca and Mn/Ca ratios can

occur within one structural layer of shell calcite precipitated at a single and constant seawater temperature and via deposition from the same marginal extra-pallial space (EPS), albeit a non-permanent EPS in *Pecten maximus*. Such significant small-scale heterogeneity of the Mg, Sr and Mn content in the shells of *Mytilus edulis* and *P. maximus* has profound implications for the application of these geochemical proxies in bivalve calcite. First, the deposition of elaborate shell features and surface disturbance growth marks, the latter ubiquitous features of shells of many bivalve shells, is associated with highly variable element/Ca ratios. Second, factors/processes that may influence elemental incorporation into bivalve calcite potentially do not just operate at the scale of whole shells, or even within a single shell structural layer, but can vary at tens of microns scale. Third, users of large-scale 'bulk' shell sampling methods, and even micro-sampling methods such as micro-milling or laser ablation sampling, need to consider carefully which section, or sections, of the shell are sampled, otherwise they risk obtaining a large variability in element/Ca ratio measurements that do not relate to any change in environmental conditions. Finally, Mg, Sr and Mn incorporation into bivalve calcite most likely is under the control of multiple factors (e.g. Mg content, organic matrix content, mantle metabolic activity, and transport and activity conditions at the shell crystal-solution interface) and that the relative influence of any one factor most likely varies with time and with the location of the shell deposition.

In particular, significant small-scale heterogeneity (i.e. tens of microns) in bivalve shell Mg/Ca ratios is potentially a significant source of error when attempting to use Mg/Ca ratios of these biogenic calcites in palaeotemperature reconstructions. For instance, in *Mytilus edulis* and *Pecten maximus* specimens grown in the same experiment as the ones analysed by SIMS in the present study, but sampled by surface milling, displayed a large variability in Mg/Ca ratios at constant temperature and a weak correlation between shell Mg/Ca ratios and seawater temperature (r^2 = 0.37, $p < 0.001$ and $r^2 = 0.21$, $p < 0.001$, respectively) was observed over a range from 10 to 20°C (Chapter 4). It is clear from the ion microprobe data obtained in this study that small-scale variability in the Mg content is one possible reason why such a weak relationship was observed between shell Mg/Ca ratios and seawater temperature. The inclusion of variable amounts of material from parts of the shell structure with different Mg/Ca ratios, as well as the sampling of shell areas with

striae and/or surface disturbance marks, may provide an explanation for the large variability observed in Mg/Ca ratios from shell calcite grown at constant temperatures. In another field culturing experiment study, the unexpected increase in Mg/Ca ratios of *P. maximus* specimens grown in a field-based culturing experiment at low winter temperatures reported in chapter 3 could now be explained by a higher number of striae (ca. 12 striae/mm) being milled and included in each 'winter' powder sample, compared to Mg/Ca ratios in spring and summer samples with a lower number of stria (ca. 4–6 striae/mm), which had a more robust relationship to water temperatures.

In *Mytilus edulis* there is some evidence that Mg/Ca ratios vary significantly depending on whether shell deposition occurs at the shell margin or on the inner shell surface away from it. The observation that *M. edulis* shell Mg/Ca ratios are influenced by disturbance marks formed during emersion could be particularly significant since in a natural inter-tidal environment the twice daily emersion–immersion cycles control the internal and surficial growth banding of *M. edulis* shells. Furthermore, disturbance marks are ubiquitous in *M. edulis* shells, as well as in other bivalve species, and can reflect interruption of shell deposition during periods of non-tidal environmental and/or physiological stress (Klein et al., 1996a). Such observations further question the validity, and indicate the difficulty, of using Mg/Ca ratios in *M. edulis* as a palaeotemperature proxy, despite a previous study that demonstrated a Mg/Ca ratio–temperature relationship in the closely related species *Mytilus trossulus* (Lorens and Bender, 1977; Lorens and Bender, 1980; Rosenberg and Hughes, 1991; Vander Putten et al., 2000; Rosenberg et al., 2001; Markich et al., 2002; Lazareth et al., 2003; Takesue and van Geen, 2004; Gillikin et al., 2005a; Lorrain et al., 2005; Carré et al., 2006; Gillikin et al., 2006a; Pearce and Mann, 2006).

Chapter VIII

Conclusions

Chapter 8

Conclusions

VIII - Conclusions

Geochemical proxies have been comprehensively studied and used in marine biogenic carbonates as proxies for environmental conditions. Bivalve shells have also been expected to contain valid and useful geochemical proxies of the environmental conditions under which the shell was deposited. Previous studies have expanded the knowledge on the controls of the stable-isotopic and elemental composition of bivalve shells (e.g. Krantz et al., 1988; Klein et al., 1996a; Hickson et al., 1999; Chauvaud et al., 2005; Gillikin et al., 2006a; Wanamaker et al., 2007). Such studies have shown the stable oxygen isotopic composition of bivalve shell carbonates to be deposited in or close to isotopic equilibrium, while elemental/Ca ratios in bivalve shells, in spite of some promising results (e.g. Klein et al., 1996a; Vander Putten et al. 2000; Gillikin et al., 2006a; Langlet et al., 2006), are not yet reliable and accurate proxies for environmental conditions and are influenced at variable degrees by secondary control factors, e.g. physiological processes or precipitation rate.

The present study has focused on validating the use of elemental/Ca ratios (Mg/Ca, Sr/Ca and Mn/Ca) in bivalve calcite as geochemical proxies of environmental conditions (temperature, salinity, dissolved or particulate Mn, respectively). The species used have previously been proposed, as well as closely related taxa, as potential archives for palaeoceanographic studies (e.g. Krantz et al., 1988; Klein et al., 1996a; Hickson et al., 1999; Kennedy et al., 2001; Chauvaud et al., 2005; Gillikin et al., 2006a; Wanamaker et al., 2007).

The temperature dependence of shell Mg/Ca ratios was found to be generally weak in bivalve calcite, as well as the occurrence of a large degree of variability of Mg/Ca ratios, and thus clearly suggests that bivalve Mg/Ca ratios do not yet appear to be a reliable and precise temperature proxy, at least in most of the species studied to date (Chapters 2, 3 and 4). Such variability is significant at the species, inter- and intra-individual shell levels, and thus suggests a strong physiological control (metabolic and/or kinetic factors) of calcite Mg/Ca ratios during shell biomineralization. Nevertheless, shell Mg/Ca ratios in field grown specimens of *Pinna nobilis* are a

valid temperature proxy during the first 4 to 5 years of growth, after which ontogenetic effects decouple significantly the relationship between shell Mg/Ca ratios and calcification temperature (Chapter 2).

Seawater temperature was not a significant control of shell calcite Sr/Ca ratios in the three species studied *Pinna nobilis*, *Pecten maximus* and *Mytilus edulis* (Chapters 2, 3, and 5). Shell Sr/Ca ratios thus appear to be influenced by physiological controls. Shell growth rate, assumed to indicate a precipitation rate control, was significantly, correlated to shell calcite Sr/Ca ratios in field- and laboratory-grown *P. maximus* and *M. edulis* (Chapters 3 and 5), albeit not as strongly as previously reported for *P. maximus* (Lorrain et al., 2005). Generally, shell Mg content did not influence shell Sr/Ca ratios, albeit a significant but weak control of Sr/Ca ratios was observed in both field- and laboratory-grown specimens of *P. maximus* (Chapters 3 and 5). The positive relationship observed between absolute respiration rate and Sr/Ca in *M. edulis* grown both in laboratory and field culturing experiments provides the first direct evidence of a physiological control on bivalve calcite Sr/Ca ratios (Chapter 5). Further support for a physiological control of shell Sr/Ca ratios also comes from the significant inverse relationship between shell Sr/Ca and $\delta^{13}C$ ratios in *M. edulis*, *P. maximus* and *P. nobilis*. However, such physiological control of Sr/Ca ratios cannot be applied to bivalves in general, which can be absent (e.g. Gillikin et al., 2005b), inverse (Chapter 2 and 5) or even positive (Klein et al., 1996b). Shell calcite Sr/Ca ratios thus appear to be under the control of more than a single factor (shell growth rate, metabolic activity and even shell Mg content), which may differ from one species to another (Chapter 5), but also temporally in a single species (Chapter 3).

A significant relationship between bivalve calcite Mn/Ca ratios and dissolved Mn^{2+} concentrations was suggested (Chapter 3) from the similar intra-annual variations of shell Mn/Ca in field-grown specimens of *Pecten maximus* and previously described seawater dissolved Mn^{2+} concentrations (Morris, 1974). In field-grown specimens of *Mytilus edulis*, shell Mn/Ca ratios were found not to be influenced by either dissolved or particulate Mn^{2+} concentrations. Shell Mn/Ca ratios and shell growth rates showed a remarkably similar seasonal variation, which was not indicative of a precipitation rate control. The influence of shell growth rate on shell Mn/Ca ratios must reflect a physiological control most likely acting through an increase in the

transport of Mn into the extra-pallial fluid, raising its Mn content, and ultimately causing higher shell Mn/Ca ratios (Chapter 6).

Significant small-scale heterogeneity in Mg/Ca, Sr/Ca and Mn/Ca ratios in the shells of *P. maximus* and *M. edulis* deposited at a constant temperature of was observed (Chapter 7). It is clear from the ion microprobe data obtained in this study that differences in the relative contribution of specific shell features, i.e. the number and size of stria and surface disturbance growth marks milled, as well as the depth of milling through regions of shell with variable Mg/Ca, Sr/Ca and Mn/Ca ratios, can explain some of the variability in elemental/Ca ratios observed previously for *M. edulis* and *P. maximus* shells (Chapters 3, 4, 5 and 6). In particular, the unexpected increase in Mg/Ca ratios at low winter temperatures of field grown *P. maximus* specimens (chapter 3) could potentially be explained by a higher number of stria (ca. 12 striae/mm) being milled and included in each 'winter' powder sample, compared to Mg/Ca ratios in spring and summer samples with a lower number of stria (ca. 4–6 striae/mm). However, such small-scale heterogeneity in shell elemental/Ca ratios cannot be attributed to particular structural shell layers. Most importantly, in both bivalve species studied, elemental/Ca ratios vary significantly in shell deposited from the same EPF and thus strongly suggests that element incorporation in to the shell carbonate at the crystal-solution interface is a key control step in determining the element composition of shell calcite.

Most of the results presented in this dissertation do not support the use of the elemental/Ca ratios studied in bivalve calcite, and contribute to the growing evidence that bivalve calcite element composition is controlled by physiological factors that underlie a tight control of element incorporation during shell biomineralization. Such physiological control of shell elemental composition in bivalves could be associated in some occasions to particular processes, such as shell growth rate or metabolic activity (chapter 3, 5 and 6). Furthermore, elaborate shell features and disturbance growth marks, which are ubiquitous in bivalve shells, were associated with significant variations of the elemental content of the shell calcite and thus may represent an important interference in the use of geochemical proxies in bivalve shell calcite.

The results of the present work suggest that specimens or species, subject during their lives to a disturbing and stressful environment are most likely unsuitable for palaeoenvironmental reconstructions using elemental/Ca ratios. The use of bivalve shells in palaeoenvironmental reconstruction studies relies on the use of fossil shells and more often than not the choice of specimens, and even of species, to be used in such studies is limited for practical reasons (e.g. location, presence in the deposit, preservation, etc). Sources of metabolic stress and growth disturbance are ubiquitous during the life of many bivalve species and will no doubt influence the elemental/Ca records preserved in their shells. In particular, most bivalve species used in palaeoenvironmental studies often occupy coastal or estuarine environments and are exposed to stressful factors such as: exposure to air in inter-tidal areas; variations in salinity, pH and oxygen concentrations; presence of harmful substances and even toxic phytoplankton. Furthermore, growth in bivalves can be disturbed by storms, strong currents, sediment transport and predation, which causes disturbance growth marks in the shell, and even endogenous factors such as reproduction, may be a source of metabolic stress to the animals. For instance, *Mytilus edulis* can live in a wide range of habitats, from inter-tidal to sub-tidal areas, from fully marine to estuarine areas and in hard or soft substrates. It is reasonable to assume that contemporaneous *M. edulis* specimens from the same location, but that grew in different habitats, such as adjacent inter-tidal and sub-tidal areas, will have distinct elemental/Ca ratios and thus invalidate any reconstructions of past or present environmental conditions.

Unless the secondary controls (i.e. metabolic and/or kinetic factors) on element incorporation, in particular their influence on the small-scale heterogeneity of shell elemental composition, can be understood in more detail, and eventually compensated for, the use of the geochemical proxies Mg/Ca, Sr/Ca and Mn/Ca ratios in bivalves for reliable and accurate reconstructions of past or present environmental conditions remains unlikely, at least in the species studied to date. Nevertheless, shell Mg/Ca ratios in the earlier years of growth in *Pinna nobilis* and particularly in the inner regions of *Pecten maximus* shells promise the potential of valid palaeotemperature proxies that deserve further investigation.

In the present study, a complementary field and laboratory experimental approach was used with constrained or monitored environmental and physiological conditions during new shell growth. Laboratory aquaria are not a true representation of the animal's natural habitat and the outcomes of laboratory culturing studies are only of value when validated by field-based studies, albeit with the latter suffering from a lesser degree of constraint of environmental variables. The constrained chronology of new shell growth obtained for both field and laboratory experimentally grown animals has thus allowed completion of a reliable comparison of shell elemental/Ca ratios to measurements of contemporaneous seawater temperature, salinity and other relevant environmental variables, as well as to biological variables such as shell growth rate, size and metabolic activity. The approach used in the present study is thus a significant advancement on previous studies of elemental/Ca ratios in bivalve shells, providing which have often relied on $\delta^{18}O$-derived calcification temperature, unconstrained growth and variation of environmental and physiological variables. Furthermore, an initial assessment of the extent of any small-scale heterogeneity in Mg/Ca, Sr/Ca and Mn/Ca ratios in bivalve shell calcite laboratory-grown specimens of *Pecten maximus* and *Mytilus edulis* under constant temperature has also been investigated.

The present thesis was presented with increasing degrees of experimental constrain of environmental and physiological conditions from chapter 2 and 3 to chapters 4, 5 and 6. For instance, in chapter 2, the field calibration of the Mg/Ca temperature proxy in *Pinna nobilis* was done using calcification temperatures derived from shell $\delta^{18}O$, assuming an annual mean value for $\delta^{18}O_{water}$, since no seawater temperature or were available. However, in chapter 3, seawater temperature and $\delta^{18}O_{water}$ data during growth were available, but *Pecten maximus* shell growth during the one-year experiment was not constrained and a shell growth model had to be constructed. In the laboratory and field culturing experiments used in chapters 4, 5 and 6 (field only) a constrained chronology of new shell growth was obtained and environmental and physiological variables were either monitored or constrained.

Studies on the evaluation and calibration of geochemical proxies in marine biogenic carbonates should move, and are already moving, from studies with loosely constrained growth and environmental conditions towards well constrained field and

laboratory calibration studies. In addition, the questions raised in the present work, but also from previous studies, suggest that only with high-resolution techniques such as SIMS, it is possible to understand the physiological and biomineralization processes that underline the larger scale variability of elemental/Ca ratios observed in bivalve shells. For instance, such high-resolution techniques will be necessary to explain why the variability of Mg/Ca ratios from shell deposited at constant temperature is so large; why shell deposited contemporaneously from the same extra-pallial fluid, but at different locations along the inner shell surface, has different elemental/Ca ratios; how changes in shell biomineralization processes associated with the deposition of disturbance growth marks and elaborate shell features influence the shell elemental composition and also what is the role of the organic matrix on the elemental composition of bivalve shells.

Finally, the findings of the present work should be considered in the development of future work on the use of geochemical proxies in bivalve shells, either guiding future research on the proxies studied here (see above) or as potential problems to be encountered in the development of recent and novel geochemical proxies in bivalve shells, such as potential palaeotemperature proxies already investigated in other marine biogenic carbonates, e.g. Li/Ca, U/Ca and Mg isotopes.

References

Addadi, L., Joester, D., Nudelman, F. and Weiner, S., 2006. Mollusk shell formation: A source of new concepts for understanding biomineralization processes. *Chemistry European Journal*, 12: 980-987.

Adkins, J., Boyle, E., Curry, W. and Lutringer, T., 2003. Stable isotopes in deep-sea and new mechanism for "vital effects". *Geochimica et Cosmochimica Acta*, 67(6): 1129-1143.

Allison, N., 1996. Comparative determination of trace and minor elements in coral aragonite by ion microprobe analysis, with preliminary results from Phuket, southern Thailand. *Geochimica et Cosmochimica Acta*, 60(18): 3457-3470.

Allison, N. and Austin, W., 2003. The potential of ion microprobe analysis in detecting geochemical variations across individual foraminifera tests. *Geochemistry, Geophysics, Geosystems*, 4(2): 8403, doi:10.1029/2002GC000430.

Andreasson, F. and Schmitz, B., 1998. Tropical Atlantic seasonal dynamics in the early middle Eocene from stable oxygen and carbon isotope profiles of mollusc shells. *Paleoceanography*, 13(2): 183-192.

Arthur, M., Dean, W. and Claypool, G., 1985. Anomalous ^{13}C enrichment in modern marine organic carbon. *Nature*, 315: 216-219.

Arthur, M., Williams, D. and Jones, D., 1983. Seasonal temperature-salinity changes and thermocline development in the mid-Atlantic Bight as recorded by the isotopic composition of bivalves. *Geology*, 11: 655-659.

Balistrieri, L. and Murray, J., 1986. The surface chemistry of sediments from the Panama Basin: The influence of Mn oxides on metal adsorption. *Geochimica et Cosmochimica Acta*, 50: 235-243.

Bayne, B. and Newell, R., 1983. Physiological energetics of marine molluscs. In: A. Saleuddin and K. Wilbur (Editors), *The Mollusca*. Academic Press, New York, pp. 407-515.

Bayne, B. and Worral, C., 1980. Growth and production of mussels (*Mytilus edulis*) from two populations. *Marine Ecology Progress Series*, 3: 317-328.

Beck, J., Edwards, R., Ito, E., Taylor, F., Recy, J., Rougerie, F., Joannot, P. and Henin, C., 1992. Sea surface temperature from skeletal Sr/Ca ratios. *Science*, 257: 644-647.

Belcher, A., Wu, X., Christensen, R., Hansma, P., Stucky, G. and Morse, D., 1996. Control of crystal phase switching and orientation by soluble mollusc-shell proteins. *Nature*, 381: 56-58.

Bemis, B., Spero, H., Bijma, J. and Lea, D., 1998. Reevaluation of the isotopic composition of planktonic foraminifera: experimental results and revised paleotemperature equations. *Paleoceanography*, 13(2): 150-160.

Benninger, P. and Le Pennec, M., 1991. Functional Anatomy of Scallops. In: S. Shumway (Editor), *Scallops: Biology, Ecology and Aquaculture*. Elsevier, Amsterdam, pp. 133-223.

Bentov, S. and Erez, J., 2005. Novel observations on biomineralization processes in foraminifera and implications for Mg/Ca ratio in the shells. *Geology*, 33(11): 841-844.

Berelson, W., MacManus, J., Coale, K., Johnson, K., Burdige, D., Kilgore, T., Colodner, D., Chavez, F., Kudela, R. and Boucher, J., 2003. A time series of benthic flux measurements from Monterey Bay, CA. *Continental and Shelf Research*, 23: 457-481.

Berner, R., 1975a. The role of magnesium on the crystal growth of calcite and aragonite in seawater. *Geochimica et Cosmochimica Acta*, 39: 489-504.

Berner, R., 1975b. The role pf magnesium on the crystal growth of calcite and aragonite in seawater. *Geochimica et Chosmochimica Acta*, 39: 489-504.

Bice, K., Layne, G. and Dahl, K., 2005. Application of secondary ion mass spectrometry to the determination of Mg/Ca in rare, delicate, or altered planktonic foraminifera: Examples from the Holocene, Paleogene, and Cretaceous. *Geochemistry, Geophysics, Geosystems*, 6(12): Q12P07, doi:10.1029/2005GC000974.

Bigg, G. and Rohling, E., 2000. An oxygen isotope dataset for marine waters. *Journal of Geophysical Research - Oceans*, 105(C4): 8527-8535.

Bijma, J., Hemleben, C., Huber, B.T., Erlenkeuser, H. and Kroon, D., 1998. Experimental determination of the ontogenetic stable isotope variability in two morphotypes of *Globigerinella siphonifera* (d'Orbigny). *Marine Micropaleontology*, 35: 141-160.

Blight, S., Bentley, T., Lefevre, D., Robinson, C., Rodrigues, R., Rowlands, J. and Williams, P., 1995. Phasing of autotrophic and heterotrophic plankton metabolism in a temperature coastal ecosystem. *Marine Ecology Progress Series*, 128: 61-75.

Bohm, F., Joachimski, M., Dullo, W., Einsenhauer, A., Lehnert, H., Reitner, J. and Worheide, G., 2000. Oxygen isotope fractionation in marine aragonite of coralline sponges. *Geochimica et Cosmochimica Acta*, 64(10): 1695-1703.

Brand, A., 1991. Scallop Ecology: Distributions and Behaviour. In: S. Shumway (Editor), *Scallops: Biology, Ecology and Aquaculture*. Elsevier, Amsterdam, pp. 517-584.

Bricelj, V. and Shumway, S., 1991. Physiology: Energy acquisition and utilization. In: S. Shumway (Editor), *Scallops: Biology, Ecology and Aquaculture*. Elsevier, Amsterdam, pp. 305-346.

Broecker, W. and Peng, T., 1982. Tracers in the Sea. Lamont Doherty Geological Observatory, Palisades, 690 pp.

Bruland, K., 1983. Trace elements in sea water. In: R. Chester (Editor), *Chemical Oceanography*. Academic Press, London, pp. 157-220.

Buick, D. and Ivany, L., 2004. 100 years in the dark: longevity of Eocene bivalves from Antartica. *Geology*, 32: 921-924.

Burdige, D., 1993. The biogeochemistry of manganese and iron reduction in marine sediments. *Earth-Science Reviews*, 35: 249-284.

Burnett, W., Bokuniewicz, H., Huttel, M., Moor, W. and Taniguchi, M., 2003. Groundwater and pore water inputs to the coastal zone. *Biogeochemistry*, 66: 3-33.

Burton, E. and Walter, L., 1987. Relative precipitation rates of aragonite and Mg calcite from seawater: Temperature or carbonate ion control? *Geology*, 15: 111-114.

Burton, J. and Statham, P., 1988. Trace Metals as Tracers in the Ocean. *Philosophical Transactions of the Royal Society London, Series A*, 325(1583): 127-144.

Carpenter, S. and Lohmann, K., 1992. Sr/Mg ratios of modern marine calcite: Empirical indicators of ocean chemistry and precipitation rate. *Geochimica et Cosmochimica Acta*, 56: 1837-849.

Carré, M., Bentaleb, I., Bruguier, O., Ordinola, E., Barret, N. and Fontugne, M., 2006. Calcification rate influence on trace element concentrations in aragonitic bivalve shells: Evidences and mechanisms. *Geochimica et Cosmochimica Acta*, 70: 4906-4920.

Carriker, M., 1992. Prismatic shell formation in constinously isolated (*Mytilus edulis*) and periodically exposed (*Crassostrea virginica*) extrapallial spaces - Explicable by the same concept. *American Malacological Bulletin*, 9(2): 193-197.

Carter, J., 1980. Controls of bivalve shell mineralogy and microstructure. In: D. Rhoads and R. Lutz (Editors), *Skeletal growth of aquatic organisms*. Plenum Press, New York, pp. 69-113.

Carter, J., 1990a. Shell Microstructural Data for the Bivalvia. Part V. Order Pectinoida. In: J. Carter (Editor), *Skeletal Biomineralization: Patterns, Processes and Evolutionary Trends*. Van Nostrand Reinhold, New York, pp. 363-389.

Carter, J., 1990b. Shell Microstructural Data for the Bivalvia. Part VI. Order Mytiloida. In: J. Carter (Editor), *Skeletal Biomineralization: Patterns, Processes and Evolutionary Trends*. Van Nostrand Reinhold, New York, pp. 390-.

Chauvaud, L., Lorrain, A., Dunbar, R., Paulet, Y.M., Thouzeau, G., Jean, F., Guarini, J. and Mucciarone, D., 2005. Shell of the Great Scallop *Pecten maximus* as a high-frequency archive of paleoenvironmental changes. *Geochemistry, Geophysics, Geosystems*, 6(8).

Chauvaud, L., Thouzeau, G. and Paulet, Y.M., 1998a. Effects of environmental factors on the daily growth rate of *Pecten maximus* juveniles in the Bay of Brest (France). *Journal of Experimental Marine Biology and Ecology*, 227: 83-111.

Chauvaud, L., Thouzeau, G. and Paulet, Y.M., 1998b. Effects of environmental factors on the daily growth rate of *Pecten maximus* juvenites in the Bay of Brest, (France). *Journal of Experimental Marine Biology and Ecology*, 227: 83-111.

Chave, K., 1954. Aspects of the biogeochemistry of magnesium 1. Calcareous marine organisms. *Journal of Geology*, 62: 266-283.

Checa, A., 2000. A new model for periostracum and shell formation in Unionidae (Bivalvia, Mollusca). *Tissue and Cell*, 32(5): 405-416.

Chilingar, G.V., 1962. Dependence on temperature of Ca/Mg ratio of skeletal structures of organisms and direct chemical precipitates out of seawater. *Bulletin of the Southern California Academy of Sciences*, 61(1): 45-61.

Clark II, G., 1974. Calcification on an unstable substrate: marginal growth in the mollusc *Pecten diagenensis*. *Science*, 183: 968-970.

Cohen, A. and Branch, G., 1992. Environmentally controlled variation in the structure and mineralogy of *Patella granularis* shells from the coast of southern Africa: implications for paleotemperature assessments. *Palaeogeography Palaeoclimatology Palaeoecology*, 91: 49-57.

Cohen, A., Layne, G., Hart, S. and Lobel, P., 2001. Kinetic control of skeletal Sr/Ca in a symbiotic coral: Implications for the paleotemperature proxy. *Paleoceanography*, 16(1): 20-26.

Cohen, A. and McConnaughey, T., 2003. Geochemical Perspectives on Coral Mineralization. In: P. Dove, J. De Yoreo and S. Weiner (Editors), *Biomineralization*. Reviews in Mineralogy and Geochemistry. Mineralogical Society of America, Washington, USA, pp. 151-187.

Comans, R.N.J. and Middelburg, J.J., 1987. Sorption of trace metals on calcite: Applicability of the surface precipitation model. *Geochimica et Cosmochimica Acta*, 51(9): 2587-2591.

Coote, G.E. and Trompetter, W.J., 1995. Proton microprobe studies of fluorine distributions in mollusc shells. *Nuclear Instruments and Methods in Physics Research Section B: Beam Interactions with Materials and Atoms*, 104(1-4): 333.

Coplen, T.B., Kendall, C. and Hopple, J., 1983. Comparison of stable isotope reference samples. *Nature*, 302: 236-238.

Correge, T. and Deckker, P., 1997. Faunal and geochemical evidence for changes in intermediate water temperature and salinity in the western Coral Sea (northeast Australia) during the Late Quaternary. *Palaeogeography, Palaeoclimatology, Palaeoecology*, 313: 183-205.

Craig, H., 1953. The geochemistry of stable carbon isotopes. *Geochimica et Cosmochimica Acta*, 3: 53-92.

Crenshaw, M., 1972. The inorganic composition of molluscan extrapallial fluid. *Biological Bulletin*, 143: 505-512.

Crenshaw, M., 1975. Histochemical and structural study of nautiloid septal nacre. *Biomineralisation*, 8: 1-8.

Crenshaw, M., 1980. Mechanisms of shell formation and dissolution. In: D. Rhoads and R. Lutz (Editors), *Skeletal growth of aquatic organisms*. Plenum Press, New York, pp. 115-132.

Currey, J., 1988. Shell Form and Strength. In: E.R. Trueman and M.R. Clarke (Editors), *The Mollusca*. Academic Press, New York, pp. 183-210.

Dalbeck, P., England, J., Cusack, M., Lee, M. and Fallick, A., 2006. Crystallography and chemistry of the calcium carbonate polymorph switch in *M. edulis* shells. *European Journal of Mineralogy*, 18(5): 601-609.

Dansgaard, W., 1964. Stable isotopes in precipitation. *Tellus*, 16: 436-468.

Dare, P. and Deith, M., 1991. Problems with reconstructing sea - water temperature records from oxygen stable isotopic profiles in shells of the Scallop *Pecten maximus*, 8th International Pectinid Workshop, Cherbourg, France.

Dauphin, Y., Cuif, J.P., Doucet, J., Salome, M., Susini, J. and Willams, C.T., 2003. In situ chemical speciation of sulfur in calcitic biominerals and the simple prism concept. *Journal Of Structural Biology*, 142(2): 272-280.

Dauphin, Y., Cuif, J.P., Salome, C. and Susini, J., 2005. Speciation and distribution of sulfur in a mollusk shell as revealed by in situ maps using X-ray absorption near-edge structure (XANES) spectroscopy at the SK-edge. *American Mineralogist*, 90(11-12): 1748-1758.

Davidson, A. and Marchant, H., 1987. Binding of manganese by Antartic *Phaeocystis pouchetii* and the role of bacteria in its release. *Marine Biology*, 95: 481-487.

Davis, J.A., Fuller, C.C. and Cook, A.D., 1987. A model for trace metal sorption processes at the calcite surface: Adsorption of Cd^{2+} and subsequent solid solution formation. *Geochimica et Cosmochimica Acta*, 51(6): 1477-1490.

de Villiers, S., Greaves, M. and Elderfield, H., 2002. An intensity ratio calibration method for the accurate determination of Mg/Ca and Sr/Ca of marine carbonates by ICP-AES. *Geochemistry, Geophysics, Geosystems*, 3: 10.1029/2001GC000169.

de Villiers, S., Nelson, B. and Chivas, A., 1995. Biological controls on coral Sr/Ca and $\delta^{18}O$ reconstructions of sea surface temperatures. *Science*, 269: 1247-1249.

De Zwaan, A. and Mathieu, M., 1992. Cellular biochemistry and endocrinology. In: E. Gossling (Editor), *The Mussel Mytilus: Ecology, Physiology, Genetics and*

Culture. Developments in Aquaculture and Fisheries Science, 25. Elsevier Science Publishers, Amsterdam, pp. 223-307.

Debeney, J., Guillou, J., Geslin, E. and Lesourd, M., 2000. Crystallization of calcite in foraminiferal tests. *Micropaleontology*, 46: 87-94.

Dehairs, F., Baeyens, W. and Van Gansbeke, D., 1989. Tight coupling between enrichment of iron and manganese in North Sea suspended matter and sedimentary redox processes: Evidence for seasonal variability. *Estuarine, Coastal and Shelf Science*, 29: 457-471.

Delaney, M.L., Linn, L.J. and Druffel, E.R.M., 1993. Seasonal cycles of manganese and cadmium in coral from the Galapagos Islands. *Geochimica et Cosmochimica Acta*, 57(2): 347-354.

Delaney, M.L., W.H. Be, A. and Boyle, E.A., 1985. Li, Sr, Mg, and Na in foraminiferal calcite shells from laboratory culture, sediment traps, and sediment cores. *Geochimica et Cosmochimica Acta*, 49(6): 1327-1341.

Dellwig, O., Bosselmann, K., Kolsch, S., Hentscher, M., Hinrichs, J., Bottcher, M., Reuter, R. and Brumsack, H., 2007. Sources and fate of manganese in a tidal basin of the German Wadden Sea. *Journal of Sea Research*, 57: 1-18.

Dietzel, M., Gussone, N. and Einsenhauer, A., 2004. Co-precipitation of Sr^{2+} and Ba^{2+} with aragonite by membrane diffusion of CO_2 between 10 and 50°C. *Chemical Geology*, 203: 139-151.

Dillaman, R. and Ford, S., 1982. Measurement of calcium-carbonate deposition in mollusks by controlled etching of radioactively labeled shells. *Marine Biology*, 66: 133-143.

Dodd, J., 1965. Environmental control of strontium and magnesium in *Mytilus*. *Geochimica et Cosmochimica Acta*, 29: 385-398.

Dodd, J. and Crisp, E., 1982. Non-linear variation with salinity of Sr/Ca and Mg/Ca ratios in water and aragonitic bivalve shells and implications for paleosalinity studies. *Palaeogeography, Palaeoclimatology, Palaeoecology*, 38: 45-56.

Dromgoole, E. and Walter, L., 1990. Iron and manganese incorporation into calcite: effects of growth kinetics, temperature and solution chemistry. *Chemical Geology*, 81: 311-336.

Druffel, E., 1997. Geochemistry of corals: Proxies of past ocean chemistry, ocean circulation, and climate. *Proceedings of the National Academy of Sciences of the United States of America*, 94: 8354-8361.

Duinker, J., Hillebrand, M., Nolting, R. and Wellershaus, S., 1982. The river Weser: Processes affecting the behaviour of metals and organochlorines during estuarine mixing. *Netherlands Journal of Sea Research*, 15: 170-195.

Dwyer, G., Cronin, T., Baker, P., Raymo, M., Buzas, J. and Correge, T., 1995. North Atlantic deepwater temperature change during late Pliocene and late Quaternary climatic cycles. *Science*, 270: 1347-1351.

Dwyer, G., Cronin, T., Baker, P. and Rodriguez-Lazaro, J., 2000. Changes in North Atlantic deep sea temperature during climate fluctuations of the last 25,000 years based on ostracode Mg/Ca ratios. *Geochemistry, Geophysics, Geosystems*, 1(12): DO 10.1029/2000GC000046.

Eggins, S., Sadekov, A. and Deckker, P., 2004. Modulation and daily banding of Mg/Ca in *Orbulina universa* test by symbiont photosynthesis and respiration: A complication for seawater thermometry? *Earth and Planetary Science Letters*, 225: 411-419, doi: 10.1016/j.epsl.2004.06.019.

Elderfield, H., Bertram, C. and Erez, J., 1996. A biomineralization model for the incorporation of trace elements into foraminiferal calcium carbonate. *Earth and Planetary Science Letters*, 142: 409-423.

Elderfield, H. and Ganssen, G., 2000. Past temperature and $\delta^{18}O$ of surface ocean waters inferred from foraminiferal Mg/Ca ratios. *Nature*, 405: 442-445.

Elderfield, H., Vautravers, M. and Cooper, M., 2001. The relationship between shell size and Mg/Ca, Sr/Ca, $\delta^{18}O$,and $\delta^{13}C$ of species of planktonic foraminifera. *Geochemistry, Geophysics, Geosystems*, 3(8): 10.1029/2001GC000194.

Elliot, M., deMenocal, P., Linsley, B. and Howe, S., 2003. Environmental controls on the stable isotopic composition of *Mercenaria mercenaria*: Potential application to paleoenvironmental studies. *Geochemistry, Geophysics, Geosystems*, 4(7): 1056, doi:10.1029/2002GC000425.

Emerson, S., Kalhorn, S., Jacobs, S., Tebo, B., Nealson, K. and Rosson, R., 1982. Environmental oxidation rate of manganese(II): bacterial catalysis. *Geochimica et Cosmochimica Acta*, 46: 1073-1079.

Emiliani, C., 1955. Pleistocene Temperatures. *Journal of Geology*, 63: 538-578.

Emiliani, C., 1966. Isotopic paleotemperatures. *Science*, 154: 851-857.

England, J., Cusack, M. and Lee, M., 2007. Magnesium and sylphur in the calcite shells of two brachiopods, *Terebratulina retusa* and *Novocrania anomala*. *Lethaia*, 40(1): 2-10.

Epstein, S., Buchsbaum, R., Lowenstam, H. and Urey, H., 1951. Carbonate-water isotopic temperature scale. *Bulletin of the Geological Society of America*, 62(417-436).

Epstein, S., Buchsbaum, R., Lowenstam, H. and Urey, H., 1953. Revised carbonate-water isotopic temperature scale. *Bulletin of the Geological Society of America*, 64: 1315-1326.

Epstein, S. and Mayeda, T., 1953a. Variation of $\delta^{18}O$ content waters from natural waters. *Geochimica et Cosmochimica Acta*, 4: 213-224.

Epstein, S. and Mayeda, T., 1953b. Variation of $\delta^{18}O$ content waters from natural waters. *Geochimica et Chosmochimica Acta*, 4: 213-224.

Erez, J., 1978. Vital effect on stable-isotope composition seen in foraminifera and coral skeletons. *Nature*, 273: 199-202.

Erez, J., 2003. The source of ions for biomineralization in foraminifera and their implications for paleoceanographic proxies. In: P. Dove, J. De Yoreo and S. Weiner (Editors), *Biomineralization*. Reviews in Mineralogy and Geochemistry. Mineralogical Society of America, Washington, USA, pp. 115-149.

Falini, G., Albeck, S., Weiner, S. and Addadi, L., 1996. Control of aragonite or calcite polymorphism by mollusc shell macromolecules. *Science*, 271: 67-69.

Feng, Q.L., Pu, G., Pei, Y., Cui, F.Z., Li, H.D. and Kim, T.N., 2000. Polymorph and morphology of calcium carbonate crystals induced by proteins extracted from mollusk shell. *Journal of Crystal Growth*, 216(1-4): 459-465.

Franklin, M. and Morse, J., 1983. The interaction of manganese (II) with the surface of calcite in dilute solutions and seawater. *Marine Chemistry*, 12: 241-254.

Freitas, P., Clarke, L., Kennedy, H., Richardson, C.A. and Abrantes, F., 2005. Mg/Ca, Sr/Ca and stable-isotope ($\delta^{18}O$ and $\delta^{13}C$) ratio profiles from the fan mussel *Pinna nobilis*: Seasonal records and temperature relationships. *Geochemistry, Geophysics, Geosystems*, 6(4): Q04D14, doi:10.1029/2004GC000872.

Freitas, P., Clarke, L., Kennedy, H., Richardson, C.A. and Abrantes, F., 2006. Environmental and biological controls on elemental (Mg/Ca, Sr/Ca and Mn/Ca) ratios in shells of the king scallop *Pecten maximus*. *Geochimica et Cosmochimica Acta*, 70: 5119-5133.

Fuge, R., Palmer, T., Pearce, N. and Perkins, W., 1993. Minor and trace element chemistry of modern shells: A laser ablation inductively coupled plasma mass spectrometry study. *Applied Geochemistry*, Suppl. Issue No. 2: 111-116.

Furla, P., Galgani, I., Durand, I. and Allemand, D., 2000. Sources and mechanisms of inorganic carbon transport for coral calcification and photosynthesis. *Journal of Experimental Biology*, 203: 3445-3457.

Gabitov, R. and Watson, E., 2006. Partitioning of strontium between calcite and fluid. *Geochemistry, Geophysics, Geosystems*, 7(11): Q11004, doi:10.1029/2005GC01216.

Gagan, M., Ayliffe, L., Beck, J., Cole, J., Druffel, E., Dunbar, R. and Schrag, D., 2000. New views of tropical paleoclimates from corals. *Quaternary Science Reviews*, 19: 45-64.

Garlick, G., 1974. The stable isotopes of oxygen, carbon, hydrogen in the marine environment. In: E. Goldberg (Editor), *The Sea*. John Wiley & Sons, New York, pp. 393-425.

Gill, R., 1997. Modern analytical geochemistry: An introduction to quantitative chemical analysis fro earth, environmental and material scientists. Longman, Harlow.

Gillikin, D., 2005. Geochemistry of Marine Bivalve Shells: the potential for paleoenvironmental reconstruction, Vrije Universiteit Brussel, Brussels.

Gillikin, D., Dehairs, F., Baeyens, W., Navez, J., Lorrain, A. and Andre, L., 2005a. Inter- and intra-annual variations of Pb/Ca ratios in clam shells (*Mercenaria mercenaria*): A record of anthropogenic lead pollution. *Marine Pollution Bulletin*, 50: 1530-1540.

Gillikin, D., Dehairs, F., Lorrain, A., Steenmans, D., Baeyens, W. and Andre, L., 2006a. Barium uptake into the shell of the common mussel (*Mytilus edulis*) and the potential for paleo-chemistry reconstruction. *Geochimica et Cosmochimica Acta*, 70: 395-407.

Gillikin, D., Lorrain, A., Bouillon, S., Willenz, P. and Dehairs, F., 2006b. Stable carbon isotopic composition of *Mytilus edulis* shells: relation to metabolism, salinity, $\delta^{13}C_{DIC}$ and phytoplankton. *Organic Geochemistry*, 37: 1371-1382.

Gillikin, D., Lorrain, A., Meng, L. and Dehairs, F., 2007. A large metabolic carbon contribution to the $\delta^{13}C$ record in marine aragonitic bivalve shells. *Geochimica et Cosmochimica Acta*, 71: 2936-2946.

Gillikin, D., Lorrain, A., Navez, J., Taylor, J., Andre, L., Keppens, E., Baeyens, W. and Dehairs, F., 2005b. Strong biological controls on Sr/Ca ratios in aragonitic marine bivalve shells. *Geochemistry, Geophysics, Geosystems*, 6(5): Q05009, doi:10.1029/2004GC000874.

Gillikin, D., Ulens, H., De Ridder, F., Elskens, M., Keppens, E., Baeyens, W. and Dehairs, F., 2005c. Assessing the reproducibility and reliability of estuarine bivalve shells (*Saxidomus gigateus*) for sea surface temperature reconstructions: implications for paleoclimate studies. *Palaeogeography, Palaeoclimatology, Palaeoecology*, 228: 70-85.

Glasby, C.P., 1984. Maganese in the marine environment. *Oceanography and Marine Biology Annual Review*, 22: 169-194.

Glasby, G.P. and Schulz, H., 1999. E_H, pH diagrams for Mn, Fe, Co, Ni, Cu and As under seawater conditions: application of two new types of E_H, pH diagrams to the study of specific problems in marine geochemistry. *Aquatic Geochemistry*, 5: 227-248.

Goodfriend, C.A., 1992. Rapid racemization of aspartic acid in mollusk shells and potential for dating over recent centuries. *Nature*, 357: 399-401.

Goodwin, D., Flessa, K., Schone, B. and Dettman, D., 2001. Cross-calibration of daily growth increments, stable isotope variation and temperature in the Gulf of California bivalve mollusk *Chione cortezi*: Implications for paleoenvironmental analysis. *Palaios*, 16(4).

Goodwin, D., Flessa, K., Tellez-Duarte, M., Dettman, D., Schone, B. and Avila-Serrano, G., 2004. Detecting time-averaging and spatial mixing using oxygen isotope variation:a case study. *Palaeogeography Palaeoclimatology Palaeoecology*, 205: 1-21.

Goodwin, D., Schoene, B. and Dettman, D., 2003. Resolution and fidelity of oxygen isotopes as paleotemperature proxies in bivalve mollusk shells: Models and Observations. *Palaios*, 18: 110-125.

Gosling, E., 1992. The mussel Mytilus: Ecology, Physiology, Genetics and Culture. Elsevier, Amsterdam.

Gosling, E., 2003. Bivalve Molluscs: Biology, Ecology and Culture. Fishing News Books. Blackwell Scientific Publications, Oxford, 443 pp.

Grasshof, K., Wehrhardt, M. and Kremling, K. (Editors), 1983. Methods of Seawater Analysis. Verlag Chemie, Weinheim.

Greaves, M., Barker, S., Daunt, C. and Elderfield, H., 2005. Accuracy, standardization, and interlaboratory calibration standards for foraminiferal Mg/Ca thermometry. *Geochemistry, Geophysics, Geosystems*, 6(2): Q02D13, doi:10.1029/2004GC000790.

Grossman, E.L., 1987. Stables isotopes in modern benthic foraminifera: a study of vital effect. *Journal of Foraminifera Research*, 17(1): 48-61.

Grossman, E.L. and Ku, T., 1986. Oxygen and carbon isotope fractionation in biogenic aragonite: Temperature effects. *Chemical Geology*, 59: 59-74.

Guilderson, T., Fairbanks, R. and Rubenstone, J., 1994. Tropical temperatures variations sice 20,000 years ago: Modulating interhemispheric climate change. *Science*, 263(5147): 663-665.

Hales, B., van Geen, A. and Takahashi, T., 2004. High-frequency measurement of seawater chemistry: Flow-injection analysis of macronutrients. *Limnology and Oceanography: Methods*, 2: 91-101.

Hall, I., Hydes, D., Statham, P. and Overnell, J., 1999. Seasonal variations in the cycling of aluminium, cadmium and manganese in a Scottish sea loch: biogeochemical processes involving suspended particles. *Continental and Shelf Research*, 19: 1783-1808.

Hare, P., 1963. Amino acids in the proteins from aragonite and calcite in the shells of *Mytilus californianus*. *Science*, 139: 216-217.

Hare, P. and Abelson, P., 1965. Amino acids composition of some calcified proteins. *Yearbook Carnegie Institution Washington*, 64: 223-232.

Harper, E., 1991. Post-larval cementation in the Ostreidae and its implications for other cementing Bivalvia. *Journal of Molluscan Studies*, 58: 37-48.

Harper, E., 1997. The molluscan periostracum: an important constraint in bivalve evolution. *Palaeontology*, 40: 71-97.

Harvey, J., 1968. The flow of water through the Menai Strait. *Geophysical Journal of the Royal Astronomical Society*, 15: 517-528.

Hathorne, E., Alard, O., James, R. and Rogers, N., 2003. Determination of intratest variability of trace elements in foraminifera by laser ablation inductively coupled plasma-mass spectrometry. *Geochemistry, Geophysics, Geosystems*, 4: 8408DEC52003.

Hattan, S.J., Laue, T.M. and Chasteen, N.D., 2001. Purification and characterization of a novel calcium-binding protein from the extrapallial fluid of the mollusc, Mytilus edulis. *Journal of Biological Chemistry*, 276(6): 4461-4468.

Hawkins, A. and Bayne, B., 1992. Physiological interrelations, and the regulation of production. In: E. Gossling (Editor), *The Mussel Mytilus: Ecology, Physiology, Genetics and Culture*. Developments in Aquaculture and Fisheries Science, 25. Elsevier Science Publishers, Amsterdam, pp. 171-221.

He, G. and Mai, K., 2001. Ontogenetic trends of mineralogy and elements in the shell of abalone, *Haliotis discus* hannai Ino. *Journal of Shellfish Research*, 20(2): 685-687.

Hickson, J.A., Johnson, A.L.A., Heaton, T.H.E. and Balson, P.S., 1999. The shell of the Queen Scallop *Aequipecten opercularis* (L.) as a promising tool for palaeoenvironmental reconstruction: evidence and reasons for equilibrium stable-isotope incorporation. *Palaeogeography Palaeoclimatology Palaeoecology*, 154(4): 325-337.

Hillbish, T., 1986. Growth trajectories of shell and soft tissue in bivalves: seasonal variation in *Mytilus edulis*. *Journal of Experimental Marine Biology and Ecology*, 96: 103-113.

Hinton, R., 1995. Ion microprobe analysis in geology. In: P.J. Potts and e. al. (Editors), *Microprobe Techniques in the Earth Sciences*. Chapman and Hall, New York, pp. 235-290.

Hoefs, J., 1997. Stable Isotope Geochemistry. Springer-Verlag, Berlin, 201 pp.

Hughen, K., Schrag, D., Jacobsen, S. and Hantoro, W., 1999. El Nino during the last interglacial period recorded by a fossil coral from Indonesia. *Geophysical Research Letters*, 26: 3129-3132.

Hunt, C., 1983. Variability in the benthic Mn flux in coastal marine ecosystems resulting from temperature and primary production. *Limnology and Oceanography*, 28: 913-923.

Hunt, C. and Kelly, J., 1988. Manganese cycling in coastal regions: Response to eutrophication. *Estuarine, Coastal and Shelf Science*, 26: 527-558.

Hut, G., 1987. Consultants group meeting on stable isotope reference samples for geochemical and hydrological investigations, Rep. to Dir. Gen., Int. At. Energy Agency, Vienna.

Immenhauser, A., Nagler, T., Steuber, T. and Hippler, D., 2005. A critical assessment of mollusk $^{18}O/^{16}O$, Mg/Ca and $^{44}Ca/^{40}Ca$ ratios as proxies for Cretaceous seawater temperature seasonality. *Palaeogeography, Palaeoclimatology, Palaeoecology*, 215: 221-237.

Ingram, B.L., Conrad, M. and Ingle, J., 1996a. Stable isotope and salinity systematics in estuarine waters and carbonates: San Francisco Bay. *Geochimica et Cosmochimica Acta*, 60(3): 455-467.

Ingram, L., Ingle, J. and Conrad, M., 1996b. Stable isotope record of late Holocene salinity and river discharge in San Francisco Bay, California. *Earth and Planetary Science Letters*, 141: 237-247.

Ivany, L., Wilkinson, B. and Jones, D., 2003. Using stable isotopic data to resolved rate and duration of growth throughout ontogeny: An example from the surf clam, *Spisula solidissima*. *Palaios*, 18: 126-137.

Jeffree, R., Markich, S., Lefebvre, F., Thellier, M. and Ripoll, C., 1995. Shell microlaminations of the fresh-water bivalve *Hyridella depressa* as an archival monitor of manganese concentration - Experimental investigation by depth profiling using secondary-ion mass-spectrometry (SIMS). *Experientia*, 51(8): 838-848.

Johnson, K., 1982. Carbon dioxide hydration and dehydration kinetics in seawater. *Limnology and Oceanography*, 27: 849-855.

Jones, D., 1983. Sclerochronology: reading the record of the molluscan shells. *American Scientist*, 71(4): 384-391.

Jones, D. and Quitmyer, I., 1996. Marking time with bivalves shells: Oxygen isotopes and season of annual increment formation. *Palaios*, 11(4): 340-346.

Kaplan, D.L., 1998. Mollusc shell structures: novel design strategies for synthetic materials. *Current Opinion in Solid State & Materials Science*, 3(3): 232-236.

Katz, A., 1973a. The interaction of magnesium with calcite during crystal growth at 25-90 °C and one atmosphere. *Geochimica et Cosmochimica Acta*, 37: 1563-1586.

Katz, A., 1973b. The interaction of magnesium with calcite during crystal growth at 25-90 °C and one atmosphere. *Geochimica et Chosmochimica Acta*, 37: 1563-1586.

Keith, M. and Weber, J., 1965. Systematic realtionships between modern carbon and oxygen isotopes in carbonates deposited by modern corals and algae. *Science*, 150: 498-501.

Keller, N., Del Piero, D. and Longinelli, A., 2002. Isotopic composition, growth rates, and biological behaviour of *Chamelea gallina* and *Callista chione* from the Gulf of Trieste (Italy). *Marine Biology*, 140: 9-15.

Kennedy, H., Richardson, C., Duarte, C. and Kennedy, D.P., 2001. Oxygen and carbon stable isotopic profiles of the fan mussel, *Pinna nobilis*, and reconstruction of sea surface temperatures in the Mediterranean. *Marine Biology*, 139: 1115-1124.

Killingley, J. and Berger, W., 1979. Stable isotopes in a mollusk shell: Detection of upwelling events. *Science*, 205(186-188).

Kim, S.-T. and O'Neil, J.R., 1997. Equilibrium and nonequilibrium oxygen isotope effects in synthetic carbonates. *Geochimica et Cosmochimica Acta*, 61(16): 3461-3475.

Kinsman, D. and Holland, H., 1969a. The co-precipitation of cations with $CaCO_3$ - IV. The co-precipitation of Sr^{2+} with aragonite between 16° and 96°C. *Geochimica et Cosmochimica Acta*, 33: 1-17.

Kinsman, D. and Holland, H., 1969b. The co-precipitation of cations with $CaCO_3$ IV. The co-precipitation of Sr^{2+} with aragonite between 16° and 96°C. *Geochimica et Cosmochimica Acta*, 33: 1-17.

Kitano, Y., Kanmori, N. and Yoshioka, S., 1976. Influence of chemical species on the type of calcium carbonate. In: N. Watabe and K. Wilbur (Editors), *The mechanisms of mineralization in the invertebrates and plants*. Univ. of South Carolina Press, Columbia, pp. 191-202.

Klein, R., Lohmann, K. and Thayer, C., 1996a. Bivalve skeletons record sea-surface temperatures and $\delta^{18}O$ via Mg/Ca and $^{18}O/^{16}O$ ratios. *Geology*, 24(5): 415-418.

Klein, R., Lohmann, K. and Thayer, C., 1996b. Sr/Ca and $^{13}C/^{12}C$ ratios in skeletal calcite of *Mytilus trossulus*: Covariation with metabolic rate, salinity and carbon isotopic composition of seawater. *Geochimica et Cosmochimica Acta*, 60(21): 4207-4221.

Klein, R.T., Lohmann, K.C. and Kennedy, G.L., 1997. Elemental and isotopic proxies of paleotemperature and paleosalinity: Climate reconstruction of the marginal northeast Pacific ca 80 ka. *Geology*, 25(4): 363-366.

Klinkhammer, G. and McManus, J., 2001. Dissolved manganese in the Columbia River estuary: Production in the water column. *Geochimica et Cosmochimica Acta*, 65(17): 2835-2841.

Kobayashi, I., 1981. Internal Shell structure and its paleontological significance in molluscs - especially in Bivalvia. In: T. Habe and M. Omori (Editors), *Study of Molluscan Paleobiology*. Niigata University, Niigata, pp. 47-62.

Koziol, A. and Newton, R., 1995. Experimental determination of reactions magnesite + quartz = periclase + CO_2 and the enthalpies of formation of enstatite and magnesite. *American Mineralogist*, 80: 1252-1260.

Krantz, D., Jones, D. and Williams, D., 1987. Ecological and paleoenvironmental information using stable isotope profiles from living and fossil mollusks. *Palaeogeography, Palaeoclimatology, Palaeoecology*, 58: 249-266.

Krantz, D., Kronick, A. and Williams, D., 1988. A model for interpreting continental shelf hydrographic processes from the stable isotope and cadmium: calcium profiles of scallop shells. *Palaeogeography Palaeoclimatology Palaeoecology*, 64: 123-140.

Krantz, D., Williams, D. and Jones, D., 1984. Growth rates of the sea scallop, *Placopecten magellanicus*, determined from the $^{18}O/^{16}O$ record in shell calcite. *Biological Bulletin*, 167: 186-199.

Kratzer, S., Bowers, D. and Tett, P., 2000. Seasonal changes in colour ratios and optically active constituents in the optical case-2 waters of the Menai Strait, North Wales. *International Journal of Remote Sensing*, 21: 2225-2246.

Kratzer, S., Buchan, S. and Bowers, D., 2003. Testing long-term trends in turbidity in the Menai Strait, North Wales. *Estuarine, Coastal and Shelf Science*, 56: 221-226.

Kurunczi, S., Torok, S. and Chevallier, P., 2001. A micro-XRF study of the element distribution on the growth front of mussel shell (Species of Unio crassus Retzius). *Mikrochimica Acta*, 137(1-2): 41-48.

Laing, I., 2000. Effect of temperature and ration on growth and condition of king scallop (*Pecten maximus*) spat. *Aquaculture*, 183: 325-334.

Langlet, D., Alleman, L., Plisnier, P.-D., Hughes, H. and André, L., 2007. Manganese content records seasonal upwelling in Lake Tanganyika. *Biogeosciences*, 4: 195-203.

Langlet, D., Alunno-Bruscia, M., Rafelis, M., Renard, M., Roux, M., Schein, E. and Buestel, D., 2006. Experimental and natural cathodoluminescence in the shell of *Crassostrea gigas* from Thau lagoon (France): ecological and environmental implications. *Marine Ecology Progress Series*, 317: 143-156.

Laslett, R., 1995. Concentrations of dissolved and suspended particulate Cd, Cu, Mn, Ni, Pb and Zn in surface waters around the coasts of England and Wales and in adjacent seas. *Estuarine, Coastal and Shelf Science*, 40: 67-85.

Lazareth, C.E., Vander Putten, E., Andre, L. and Dehairs, F., 2003. High-resolution trace element profiles in shells of the mangrove bivalve *Isognomon*

ephippium: a record of environmental spatio-temporal variations? *Estuarine Coastal and Shelf Science*, 57(5-6): 1103-1114.

Lea, D. and Boyle, E., 1989. Barium content of benthic foraminifera controlled by bottom-water composition. *Nature*, 338: 751-753.

Lea, D.W., 2003. Elemental and isotopic proxies of past ocean temperatures. In: H. Elderfield (Editor), *The oceans and marine geochemistry*. Elsevier-Pergamon, Oxford, pp. 365-390.

Lea, D.W., Mashiotta, T. and Spero, H., 1999. Controls on magnesium and strontium uptake in planktonic foraminifera determined by live culturing. *Geochimica et Cosmochimica Acta*, 63(16): 2369-2379.

Lea, D.W., Pak, D. and Spero, H., 2000. Climate impact of late Quaternary equatorial Pacific sea surface temperature variations. *Science*, 289(5486): 1719-1724.

Lea, D.W., Shen, G. and Boyle, E., 1989. Coralline barium records temporal variability in equatorial upwelling. *Nature*, 340: 373-376.

Lear, C., Rosenthal, Y. and Slowey, N., 2002. Benthic foraminiferal Mg/Ca-paleothermometry: A revised core-top calibration. *Geochimica et Cosmochimica Acta*, 66(19): 3375-3387.

Leng, M. and Pearce, N., 1999. Seasonal variation of trace element and isotopic composition in the shell of a coastal mollusk, *Mactra isabelleana*. *Journal of Shellfish Research*, 18(2): 569-574.

Lewis, D. and Cerrato, R., 1997. Growth uncoupling and the relationship between shell growth and metabolism in the soft shell clam *Mya arenaria*. *Marine Ecology Progress Series*, 158: 177-189.

Lindh, U., Mutvei, H., Sunde, T. and Westermark, T., 1988. Environmental history told by mussel shells. *Nuclear Instruments & Methods In Physics Research Section B-Beam Interactions With Materials And Atoms*, 30: 388-392.

Lipmann, F., 1973. Sedimentary carbonate minerals. Springer-Verlag, Berlin.

Lorens, R., 1981a. Sr, Cd, Mn and Co distribution coefficients in calcite as a function of calcite precipitation rate. *Geochimica et Cosmochimica Acta*, 45: 553-561.

Lorens, R., 1981b. Sr, Cd, Mn and Co distribution coefficients in calcite as a function of calcite precipitation rate. *Geochimica et Chosmochimica Acta*, 45: 553-561.

Lorens, R. and Bender, M., 1977. Physiological exclusion of magnesium from *Mytilus edulis* calcite. *Nature*, 269: 793-794.

Lorens, R. and Bender, M., 1980. The impact of solution chemistry on *Mytilus edulis* calcite and aragonite. *Geochimica et Cosmochimica Acta*, 44: 1265-1278.

Lorrain, A., Gillikin, D., Paulet, Y.M., Chavaud, L., Lemercier, A., Navez, J. and Andre, L., 2005. Strong kinetic effects on Sr/Ca ratios in the calcitic bivalve *Pecten maximus*. *Geology*, 33: 965-968.

Lorrain, A., Paulet, Y.-M., Chauvaud, L., Savoye, N., Donval, A. and Saout, C., 2002. Differential $\delta^{13}C$ and $\delta^{15}N$ signatures among scallop tissues: implications for ecology and physiology. *Journal of Experimental Marine Biology and Ecology*, 275(1): 47-61.

Lorrain, A., Paulet, Y.M., Chauvaud, L., Savoye, N., Nezan, E. and Guerin, L., 2000. Growth anomalies in *Pecten maximus* from coastal waters (Bay of Brest, France): relationship with diatom blooms. *Journal of the Marine Biological Association of the United Kingdom*, 80: 667-673.

Lorrain, A., Paulet, Y.M., Chavaud, L., Dunbar, R., Mucciarone, D. and Fontugne, M., 2004. $\delta^{13}C$ variation in scallop shells: Increasing metabolic carbon

contribution with body size. *Geochimica et Cosmochimica Acta*, 68(17): 3509-3519.

Lowenstam, H. and Weiner, S., 1989. On Biomineralization. Oxford University Press, New York.

Lubbers, G., Giesles, W., del Castillo, P., Salomons, W. and Bril, J., 1990. Manganese accumulation in the high pH microenvironments of *Phaeocystis* sp. (Haptophyceae) colonies from the North Sea. *Marine Ecology Progress Series*, 59: 285-293.

Lutz, R., 1981. Electron probe analysis of strontium in mussel (Bivalvia: Mytilidae) shells: Feasability of estimating water temperature. *Hydrobiologia*, 83: 377-382.

Lutz, R. and Rhoads, D., 1980. Growth patterns within the molluscan shell: an overview. In: D. Rhoads and R. Lutz (Editors), *Skeletal growth of aquatic organisms*. Plenum Press, New York, pp. 203-248.

Mann, S., 2001. Biomineralization: Principles and Concepts in Bioinorganic materials Chemistry. Oxford University Press, New York.

Markich, S., Jeffree, R. and Burke, P., 2002. Freshwater bivalve shells as archival indicators of metal pollution from a copper-uranium mine in tropical northern Australia. *Environmental Science and Technology*, 36(5): 821-832.

Martin, P., Lea, D., Mashiotta, T., Papenfuss, T. and Sarthein, M., 1999. Variation of foraminiferal Sr/Ca over Quaternary glacila-interglacial cycles: Evidence for changes in mean ocean Sr/Ca? *Geochemistry, Geophysics, Geosystems*, 1: 1999GC000006.

Martin, P., Lea, D., Rosenthal, Y., Shackleton, N., Sarnthein, M. and Pappenfuss, T., 2002. Quaternary deep sea temperature histories derived from benthic foraminiferal Mg/Ca. *Earth and Planetary Science Letters*, 198: 193-209.

Mashiotta, T., Lea, D. and Spero, H., 1999. Glacial-intergalcial changes in Subantarctic sea surface temperature and $\delta^{18}O$-water using foraminiferal Mg. *Earth and Planetary Science Letters*, 170: 417-432.

McConnaughey, T., 1989a. ^{13}C and ^{18}O isotopic desequilibrium in biological carbonates: I. Patterns. *Geochimica et Cosmochimica Acta*, 53: 151-162.

McConnaughey, T., 1989b. ^{13}C and ^{18}O isotopic disequilibrium in biological carbonates:II. *In vitro* simulation of kinetic isotope effects. *Geochimica et Chosmochimica Acta*, 53: 163-171.

McConnaughey, T., 1989c. ^{13}C and ^{18}O isotopic disequilibrium in biological carbonates:II. *In vitro* simulation of kinetic isotope effects. *Geochimica et Cosmochimica Acta*, 53: 163-171.

McConnaughey, T., 2003. Sub-equilibrium oxygen-18 and carbon-13 levels in biological carbonates: carbonate and kinetic models. *Coral Reefs*, 22: 316-327.

McConnaughey, T., Burdet, J., Whelan, J. and Paull, C., 1997. Carbon isotopes in biological carbonates: Respiration and photosynthesis. *Geochimica et Cosmochimica Acta*, 61(3): 611-622.

McConnaughey, T. and Falk, R., 1996. Calcium-proton exchange during algal calcification. *Biological Bulletin*, 180: 185-195.

McCrea, J., 1950. On the isotopic chemistry of carbonates and a paleotemperature scale. *Jornal of Chemical Physics*, 18(6): 849-857.

McCulloch, M., Tudhope, A., Esat, T., Mortimer, G., Chappell, J., Pilans, B., Chivas, A. and Omuta, A., 1999. Coral record of equatorial sea-surface temperatures

during the penultimate deglaciation at Huon Peninsula. *Science*, 283: 202-204.

McKenna, V. and Prell, W., 2004. Calibration of the Mg/Ca of *Globorotalia truncatulinoides* (R) for the reconstruction of marine temperature gradients. *Paleoceanography*, 19(PA2006): 12.

McKinney, C., McCrea, J., Epstein, S., Allen, H. and Urey, H., 1950. Improvements in mass spectrometers for the measurement of small differences in isotopic ratios. *Rev. Sci. Instrum.*, 21: 724-730.

Meibom, A., Cuif, J.P., Hillion, F.O., Constantz, B.R., Juillet-Leclerc, A., Dauphin, Y., Watanabe, T. and Dunbar, R.B., 2004. Distribution of magnesium in coral skeleton. *Geophysical Research Letters*, 31(23).

Millward, G., Morris, A. and Tappin, A., 1998. Trace metals at two sites in the southern North Sea: Results from a sediment resuspension study. *Continental and Shelf Research*, 18: 1381-1400.

Misogianes, M. and Chasteen, N., 1979. A chemical and spectral characterization of the extrapallial fluid of *Mytilus edulis*. *Analytical Biochemistry*, 100: 324-334.

Mitchell, L., Fallick, A. and Curry, G., 1994. Stable carbon and oxygen isotope composition of mollusc shells from Britain and New Zealand. *Palaeogeography, Palaeoclimatology, Palaeoecology*, 111: 207-216.

Miyamoto, H., Miyashita, T., Okushima, M., Nakano, S., Morita, T. and Matsushiro, A., 1996. A carbonica anhydrase from the nacreous layer of oyster pearls. *Proceedings of the National Academy of Sciences of the United States of America*, 93: 9657-9660.

Mook, W. and Vogel, J., 1968. Isotopic equilibrium between shells and their environment. *Science*, 159: 874-875.

Moreteau, J. and Vicente, N., 1982. Evolution d'une population de *Pinna nobilis* L. (Mollusca, Bivalvia). *Malacologia*, 22: 341-345.

Morris, A., 1971. Trace metal variations in sea water of the Menai Straits caused by a bloom of *Phaeocystis*. *Nature*, 233: 427-428.

Morris, A., 1974. Seasonal variation of dissolved metals in inshore waters of the Menai Straits. *Marine Pollution Bulletin*: 54-59.

Morse, J. and Bender, M., 1990. Partition coefficients in calcite: Examination of factors influencing the validity of experimental results and their application to natural systems. *Chemical Geology*, 82: 265-277.

Mount, A., Wheeler, A., Paradkar, R. and Snider, D., 2004. Hemocyte-mediated shell mineralization in the Easten Oyster. *Science*, 304: 297-300.

Mucci, A., 1987a. Influence of temperature on the precipitation of magnesian calcite overgrowths precipitated from seawater. *Geochimica et Chosmochimica Acta*, 51: 1977-1984.

Mucci, A., 1987b. Influence of temperature on the precipitation of magnesian calcite overgrowths precipitated from seawater. *Geochimica et Cosmochimica Acta*, 51: 1977-1984.

Mucci, A., 1988. Manganese uptake during calcite precipitation from seawater: Conditions leading to the formation of pseudokutnahorite. *Geochimica et Cosmochimica Acta*, 52: 1859-1868.

Mucci, A. and Morse, J., 1983. The incorporation of Mg^{2+} and Sr^{2+} into calcite overgrowths: Influences of growth rate and solution composition. *Geochimica et Cosmochimica Acta*, 47: 217-233.

Mueller-Lupp, T., Erlenkeuser, H. and Bauch, H.A., 2003. Seasonal and interannual variability of Siberian river discharge in the Laptev Sea inferred from stable isotopes in modern bivalves. *Boreas*, 32(2): 292-303.

Murray, J., 1975. The interactions of metal ions at the manganese dioxide solution interface. *Geochimica et Cosmochimica Acta*, 39: 505-519.

Nair, P. and Robinson, W., 1998. Calcium speciation and exchange between blood and extrapallial fluid of the quahog *Mercenaria mercenaria* (L). *Biological Bulletin*, 195(1): 43-51.

Neri, R., Schifano, G. and Papanicolau, C., 1979. Effects of salinity on mineralogy and chemical composition of *Cerastoderme edule* and *Monodonta articulata* shells. *Marine Geology*, 30: 233-241.

Nico, P., Anastasio, C. and Zasoski, R., 2002. Rapid photo-oxidation of Mn (II) mediated by humic substances. *Geochimica et Cosmochimica Acta*, 66: 4047-4056.

Nurnberg, D., 1995. Magnesium in tests of *Neogloboquadrina pachyderma* sinistral from high Northern and Southern latitudes. *Journal of Foraminifera Research*, 25: 350-368.

Nurnberg, D., Bijma, J. and Hemleben, C., 1996a. Assessing the reliability of magnesium in foraminiferal calcite as a proxy for water mass temperatures. *Geochimica et Cosmochimica Acta*, 60: 803-814.

Nurnberg, D., Bijma, J. and Hemleben, C., 1996b. Erratum: Assessing the reliability of magnesium in foraminiferal calcite as a proxy for water mass temperatures. *Geochimica et Cosmochimica Acta*, 60: 2483-2484.

O'Neil, J., Clayton, N. and Mayeda, T., 1969. Oxygen isotope fractionation in divalent metal carbonates. *Journal of Chemical Physics*, 31: 5547-5558.

Ohde, S. and Kitano, Y., 1984. Coprecipitation of strontium with marine Ca-Mg carbonates. *Geochemistry Journal*, 18: 143-146.

Onuma, N., Masuda, F., Hirano, M. and Wada, K., 1979. Crystal structure control on trace element partition in molluscan shell formation. *Geochemistry Journal*, 13: 187-189.

Oomori, T., Kaneshima, H., Maezato, Y. and Kitano, Y., 1987. Distribution coefficient of Mg^{2+} ions between calcite and solution at 10-50°C. *Marine Chemistry*, 20(4): 327-336.

Owen, R., 1998. Partitioning of stable isotopes between scallop shell calcite and sea water and factors influencing shell growth and microgrowth patterns. Ph.D. Thesis, University of Wales Bangor, Bangor.

Owen, R., Kennedy, H. and Richardson, C., 2002a. Isotopic partitioning between scallop-shell calcite and seawater: effect of shell-growth rate. *Geochimica et Chosmochimica Acta*, 66(10): 1727-1737.

Owen, R., Kennedy, H. and Richardson, C., 2002b. Isotopic partitioning between scallop shell calcite and seawater: Effect of shell growth rate. *Geochimica et Cosmochimica Acta*, 66(10): 1727-1737.

Owen, R., Richardson, C. and Kennedy, H., 2002c. The influence of shell growth rate on striae deposition in the scallop *Pecten maximus*. *Journal of the Marine Biological Association of the United Kingdom*, 82(4): 621-623.

Paillaird, D., Labeyrie, L. and Yiou, P., 1996. Macintosh program performs time-series analysis. *EOS Trans. AGU*, 77(39): 379.

Paquette, J. and Reeder, R., 1995. Relationship between surface structure, growth mechanism and trace element incorporation in calcite. *Geochimica et Cosmochimica Acta*, 54: 395-402.

Parsons, T., Muita, Y. and Lalli, C., 1984. A manual of chemical and biological methods for seawater analysis. Pergamon Press, Oxford.

Pearce, N. and Mann, V., 2006. Trace metal variations in the shells of *Ensis siliqua* record pollution and environmental conditions in the sea to the west of mainland Britain. *Marine Pollution Bulletin*, 52: 739-755.

Pedersen, T.F. and Price, N.B., 1982. The geochemistry of manganese carbonate in Panama Basin sediments. *Geochimica et Cosmochimica Acta*, 46(1): 59-68.

Picco, P., 1990. Climatological atlas of the western Mediterranean. ENEA, Rome, 224 pp.

Pierre, C., 1999. The oxygen and carbon isotope distribution in the Mediterranean water masses. *Marine Geology*, 153: 41-55.

Pietrzak, J., Bates, J. and Scott, R., 1976. Constituents of unionid extrepallial fluid. ii ph and metal ion composition. *Hydrobiologia*, 50(1): 89-93.

Pingitore, J., Nicholas E., Eastman, M., Sandidge, M., Oden, K. and Freiha, B., 1988. The coprecipitation of manganese (II) with calcite: an experimental study. *Marine Chemistry*, 25: 107-120.

Pingitore, N., 1986. Modes of coprecipitation of Ba^{2+} and Sr^{2+} wiht calcite. In: J. Davis and K. Hayes (Editors), *Geochemical Processes at Mineral Surfaces*. Amer. Chem. Soc, pp. 574-586.

Pingitore, N. and Eastman, M., 1986. The coprecipitation of Sr^{2+} with calcite at 25°C and 1 atm. *Geochimica et Cosmochimica Acta*, 50: 2195-2203.

Pingitore, N.E., Lytle, F.W., Davies, B.M., Eastman, M.P., Eller, P.G. and Larson, E.M., 1992. Mode of incorporation of Sr2+ in calcite: Determination by X-ray absorption spectroscopy. *Geochimica et Cosmochimica Acta*, 56(4): 1531.

Price, G. and Pearce, N., 1997. Biomonitoring of pollution by *Cerastoderma edule* from the British Isles: a laser ablation ICP-MS study. *Marine Pollution Bulletin*, 34(12): 1025-1031.

Purton, L.M.A., Shields, G.A., Brasier, M.D. and Grime, G.W., 1999. Metabolism controls Sr/Ca ratios in fossil aragonitic mollusks. *Geology*, 27(12): 1083-1086.

Raith, A., Perkins, W., Pearce, N. and Jeffries, T., 1996. Environmental monitoring on shellfish using UV laser ablation ICP-MS. *Fresenius Journal of Analytical Chemistry*, 355(7-8): 789-792.

Reeder, R., 1996. Interaction of divalent cobalt, zinc, cadmium and barium with calcite surface during layer growth. *Geochimica et Chosmochimica Acta*, 60: 1543-1552.

Reeder, R. and Paquette, J., 1989. Sector zoning in natural and synthetic calcites. *Sedimentary Geology*, 65: 239-247.

Reeder, R.J. and Grams, J.C., 1987. Sector zoning in calcite cement crystals: Implications for trace element distributions in carbonates. *Geochimica et Cosmochimica Acta*, 51(2): 187-194.

Richardson, C., 2001. Molluscs as archives of environmental change. *Oceanography and Marine Biology*, 39: 103-164.

Richardson, C., Kennedy, H., Duarte, C., Kennedy, D. and Proud, S., 1999. Age and growth of the fan mussel *Pinna nobilis* from south-east spanish Mediterranean seagrass (*Posidonia oceanica*) meadows. *Marine Biology*, 133: 205-212.

Richardson, C.A., Peharda, M., Kennedy, H., Kennedy, P. and Onofri, V., 2004. Age, growth rate and season of recruitment of *Pinna nobilis* (L) in the

Croatian Adriatic determined from Mg:Ca and Sr:Ca shell profiles. *Journal of Experimental Marine Biology and Ecology*, 299(1): 1-16.

Richardson, L., Aguilar, C. and Nealson, K., 1988. Manganese oxidation in pH and O_2 microenvironments produced by phytoplankton. *Limnology and Oceanography*, 33(3): 352-363.

Richardson, L. and Stolzenbach, K., 1995. Phytoplankton cell size and the development of microenvironments. *FEMS Microbiology Ecology*, 16: 185-192.

Rickaby, R., Schrag, D., Zondervan, I. and Riebell, U., 2002. Growth-rate dependence of Sr incorporation during calcification of *Emiliana huxley*. *Global Biogeochemical Cycles*, 16(1): art. no. 1006 mar 2002.

Rimstidt, J.D., Balog, A. and Webb, J., 1998. Distribution of trace elements between carbonate minerals and aqueous solutions. *Geochimica et Cosmochimica Acta*, 62(11): 1851-1863.

Rio, M., Bodergat, A., Carbonnel, G. and Keyser, D., 1997. Anisotropie chimique de la carapace des ostracodes. Exemple de *Leptocythere psammophila*. *Comptes Rendus de l'Academie des Sciences - Series II a*, 324: 827-834.

Roitz, J., Flegal, A. and Bruland, K., 2002. The biogeochemical cycling of manganese in San Francisco Bay: Temporal and spatial variations in surface water concentrations. *Estuarine, Coastal and Shelf Science*, 54: 227-239.

Rollion-Bard, C., Chaussidon, M. and France-Lanord, C., 2003. pH control on oxygen isotopic composition of symbiotic corals. *Earth and Planetary Science Letters*, 215: 275-288.

Romanek, C.S., Grossman, E.L. and Morse, J.W., 1992. Carbon isotopic fractionation in synthetic aragonite and calcite: Effects of temperature and precipitation rate. *Geochimica et Cosmochimica Acta*, 56(1): 419-430.

Rosenberg, G., 1980. An ontogenetic approach to the environmental significance of bivalve shell chemistry. In: D. Rhoads and R. Lutz (Editors), *Skeletal Growth of Aquatic Organisms: Biological records of environmental change*. Plenum Press, New York, pp. 133-168.

Rosenberg, G. and Hughes, W., 1991. A metabolic model for the determination of shell composition in the bivalve mollusc, *Mytilus edulis*. *Lethaia*, 24: 83-96.

Rosenberg, G.D., Hughes, W.W., Parker, D.L. and Ray, B.D., 2001. The geometry of bivalve shell chemistry and mantle metabolism. *American Malacological Bulletin*, 16(1-2): 251-261.

Rosenheim, B., Swart, P.K., Thorrold, S., Willenz, P., Berry, L. and Latkcoczy, C., 2004. High-resolution Sr/Ca records in sclerosponges calibrated to temperature in situ. *Geology*, 32(2): 145-148.

Rosenthal, Y., Boyle, E. and Slowey, N., 1997. Temperature control on the incorporation of magnesium, strontium, fluorine and cadmium into benthic foraminiferal shells from Little Bahamas Bank: Prospects for thermocline paleoceanography. *Geochimica et Cosmochimica Acta*, 61(17): 3633-3643.

Russell, A., Emerson, S. and Mix, A., 1996. The use of foraminiferal uranium/calcium ratios as an indicator of changes in seawater uranium content. *Paleoceanography*, 11(6): 649-663.

Russell, A., Honisch, B., Spero, H. and Lea, D., 2004. Effects of seawater carbonate ion concentration and temperature on shell U, Mg and Sr in cultured planktonic foraminifera. *Geochimica et Cosmochimica Acta*, 68(21): 4347-4361.

Sadekov, A., Eggins, S. and Deckker, P., 2005. Characterization of Mg/Ca distributions in planktonic foraminifera species by electron microprobe mapping. *Geochemistry, Geophysics, Geosystems*, 6: Q12P06DEC132005.

Saleuddin, A. and Petit, H., 1983. The mode of formation and the structure of the periostracum. In: A. Saleuddin and K. Wilbur (Editors), *The Mollusca*. Academic Press, New York, pp. 199-235.

Schoemann, V., de Baar, H., de Jong, J. and Lancelot, C., 1998. Effects of phytoplankton blooms on the cycling of manganese and iron in coastal waters. *Limnology and Oceanography*, 43(7): 1427-1441.

Schoene, B., Castro, A., Fiebig, J., Houk, S., Oschmann, W. and Kroncke, I., 2004. Sea surface water temperatures over the period 1884-1983 reconstructed from oxygen isotope ratios of a bivalve mollusk shell (*Artica islandica*, southern North Sea). *Palaeogeography Palaeoclimatology Palaeoecology*, 212: 215-232.

Schoene, B., Tanabe, K., Dettman, D. and Sato, S., 2003. Environmental controls on shell growth rates and $\delta^{18}O$ of the shallow-marine bivalve mollusk *Phacosoma japonicum* in Japan. *Marine Biology*, 142: 473-485.

Schöne, B., Fiebig, J., Pfeiffer, M., Gleß, R., Hickson, J., Johnson, A., Dreyer, W. and Oschmann, W., 2005. Climate records from a bivalved Methuselah (*Artica islandica*, Mollusca; Iceland). *Palaeogeography, Palaeoclimatology, Palaeoecology228*(130-148).

Seed, R., 1976. Ecology. In: B. Bayne (Editor), *Marine Mussels: their ecology and physiology*. Cambridge University Press, Cambridge, pp. 13-65.

Seed, R. and Suchanek, T., 1992. Population and community ecology of *Mytilus*. In: E. Gossling (Editor), *The mussel Mytilus: Ecology, Physiology, Genetics and Culture*. Developments in aquaculture and fisheries science. Elsevier, pp. 87-170.

Shackleton, N., 1967. Oxygen isotopes analyses and Pleistocene temperatures re-assessed. *Nature*, 215: 15-17.

Shackleton, N., 1977. ^{13}C in Uvigerina: tropical rainforest history and the equatorial Pacfic carbonate dissolution cycles. In: N. Anderson and A. Malahof (Editors), *Fate of Fossil Fuel CO_2 in the Oceans*. Plenum, New York, pp. 401-427.

Shackleton, N. and Opdyke, N., 1973. Oxyegn isotope and paleomagnetic stratigraphy of equatorial Pacific core V28-238: Oxyegn isotope temperatures and ice volumes on a 10^5 and 10^6 year scale. *Quaternary Research*, 3: 39-55.

Siegele, R., Orlic, I., Cohen, D., Markich, S. and Jeffree, R., 2001. Manganese profiles in freshwater mussel shells. *Nuclear Instruments and Methods in Physics Research Section B: Beam Interactions with Materials and Atoms*, 181: 593-597.

Simkiss, K. and Mason, A., 1983. Metal Ions: Metabolic and toxic effects. In: P.W. Hochachka (Editor), *The Mollusca*, pp. 102-164.

Simkiss, K. and Wilbur, K., 1989. Biomineralisation: Cell biology and mineral deposition. Academic Press, San Diego.

Skinner, L. and Elderfield, H., 2005. Constraining ecological and biological bias in planktonic foraminiferal Mg/Ca and $\delta^{18}Occ$: A multispecies approach to proxy calibration testing. *Paleoceanography*, 20: PA1015, doi10.1029/2004PA001058.

Slomp, C., Malschaert, F., Lohse, L. and Van Raaphorst, W., 1997. Iron and manganese cycling in different sedimentary environments on the North Sea continental margin. *Continental and Shelf Research*, 17: 1083-1117.

Speer, J., 1983. Crystal chemistry and phase relations of orthorhombic carbonates. In: R. Reeder (Editor), *Carbonates: Mineralogy and Chemistry*. Rev. Mineral., pp. 145-190. Mineralogical Society of America.

Spero, H., Bijma, J., Lea, D. and Bemis, B., 1997. Effect of seawater carbonate concentration on foraminiferal carbon and oxygen isotopes. *Nature*, 390: 497-500.

Spero, H. and Deniro, M., 1987. The influence of symbiont photosynthesis on the $\delta^{18}O$ and $\delta^{13}C$ of planktonic foraminiferal shell calcite. *Symbiosis*, 4: 213-228.

Spero, H. and Lea, D., 1993. Intraspecific stable isotope variability in the planktonic foraminifera *Globigerinoides sacculifer*: Results from laboratory experiments. *Marine Micropaleontology*, 22: 221-234.

Spero, H. and Lea, D., 1996. Experimental determination of stable isotope variability in *Globigerina bulloides*: implications for paleoceonographic reconstructions. *Marine Micropaleontology*, 28: 231-246.

Stecher, H., Krantz, D., Lord III, C., Luter III, G. and Bock, K., 1996. Profiles of strontium and barium in *Mercenaria mercenaria* and *Spisula solidissima* shells. *Geochimica et Cosmochimica Acta*, 60(18): 3445-3456.

Stipp, S.L., Hochella, J., Michael F., Parks, G.A. and Leckie, J.O., 1992. Cd^{2+} uptake by calcite, solid-state diffusion, and the formation of solid-solution: Interface processes observed with near-surface sensitive techniques (XPS, LEED, and AES). *Geochimica et Cosmochimica Acta*, 56(5): 1941-1954.

Stoll, H., Ruiz Encinar, J., Garcia Alonso, J.I., Rosenthal, Y., Klaas, C. and Probert, I., 2001. A first look at paleotemperatures prospects from Mg in coccolith carbonate: Cleaning techniques and culture measurments. *Geochemistry, Geophysics, Geosystems*, 2: 2000GC000144.

Stoll, H. and Schrag, D., 2000. Coccolith Sr/Ca as a new indicator of coccolithphorid calcification and growth rate. *Geochemistry, Geophysics, Geosystems*, 1: doi:10.1029/2000GC000144.

Stoll, H., Ziveri, P., Geisen, M., Probert, I. and Young, J., 2002a. Potential and limitations of Sr/Ca ratios in coccolith carbonate: new perspectives from cultures and monospecific samples from sediments. *Philosophical Transactions of the Royal Society London, Series A*, 360: 719-747.

Stoll, H.M., Klaas, C.M., Probert, I., Ruiz Encinar, J. and Garcia Alonso, J.I., 2002b. Calcification rate and temperature effects on Sr partitioning in coccoliths of multiple species of coccolithophorids in culture. *Global and Planetary Change*, 34(3-4): 153-171.

Stoll, H.M., Schrag, D.P. and Clemens, S.C., 1999. Are seawater Sr/Ca variations preserved in quaternary foraminifera? *Geochimica et Cosmochimica Acta*, 63(21): 3535-3547.

Su, P. and Huang, S., 1998. Direct and simultaneous determination of copper and manganese in seawater with a multielement graphite furnace atomic absorption spectrometer. *Spectrochimica Acta Part B-Atomic Spectroscopy*, 53(5): 699-708.

Sunda, W. and Huntsman, S., 1985. Regulation of cellular manganese and manganese transport rates in unicellular alga *Chlamydomonas*. *Limnology and Oceanography*, 30: 71-80.

Sunda, W. and Huntsman, S., 1987. Microbial oxidation of manganese in a North Carolina Estuary. *Limnology and Oceanography*, 32(3): 552-564.

Sundby, B., Anderson, L., Hall, P., Iverfeldt, A., Rutgers, V., Der Loeff, M. and Westerlund, S., 1986. The effect of oxygen on release and uptake of cobalt, manganese, iron and phosphate at the sediment-water interface. *Geochimica et Cosmochimica Acta*, 50: 1281-1288.

Sundby, B., Silverberg, N. and Chesselet, R., 1981. Pathways of manganese in an open estuarine system. *Geochimica et Cosmochimica Acta*, 45: 293-307.

Swann, C.P., Hansen, K.M., Price, K. and Lutz, R., 1991. Application Of Pixe In The Study Of Shellfish. *Nuclear Instruments & Methods In Physics Research Section B-Beam Interactions With Materials And Atoms*, 56-7: 683-686.

Swart, P.K., 1983. Carbon and oxygen isotope fractionation in scleratinian corals: a review. *Earth-Science Reviews*, 19: 51-80.

Swart, P.K. and Grottoli, A., 2003. Proxy indicators of climate in coral skeletons: a perspective. *Coral Reefs*, 22: 313-315.

Takesue, R. and van Geen, A., 2004. Mg/Ca, Sr/Ca and stable isotopes in modern and holocene *Protothaca staminea* shells from a northern California coastal upwelling region. *Geochimica et Cosmochimica Acta*, 68(19): 3845-3861.

Tan, F., Cai, D. and Roddick, D., 1988. Oxygen isotope studies on Sea Scallops *Placopecten magellanicus*, from Brown's Bank, Nova Scotia. *Canadian Journal of Fisheries and Aquatic Sciences*, 45: 1378-1385.

Tanaka, N., Monaghan, M. and Rye, D., 1986. Contribution of metabolic carbon to mollusc and barnacle shell carbonate. *Nature*, 320: 520-523.

Tappin, A., Millward, G., Statham, P., Burton, J. and Morris, A., 1995. Trace-metals in the central and southern North Sea. *Estuarine, Coastal and Shelf Science*, 41: 275-323.

Tarutani, T., Clayton, N. and Mayeda, T., 1969. Effect of polymorphism and magnesium substitution on oxygen isotope fractionation between calcium carbonate and water. *Geochimica et Cosmochimica Acta*, 33(8): 987-996.

Taylor, J.D., Kennedy, W.J. and Hall, A., 1969. The shell structure and mineralogy of the Bivalvia: Introduction, Nuculacea-Trigonacea. *Bulletin Brithish Museum (Nat. Hist.) Zoology*, 3: 1-125.

Taylor, J.D., Kennedy, W.J. and Hall, A., 1973. The shell structure and mineralogy of the Bivalvia: Introduction: Nuculacea-Clavagellacea: conclusions. *Bulletin Br. Mus. (Nat. Hist.) Zool.*, 22: 253-294.

Taylor, J.D. and Reid, D., 1990. Shell microstructure and mineralogy of the Littorinidae: Ecological and evolutionary significance. *Hydrobiologia*, 193: 199-215.

Tesoriero, A. and Pankow, J., 1996. Solid solution partitioning of Sr^{2+}, Ba^{2+} and Cd^{2+} to calcite. *Geochimica et Cosmochimica Acta*, 60: 1053-1063.

Thamdrup, B., Fossing, H. and Jorgensen, B., 1994. Manganese, iron, and sulfur cycling in a coastal marine sediment, Aarhus Bay, Denmark. *Geochimica et Cosmochimica Acta*, 58(23): 5115-5129.

Thorn, K., Cerrato, R. and Rivers, M., 1995. Elemental distributions in marine bivalves shells as measured by synchroton X-ray fluorescence. *Biological Bulletin*, 188(1): 57-67.

Toland, H, Perkins, B., Pearce, N., Keenan, F. and Leng, M., 2000. A study of sclerochronology by laser ablation ICP-MS. *Journal of Analytical Atomic Spectrometry*, 15(9): 1143-1148.

Toyofuku, T., Kitazato, H., Kawahata, H., Tsuchiya, M. and Nohara, M., 2000. Evaluation of Mg/Ca thermometry in foraminifera: Comparison of experimental results and measurements in nature. *Paleoceanography*, 15(4): 456-464.

Turekian, K., 1977. The fate of metals in the oceans. *Geochimica et Cosmochimica Acta*, 41: 1139-114.

Turner, A. and Millward, G., 2000. Particle dynamics and trace metal reactivity in estuarine plumes. *Estuarine, Coastal and Shelf Science*, 50: 761-774.

Turner, J., 1982. Kinetic fractionation of carbon-13 during calcium carbonate precipitation. *Geochimica et Chosmochimica Acta*, 46: 1183-1191.

Urey, H., 1947. The thermodynamic properties of isotopic substances. *Journal of the Chemical Society*, 1: 562-581.

Urey, H., Epstein, S. and McKinney, C., 1951. Measurement of paleotemperatures and temperatures of the Upper Cretaceous of England, Denmark, and the shoutheastern United States. *Geological Society of America Bulletin*, 62: 399-416.

Usdowski, E. and Hoefs, J., 1993. Oxygen isotope exchange between carbonic acid, bicarbonate, carbonate, and water: A re-examination of the data of McCrea (1950) and and expression for the overall partitioning of oxygen isotopes between the carbonate species and water. *Geochimica et Cosmochimica Acta*, 57: 3815-3818.

Usdowski, E., Michaelis, J., Böttcher, M. and Hoefs, J., 1991. Factors for the oxygen isotope equilibrium fractionation between aqueous and gaseous CO_2, carbonic acid, bivarbonate, carbonate, and water (19C). *Z. Phys. Chem.*, 170: 237-249.

Vander Putten, E., Dehairs, F., André, L. and Baeyens, W., 1999. Quantitative in situ microanalysis and trace elements in biogenic calcite using infrared laser ablation-inductively coupled plasma mass spectrometry. *Analytica Chimica Acta*, 378: 261-272.

Vander Putten, E., Dehairs, F., Keppens, E. and Baeyens, W., 2000. High resolution distribution of trace elements in the calcite shell layer of modern *Mytilus edulis*: Environmental and biological controls. *Geochimica et Cosmochimica Acta*, 64(6): 997-1011.

Vasil'ev, A., 2005. Calcium-Magnesium Paleothermometry and Biochemical Adaptations of Mollusks. *Paleontological Journal*, 39(3): 248-250.

Vinot-Bertouille, A. and Duplessy, J., 1973. Individual isotope fractionation of carbon and oxygen in benthic foraminifera. *Earth and Planetary Science Letters*, 18: 247-252.

Wada, K. and Fujinuki, T., 1974. Biomineralization in bivalve molusca with emphasis on the chemical composition of extrapallial fluid. In: N. Watabe and K. Wilbur (Editors), *The Mechanisms of Mineralization in the Invertebrates and Plants*. Univ. of South Carolina Press, Columbia, pp. 175-188.

Wada, K. and Fujinuki, T., 1976. Biomineralization in bivalve molusca with emphasis on the chemical composition of extrapallial fluid. In: N. Watabe and K. Wilbur (Editors), *The Mechanisms of Mineralization in the Invertebrates and Plants*. Univ. of South Carolina Press, Columbia, pp. 175-188.

Wanamaker, A., Kreutz, K., Borns, H., Introne, D., Feindel, S. and Barber, B., 2006. An aquaculture-based method for calibrated bivalve isotope

paeothermometry. *Geochemistry, Geophysics, Geosystems*, 7(9): Q09011, doi:10.1029/2005GC001189.

Wanamaker, A., Kreutz, K., Borns, H., Introne, D., Feindel, S., Funder, S., Rawson, P. and Barber, B., 2007. Experimental determination of salinity, temperature, growth, and metabolic effects on shell isotope chemistry of *Mytilus edulis* collected from Maine and Greenland. *Paleoceanography*, 22: doi:10.1029/2006PA001352.

Wara, M., Anderson, Schellenberg, S., Franks, R., Ravelo, A. and Delaney, M., 2003. Application of a radially viewed inductively coupled plasma-optical emission spectrophotometer to simultaneous measurement of Mg/Ca, Sr/Ca and Mn/Ca ratios in marine biogenic carbonates. *Geochemistry, Geophysics, Geosystems*, 4(8): 1-14.

Warren, C. and Davis, G., 1967. Laboratory studies on the feeding, bioenergetics, and growth of fish. In: S. Gerking (Editor), *The Biological Basis of Freshwater Fish Production*. Blackwell Scientific Publications, Oxford, pp. 175-214.

Wasylenki, L., Dove, P. and De Yoreo, J., 2005a. Effects of temperature and transport conditions on calcite growth in the presence of Mg^{2+}: Implications for paleothermometry. *Geochimica et Cosmochimica Acta*, 69(17): 4227-4236.

Wasylenki, L., Dove, P., Wilson, D. and De Yoreo, J., 2005b. Nannoscale effects of strontium on calcite growth: An in situ AFM study in the absence of vital effects. *Geochimica et Cosmochimica Acta*, 69(12): 3017-3027.

Watabe, N., 1988. Shell structure. In: E.R. Trueman and M.R. Clarke (Editors), *The Mollusca*. Academic Press, New York, pp. 69-74.

Watson, E., 1996. Surface enrichment and trace-element uptake during crystal growth. *Geochimica et Cosmochimica Acta*, 60(24): 5013-5020.

Watson, E., 2004. A conceptual model for near-surface kinetic controls on the trace element and stable isotopic composition of abiogenic calcite crystals. *Geochimica et Cosmochimica Acta*, 68(7): 1473-1488.

Weber, J., 1973. Incorporation of strontium into reef coral skeletal carbonate. *Geochimica et Cosmochimica Acta*, 37: 2173-2190.

Weber, J. and Woodhead, P., 1970. Carbon and oxygen isotope fractionation in the skeletal carbonate of reef building corals. *Chemical Geology*, 6: 93-117.

Wefer, G. and Berger, W., 1991. Isotope palaeontology: growth and composition of extant calcareous species. *Marine Geology*, 100: 207-248.

Wefer, G., Berger, W., Bijma, J. and Fischer, G., 1999. Clues to Ocean History: a Brief Overview of Proxies. In: G. Fischer and G. Wefer (Editors), *Use of Proxies in Paleocenography: Examples from the South Atlantic*. Springer-Verlag, Berlin Heidelberg, pp. 1-68.

Weidman, C., Jones, G. and Kyger, 1994. The long-lived mollusk *Artica islandica* - A new paleoceanographic tool for the reconstruction of bottom temperatures for the continental shelves of the northern North Atlantic Ocean. *Journal of Geophysical Research*, 99(C9): 18305-18314.

Weiner, S. and Dove, P., 2003. Overview of Biomineralization Processes and the Problem of the Vital Effects. In: P. Dove, J. De Yoreo and S. Weiner (Editors), *Biomineralization*. Reviews in Mineralogy and Geochemistry. Mineralogical Society of America, Washington, USA, pp. 1-29.

Wheeler, A., 1975. Oyster mantle carbonic anhydrase: Evidence for plasma membrane-bound activity and for a role in bicarbonate trasnport, Duke University, Durham, North carolina.

Wheeler, A., 1992. Mechanisms of molluscan shell formation. In: E. Bonucci (Editor), *Calcification in Biologycal Systems*. CRC Press, pp. 179-216.

Wilbur, D. and Saleuddin, A., 1983. Shell formation. In: A. Saleuddin and K. Wilbur (Editors), *The Mollusca*. Academic Press, New York, pp. 236-287.

Wilbur, K., 1976. Recent studies of invertebrate mineralization. In: N. Watabe and K. Wilbur (Editors), *The mechanisms of mineralization in the invertebrates and plants*. Univ. of South Carolina Press, Columbia, pp. 79-108.

Wilkinson, B. and Ivany, L., 2002. Paleoclimatic inference from stable isotope profiles of accreationary biogenic hardparts - a quantitative approach to the evaluation of incomplete data. *Palaeogeography Palaeoclimatology Palaeoecology*, 185: 95-114.

Williams, D., Arthur, M., Jones, D. and Healy-Williams, N., 1982. Seasonality and mean annual sea surface temperatures from isotopic and sclerochronological records. *Nature*, 296: 432-434.

Wilson, D.E., 1980. Surface and complexation effects on the rate of Mn(II) oxidation in natural waters. *Geochimica et Cosmochimica Acta*, 44(9): 1311-1317.

Wolf-Gladrow, D., Bijma, J. and Zeebe, C., 1999. Model simulation of the carbonate chemistry in the microenvironment of symbiont bearing foraminifera. *Marine Chemistry*, 64: 181-198.

Woodward, C. and Davidson, E., 1968. Structure-function relationships of protein polysaccharide complexes: specific ion-binding properties. *Biochemistry*, 60: 201-205.

Zachara, J., Cowan, C. and Resch, C., 1991. Sorption of divalent metals on calcite. *Geochimica et Cosmochimica Acta*, 55: 1549-1562.

Zachara, J.M., Kittrick, J.A. and Harsh, J.B., 1988. The mechanism of Zn^{2+} adsorption on calcite. *Geochimica et Cosmochimica Acta*, 52(9): 2281-2291.

Zeebe, C., 1999a. An explanation of the effect of seawater carbonate concentration on foraminiferal oxygen isotopes. *Geochimica et Chosmochimica Acta*, 63(13/14): 2001-2007.

Zeebe, R., 1999b. An explanation of the effect of seawater carbonate concentration on foraminiferal oxygen isotopes. *Geochimica et Cosmochimica Acta*, 63(13/14): 2001-2007.

Zeebe, R., Bijma, J. and Wolf-Gladrow, D., 1999. A diffusion-reaction model of carbon isotope fractionation in foraminifera. *Marine Chemistry*, 64: 199-227.

Zhong, S. and Mucci, A., 1989. Calcite and aragonite precipitation from seawater solutions of various salinities: Precipitation rates and overgrowth compositions. *Chemical Geology*, 78: 283-299.